

**MASS SPECTROMETRIC DETECTION OF INDOPHENOLS FROM THE
GIBBS REACTION FOR PHENOLS ANALYSIS**

by
Sabyasachy Mistry

A Dissertation

*Submitted to the Faculty of Purdue University
In Partial Fulfillment of the Requirements for the degree of*

Doctor of Philosophy



Department of Chemistry
West Lafayette, Indiana
May 2020

THE PURDUE UNIVERSITY GRADUATE SCHOOL
STATEMENT OF COMMITTEE APPROVAL

Dr. Paul G. Wenthold, Chair

Department of Chemistry

Dr. Garth J. Simpson

Department of Chemistry

Dr. Chengde Mao

Department of Chemistry

Dr. Julia Laskin

Department of Chemistry

Approved by:

Dr. Christine A. Hrycyna

Dedicated to all the FREEDOM FIGHTERS of Bangladesh

ACKNOWLEDGMENTS

The accomplishments I have enjoyed in my graduate school career at Purdue University would be naught without the support of my principal investigator (PI), lab colleagues, Chemistry Department, my friends, family, and loving wife. There are many folks and groups to acknowledge and I object is to name you all here.

I am thankful for my PhD advisor, Prof. Paul G. Wenthold, for offering me the academic freedom and support to solve different challenging problems in my time at Purdue. The atmosphere that you have created and managed in your laboratory is unique and admirable. I am very thankful to have been accepted into your research group and to have worked with you over the past five and half years. Prof. Wenthold appeared to be the most resourceful person in every aspect during my graduate school. His motivation and patience about science always encourage me to think beyond the capability. Thank you so much for your great support since my graduate time at Purdue.

Besides my advisor, I am thankful to the rest of my dissertation committee: Prof. Chengde Mao, Garth Simpson, Julia Laskin and Yu Xia for their time and enagernees in helping me. I am grateful that they were very approachable for anything I needed in my Purdue time.

I learned many new skills from senior and junior of 'Purdue Center for Negative Ion Research' lab colleagues while at Purdue. Thank you to Damodar Koirala, Chris Haskins, Harshal Jawale, Cory Conder, James Langford, Bryan Smith, Chris Brown, Evan Reeves, Rachael Marie Knieser for sharing your skills with me. In addition, I have had the pleasure of working with all of you.

I am thanking to all the staff of the Chemistry Department for their valuable support at my graduate school. I want to mention Mark Carlsen and Konrad Kliewer of Jonathan Amy Facility

for Chemical Instrumentation and Robert A. Reason of Chemistry Copy Center for their generous help. Without the help of the first two staff it would be very difficult to keep running instruments (Thermo Finnigan LCQ-Deca and Waters micromas Ultima) in our lab. Rob was always helping to print posters for the conferences. I am grateful to all of you.

Thank you to my graduate school friends, Sarju Adhikari, Clint Alfaro, Patrick Fedrick, Stevie Norcross, Sreya Sarkar, Mack Shih, Dalton Snyder, Janny Dinh, Anindya Sarkar, Amartyo Jiban Basu, Azhad U. Chowdhury, Bharat Mankani, Ameya Kulkarni, Priya Murria, Hari Raj Khatri, Manish Nepal and others for helping keep me centered at Purdue. I am thanking also to Biddut Sharker and Kamol Das for their valuable advice and help at my time at Purdue.

I am extremely grateful for the support from my undergraduate (Prof. Iqbal Rouf Mamun) and masters research advisor (Prof. Nilufar Nahar) at the University of Dhaka for being an inspiring scientist, mentor, role model, and friend. I would not be pursuing analytical chemistry research and writing this dissertation if not for your contagious enthusiasm. Your ability to inspire students is an amazing skill. In addition, I am very thankful to Prof. Ernesto Abel-Santos of University of Nevada Las Vegas for helping me to consider Purdue University for my PhD.

The Bangladeshi community at Purdue is a very helpful and knowledgeable community. They make me feel like I have never been away from my country. They are always there during the time of difficulties and challenges. I had pleasure serving as a vice-president (2017-2018) of Bangladesh Student Association – Purdue (BDSA).

I am incredibly grateful for the support from my family in pursuing my career goals. My parents, Nil Ratan Mistry and Sandhya Rani Samaddar, provide unwavering moral support and convince me that I can achieve anything despite how difficult the journey may be. My uncle,

Shishir Mistry and Nripendra Nath Mistry, give me constant reassurance and remind me that I am valued. Thank all of you for your encouragement.

Finally, I feel loved to have Amity Saha as my wife who is with me on every twist and turns. She has helped me since 2017. Without your support and encouragement, my graduate time would be much more difficult. Thank you so much for your great support.

TABLE OF CONTENTS

LIST OF TABLES.....	12
LIST OF FIGURES.....	13
ABSTRACT.....	20
CHAPTER 1. PHENOLS AND GUIDE TO DISSERTATION.....	23
1.1 Phenol.....	23
1.2 History and uses of phenols.....	23
1.3 Toxic effects of phenolic compounds.....	25
1.4 The identification and measurements of phenolics.....	26
1.4.1 Determination of phenolic compounds using classical colorimetric methods.....	26
1.4.2 Determination of total content of flavonoids and anthocyanins.....	26
1.4.3 Determination of condensed tannins.....	27
1.4.4 Determination of total phenolic content.....	28
1.4.5 Chromatography.....	28
1.4.6 Mass Spectrometry.....	30
1.4.7 NMR Spectroscopy.....	31
1.5 Proposed techniques and guide to dissertation.....	32
1.6 References.....	33
CHAPTER 2. HISTORY AND MECHANISM OF THE GIBBS REACTION.....	40
2.1 Background of Gibbs reaction.....	40
2.2 Mechanism of the Gibbs reaction.....	42
2.3 Examples of Gibbs reaction.....	48
2.4 Conclusion.....	50
2.5 References.....	50
CHAPTER 3. MASS SPECTROMETRIC DETECTION OF THE GIBBS REACTION FOR PHENOL ANALYSIS.....	54
3.1 Introduction.....	54
3.2 Experimental.....	56
3.2.1 Sample preparation – general procedures.....	56
3.2.2 Sample preparation – liquid smoke.....	57

3.2.3	Spectra collection.....	57
3.2.4	Spectral analysis	58
3.2.5	Materials.....	58
3.3	Results.....	59
3.3.1	Phenol.....	59
3.3.2	Substituted phenols.....	60
3.3.3	Isomer distinction	69
3.3.4	Mixture analysis and signal time dependence	72
3.3.5	Sensitivity.....	73
3.3.6	Application: Analysis of “Hickory” and “Mesquite” Liquid Smoke	74
3.4	Conclusions	76
3.5	References.....	77
CHAPTER 4. RAPID QUANTIFICATION OF PHENOLIC COMPOUNDS IN LIQUID SMOKE BY USING MASS SPECTROSCOPY		82
4.1	Introduction	82
4.2	Materials and methods	83
4.2.1	Chemicals.....	83
4.2.2	Samples	83
4.2.3	Analysis of Liquid Smoke.....	84
4.2.4	Calibration Curve.....	85
4.2.5	Spectra collection.....	85
4.2.6	Spectral analysis	85
4.3	Results.....	86
4.3.1	Identification of the phenols in liquid smokes	86
4.3.2	Internal standard for the analysis.....	101
4.3.3	Preparation of calibration curves	102
4.3.4	Limit of detection (LOD) and limit of quantification (LOQ)	103
4.3.5	Quantification of Colgin Natural Liquid Smoke	104
4.4	Discussion.....	107
4.5	Conclusion	108
4.6	References.....	108

CHAPTER 5. HOW SMOKEY THE WHISKEY IS: A QUANTITATIVE APPROACH ON CHEMISTRY ASPECT	112
5.1 Introduction	112
5.2 Materials and methods	115
5.2.1 Chemicals	115
5.2.2 Scotch Whiskey Samples	115
5.2.3 Calibration Curve.....	116
5.2.4 Analysis of Whiskey.....	117
5.2.5 Spectra collection.....	117
5.2.6 Spectral analysis	118
5.3 Results.....	118
5.3.1 Identification of the phenols in whiskey	118
5.3.2 Preparation of calibration curves	132
5.3.3 Limit of quantification (LOQ)	133
5.3.4 Quantification of Phenols in Whiskeys	134
5.4 Discussion.....	136
5.5 Conclusion	140
5.6 References.....	141
CHAPTER 6. MASS SPECTROSCOPIC ANALYSIS OF L-DOPA NEUROTRANSMITTER AND IT'S METABOLITES BY USING GIBBS REACTIO.....	147
6.1 Introduction	147
6.2 Experiment.....	149
6.2.1 Chemicals	149
6.2.2 Stock solution.....	150
6.2.3 Sample preparation – general procedures	150
6.2.4 L-DOPA methyl ester formation	150
6.2.5 Spectra collection.....	150
6.2.6 Spectral analysis	151
6.3 Results.....	151
6.3.1 L-Dopa.....	151
6.3.2 <i>iso</i> -Homovanillic acid (<i>iso</i> -HVA)	153

6.3.3	Dopamine	155
6.3.4	3,4-Dihydroxyphenylacetic acid (DOPAC)	156
6.3.5	3-Methoxytyramine (3-MT).....	157
6.3.6	Norepinephrine (noradrenaline).....	158
6.4	Discussion.....	159
6.5	Conclusion	160
6.6	References.....	160
CHAPTER 7. SPECIFICITY OF <i>PARA</i> -SUBSTITUTED PHENOLS IN GIBBS REACTIO _n ...		
	165
7.1	Introduction	165
7.2	Experimental.....	166
7.2.1	Chemicals	166
7.2.2	Sample preparation	167
7.2.3	Purification of the Gibbs product	167
7.2.4	Spectra collection.....	167
7.2.5	Spectral analysis	168
7.3	Results.....	168
7.3.1	Direct substitution of X	170
7.3.2	Substitution at ortho position	171
7.3.3	Substitution and second addition of X	175
7.3.4	No reaction	180
7.3.5	Structure of the condensation product (CP)	181
7.4	Conclusion	183
7.5	References.....	183
CHAPTER 8. FRAGMENTATION MECHANISM OF PROLINE CONTAINING DIPEPTIDES		186
8.1	Introduction	186
8.2	Experimental.....	188
8.2.1	Mass spectrometric analysis.....	188
8.2.2	Computational methods.....	188
8.2.3	Synthesis of amino acid esters	189

8.2.4	Synthesis of Boc protected amino acid	189
8.2.5	Synthesis of Pro-Phe*OH and Phe*-ProOH dipeptides and their methyl ester	190
8.2.6	Synthesis of Diketopiperazine	191
8.2.7	Synthesis of oxazolone (from ProPhe*)	191
8.3	Result	192
8.3.1	Formation of Phe*-ProOH and Pro-Phe*OH.....	192
8.3.2	Analysis of Phe*-ProOH and Pro-Phe*OH	194
8.3.3	Analysis of Phe*ProOMe and ProPhe*OMe	196
8.3.4	Comparison to Authentic Diketopiperazine and Oxazolones	198
8.3.5	Deuterium labelling	200
8.4	Conclusion	204
8.5	References.....	205
VITA.....		210
PUBLICATIONS		211
APPENDIX. PATENT		229

LIST OF TABLES

Table 2.1. Examples of the applications of the Gibbs Reactions	48
Table 4.1. Tandem mass spectrometry of indophenols formed from the reaction of Gibbs reagent and dihydroxybenzene, methoxyphenol, and dimethoxyphenol isomers, and four different flavours of liquid smoke. CID fragmentation (peaks with intensity of more than 5% of the base peak). .	100
Table 4.2. Limit of detection (LOD) and limit of quantification (LOQ) of catechol, guaiacol, and syringol.....	104
Table 4.3. Concentration of catechol, guaiacol, and syringol in mg/L in four different flavored colgin® liquid some.	106
Table 5.1. Tandem mass spectrometry of indophenols formed from the reaction of Gibbs reagent and cresol, methoxyphenol, and dimethoxyphenol isomers, and four different brands of whiskey. CID fragmentation (peaks with intensity of more than 5% of the base peak).....	131
Table 5.2. Limit of detection and limit of quantification of catechol, guaiacol, and syringol.....	134
Table 5.3. Concentration of <i>o</i> -cresol, guaiacol, and syringol in Johnnie Walker Double Black, Tomintoul, Laphroaig, and Gordon Graham Black Bottle Blended Whiskey in mg/L (or ppm).	135
Table 6.1. Indophenol peak analysis of L-Dopa and it's metabolites	159
Table 7.1. List of <i>para</i> -substituted phenols that were analyzed	169
Table 8.1. Calculated Relative Energies of b ₂ ions in kcal/mol at B3LYP/6-31+G* optimized geometries.	203

LIST OF FIGURES

Figure 2.1. Formation of Indophenol color (blue) when phenol reacts with 2,6-dichloroquinone-4-chloroimide. The concentration of phenol increases from left to right and thus the color is changing from light blue to deep blue.	41
Figure 3.1. ESI mass spectra of products of phenol reaction with the Gibbs reagent. a) Gibbs reagent alone in buffer; b) phenol alone in buffer; c) phenol and Gibbs reagent mixture in buffer, 5 minutes after mixing; d) mixture mass spectrum deconvoluted for the 2-chlorine isotope pattern.	60
Figure 3.2. Structures of phenolic derivatives with <i>ortho</i> - and <i>meta</i> -substituted and bicyclic phenols.....	61
Figure 3.3. ESI mass spectra of products of <i>o</i> -cresol reaction with the Gibbs reagent. a) Gibbs product in buffer reaction, 5 minutes after mixing; b) mixture mass spectrum deconvoluted for the 2-chlorine isotope pattern.....	61
Figure 3.4. ESI mass spectra of products of <i>m</i> -cresol reaction with the Gibbs reagent. a) Gibbs product in buffer reaction, 5 minutes after mixing; b) mixture mass spectrum deconvoluted for the 2-chlorine isotope pattern.....	62
Figure 3.5. ESI mass spectra of products of <i>o</i> -methoxyphenol or guaiacol reaction with the Gibbs reagent. a) Gibbs product in buffer reaction, 5 minutes after mixing; b) mixture mass spectrum deconvoluted for the 2-chlorin.....	62
Figure 3.6. ESI mass spectra of products of <i>m</i> -methoxyphenol reaction with the Gibbs reagent. a) Gibbs product in buffer reaction, 5 minutes after mixing; b) mixture mass spectrum deconvoluted for the 2-chlorine isotope pattern.....	63
Figure 3.7. ESI mass spectra of products of catechol reaction with the Gibbs reagent. a) Gibbs product in buffer reaction, 5 minutes after mixing; b) mixture mass spectrum deconvoluted for the 2-chlorine isotope pattern.....	63
Figure 3.8. ESI mass spectra of products of <i>o</i> -aminophenol reaction with the Gibbs reagent. a) Gibbs product in buffer reaction, 5 minutes after mixing; b) mixture mass spectrum deconvoluted for the 2-chlorine isotope pattern.....	64
Figure 3.9. ESI mass spectra of products of 1-naphthol reaction with the Gibbs reagent. a) Gibbs product in buffer reaction, 5 minutes after mixing; b) mixture mass spectrum deconvoluted for the 2-chlorine isotope pattern.....	64
Figure 3.10. ESI mass spectra of products of 5,6,7,8-tetrahydro-1-naphthol reaction with the Gibbs reagent. a) Gibbs product in buffer reaction, 5 minutes after mixing; b) mixture mass spectrum deconvoluted for the 2-chlorine isotope pattern.....	65
Figure 3.11. Structures of phenolic derivatives with <i>para</i> -substitution.....	65

Figure 3.12. ESI mass spectra of products of <i>p</i> -chlorophenol reaction with the Gibbs reagent. a) Gibbs product in buffer reaction, 5 minutes after mixing; b) mixture mass spectrum deconvoluted for the 2-chlorine isotope pattern.....	66
Figure 3.13. ESI mass spectra of products of <i>p</i> -methoxyphenol reaction with the Gibbs reagent. a) Gibbs product in buffer reaction, 5 minutes after mixing; b) mixture mass spectrum deconvoluted for the 2-chlorine isotope pattern.....	67
Figure 3.14. ESI mass spectra of products of <i>p</i> -fluorophenol reaction with the Gibbs reagent. a) Gibbs product in buffer reaction, 5 minutes after mixing; b) mixture mass spectrum deconvoluted for the 2-chlorine isotope pattern.....	67
Figure 3.15. ESI mass spectra of products of <i>p</i> -cresol reaction with the Gibbs reagent. a) Gibbs product in buffer reaction, 5 minutes after mixing; b) mixture mass spectrum deconvoluted for the 2-chlorine isotope pattern.....	68
Figure 3.16. ESI mass spectra of products of <i>p</i> -ethylphenol reaction with the Gibbs reagent. a) Gibbs product in buffer reaction, 5 minutes after mixing; b) mixture mass spectrum deconvoluted for the 2-chlorine isotope pattern.....	68
Figure 3.17. MS/MS of substituted phenols examined in this work	69
Figure 3.18. CID spectra of indophenols formed from a) <i>ortho</i> - and b) <i>meta</i> -cresol, with a normalized energy of 25%.	69
Figure 3.19. CID spectra of indophenols formed from a) <i>ortho</i> - and b) <i>meta</i> -methoxyphenol, with a normalized energy of 25%.	70
Figure 3.20. CID spectra of indophenols formed from a) catechol and b) resorcinol, with a normalized energy of 25%.	71
Figure 3.21. CID spectra of indophenols formed from a) <i>ortho</i> - and b) <i>meta</i> -aminophenol, with a normalized energy of 32%.	71
Figure 3.22. Deconvoluted ESI-mass spectrum of Gibbs products obtained from a 1:1 mixture of phenol and <i>o</i> -cresol, taken a) 5 minutes and b) 30 minutes after mixing. The spectrum in Figure 2a was taken 5 minutes after mixing the phenols with the Gibbs reagent.	72
Figure 3.23. Relative intensities of phenol (m/z 266) and <i>o</i> -cresol (m/z 280) Gibbs products as a function of phenol concentration. The <i>o</i> -cresol is present at a concentration of 3 μ mol/L.	74
Figure 3.24. 2,6-Dimethoxyphenol or syringol is found in liquid smoke.....	75
Figure 3.25. Deconvoluted mass spectrum of the Gibbs products obtained from analysis of a) Natural Hickory and b) Natural Mesquite flavors of colgin® brand liquid smoke.	75
Figure 4.1. Commercially available four different flavored Colgin Assorted Liquid Smoke was examined in this work. The four different flavors are – (from left to right) Hickory, Mesquite, Apple and Pecan.	84
Figure 4.2. Full MS (top) and deconvoluted MS (bottom) of the Gibbs product of Hickory liquid some.....	87

Figure 4.3. Full MS (top) and deconvoluted MS (bottom) of catechol, resorcinol, and hydroquinone, respectively. At 5 minute reaction hydroquinone gives peak at m/z 266, whereas it gives an additional peak at m/z 266 in longer reaction time.	88
Figure 4.4. MS/MS of m/z 282 of indophenol from Hickory, <i>ortho</i> -, <i>meta</i> -, and <i>para</i> -hydroxyphenol, respectively, with CID energy of 45%.	89
Figure 4.5. (From left to right) Full MS (top) and deconvoluted MS (bottom) of <i>ortho</i> -, <i>meta</i> -, and <i>para</i> -methoxyphenol, respectively. All of them give indophenol peak at m/z 296. In addition, <i>p</i> -methoxy phenol gives a characteristic peak among these isomers at m/z 388.	90
Figure 4.6. MS/MS of m/z 296 of indophenols formed by Hickory liquid smoke, <i>o</i> -, and <i>m</i> -methoxyphenol. CID energy of 32% is used for all experiments. <i>m</i> -isomer can be distinguished by the appearance of daughter ion at m/z 122.	91
Figure 4.7. Full MS (top) and deconvoluted MS (bottom) of 2,6-, 2,3-, and 2,5-dimethoxyphenol, respectively.	92
Figure 4.8. Full MS (top) and deconvoluted MS (bottom) of 2,4-, and 3,4-dimethoxyphenol, respectively.	93
Figure 4.9. (From top to bottom) MS/MS (left) and MS/MS/MS (right) of indophenols formed from m/z 326 from Hickory, 2,6-, 2,3-, 2,5-, and 3,5-dimethoxyphenols, respectively. The collision energy for MS/MS is 35% and for MS ³ is of 30%.	95
Figure 4.10. (From left to right) Full MS and deconvoluted MS of Mesquite, Pecan, and Apple liquid smokes, respectively.	96
Figure 4.11. (From top to bottom) MS/MS (left) of m/z 282 (right) of Mesquite, Pecan, and Apple liquid smokes, respectively, at CID energy of 32%.	97
Figure 4.12. (Top to bottom) MS/MS of m/z 296 of Mesquite, Pecan, and Apple liquid smokes, respectively, at CID energy of 32%.	98
Figure 4.13. (From top to bottom) MS/MS (left) and MS ³ (right) of indophenols formed at m/z 326 from Mesquite, Pecan, and apple liquid smokes, respectively.	99
Figure 4.14. ESI mass spectra of products of phenol, 1-naphthol, and 5,6,7,8-tetrahydro-1-naphthol (THN) reaction with Gibbs reagent. a) phenol, 1-naphthol, and 5,6,7,8-tetrahydro-1-naphthol and Gibbs reagent mixture in buffer after 5 minutes; b) mixture mass spectrum deconvoluted for the 2-chlorine isotope pattern.	102
Figure 4.15. Calibration plots for Gibbs product formation compared to the internal standard for a) catechol, b) guaiacol and c) syringol obtained 5 minutes after mixing with the Gibbs reagent. The internal standard, 5,6,7,8-tetrahydro-1-naphthol, is present at a concentration of 0.20 mg/L.	103
Figure 4.16. Deconvoluted ESI-mass spectra of Gibbs product obtained from Hickory (a), Mesquite (b), Pecan (c) and Apple (d) flavored “colgin® All Natural” liquid smokes obtained by mixing 0.2 mg/L (1.5 μmol/L) 5,6,7,8-tetrahydro-1-naphthol as internal standard.	105
Figure 4.17. Comparison of the concentrations of catechol (black), guaiacol (red), and syringol (green) in mg/L in hickory, mesquite, pecan and apple flavored “Colgon All Natural” liquid smoke.	

For the better comparison, the concentration of guaiacol and syringol makes fifty times in the bar-chart.	107
Figure 5.1. Four different brands of whiskey: (from left to right) Tomintoul 10 years aged; Johnnie Walker Double Black Blended Scotch Whiskey; Laphroaig Islay Single Malt Scotch Whiskey, 10 years aged; and Gordon Graham's Black Bottle Blended Scotch whiskey.	116
Figure 5.2. Full MS (top) and deconvoluted MS (bottom) of the Gibbs product of Laphroaig Islay Single Malt Scotch Whiskey, Aged 10 Years.	119
Figure 5.3. Full MS (top) and deconvoluted MS (bottom) of <i>ortho</i> -, <i>meta</i> -, and <i>para</i> -cresol, respectively.	120
Figure 5.4. (From top to bottom) MS/MS of m/z 280 of indophenol from Laphroaig, <i>o</i> -cresol, <i>m</i> -cresol, <i>p</i> -cresol with CID energy of 45%.	121
Figure 5.5. (From top to bottom) Full MS (top) and deconvoluted MS (bottom) of <i>ortho</i> -, <i>meta</i> -, and <i>para</i> -methoxyphenol, respectively. The first two isomers give indophenol peak at m/z 296 and <i>p</i> -methoxyphenol gives a characteristic peak among these isomers at m/z 388 along with another indophenol at m/z 266.	122
Figure 5.6. (From top to bottom) MS/MS of m/z 296 of indophenols formed by Laphroaig, <i>o</i> -, and <i>m</i> -methoxyphenol. CID energy of 32% is used for all experiments. <i>m</i> -isomer can be distinguished by the appearance of daughter ion at m/z 122.	123
Figure 5.7. (From left to right) Full MS (top) and deconvoluted MS (bottom) of 2,6-, 2,3-, and 2,5-dimethoxyphenol, respectively.	124
Figure 5.8. Full MS (top) and deconvoluted MS (bottom) of 3,5-, 2,4-, and 3,4-dimethoxyphenol, respectively.	125
Figure 5.9. (From top to bottom) MS/MS (left) and MS/MS/MS (right) of indophenols formed from 2,6-, 2,3-, 2,5-, and 3,5-dimethoxyphenols, respectively. The collision energy for MS/MS is 35% and for MS ³ is of 30%.	127
Figure 5.10. (From left to right) Full MS (top) and deconvoluted MS (bottom) of Tomintoul Scotch Whiskey, Gordon Graham's Black Bottle Blended Scotch whiskey and Johnnie Walker Double Black Blended Scotch Whiskey, respectively.	128
Figure 5.11. (From top to bottom) MS/MS of m/z 296 of Tomintoul Scotch Whiskey, Gordon Graham's Black Bottle Blended Scotch whiskey and Johnnie Walker Double Black Blended Scotch Whiskey, respectively, at CID energy of 32%.	129
Figure 5.12. (From top to bottom) MS/MS (left) and MS ³ (right) of indophenols at m/z 326 from Tomintoul, Gordon Graham's Black Bottle Blended, and Johnnie Walker Double Black Blended whiskeys, respectively.	130
Figure 5.13. Relative intensities of each of <i>o</i> -cresol (m/z 280) (a), guaiacol (m/z 296) (b), syringol (m/z 326) (c) to 5,6,7,8-tetrahydro-1-naphthol (m/z 320) Gibbs products as a function of concentration of the compounds. The 5,6,7,8-tetrahydro-1-naphthol is present at a concentration of 1.25 μ mole/L or 0.20 mg/L.	133

Figure 5.14. Amount of different phenols in all four different whiskies. Laphroaig contains all three phenols: <i>o</i> -cresol, guaiacol, and syringol, whereas other three whiskies contain only guaiacol and syringol.....	135
Figure 6.1. Full MS of L-DOPA methyl ester	152
Figure 6.2. (a) Full MS and (b) deconvoluted MS of the Gibbs products from L-DOPA-methyl ester.....	153
Figure 6.3. (a) Full MS and (b) deconvoluted MS of the Gibbs products from <i>iso</i> -Homovanillic acid.....	154
Figure 6.4. (a) Full MS and (b) deconvoluted MS of the Gibbs products from dopamine. Dopamine gives only indophenol at <i>m/z</i> 325.....	155
Figure 6.5. (a) Full MS and (b) deconvoluted MS of the Gibbs products from DOPAC.	156
Figure 6.6. (a) Full MS and (b) deconvoluted MS of the Gibbs products from 3-methoxytyramine.	157
Figure 6.7. (a) Full MS and (b) deconvoluted MS of the Gibbs products from norepinephrine or noradrenaline.....	158
Figure 7.1. The Gibbs reaction of 4-aminophenol after (a) 5 minute and (b) 30-minute reaction. a1 is the full MS and a2 is corresponding deconvoluted MS. After 5-minute reaction, 4-aminophenol gives no substitution product and no condensation product. The peak formed at <i>ortho</i> -substitution (at <i>m/z</i> 281) is also missing. However, after 30-minute reaction, it gives only substitution product at <i>m/z</i> 266 (b1 and b2). The peak formed by <i>ortho</i> -substitution (at <i>m/z</i> 281) is also missing even after 30-minute reaction.	171
Figure 7.2. The Gibbs products of 4-methylphenol or <i>p</i> -cresol after 5 minute reaction. (a) is the Full MS of the reaction solution and (b) is the deconvoluted MS. 4-Methylphenol gives neither the substitution product nor the condensation product. It is proposed that the peak at <i>m/z</i> 280 is formed from the substitution of <i>ortho</i> -position instead of <i>para</i> -substitution.	172
Figure 7.3. The Gibbs products of hydroxyquinone after 5 minute reaction (a1 and a2) and 30 minute reaction (b1 and b2). Only <i>ortho</i> -substituted product forms after 5 minutes and both <i>ortho</i> - and <i>para</i> -substituted products form in longer reaction time.	173
Figure 7.4. The Gibbs products of <i>p</i> -ethylphenol after 5 minute reaction (a1 and a2) and 30 minute reaction (b1 and b2). Only <i>ortho</i> -substituted product forms after 5 minutes and both <i>ortho</i> - and <i>para</i> -substituted products form in longer reaction time.	174
Figure 7.5. The Gibbs products of <i>p</i> -phenoxyphenol after 5 minute reaction. (a) is the Full MS of the reaction solution and (b) is the deconvoluted MS. 4-phenoxyphenol gives <i>ortho</i> -substituted indophenol at <i>m/z</i> 266 and <i>para</i> -substituted indophenol at <i>m/z</i> of 358.....	175
Figure 7.6. The Gibbs products of 4-fluorophenol after 5 minutes reaction. (a) is the Full MS of the reaction solution and (b) is the deconvoluted MS. 4-fluorophenol gives both substituted product, indophenol, at <i>m/z</i> 266 and an adduct at <i>m/z</i> 376.	176

Figure 7.7. The Gibbs products of 4-chlorophenol after 5 minutes reaction. (a) is the Full MS and (b) is the deconvoluted MS. 4-chlorophenol gives both substituted product, indophenol, at m/z 266 and an adduct at m/z 392.....	177
Figure 7.8. The Gibbs products of 4-bromophenol after 5 minutes reaction. (a) is the Full MS and (b) is the deconvoluted MS. 4-bromophenol gives both substituted product, indophenol, at m/z 266 and an adduct at m/z 436.....	178
Figure 7.9. The Gibbs products of 4-methoxyphenol after 5 minutes reaction. (a) is the Full MS and (b) is the deconvoluted MS. 4-methoxyphenol gives both substituted product, indophenol, at m/z 266 and an adduct at m/z 388.	178
Figure 7.10. The Gibbs products of 4-ethoxyphenol after 5 minutes reaction. (a) is the Full MS and (b) is the deconvoluted MS. 4-ethoxyphenol gives both substituted product, indophenol, at m/z 266 and an adduct at m/z 402.	179
Figure 7.11. The Gibbs products of 4- <i>n</i> -propoxyphenol after 5 minutes reaction. (a) is the Full MS and (b) is the deconvoluted MS. 4- <i>n</i> -propoxyphenol gives both substituted product, indophenol, at m/z 266 and an adduct at m/z 416.	179
Figure 7.12. The Gibbs products of 4- <i>n</i> -butoxyphenol after 5 minutes reaction. (a) is the Full MS and (b) is the deconvoluted MS. 4- <i>n</i> -butoxyphenol gives both substituted product, indophenol, at m/z 266 and an adduct at m/z 430.	180
Figure 7.13. Solution of pure indophenol (m/z 266) and pure condensation product (m/z 376) in ethyl acetate. Indophenol gives brown colored solution, whereas condensation product gives orange colored solution in ethyl acetate.	182
Figure 7.14. The Gibbs products of 4-fluorophenol after separation of the second product. (a) is the Full MS of the reaction solution and (b) is the deconvoluted MS.....	182
Figure 7.15. Crystal structure of indophenol	183
Figure 8.1. Dipeptide formed by phenylalanine with sulfonated tag and proline (Phe*-Pro). (a) dipeptide having 'Boc' as protecting group (Phe*(Boc)-ProOH), whereas (b) is after deprotected (Phe*-ProOH).	193
Figure 8.2. Dipeptide formed by proline and phenylalanine with sulfonated tag (Pro-Phe*). (a) dipeptide having 'Boc' as protecting group (Pro(Boc)-Phe*), whereas (b) is after deprotected (Pro-Phe*).....	194
Figure 8.3. MS/MS mass spectra for Full MS of the reaction mixtures of (a) Phe*-Pro dipeptide and (b) Pro-Phe*	195
Figure 8.4. Proposed mechanism for formation of common structure from ProPhe*OH and Phe*ProOH. Both of the dipeptides rearranged to a common structure before fragmentation. ..	196
Figure 8.5. a) CID of Phe*ProOCH ₃ and b) ProPhe*OCH ₃ with 35% energy. Formation of methyl esters block the rearrangement of the dipeptides.....	197

Figure 8.6. CID of b_2 ions from dipeptides methyl ester. (a) is MS^3 spectra of Phe*ProOCH₃ and (b) is MS^3 spectra of ProPhe*OCH₃. The different isomers give different products in MS^3 , which reveals that the isomers fragment without going through a common structure.198

Figure 8.7. CID spectra of authentic structures of m/z 323 ions derived from the dipeptide (a) diketopiperazine is from Phe*Pro and (b) oxazolone is from Pro-Phe*199

Figure 8.8. MS/MS spectra of deuterated a) Phe*ProOH and b) ProPhe*OH. The removal of D₂O (formation of m/z 323, M – D₂O) and DOH (formation of m/z 324, M – DOH) depict that there are two different options for transferring protons.201

Figure 8.9. Proton transfer mechanism for the b_2 ion formation from ProPhe*OH202

Figure 8.10. Lowest energy structures of possible b_2 ion structures.204

ABSTRACT

Phenols are ubiquitous in our surroundings including biological molecules such as L-Dopa metabolites, food components, such as whiskey and liquid smoke, etc. This dissertation describes a new method for detecting phenols, by reaction with Gibbs reagent to form indophenols, followed by mass spectrometric detection. Unlike the standard Gibbs reaction which uses a colorimetric approach, the use of mass spectrometry allows for simultaneous detection of differently substituted phenols. The procedure is demonstrated to work for a large variety of phenols without *para*-substitution. With *para*-substituted phenols, Gibbs products are still often observed, but the specific product depends on the substituent. For *para* groups with high electronegativity, such as methoxy or halogens, the reaction proceeds by displacement of the substituent. For groups with lower electronegativity, such as amino or alkyl groups, Gibbs products are observed that retain the substituent, indicating that the reaction occurs at the *ortho* or *meta* position. In mixtures of phenols, the relative intensities of the Gibbs products are proportional to the relative concentrations, and concentrations as low as 1 $\mu\text{mol/L}$ can be detected. The method is applied to the qualitative analysis of commercial liquid smoke, and it is found that hickory and mesquite flavors have significantly different phenolic composition.

In the course of this study, we used this technique to quantify major phenol derivatives in commercial products such as liquid smoke (catechol, guaiacol and syringol) and whiskey (*o*-cresol, guaiacol and syringol) as the phenol derivatives are a significant part of the aroma of foodstuffs and alcoholic beverages. For instance, phenolic compounds are partly responsible for the taste, aroma and the smokiness in Liquid Smokes and Scotch whiskies.

In the analysis of Liquid Smokes, we have carried out an analysis of phenols in commercial liquid smoke by using the reaction with Gibbs reagent followed by analysis using electrospray ionization mass spectrometry (ESI-MS). This analysis technique allows us to avoid any separation and/or solvent extraction steps before MS analysis. With this analysis, we are able to determine and compare the phenolic compositions of hickory, mesquite, pecan and apple wood flavors of liquid smoke.

In the analysis of phenols in whiskey, we describe the detection of the Gibbs products from the phenols in four different commercial Scotch whiskies by using simple ESI-MS. In addition, by addition of an internal standard, 5,6,7,8-tetrahydro-1-naphthol (THN), concentrations of the major phenols in the whiskies are readily obtained. With this analysis we are able to determine and compare the composition of phenols in them and their contribution in the taste, smokey, and aroma to the whiskies.

Another important class of phenols are found in biological samples, such as L-Dopa and its metabolites, which are neurotransmitters and play important roles in living systems. In this work, we describe the detection of Gibbs products formed from these neurotransmitters after reaction with Gibbs reagent and analysis by using simple ESI-MS. This technique would be an alternative method for the detection and simultaneous quantification of these neurotransmitters.

Finally, in the course of this work, we found that the positive Gibbs tests are obtained for a wide range of *para*-substituted phenols, and that, in most cases, substitution occurs by displacement of the *para*-substituent. In addition, there is generally an additional unique second-phenol-addition product, which conveniently can be used from an analytical perspective to distinguish *para*-substituted phenols from the unsubstituted versions. In addition to using the

methodology for phenol analysis, we are examining the mechanism of indophenol formation, particularly with the *para*-substituted phenols.

The importance of peptides to the scientific world is enormous and, therefore, their structures, properties, and reactivity are exceptionally well-characterized by mass spectrometry and electrospray ionization. In the dipeptide work, we have used mass spectrometry to examine the dissociation of dipeptides of phenylalanine (Phe), containing sulfonated tag as a charge carrier (Phe*), proline (Pro) to investigate their gas phase dissociation. The presence of sulfonated tag (SO_3^-) on the Phe amino acid serves as the charge carrier such that the dipeptide backbone has a canonical structure and is not protonated. Phe-Pro dipeptide and their derivatives were synthesized and analyzed by LCQ-Deca mass spectroscopy to get the fragmentation mechanism. To confirm that fragmentation path, we also synthesized dikitopeparazines and oxazolines from all combinations of the dipeptides. All these analyses were confirmed by isotopic labeling experiments and determination and optimization of structures were carried out using theoretical calculation. We have found that the fragmentation of Phe*Pro and ProPhe* dipeptides form sequence specific b_2 ions. In addition, not only is the ‘mobile proton’ involved in the dissociation process, but also is the ‘backbone hydrogen’ is involved in forming b_2 ions.

CHAPTER 1. PHENOLS AND GUIDE TO DISSERTATION

1.1 Phenol

Phenols (sometimes called phenolics) are a class of chemical compounds consisting of a hydroxyl group (-OH) bonded directly to a phenyl group. These compounds are found in fruits, vegetables, nuts, plant-derived beverages such as tea and wine, traditional Eastern medicines, and a plethora of herbal dietary supplements.¹ Dietary phenols have been consumed by humans since the beginning of human history. So far, more than 8000 different naturally occurring phenols have been listed, and this list is still growing.¹⁻³ These phenols can be classified into several groups – simple phenols, quinones, naphthoquinones, anthraquinones, xanthenes, coumarins (including furanocoumarins and chromones), flavonoids, tannins, and lignin and lignans.⁴ These compounds have been produced by plants as secondary metabolites in diverse processes, such as growth, lignification, pigmentation, pollination, and resistance against pathogens, predators, and environmental stresses.⁴⁻⁶ Over the centuries, these compounds have been known as plant pigments and are present within a variety of foods that come from plants. Thus, these compounds are present in many foods. In North America, people consume around one gram of phenols daily.⁷

1.2 History and uses of phenols

Phenols have been used as deodorants, antiseptics, disinfectants, preservatives, and as constituents of aromatic vapors from the earliest antiquity because of their pleasant odor and their ability to counteract malodor. During the eighteenth century, phenol and other volatile alkyl phenols become available due to coal carbonization, and people started using these compounds as deodorants because of their pleasant smells.⁸ On the other hand, the nonvolatile residue, coal tar, from carbonization was used as a substitute for wood tar, especially in the ship-building industry.⁹

Although phenols and similar compounds have always been used, phenol was first isolated by a German chemist Runge from coal tar in 1834, and its structure was proved by Laurant in 1842.⁹ Around twenty years later, Küchenmeister used pure phenol as a dressing for wounds, and coal tar was being used as antiseptic and disinfectant as early as 1815.^{8,9} At that time, pharmacists and surgeons used these compounds as a disinfectant,^{10,11} although it was found later that some of these compounds are corrosive and escharotic on open wounds. At this time, a variety of phenol homologues came when the procedure for distillation and separation of natural products was improving, and their uses were explored by chemists, pharmacists, and surgeons. Some of them are still used today. For instance, the creosote (mixture of cresols, xylenols, and ethylphenol)/soap complex has been used as a disinfectant since 1877.⁹ Later, antibacterial properties of individual phenolic compounds and their derivatives were examined. For instance, cresols (1886), β -naphthol and polyhalogenated phenols (1906), alkylrecorcinol or alkyl *m*-dihydroxy benzenes (1921), other alkyl phenols (1930), polyhydroxyphenols (1932), and dimethylphenols (1933) were found to have more active bactericides and/or more disinfectant than phenol.⁹ In addition, since introduced, chlorocresols (1933), chloroxylenol (1927) in castor oil soap solution have been used as a commercial disinfectant, and methylphenols (1929) have been used as preservatives.^{12,13} Similar to alkylphenol, arylphenols are also being used in variety of applications. For instance, 2-, 4-phenylphenols used as a pain reducers and halogenated dihydroxydiphenylmethanes are being used as antiseptics in soaps and dusting powers.⁹ An analogue of these compound, 2,2'-dihydroxy-5,5'-dichlorodephenyl-sulphide, is being used as an antifungal agent both in medicine and in the textile industry.⁹ On the other hand, nitrated phenols (2,4-dinitrophenol, 2,4-dinitro-*o*-cresol) are also widely used for the treatment of obesity or agaricide and ovicide. Complex formulation of higher phenols is used as black and white fluids. Over time, the use of phenols has grown and

currently phenols are not only being used in household products, but also in industry for making plastics, explosives, drugs, etc.

1.3 Toxic effects of phenolic compounds

Though phenolic compounds have been used for hundreds of years, they have a significant number of toxic effects on humans. The human body can easily absorb most of the phenolic compounds through the skin and in the gastrointestinal tract. Once in the system, they are transformed into various reactive intermediate through metabolic processes. These intermediates interact with proteins to exert toxic effects. Most toxic phenols are chlorophenols, aminophenols, chlorocatechols, nitrophenols, methylphenols.^{14, 15} Apart from these compounds, bisphenol A and some alkylphenols can alter mammary glands which may cause of endocrine disruption in humans.^{16, 17} Consumption of high concentrations of phenols may cause a number of problems including in the gastrointestinal tract; muscle tremor with difficulty in walking; blisters and burns on the skin; heart, kidneys, and liver damage.^{18, 19} As phenols are readily oxidized to form radicals, some proteins can be arylated and/or destroyed, and transportation of electrons in energy transducing membranes can be disrupted.¹⁴ DNA can also be damaged by phenolic compound in the presence of metal ion.²⁰ Burning in the mouth and throat, necrotic lesions in the mouth, stomach and oesophagus, abnormal temperature and pulse fluctuation, weak muscles and convulsion may be due to chlorophenol poisoning.²¹ Poisoning of chlorophenols may result damage to the liver, kidneys, lungs, skin and digestive tract.²² Chromosomes can be damaged by hydroquinone. *p*-Cresol and 2,4-dimethylphenol are potentially carcinogenic.²³

1.4 The identification and measurements of phenolics

There is a wide variety of studies about the improvement of new techniques for quantification of phenols.²⁴ Although, high-performance liquid chromatography (HPLC) and gas chromatography (GC) coupled with or without mass spectrometry (MS) are the most commonly used techniques to analyze them, the classical spectrophotometric assay is still used, even though its results are inadequate.²⁵ A few of the currently used techniques are discussed below.

1.4.1 Determination of phenolic compounds using classical colorimetric methods

Among the classical techniques, one widely-used method is spectrophotometry UV/Vis for the analysis of total phenolic content.²⁶ In this method, phenolic compounds are reduced chemically in an alkaline medium to form a blue solution, which can be quantified by visible-light spectrophotometry at a range of 520 to 770 nm.^{26, 27} Although this technique is easy to perform, cost effective, rapid and widely used, it is not accurate. Moreover, the reagents used in this method react not only with the targeted phenols but also with any reducing substance in the system like ascorbic acid, pigments, aromatic amines, sugars, with some nitrogen-containing compounds such as hydroxylamine and guanidine, thiols, many vitamins and some inorganic ions.²⁸⁻³⁰ Thus, this technique is used to get an idea about the total reduction capacity and not for a specific quantification of phenolic derivatives. However, it is still considered a useful method for the rapid and prior screening of numerous samples for the total phenol content.^{25, 31}

1.4.2 Determination of total content of flavonoids and anthocyanins

Aluminum chloride is usually used to determine total content of flavonoids and flavones. The formation of an aluminum-flavonoid complex having an absorptivity maximum at 510 nm is the basis of this technique. Total flavonoid content is measured by comparing with a calibration

curve which is done by using rutin (quercetin-3-O-rutinoside) or quercetin (5,7,3',4'-flavon-3-ol.) as an internal standard.³²⁻³⁴

The most common method for anthocyanins analysis is a pH differential.^{24, 35} This analysis is based on the formation of a bright red color of the flavilium cation in acidic solutions, which becomes a colorless carbonol when the pH increases. Anthocyanin solution with a pH = 1 and pH = 4.5 have absorptions of 510 and 700 nm, respectively, and these absorptions are proportional to the quantity of anthocyanins.

1.4.3 Determination of condensed tannins

Among the all reported methods, the acid-butanol assay and vanilline assay are the most commonly used for the quantification of proanthocyanidins (condensed tannins). In the first method, acid is used for the oxidative-depolymerization of condensed tannins to yield red anthocyanidins. Proanthocyanidins depolymerize to colored anthocyanidins when treated with mineral acid. The products of this process have an absorption maximum around 550 nm.³⁶⁻³⁹ Although this method is simple and gives good indication of the presence of condensed tannins, the color-intensity can be effected by the acid-butanol ratio, the presence of water in the sample, and the chemical characteristics of the analytes.^{40, 41} Another issue of this method is the choice of standard due to the heterogenicity of the condensed tannins. This issue is partially overcome by using the plant materials under study as an internal standard.⁴²⁻⁴⁴

Another method involves the reaction of vanillin (4-hydroxy-3-methoxybenzaldehyde) with the *meta*-substituted ring of flavonols to yield a red adduct. Although this method has been used for quantifying condensed tannins for a long time, the reaction is not specific for tannins, and any appropriately substituted flavonol can react in this assay. Moreover, catechin is using as the internal standard, which has different reaction rate that could lead to wrong results.^{40, 44-47}

1.4.4 Determination of total phenolic content

The Folin Ciocalteu reagent is used to determine the total phenolic content of plant extracts. In this technique, phenolic ion is oxidized and coupled with reduced phosphotungstic-phosphomolybdic reagent to give blue chromophore followed by an absorption maxima measurement at 750 nm. A calibration curve is used to express the total phenolic content. Although this assay is popular due to the simplicity, rapidity and little interferences by nonphenolic compounds, the accuracy depends on the temperature, pH, and order in which the reagents are added.^{24, 45, 48, 49}

1.4.5 Chromatography

Due to their structural diversity, phenolic compounds vary significantly in their physiochemical properties; thus, it is a great challenge to separate and quantify them.³¹ While developing a generalized protocol for analysis of all kinds of phenols is almost impossible, there are some advanced analytical techniques to analyze them. Examples include the development of new technology and software for more efficient separation, identification and, quantification. The main idea behind these techniques is when any mixture passes through two phases, a mobile phase (gas or liquid) and a stationary phase (solid, liquid or gel), the components are separated based on their interaction with phases. This technique is used for the qualitative and quantitative analysis of a mixture. There are many different choices available for the two phases.²⁵

The first of this class is gas chromatography (GC). GC uses vaporization temperature to separate each component from a solution when the sample is passing through a heated column. In this process, the compound is separated between an inert gas (helium, nitrogen, etc.) and a nonvolatile liquid coated on an inert support inside the column.⁵⁰ Each molecule has a specific affinity to the stationary phase, and that determines the retention time (RT) of that analyte in the

column. Each compound has a specific RT in a specific system. When the compounds of a solution traveling through the column have nearly the same rate, they will elute within a narrow time band according to their retention time. Thus, according to their retention time, the components of a solution will be separated physically for presentation to a detector and analyzer. Although GC has many advantages, the analysis of phenolic compounds is relatively restricted due to their lack of volatility³¹ Therefore, in order to analyze phenols, it is necessary to improve their vaporization capacity by replacing the hydroxyl groups of phenols by other nonpolar chemical groups like trimethylsilyl before analysis.⁵¹⁻⁵³ Hence the gas chromatographic analysis of phenolic compounds are limited; however, the use of mass spectrometry (MS) with GC can improve the detection stage.^{31, 54}

Another common example of this type of technique for phenolic analysis is high-performance liquid chromatography (HPLC) due to its high selectivity, sensitivity, resolution, precision, and sample preparation.^{25, 55-57} Polarity, solubility, and size properties of each compound is the basis of compound separation by using this technique. In addition, combination of a photodiode-array detector with HPLC (HPLC-DAD) provides extensive information about structures of phenols.⁵⁸ The most common practice to get the identity of the compounds using this method is to compare the retention time (RT) with the standards.⁵⁹ In addition, for quantitative determination a series of standards is analyzed to get a calibration curve for the range of interest for each compound and compare with the unknown sample.⁶⁰ However, HPLC analysis of phenols is limited due to the lack of standards for some classes of phenols like flavonoid, glycosides, and proanthocyanides. Hydrolyzation of these types of compounds to aglycones prior to analysis is a common practice.³¹ Another limitation of HPLC is the detection and quantification limit of phenols in a crude mixture because UV- based detection and retention time of standards can lead

to a wrong identification of the phenols.³¹ In this context, mass spectrometry (MS) coupled with HPLC is considered the better characterization technique.

Another two techniques for the analysis of phenols are ion exchange chromatography (IEC) and affinity chromatography (AC). An IEC separation is done when charged molecules bind with the binding site of the stationary phase, whereas in AC the analyte is modified by attaching another compound with a specific affinity. The first method is mainly used for purification of biological materials, and the latter one is used for advanced processes of purification because of the requirement of the analyte to be inert and easily modifiable.

1.4.6 Mass Spectrometry

Mass spectrometry (MS) is a widely used method of identifying phenols due to its ability to eliminate some of the ambiguity associated with the previously discussed methods. The high sensitivity and ability of using chromatography (GC/MS, LC/MS) makes it the most appropriate physicochemical method for the analysis of phenols in a matrix. Addition of chromatography with MS allows the selective molecular detection of phenols. The molecular ion and characteristic fragmentation ions are used to identify the desired components of a sample. This can be done with or without a standard.⁶⁰⁻⁶³

The difference in the mass-to-charge ratio (m/z) of ionized molecules is used by MS to distinguish between ions.⁵² The commonly used ionization sources to analyze phenolic compounds are electron impact (EI), chemical ionization (CI), fast atom bombardment (FAB), atmospheric pressure ionization (API includes atmospheric pressure chemical ionization (APCI) and atmospheric pressure photo-ionization (APPI)), electrospray ionization (ESI), and matrix-assisted laser desorption ionization (MALDI).⁵¹⁻⁵³ Among these, EI and CI are relatively harsh techniques involving volatilization of the sample to gas phase. Soft ionization techniques (FBA, MALDI for

ionization without evaporation in high vacuum, or ESI, APCI for atmospheric ionization) are used for the thermally labile compounds to avoid decomposition at higher temperature.^{24, 45, 64, 65} Among these, ESI and APCI are the most widely used ionization methods for characterization of phenolic compounds as they can produce stable ions in both negative and positive ion modes with low spontaneous fragmentation.⁵⁶ For ionizing polar and nonvolatile molecules, tannins and anthocyanidins, ESI is used, whereas APCI is suitable for less polar and nonionic compounds – flavonols, flavones, flavanones, and chalcones.^{51, 63, 66} Finally, MALDI is used for the analysis of phenols of higher molecular weight and complex matrices. In addition, the use of tandem mass spectrometry may help improve sensitivity and selectivity.^{66, 67} MS/MS and MS³ give more fragmentation of the precursors and daughter ions, thus providing more structural information for the identification of phenols in a mixture.³¹

1.4.7 NMR Spectroscopy

Nuclear magnetic resonance (NMR) spectroscopy is the most promising spectroscopic technique for the analysis of a complex matrix. Fast (less than 5 minutes for one-dimensional ¹H and ¹³C-NMR), simple sample preparation, measurement procedures, instrumental stability, and easy spectra interpretation procedure are the advantages of this technique. Moreover, coupling of LC with NMR can provide valuable structural information in the analysis of mixed samples. This technique can be used for a proper identification of compounds which are indistinguishable using other methods.⁶⁸ Nevertheless, the disadvantages of NMR spectroscopy are low sensitivity compared with MS and chromatographic techniques, high cost of the NMR spectrometers. Additionally, the sensitivity for direct measurement in the LC-NMR mode is not sufficient due to the low natural abundance of the ¹³C isotope (1.1%).^{64, 69, 70}

1.5 Proposed techniques and guide to dissertation

Mass spectroscopy (MS) has been used as an important quantitative tool to measure the mass-to-charge (m/z) ratio of ions for many years, and its use is still growing. For more than a decade, our group has used MS to analyze small molecules in the gas phase as well as in a matrix. All the experimental results in this thesis were obtained from two commercial MS – Thermo Finnigan LCQ-Deca Ion Trap Mass Spectrometer and Waters micromass ultima triple quadrupole mass spectrometer. Detail instrumental conditions are explaining in Chapter 3 to Chapter 8. chapter 2 discusses the history of identification of phenols and the development of the Gibbs reaction. It is also discussing the development of the mechanism of this reaction. In addition, this chapter also has the detection techniques of the Gibbs product formed by phenolic compounds.

Chapter 3 discusses the detection of Gibbs products by using simple electrospray-ionization mass spectrometry (ESI-MS). We found that indophenols are naturally anionic, thus, they are readily detected by ESI-MS. Another important advantage of using mass spectrometry for the detection of indophenols is that it readily distinguishes between different types of substituted phenols. In that chapter, we are reporting ESI mass spectra for indophenols obtained in the Gibbs reaction of simple substituted phenols and show its application for simultaneous detection of components in a mixture, including quantification. This approach using the Gibbs reagent to form indophenols provides an alternative to previously reported derivatization methods, such as acetylation or conversion to the imidazolium ether. In the following chapter, the analysis of phenols in commercial liquid smoke by using Gibb's reaction followed by electrospray ionization mass spectrometry (ESI-MS) detection is discussed. In this chapter, we quantify the three major phenols by using an internal standard. Finally, those three different phenols are analyzed in four different commercial liquid smokes and are compared to their taste according to the presence of those three compounds. In chapter 5, we analyze the major phenols in four different scotch

whiskies using Gibbs reaction. The reaction products are analyzed by ESI-MS and the quantity of phenol is measured by using calibration curves. The smokiness of the analyzed scotch whiskeys is correlated with the presence of the three major phenols. In the course of this study, we are discussing the analysis of L-Dopa and metabolite neurotransmitters after a reaction with the Gibbs reagent followed by simple electrospray-ionization mass spectrometry (ESI-MS). In addition, L-Dopa is converted to its methyl ester before reacting with the Gibbs reagent as it does not react with Gibbs reagent on its own.

There is a debate about the product of the *para*-substituted phenols with the Gibbs reagent. However, we are showing using ESI-MS that there are four different types of reactions showing *para*-substituted phenols. One type of phenol reacts by substituting at the *para*-position, whereas another group gives not only this product but also an additional product. A third group of phenols gives this reaction by substituting at the *ortho*-position. Finally, there is another group of phenols who do not undergo this reaction. This observation is discussed in chapter 7.

Finally, chapter 8 is discusses the use of mass spectrometry to examine the fragmentation of dipeptides that include *para*-sulfonated phenyl alanine (PheSO₃⁻ or Phe*) connected with proline (Pro) to form Phe*ProOH and ProPhe*OH dipeptides. These dipeptides are similar to Phe*GlyOH and GlyPhe*OH with respect to carrying charges such that the dipeptide backbone has a canonical structure and is not protonated.

1.6 References

1. Kyselova, Z., Toxicological aspects of the use of phenolic compounds in disease prevention. *Interdisciplinary toxicology* **2011**, 4 (4), 173-183.
2. Middleton, E.; Kandaswami, C.; Harborne, J., The flavonoids: advances in research since 1986. *Chapman & Hall/CRC, New York* **1993**.

3. Bravo, L., Polyphenols: chemistry, dietary sources, metabolism, and nutritional significance. *Nutrition reviews* **1998**, *56* (11), 317-333.
4. Aldred, E. M., *Pharmacology E-Book: A Handbook for Complementary Healthcare Professionals*. Elsevier Health Sciences: 2008.
5. Duthie, G. G.; Gardner, P. T.; Kyle, J. A., Plant polyphenols: are they the new magic bullet? *Proceedings of the Nutrition Society* **2003**, *62* (3), 599-603.
6. Fraga, C. G.; Galleano, M.; Verstraeten, S. V.; Oteiza, P. I., Basic biochemical mechanisms behind the health benefits of polyphenols. *Molecular aspects of medicine* **2010**, *31* (6), 435-445.
7. Formica, J.; Regelson, W., Review of the biology of quercetin and related bioflavonoids. *Food and chemical toxicology* **1995**, *33* (12), 1061-1080.
8. Kuchenmeister, F., Ueber Desinfectionsmittel im Allgemeinen, das Spirol und seine therapeutische Verwendung im Bsondern. *Deutsche Klinik am Eingange des zwanzigsten Jahrhunderts* **1860**, *12*, 123-4.
9. Hugo, W., Phenols: a review of their history and development as antimicrobial agents. *Microbios* **1978**, *23* (92), 83-85.
10. Lister, J., On the antiseptic principle in the practice of surgery. *British medical journal* **1867**, *2* (351), 246.
11. Miles, A., Lister's contributions to microbiology. *British Journal of Surgery* **1967**, *54* (13), 415-418.
12. Larson, E.; Talbot, G. H., An approach for selection of health care personnel handwashing agents. *Infection Control & Hospital Epidemiology* **1986**, *7* (8), 419-424.
13. Organization, W. H., WHO Model List of Essential Medicines-19th List. April 2015-Amended November 2015. Available at: who.int/medicines/publications/essentialmedicines/en/. Accessed November **2016**, *2*.
14. Schweigert, N.; Zehnder, A. J.; Eggen, R. I., Chemical properties of catechols and their molecular modes of toxic action in cells, from microorganisms to mammals: minireview. *Environmental microbiology* **2001**, *3* (2), 81-91.
15. Schweigert, N.; Hunziker, R. W.; Escher, B. I.; Eggen, R. I., Acute toxicity of (chloro-) catechols and (chloro-) catechol-copper combinations in Escherichia coli corresponds to their membrane toxicity in vitro. *Environmental Toxicology and Chemistry: An International Journal* **2001**, *20* (2), 239-247.
16. Muñoz-de-Toro, M.; Markey, C. M.; Wadia, P. R.; Luque, E. H.; Rubin, B. S.; Sonnenschein, C.; Soto, A. M., Perinatal exposure to bisphenol-A alters peripubertal mammary gland development in mice. *Endocrinology* **2005**, *146* (9), 4138-4147.

17. Vom Saal, F. S.; Hughes, C., An extensive new literature concerning low-dose effects of bisphenol A shows the need for a new risk assessment. *Environmental health perspectives* **2005**, *113* (8), 926-933.
18. Services, U. D. o. H. a. H., Agency for Toxic Substances and Disease Registry: Toxicological profile for Lead (update) PB/99/166704. *Atlanta: US Department of Health and Human Services* **1999**.
19. Anku, W. W.; Mamo, M. A.; Govender, P. P., Phenolic compounds in water: sources, reactivity, toxicity and treatment methods. *Phenolic compounds-natural sources. Importance and Applications, First Ed. InTech* **2017**, 419-443.
20. Li, Y.; Trush, M. A., Reactive oxygen-dependent DNA damage resulting from the oxidation of phenolic compounds by a copper-redox cycle mechanism. *Cancer Research* **1994**, *54* (7 Supplement), 1895s-1898s.
21. Gosselin, R. E.; Smith, R. P.; Hodge, H. C., *Clinical toxicology of commercial products*. Williams & Wilkins: 1984.
22. Schweigert, N.; Belkin, S.; Leong-Morgenthaler, P.; Zehnder, A. J.; Eggen, R. I., Combinations of chlorocatechols and heavy metals cause DNA degradation in vitro but must not result in increased mutation rates in vivo. *Environmental and molecular mutagenesis* **1999**, *33* (3), 202-210.
23. Zhang, L.; Wang, Y.; Shang, N.; Smith, M. T., Benzene metabolites induce the loss and long arm deletion of chromosomes 5 and 7 in human lymphocytes. *Leukemia research* **1998**, *22* (2), 105-113.
24. Ignat, I.; Volf, I.; Popa, V. I., A critical review of methods for characterisation of polyphenolic compounds in fruits and vegetables. *Food chemistry* **2011**, *126* (4), 1821-1835.
25. Aires, A., Phenolics in foods: Extraction, analysis and measurements. *Phenolic Compounds* **2017**, 61-88.
26. Singleton, V. L.; Rossi, J. A., Colorimetry of total phenolics with phosphomolybdic-phosphotungstic acid reagents. *American journal of Enology and Viticulture* **1965**, *16* (3), 144-158.
27. Brooker, L.; Sprague, R., Color and constitution. IV. 1 The Absorption of phenol blue. *Journal of the American Chemical Society* **1941**, *63* (11), 3214-3215.
28. Blainski, A.; Lopes, G.; de Mello, J., Application and analysis of the folin ciocalteu method for the determination of the total phenolic content from *Limonium brasiliense* L. *Molecules* **2013**, *18* (6), 6852-6865.

29. Ikawa, M.; Schaper, T. D.; Dollard, C. A.; Sasner, J. J., Utilization of Folin– Ciocalteu phenol reagent for the detection of certain nitrogen compounds. *Journal of agricultural and food chemistry* **2003**, *51* (7), 1811-1815.
30. Everette, J. D.; Bryant, Q. M.; Green, A. M.; Abbey, Y. A.; Wangila, G. W.; Walker, R. B., Thorough study of reactivity of various compound classes toward the Folin– Ciocalteu reagent. *Journal of agricultural and food chemistry* **2010**, *58* (14), 8139-8144.
31. Ignat, I.; Volf, I.; Popa, V. I., Analytical methods of phenolic compounds. *Natural Products: Phytochemistry, Botany and Metabolism of Alkaloids, Phenolics and Terpenes* **2013**, 2061-2092.
32. Makris, D. P.; Boskou, G.; Chiou, A.; Andrikopoulos, N. K., An investigation on factors affecting recovery of antioxidant phenolics and anthocyanins from red grape (*Vitis vinifera* L.) pomace employing water/ethanol-based solutions. *Am. J. Food Technol* **2008**, *3* (3), 164-173.
33. Škerget, M.; Kotnik, P.; Hadolin, M.; Hraš, A. R.; Simonič, M.; Knez, Ž., Phenols, proanthocyanidins, flavones and flavonols in some plant materials and their antioxidant activities. *Food chemistry* **2005**, *89* (2), 191-198.
34. de Rijke, E.; Out, P.; Niessen, W. M.; Ariese, F.; Gooijer, C.; Udo, A. T., Analytical separation and detection methods for flavonoids. *Journal of chromatography A* **2006**, *1112* (1-2), 31-63.
35. Balasundram, N.; Sundram, K.; Samman, S., Phenolic compounds in plants and agri-industrial by-products: Antioxidant activity, occurrence, and potential uses. *Food chemistry* **2006**, *99* (1), 191-203.
36. Gessner, M. O.; Steiner, D., Acid butanol assay for proanthocyanidins (condensed tannins). In *Methods to study litter decomposition*, Springer: 2005; pp 107-114.
37. Tuominen, A., Tannins and other polyphenols in *Geranium sylvaticum*: Identification, intraplant distribution and biological activity. **2017**.
38. Mavlyanov S M, I. S. Y., Kamaev F G, Abdullaev U A, Karimdzhall O V A K, Ismailov A I, Tannins of *Geranium sanguineum*. *Chem Nat Compd* **1997**, *33*, 179 - 184.
39. Yu, Z.; Dahlgren, R., Evaluation of methods for measuring polyphenols in conifer foliage. *Journal of Chemical Ecology* **2000**, *26* (9), 2119-2140.
40. Hagerman, A. E., Tannin Handbook. Miami University. *Oxford, OH, Available online at www.users.muohio.edu/hagermae/473* **2002**, 474, 475-476.
41. Hagerman, A. E.; Rice, M. E.; Ritchard, N. T., Mechanisms of protein precipitation for two tannins, pentagalloyl glucose and epicatechin16 (4→ 8) catechin (procyanidin). *Journal of Agricultural and Food Chemistry* **1998**, *46* (7), 2590-2595.

42. Schofield, P.; Mbugua, D.; Pell, A., Analysis of condensed tannins: a review. *Animal feed science and technology* **2001**, *91* (1-2), 21-40.
43. Luque-Rodríguez, J. M.; Pérez-Juan, P.; Luque De Castro, M. D., Extraction of polyphenols from vine shoots of *Vitis vinifera* by superheated ethanol– water mixtures. *Journal of agricultural and food chemistry* **2006**, *54* (23), 8775-8781.
44. Waterman, P.; Mole, S., *Analysis of Phenolic Plant Metabolites* Blackwell. London: 1994.
45. Bravo, L.; Mateos, R., Analysis of flavonoids in functional foods and nutraceuticals. In *Methods of analysis for functional foods and nutraceuticals*, CRC Press Boca Raton, FL: 2008; pp 148-206.
46. Mitsunaga, T.; Doi, T.; Kondo, Y.; Abe, I., Color development of proanthocyanidins in vanillin-hydrochloric acid reaction. *Journal of wood science* **1998**, *44* (2), 125-130.
47. Kelm, M. A.; Hammerstone, J. F.; Schmitz, H. H., Identification and quantitation of flavanols and proanthocyanidins in foods: How good are the datas? *Clinical and Developmental Immunology* **2005**, *12* (1), 35-41.
48. Makris, D. P.; Boskou, G.; Andrikopoulos, N. K., Recovery of antioxidant phenolics from white vinification solid by-products employing water/ethanol mixtures. *Bioresource technology* **2007**, *98* (15), 2963-2967.
49. Ciocalteu, V.; Folin, O., On tyrosine and tryptophane determination in proteins. *J. biol. Chem* **1927**, *73*, 627.
50. Volf, I.; Mamaliga, I.; Popa, V. I., Active principia with antioxidant character from vegetal by-products. II. Equilibrium study of the polyphenolic compounds extraction from wood of *Vitis* sp. *Cellulose chemistry and technology* **2006**, *40* (3-4), 211-215.
51. Maul, R.; Schebb, N. H.; Kulling, S. E., Application of LC and GC hyphenated with mass spectrometry as tool for characterization of unknown derivatives of isoflavonoids. *Analytical and bioanalytical chemistry* **2008**, *391* (1), 239-250.
52. Li, F.; Liu, Q.; Cai, W.; Shao, X., Analysis of scopoletin and caffeic acid in tobacco by GC–MS after a rapid derivatization procedure. *Chromatographia* **2009**, *69* (7-8), 743-748.
53. Fiamegos, Y. C.; Nanos, C. G.; Vervoort, J.; Stalikas, C. D., Analytical procedure for the in-vial derivatization—extraction of phenolic acids and flavonoids in methanolic and aqueous plant extracts followed by gas chromatography with mass-selective detection. *Journal of Chromatography A* **2004**, *1041* (1-2), 11-18.

54. Vinas, P.; Campillo, N.; Martínez-Castillo, N.; Hernández-Córdoba, M., Solid-phase microextraction on-fiber derivatization for the analysis of some polyphenols in wine and grapes using gas chromatography–mass spectrometry. *Journal of Chromatography A* **2009**, *1216* (9), 1279-1284.
55. Naczek, M.; Shahidi, F., Phenolics in cereals, fruits and vegetables: Occurrence, extraction and analysis. *Journal of pharmaceutical and biomedical analysis* **2006**, *41* (5), 1523-1542.
56. Almela, L.; Sánchez-Munoz, B.; Fernández-López, J. A.; Roca, M. J.; Rabe, V., Liquid chromatographic–mass spectrometric analysis of phenolics and free radical scavenging activity of rosemary extract from different raw material. *Journal of Chromatography A* **2006**, *1120* (1-2), 221-229.
57. García, Y. D.; Valles, B. S.; Lobo, A. P., Phenolic and antioxidant composition of by-products from the cider industry: Apple pomace. *Food Chemistry* **2009**, *117* (4), 731-738.
58. Rajaei, A.; Barzegar, M.; Mobarez, A. M.; Sahari, M. A.; Esfahani, Z. H., Antioxidant, anti-microbial and antimutagenicity activities of pistachio (*Pistachia vera*) green hull extract. *Food and Chemical Toxicology* **2010**, *48* (1), 107-112.
59. Kubola, J.; Siriamornpun, S., Phenolic contents and antioxidant activities of bitter melon (*Momordica charantia* L.) leaf, stem and fruit fraction extracts in vitro. *Food chemistry* **2008**, *110* (4), 881-890.
60. Fulcrand, H.; Mané, C.; Preys, S.; Mazerolles, G.; Bouchut, C.; Mazauric, J.-P.; Souquet, J.-M.; Meudec, E.; Li, Y.; Cole, R. B., Direct mass spectrometry approaches to characterize polyphenol composition of complex samples. *Phytochemistry* **2008**, *69* (18), 3131-3138.
61. López, M. J. O.; Innocenti, M.; Ieri, F.; Giaccherini, C.; Romani, A.; Mulinacci, N., HPLC/DAD/ESI/MS detection of lignans from Spanish and Italian *Olea europaea* L. fruits. *Journal of food composition and analysis* **2008**, *21* (1), 62-70.
62. Alonso-Salces, R. M.; Ndjoko, K.; Queiroz, E. F.; Ioset, J. R.; Hostettmann, K.; Berrueta, L. A.; Gallo, B.; Vicente, F., On-line characterisation of apple polyphenols by liquid chromatography coupled with mass spectrometry and ultraviolet absorbance detection. *Journal of Chromatography A* **2004**, *1046* (1-2), 89-100.
63. Reed, J. D.; Krueger, C. G.; Vestling, M. M., MALDI-TOF mass spectrometry of oligomeric food polyphenols. *Phytochemistry* **2005**, *66* (18), 2248-2263.
64. Tsao, R., Chemistry and biochemistry of dietary polyphenols. *Nutrients* **2010**, *2* (12), 1231-1246.
65. Escribano-Bailon, M.; Santos-Buelga, C., Methods in polyphenol analysis. *Polyphenol Extraction from Foods*. RSC, Cambridge, UK **2003**, 2-16.

66. Prodanov, M.; Garrido, I.; Vacas, V.; Lebrón-Aguilar, R.; Dueñas, M.; Gómez-Cordovés, C.; Bartolomé, B., Ultrafiltration as alternative purification procedure for the characterization of low and high molecular-mass phenolics from almond skins. *Analytica chimica acta* **2008**, *609* (2), 241-251.
67. Stobiecki, M., Application of mass spectrometry for identification and structural studies of flavonoid glycosides. *Phytochemistry* **2000**, *54* (3), 237-256.
68. Agiomyrgianaki, A.; Petrakis, P. V.; Dais, P., Detection of refined olive oil adulteration with refined hazelnut oil by employing NMR spectroscopy and multivariate statistical analysis. *Talanta* **2010**, *80* (5), 2165-2171.
69. Stobiecki, M.; Kachlicki, P., Isolation and identification of flavonoids. In *The science of flavonoids*, Springer: 2006; pp 47-69.
70. Naczek, M.; Shahidi, F., Extraction and analysis of phenolics in food. *Journal of chromatography A* **2004**, *1054* (1-2), 95-111.

CHAPTER 2. HISTORY AND MECHANISM OF THE GIBBS REACTION

2.1 Background of Gibbs reaction

One of the oldest methods for the identification of phenolic compounds is the test producing the beautiful, intense blue solution of indophenol salts.¹ Around 200 years ago, this intense blue color was obtained when cresol, resorcinol, and other phenols were analyzed in mixtures without a proper understanding of the reactions involved, or the identity of the colored compound.²⁻⁴ A few years later, the same color was found when phenols, including phenol, orcinol, and thymol reacted with nitrous acid⁵⁻⁷ and fuming sulfuric acid⁸ in the presence of ammonia, which is known as the Liebermann test for phenols.⁹ Though the Liebermann test was used for the analysis of phenols early on, the first approximation of the actual chemical formula of the colored compound was found by von Baeyer and Caro¹⁰ in 1874. These colorful compounds made useful dyes and were first commercially prepared by Koechlin and Witt in 1881.¹¹ However, the best laboratory method for the formation of indophenols is by condensation of quinonechloroimide and phenol, which was first described by Hirsch.¹² This reaction was developed as a very delicate qualitative and very accurate quantitative method for the estimation of the concentration of phenol in a solution by H. D. Gibbs in 1927.¹

Gibbs reported that the chloro- and bromo-substituted quinonechloroimides (2,6-dichloroquinone-4-chloroimide and 2,6-dibromoquinone-4-chloroimide) gave the most delicate results among the different quinonechloroimides tested. He found that the indophenols formed by using these reagents were the most stable. In addition, he was also able to quantify at least 1 part of phenol in 20,000,000 when reacted with 2,6-dibromoquinonechloroimide. However, not all phenols react with quinonechloroimides. Initially, it was believed that the 'para' position to the

hydroxyl must be unsubstituted.^{1, 13-15} Later on, when a larger number of phenols were examined, it was found that there were several phenols having ‘para’ substitutions that did form indophenol. However, several ‘para’ unsubstituted phenols did not form indophenol due to the influence of the adjacent substituted groups.¹ Gibbs and coworkers monitored these indophenol formations using a variety of phenolic compounds in a buffer solution and watching for the intense blue color to appear. Spectrophotometric determination of the maximum blue color was used to measure the quantity of indophenols (i.e., phenols) and charted of a number of absorption curves for those compounds. The absorption experiments were done by detecting between the wavelengths of 600 – 610 nm.¹ Figure 2.1 shows the Gibbs product from the reaction of 2,6-dichloroquinonechloroimide and phenol in buffer solution.. Lower concentrations are shown in the lower left and higher concentrations on the. The reaction gives a light blue color at lower concentrations, and the color gets more intense as the concentration increases. The increasing blue color with increasing phenol concentration explains why spectrophotometry is used to analyze phenols.

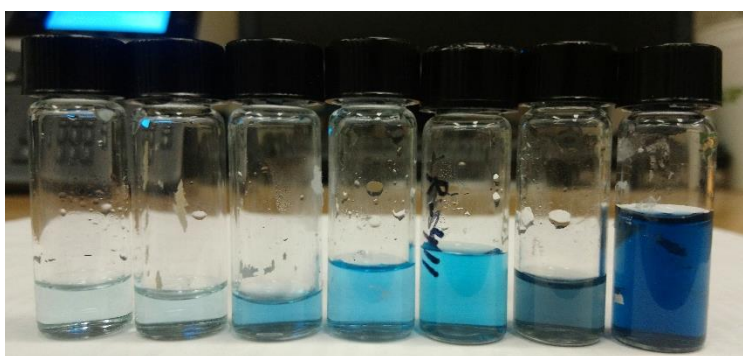
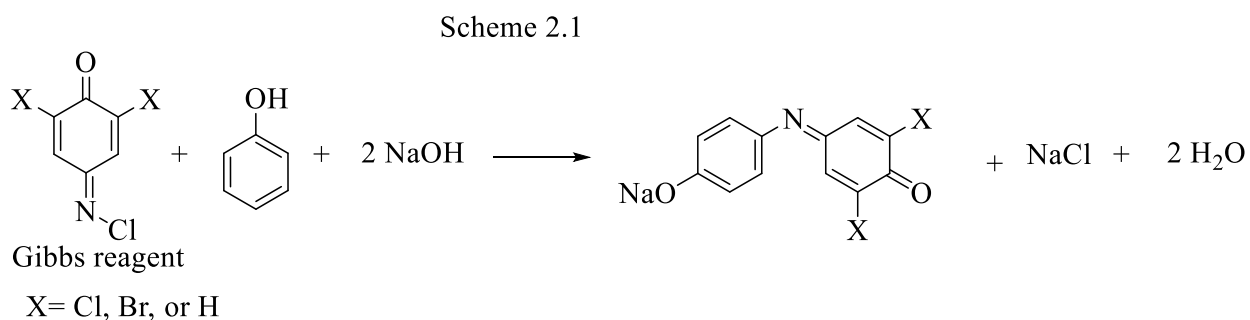


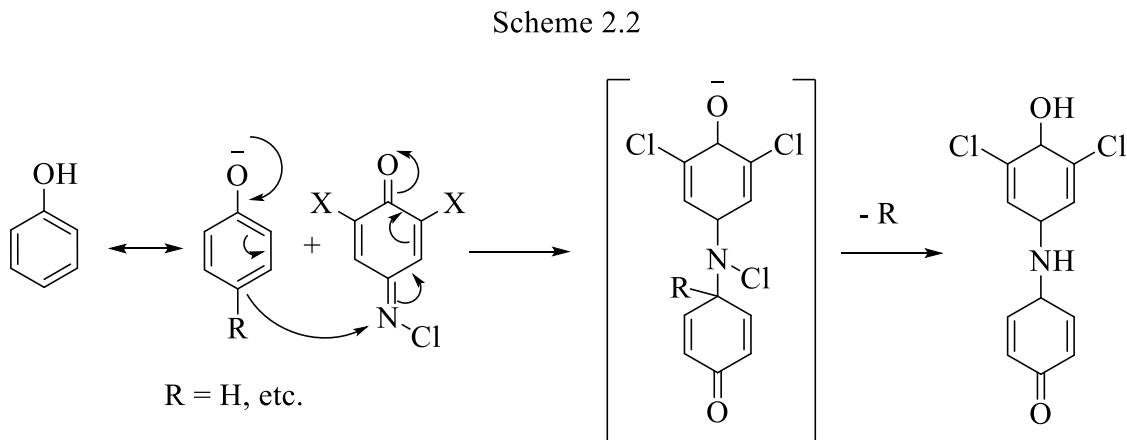
Figure 2.1. Formation of Indophenol color (blue) when phenol reacts with 2,6-dichloroquinone-4-chloroimide. The concentration of phenol increases from left to right and thus the color is changing from light blue to deep blue.

A buffer solution is essential to obtaining the best results from this reaction. A pH of 9.0 to 9.5 is typical. To obtain the best results, Palitzsch's borax buffer solution with a pH value of 9.24 has been employed. This buffer solution is prepared by following the procedure reported by Palitzsch.¹⁶ In brief, 19.108 gm of sodium borate ($\text{Na}_2\text{B}_4\text{O}_7 \cdot 10\text{H}_2\text{O}$) is dissolved in 1 liter of water to get the buffer with desired pH.¹⁶

2.2 Mechanism of the Gibbs reaction

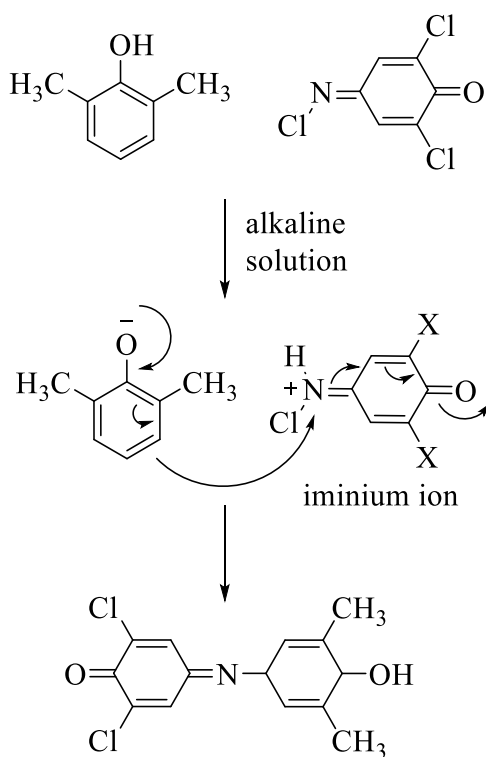


Several studies have been carried out to try establish the mechanism of the Gibbs reaction^{13, 17} since it has been introduced. Gibbs reported in his original article that equivalent amounts of unsubstituted *para* phenols reacted with 2,6-dibromobenzoquinone N-chloroimine and 2,6-dibromobenzoquinone N-chloroimine (TQI) (Scheme 2.1). Gibbs proposed a direct electrophilic substitution by TQI on the aromatic nucleus to form the indophenol (Scheme 2.2),



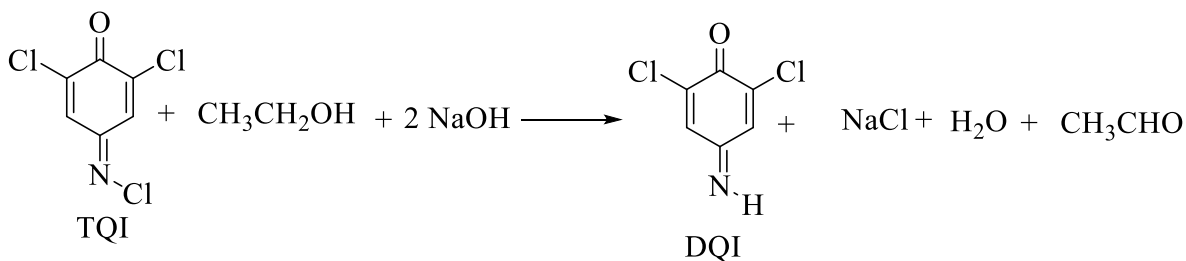
and this mechanism has been widely accepted.¹⁸⁻²⁰ However, several studies have been published proposing alternate mechanisms.²¹⁻²⁴ For instance, for the reaction with benzoquinone N-chloroimine, Ziegler and Gartler proposed an electrophilic attack by the benzoquinone iminium cation (Scheme 2.3).²⁵

Scheme 2.3

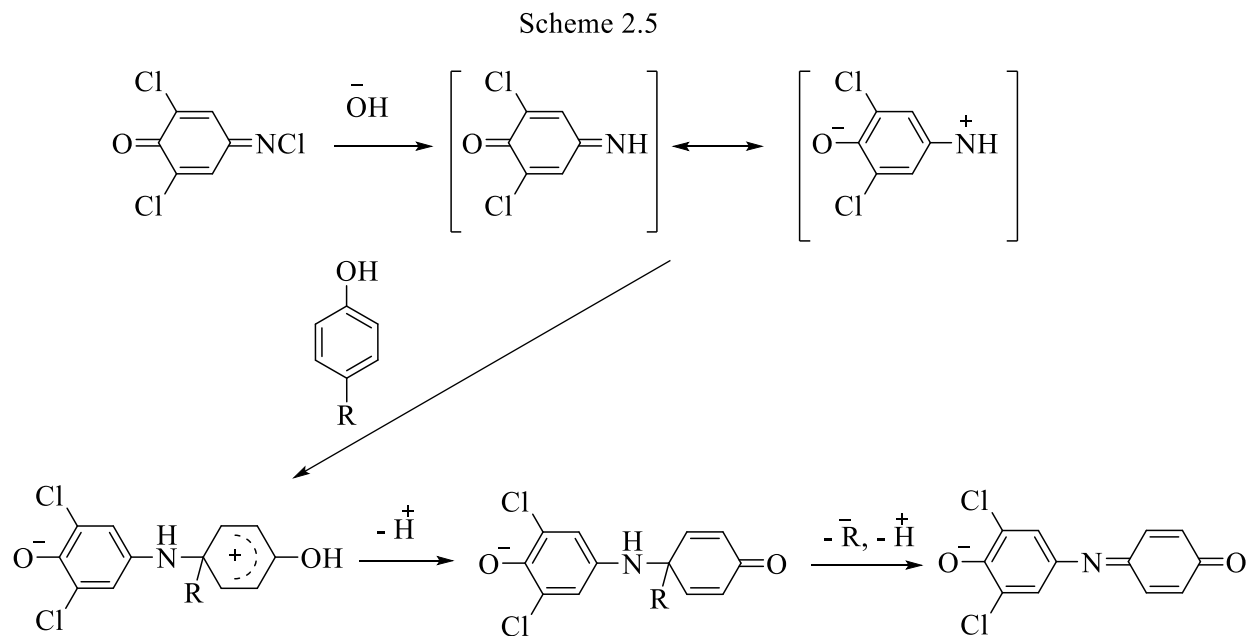


On the other hand, Svobodova and coworkers assumed that TQI was hydrolyzed to form the more reactive 2,6-dichlorobenzoquinone imine (DQI) (Scheme 2.4),²⁶ and DQI then reacts with its phenolic partner, which was studied in detail by Corbett.²⁷

Scheme 2.4



Corbett also found that one mole of phenol reacted with two moles of Gibbs reagent to give indophenol. Afterwards, Dacre examined the Gibbs reaction using a variety of *para*-substituted phenols and a spectrophotometer. He reported that the Gibbs product has a small range of absorption maxima, mostly between 580 nm to 630 nm., He concluded that the Gibbs reaction is ‘nonspecific’ for phenols.²⁸ In 1984, Josephy and Van Damme analyzed a variety of *para*-substituted phenols and reported that all of them formed indophenols by replacing the substituent at the *para*-position, which matches the way that indophenol forms from phenol itself (Scheme 2.5). They also reported that the wide range of molecular extinction coefficients (ϵ_{max}) of the Gibbs products found by Dacre was due to the varying yields of product rather than a difference in molar absorptivity.²⁹



Despite considerable efforts, none of the proposed mechanisms for indophenol formation are conclusive. Pallagi and coworkers²² disproved all of the previously proposed mechanisms for the Gibbs reaction. Depending on the *para*-substituent (R) of phenol, there are two different products – either regular indophenol (IX) where R can leave as an electrofugal leaving group (e.g., R = H, CH₂N(Me)₂, CH₂OH), or/and 4,4-disubstituted 2,5-cyclohexadien-1-one where R cannot leave as a cation (e.g., R = Me) (Figure 2.2). Additionally, when the phenol has a hydroxyl (OH) or an amino (NH₂) group at *para*-position, the phenols form the corresponding benzoquinones or benzoquinone imines, respectively, after oxidation.²² 1:1 stoichiometry was found in all of the cases, except the *para*-substituent (R = halogen, alkoxy) which can only be eliminated as a nucleofugal group. In the latter case, the reaction proceeds with a 1:2 stoichiometry to give indophenol (IX) and an oxidation product of the second mole of phenol. A second-order kinetics ($v = [\text{Gibbs reagent}] \times [\text{phenoxide}]$) was found for this reaction and the rate determining step is the single electron transfer (SET) from anion of phenol onto N-chloroimine (Gibbs reagent) to generate N-chloroimine radical anion ((III) and the neutral phenoxy radical (IV). It was found that

the initial rates depend on the reactivity of the phenol – the higher the reactivity, the greater the acceleration (pathway ‘A’ of Figure 2.2).²¹⁻²⁴ Beyond this direct combination in the solvent cage, the deviation of second-order-reaction kinetics was explained by the formation of product in a chain reaction.

The indophenol dye (IX) can be produced from N-chloroimine radical anion (III) in two different pathways – either pathway B or pathway C (Figure 2.2). In pathway B, a halogenide ion is eliminated from N-chloroimine radical anion (III) and an H-atom is abstracted from the medium to produce imine, DQI (VIII). Then, this imine (VIII) reacts with phenoxide (II) to give final product, indophenol (IX).^{21, 22} The other pathway (C) starts a radical chain reaction. At the beginning of this chain reaction, a halogen of III is displaced by phenoxide (II) in a bimolecular nucleophilic substitution to give the adduct radical (VI). An electron is transferred from N-chloroimine (I) to the newly formed VI to yield an adduct (VII) and a radical anion (III), which can enter the cycle again when substituted with another phenoxide (II). Finally, the adduct VII can easily be deprotonated to form indophenol (IX).²² This mechanism is more preferable. During the chain propagation step, the chain carrier reacts with the nucleophile in a bimolecular fashion, which is the rate determining step. This mechanism is termed $S_{RN}2$.²²

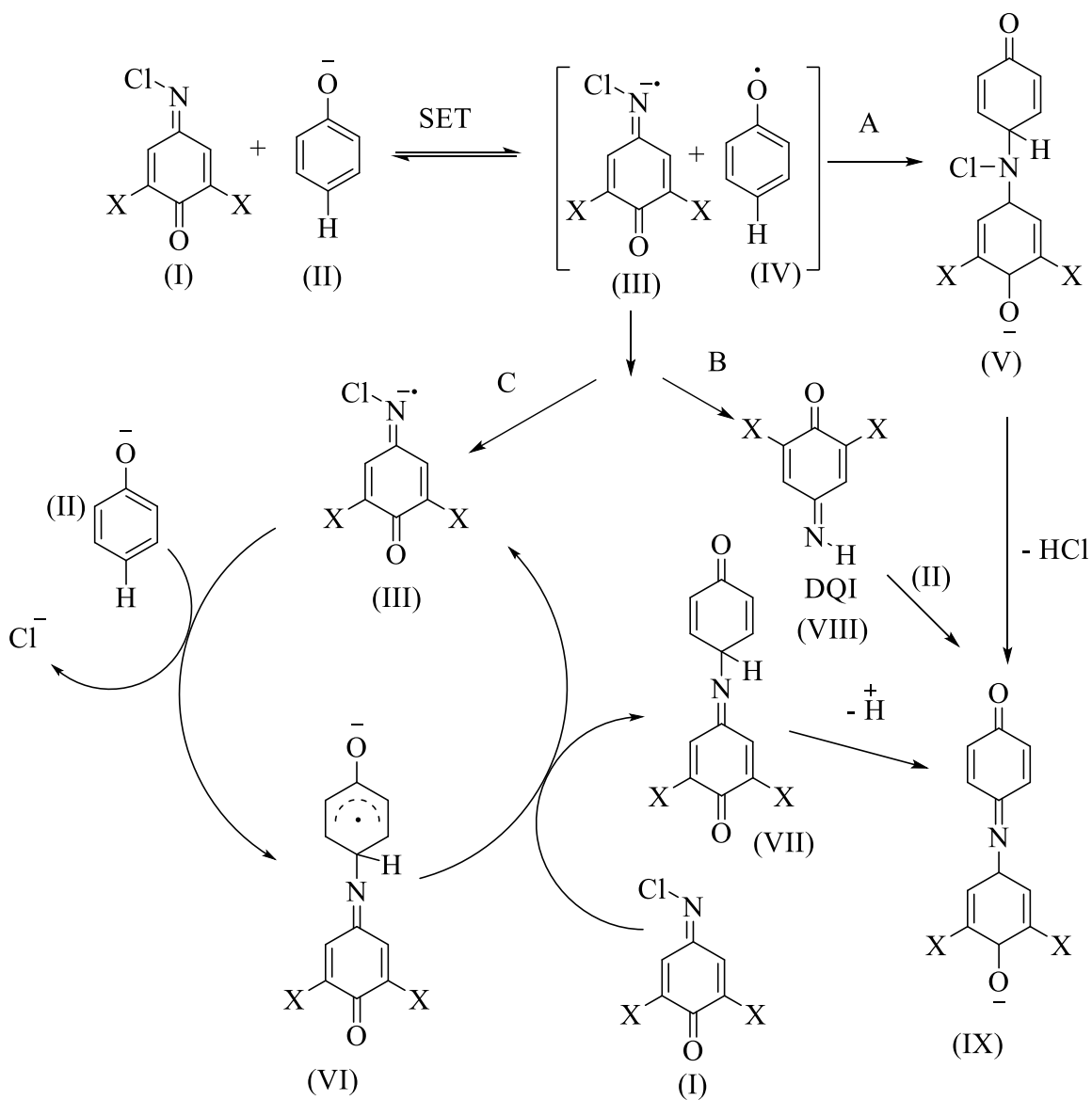


Figure 2.2. Mechanism of formation of indophenol by 2,6-Dichloroquinone-4-chloroimide when reacts with phenols. Path A is the direct combination reaction, Path B is chloride ion elimination and H-atom abstraction from the medium, and Path C is the chain reaction for the formation of indophenol.²²

2.3 Examples of Gibbs reaction

Since introduced, 2,6-dibromo-or 2,6-dichloroquinone-4-chloroimide (Gibbs' reagent) has been used widely in organic analytical chemistry for the detection of phenol analogues in reaction mixtures, biological, commercial matrixes, and in industrial waste. A few examples are shown in the following table.

Table 2.1. Examples of the applications of the Gibbs Reactions

Type of matrix	Analytes	Detection technique	References	Reported Year
Vegetation	Capsaicinoids in chili peppers	Colorimetric	Thompson, R. Q., et al. ³⁰	2012
Phenol in polluted air	Phenols	HPLC	Kuwata, K. et al. ³¹	1950
Water analysis	Phenolic contents	Spectrophotometry	Thoss, V. et al. ³²	2002
Treated wood	permethrin	Spectrophotometry	Arip, M. N. M, et al. ¹⁹	2013
Rice	Aflatoxines	spectrophotometry	Quintana, M. G., et al. ²⁰	1997
<i>Populus trichocarpa</i> Synthesis	3- <i>o</i> -Methyltransferases	Colorimetric	Bhuiya, M, et al. ¹⁸	2009
	-	Chromatography	Kang, D., et al. ³³	2016
Antioxidant BHA	Butylated hydroxyanisole (3- <i>tert</i> -butyl-4-hydroxyanisole)	spectrophotometer	Josephy, P.D., et al. ³⁴	1984
Detection	Aromatic amine (1°, 2° and 3°), carbazoles, aliphatic amines (1°, 2°), enol (2,4-pentanedione)	Thin layer chromatography (TLC)	Ross, J.H. ³⁵	1968
Synthesis of β -galactosidase substrate	7- β -D-galactopyranosyloxy-9,9-dimethyl-9H-acridin-2-one	NMR	Corey, P. F. et al. ³⁶	1991
Pharmaceutical formulations	Propranolol	Diffuse reflectance spectroscopy	Gotardo, M. A., et al. ³⁷	2008

Table 2.1 continued

Biological fluids in pregnant women	Propofol	GC and colorimetry	Ragno, G., et al. ³⁸	1997
In pharmaceutical preparation	Thymol	Colorimetry	Al-Neaimy, U. I. S. ³⁹	2009
Chili peppers	Capsaicinoids	Colorimetry	Ryu, W., et al. ⁴⁰	2017
Tablets	Levodopa	Spectrophotometry	Yi-ping, L.I.S.Y., et al. ⁴¹	2006
Pharmaceutical products	Bisoprolol	Spectrophotometry	Tuljarani, G., et al. ⁴²	2010

2.4 Conclusion

Although the Gibbs reaction was introduced a long time ago, the mechanism was unknown for a long time. There are two different types of reactions that have been accepted – direct combination, and chain reaction. Finally, the reaction has been used for detection of phenolic compounds in variety of matrixes.

2.5 References

1. Gibbs, H. D., Phenol tests III. The indophenol test. *Journal of biological chemistry* **1927**, 72 (2), 649-664.
2. Robiquet, H., Neue Beobachtungen über das Orein. *Annalen der Pharmacie*: 1835; Vol. 15, pp 289-300.
3. J Dumas, On the orcinol. *Chem Zentralbl* **1838**, 9, 690-692.
4. Kane, R., Beiträge zur chemischen Geschichte der Orseille und des Lacmus. *Justus Liebigs Annalen der Chemie* **1841**, 39 (1), 25-76.
5. Lex, R., Ueber einige neue Reactionen des Phenols. *Fresenius' Journal of Analytical Chemistry* **1871**, 10 (1), 101-102.
6. Weselsky, P., Neue Derivate des Resorcins. *Berichte der deutschen chemischen Gesellschaft* **1871**, 4 (1), 32-33.
7. Weselsky, P., Ueber die Azoverbindungen des Resorcins. *Justus Liebigs Annalen der Chemie* **1872**, 162 (2-3), 273-292.
8. Kopp, E., Über Brasilin. *Ber Chem. Ges.* **1873**, vi, 446.
9. Liebermann, C., Ueber die Einwirkung der salpetrigen Säure auf Phenole. *Berichte der deutschen chemischen Gesellschaft* **1874**, 7 (1), 247-250.
10. Baeyer, A.; Caro, H., Ueber die Einwirkung der salpetrigen Säure auf Dimethylanilin und über Nitrosophenol. *Berichte der deutschen chemischen Gesellschaft* **1874**, 7 (2), 963-968.
11. Koechlin, H., Witt, O. M., *Sur une nouvelle classe de matieres colorantes*, *Mon. SC* **1881**.
12. Hirsch, A., Ueber das Chinonchlorimid und ähnliche Substanzen. *Berichte der deutschen chemischen Gesellschaft* **1880**, 13 (2), 1903-1911.

13. Gibbs, H. D., Phenol Tests. I. A Classification of the Tests and a Review of the Literature. *Chemical Reviews* **1926**, *3* (3), 291-319.
14. Gibbs, H. D., Para-Cresol. A new method of separating paracresol from its isomers and a study of the boiling point. *Journal of the American Chemical Society* **1927**, *49* (3), 839-844.
15. Gibbs, H. D., Phenol tests II. Nitrous acid tests. The Millon and similar tests. Spectrophotometric investigations. *Journal of Biological Chemistry* **1927**, *71* (2), 445-459.
16. Palitzsch, S., Sur l'emploi de solution de borax et d'acide borique dans la détermination colorimétrique de la concentration en ions hydrogène de l'eau de mer. *Compt. rend. Lab. Carlsberg* **1916**, *11*.
17. Gibbs, H. D., Phenol Tests. IV. A Study of the Velocity of Indophenol Formation 2, 6-Dibromobenzenoneindophenol. *The Journal of Physical Chemistry* **1927**, *31* (7), 1053-1081.
18. Bhuiya, M.-W.; Liu, C.-J., A cost-effective colorimetric assay for phenolic O-methyltransferases and characterization of caffeate 3-O-methyltransferases from *Populus trichocarpa*. *Analytical biochemistry* **2009**, *384* (1), 151-158.
19. Arip, M. N. M.; Heng, L. Y.; Ahmad, M.; Hasbullah, S. A., Reaction of 2, 6-dichloroquinone-4-chloroimide (Gibbs reagent) with permethrin—an optical sensor for rapid detection of permethrin in treated wood. *Chemistry Central Journal* **2013**, *7* (1), 122.
20. Quintana, M.; Didion, C.; Dalton, H., Colorimetric method for a rapid detection of oxygenated aromatic biotransformation products. *Biotechnology techniques* **1997**, *11* (8), 585-587.
21. Pallagi, I.; Dvortsák, P., Gibbs reaction. Part 1. Reduction of benzoquinone N-chloroimines to benzoquinone imines. *Journal of the Chemical Society, Perkin Transactions 2* **1986**, (1), 105-110.
22. Pallagi, I.; Toró, A.; Horváth, G., Mechanism of the Gibbs reaction. Part 4.1 Indophenol formation via N-chlorobenzoquinone imine radical anions. The Aza-SRN2 chain reaction mechanism. Chain initiation with 1, 4-benzoquinones and cyanide ion. *The Journal of organic chemistry* **1999**, *64* (18), 6530-6540.
23. Pallagi, I.; Toro, A.; Farkas, O., Mechanism of the Gibbs Reaction. 3. Indophenol Formation via Radical Electrophilic Aromatic Substitution (SREAr) on Phenols. *The Journal of Organic Chemistry* **1994**, *59* (22), 6543-6557.

24. Pallagi, I.; Toró, A.; Müller, J., The mechanism of the gibbs reaction. Part 2: The ortho \rightleftharpoons ortho 2, 4-cyclohexadiene-1-one rearrangement of the reaction product of 2, 6-di-tert-butyl-4-chlorophenol and 2, 6-dichlorobenzoquinone N-chloroimine. *Tetrahedron* **1994**, *50* (29), 8809-8814.
25. Ziegler, E.; Gartler, K., Über Indophenole. *Monatshefte für Chemie/Chemical Monthly* **1948**, *79* (6), 637-638.
26. Svobodová, D.; Křenek, P.; Fraenkl, M.; Gasparič, J., Colour reaction of phenols with the gibbs reagent. The reaction mechanism and decomposition and stabilisation of the reagent. *Microchimica Acta* **1977**, *67* (3-4), 251-264.
27. Corbett, J. F., Benzoquinone imines. Part VIII. Mechanism and kinetics of the reaction of p-benzoquinone monoimines with monohydric phenols. *Journal of the Chemical Society B: Physical Organic* **1970**, 1502-1509.
28. Dacre, J. C., Nonspecificity of the Gibbs reaction. *Analytical Chemistry* **1971**, *43* (4), 589-591.
29. Josephy, P. D.; Van Damme, A., Reaction of Gibbs reagent with para-substituted phenols. *Analytical chemistry* **1984**, *56* (4), 813-814.
30. Thompson, R. Q.; Chu, C.; Gent, R.; Gould, A. P.; Rios, L.; Vertigan, T. M., Visualizing capsaicinoids: colorimetric analysis of chili peppers. *Journal of Chemical Education* **2012**, *89* (5), 610-612.
31. Kuwata, K.; Uebori, M.; Yamazaki, Y., Determination of phenol in polluted air as p-nitrobenzeneazophenol derivative by reversed phase high performance liquid chromatography. *Analytical Chemistry* **1980**, *52* (6), 857-860.
32. Thoss, V.; Baird, M. S.; Lock, M. A.; Courty, P. V., Quantifying the phenolic content of freshwaters using simple assays with different underlying reaction mechanisms. *Journal of Environmental Monitoring* **2002**, *4* (2), 270-275.
33. Kang, D.; Ricci, F.; White, R. J.; Plaxco, K. W., Survey of redox-active moieties for application in multiplexed electrochemical biosensors. *Analytical chemistry* **2016**, *88* (21), 10452-10458.
34. Josephy, P. D.; Lenkinski, R. E., Reaction of Gibbs reagent (2, 6-dichlorobenzoquinone 4-chloroimine) with the antioxidant BHA (3-tert.-butyl 4-hydroxyanisole): isolation and identification of the major product. *Journal of Chromatography A* **1984**, *294*, 375-379.
35. Ross, J. H., 2, 6-Dichloroquinone 4-chloroimide as a reagent for amines and aromatic hydrocarbons on thin-layer chromatograms. *Analytical Chemistry* **1968**, *40* (14), 2138-2143.

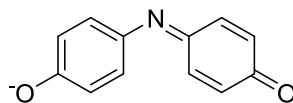
36. Corey, P. F.; Trimmer, R. W.; Biddlecom, W. G., A New Chromogenic β -Galactosidase Substrate: 7- β -D-Galactopyranosyloxy-9, 9-dimethyl-9H-acridin-2-one. *Angewandte Chemie International Edition in English* **1991**, *30* (12), 1646-1648.
37. Gotardo, M. A.; Tognolli, J. O.; Pezza, H. R.; Pezza, L., Detection of propranolol in pharmaceutical formulations by diffuse reflectance spectroscopy. *Spectrochimica Acta Part A: Molecular and Biomolecular Spectroscopy* **2008**, *69* (4), 1103-1109.
38. Ragno, G.; Cicinelli, E.; Schonauer, S.; Vetuschi, C., Propofol assay in biological fluids in pregnant women. *Journal of pharmaceutical and biomedical analysis* **1997**, *15* (11), 1633-1640.
39. Al-Neaimy, U. I., Spectrophotometric determination of thymol in pharmaceuticals with Gibb's reagent. *JOURNAL OF EDUCATION AND SCIENCE* **2009**, *22* (39), 17-26.
40. Ryu, W.-K.; Kim, H.-W.; Kim, G.-D.; Rhee, H.-I., Rapid determination of capsaicinoids by colorimetric method. *journal of food and drug analysis* **2017**, *25* (4), 798-803.
41. Yi-ping, L. S.-y. Y.; Yan-fang, C., Spectrophotometry determination of levodopa in tablets based on charge transfer complex of levodopa with 2, 6-dichloroquinone-4-chloroimide [J]. *Chinese Journal of Pharmaceutical Analysis* **2006**, *10*.
42. Tuljarani, G.; Sankar, D. G.; Kadgapathi, P.; Suthakaran, R.; Satyanarayana, B., Quantitative determination of bisoprolol fumarate in bulk and pharmaceutical dosage forms by spectrophotometry. *International Journal Of Chemical Sciences* **2010**, *8* (4), 2253-2258.

CHAPTER 3. MASS SPECTROMETRIC DETECTION OF THE GIBBS REACTION FOR PHENOL ANALYSIS

3.1 Introduction

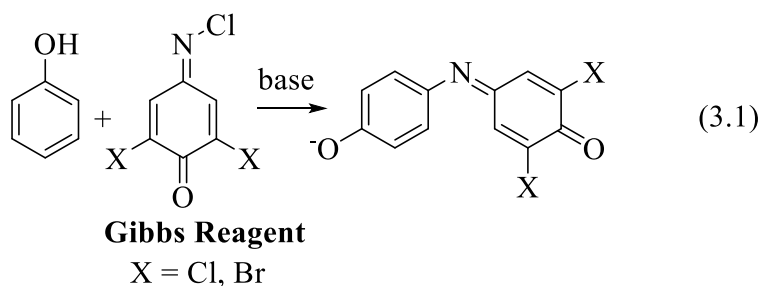
Phenols are ubiquitous in our world, and are found in all types of natural and non-natural systems. Examples of phenolic compounds that occur naturally include biological molecules, such as tyrosine and L-dopa, food components, such as capsaicin or red wine tannins, and even drugs, such as morphine and tetrahydrocannabinol. Alternatively, phenols are present due to anthropogenic sources. In particular, industrial waste can have phenol concentrations as high as 10 g/L.¹ Many methods have been used to detect phenols,² mostly relying on some sort of chromatography (LC or GC) prior to detection. Mass spectrometric detection has an advantage in that it can be used to carry out simultaneous detection of multiple phenol derivatives without requiring prior separation. However, although it is possible to detect phenols directly by using mass spectrometry, it is not specific to phenol detection. Consequently, a common approach used for the specific detection of phenols involves the use of reagents to selectively derivatize the phenols prior to detection to make them more amenable for analysis by chromatography,³⁻¹⁰ or for direct detection by mass spectrometry.^{11, 12}

In this work, we describe an approach for the analysis of phenols by using mass spectrometric detection of indophenol derivatives. The conversion of phenols to indophenols can be traced back almost 200 years, to the detection of orcinol.^{13, 14} For example, Liebermann¹⁵⁻¹⁷ showed that phenols, including phenol, orcinol and thymol, can be transformed into dark-blue-colored indophenol dyes by reaction with sulfuric acid and ammonia.



Indophenol

In 1927, Gibbs reported a convenient reagent for the detection of phenols^{18, 19} by converting them to indophenols. The Gibbs reaction (eq 3.1), utilizing the Gibbs reagent, 2,6-dichloro- or dibromo-4-(chloroimino)cyclohexa-2,5-dien-1-one, has since been a standard approach for the detection of phenols.^{20, 21}



One of the key features that makes the Gibbs procedure a useful approach for the detection of phenols is the robust color of the indophenol product,²² which allows for easy spectrophotometric detection. In recent years, applications of the Gibbs procedure have been reported for the detection of phenol-based pharmaceuticals,²³⁻³⁴ capsaicin,³⁵⁻³⁷ and for monitoring the presence of phenol.³⁸ In all of these applications, the indophenol is detected spectrophotometrically.

One of the limitations of the Gibbs approach for detection of phenols is that the absorption peak is not very sensitive to substitution of the phenol. Consequently, while the standard Gibbs method is useful for determining total phenol content,^{37, 39} it is generally not capable of distinguishing between individual substituted phenols. Therefore, a separation step is required for the detection of specific phenol derivatives. It is possible to detect the Gibbs indophenol product with other, non-colorimetric methods. For example, Lowe et al.⁴⁰ have examined and detected

the Gibbs reaction using electrochemistry and cyclic voltammetry, and have shown that it can be used to detect THC. Similarly, Josephy and Lenkinski⁴¹ have characterized the Gibbs product formed from *tert*-butylhydroxyanisole (BHA) by using electron ionization mass spectrometry, and electron-ionization spectra for some protonated indophenols (neutral phenols) are generally available.⁴²

Herein we describe the detection of Gibbs products by using simple electrospray-ionization mass spectrometry (ESI-MS). Considering that indophenols are naturally anionic, they are readily detected by ESI-MS. An important advantage of using mass spectrometry for the detection of indophenols is that it readily distinguishes between different types of substituted phenols. In this work, we report ESI mass spectra for indophenols obtained in the Gibbs reaction of simple substituted phenols, and show its application for simultaneous detection of components in a mixture, including quantification. This approach using the Gibbs reagent to form indophenols provides an alternative to previously reported derivatization methods, such as acetylation¹¹ or conversion to the imidazolium ether.¹²

3.2 Experimental

3.2.1 Sample preparation – general procedures

Samples were prepared by mixing 5 mL of a solution of Gibbs reagent in methanol (60 mmol/L) with 10 mL of an aqueous potassium phosphate dibasic solution (deionized water, 40 mmol/L, pH 9.5)⁴³ containing substrate. After mixing, the solutions were stirred at room temperature for the allotted time, after which 50 μ L of the solution was diluted to 4 mL in water-methanol solution (1:1), for ESI-MS analysis. Solutions for individual samples contained 0.25 mmol of substrate in the phosphate buffer, similar to the concentration of Gibbs reagent. Spectra are measured 5 minutes after mixing, unless otherwise noted.

For the mixture of phenol and *o*-cresol, 10 mL of the initial solution containing *o*-cresol and phenol were mixed with 5 mL methanol solution of Gibbs reagent (100 mmol/L). The reaction mixture was stirred for 5 minutes and 30 minutes before diluting with 1:1 methanol as described above, followed by mass spectrometric analysis. The concentration of *o*-cresol in the initial solution was chosen so to obtain a concentration of 3 $\mu\text{mol/L}$ in the final (electrosprayed) solution. Similarly, the concentration of phenol in the initial solution was chosen so to obtain concentrations of 1, 2, 5, 10, 25 and 50 $\mu\text{mol/L}$ in the final solution, with an excess of Gibbs reagent.

3.2.2 Sample preparation – liquid smoke

K_2HPO_4 (1 mmol, 174 mg) was added directly to 5 mL of the corresponding commercial smoke sample directly and mixed with 10 mL methanol solution of Gibbs reagent (1 mmol, 210 mg). The reaction mixture was stirred at room temperature for 5 minutes. 200 μL reaction mixture was dissolved in 4 mL water-methanol (1:1) solution for MS analysis.

3.2.3 Spectra collection

Electrospray ionization mass spectra was obtained on a commercial LCQ-DECA (Thermo Electron Corporation, San Jose, CA, USA) quadrupole ion trap mass spectrometer, equipped with electrospray ionization (ESI) source, operating in negative ion mode. Substrate solutions in a methanol:water mixture (1:1) and introduced into the source directly at a flow rate of 10 $\mu\text{L}/\text{min}$. Electrospray and ion focusing conditions were varied so that maximize the signal of the ion of interest.

3.2.4 Spectral analysis

One important advantage of using the Gibbs reagent for derivatization is that the chlorine atoms make products containing the Gibbs reagent readily detectable by the isotopic pattern. Therefore, the spectra are deconvoluted using the isotope pattern for ions containing two chlorine atoms (1:0.648:0.105) to eliminate the peaks that cannot contain the Gibbs reagent. In the deconvolution, the maximum intensity of the peak at mass M is set to be the minimum of the intensity at mass M , $I(M+2)/0.648$, or $I(M+4)/0.105$. Although this deconvolution approach does not identify peaks that must contain two chlorine atoms, as coincidental peak ratios are possible, it can be used to explicitly rule out all the signals that cannot have two chlorine atoms. For example, if the signal at mass M is 100 000, but the signal at $M + 2$ is only 100, then the signal M that contains two chlorines (and therefore could be a Gibbs product) is only 952. Technically, the intensities of the peaks remaining after deconvolution are upper limits to the signal for two-chlorine containing products, as coincidental peak ratios can result in false positives. The difference between the peak height and the Gibbs-product signal is largest when there is extensive overlap of product signals. However, the ability to specifically eliminate non-Gibbs products where possible makes the Gibbs approach preferable to simple ESI-MS of the mixture. The deconvolution is carried out using Excel.

3.2.5 Materials

All the phenols used in this work were obtained from commercial sources, and used as received. The methanol was “Reagent Grade” and used without further purification.

3.3 Results

3.3.1 Phenol

Figure 3.1 shows the ESI-MS obtained for samples of Gibbs reagent (Figure 3.1a) and phenol (Figure 3.1b). In the absence of phenol, the MS of the Gibbs reagent is non-descript, and shows a large number of unidentifiable ionic products. It is possible to detect phenoxide (m/z 93) directly under these conditions (Figure 3.1b). However, in the presence of other acidic substrates, the phenoxide product would be expected to be a minor product. Figure 3.1c shows the spectrum obtained 5 minutes after mixing Gibbs reagent and phenol in the buffer solution. The spectrum is dominated by the Gibbs indophenol product, as indicated by the characteristic isotopic pattern. Moreover, despite having phenol at the same concentration as in Figure 3.1b, the absolute intensity increases by a factor of about 100 for the detection of the Gibbs product, not taking into account the fact that signal is distributed over multiple isotope peaks. Therefore, the total signal of the phenol derivative in Figure 3.1c is nearly 200 times greater than that of phenol in Figure 3.1b (the peak below m/z 100 in Figure 1c is m/z 96, and not phenoxide, m/z 93). It has been shown previously that the detection sensitivity of phenols in mass spectrometry can be increased by derivatization, such as acetylation, before detection.¹¹ Finally, Figure 3.1d shows the spectrum obtained after deconvolution, to account for the isotope peaks. Although the initial spectrum was originally very clean, the deconvoluted spectrum is even moreso, with more than 85% of the signal attributable to indophenol.

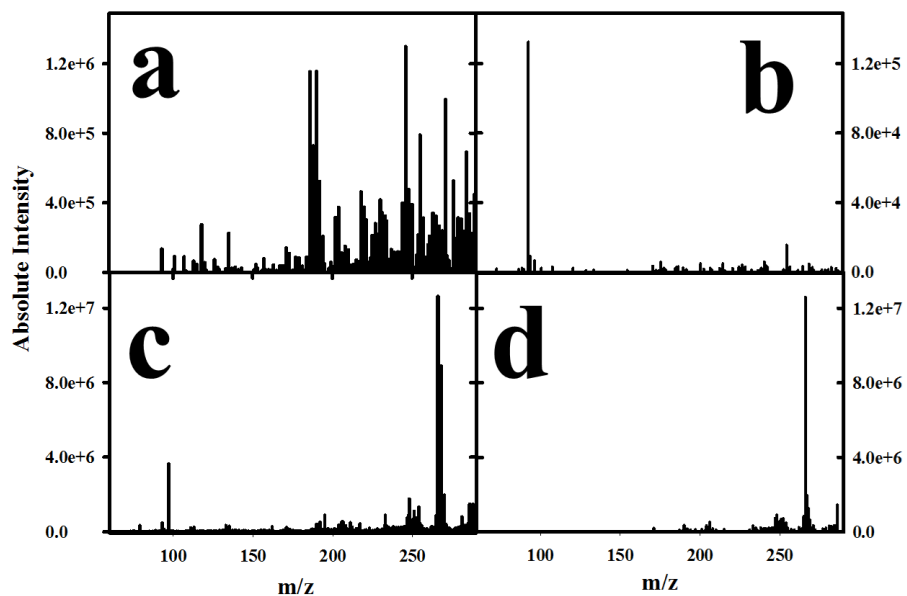


Figure 3.1. ESI mass spectra of products of phenol reaction with the Gibbs reagent. a) Gibbs reagent alone in buffer; b) phenol alone in buffer; c) phenol and Gibbs reagent mixture in buffer, 5 minutes after mixing; d) mixture mass spectrum deconvoluted for the 2-chlorine isotope pattern.

3.3.2 Substituted phenols

Gibbs products are also readily detected by ESI-MS for other substituted phenols, included *o*- and *m*-cresol (**3.1o** and **3.1m**), *o*- and *m*-hydroxyanisole (**2o** and **2m**), catechol (**3o**), resorcinol (**3m**), 2-aminophenol (**4**), 1-naphthol (**5**) and tetrahydro-1-naphthol (**6**) (see Supporting Information).

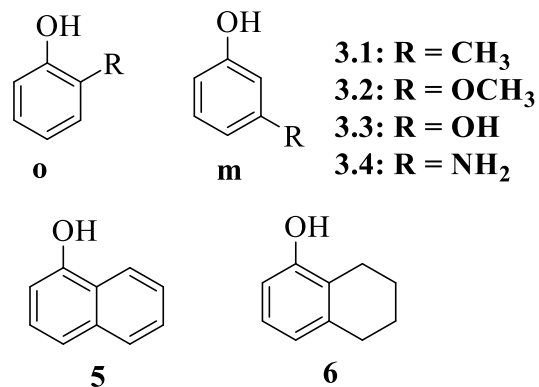


Figure 3.2. Structures of phenolic derivatives with *ortho*- and *meta*-substituted and bicyclic phenols

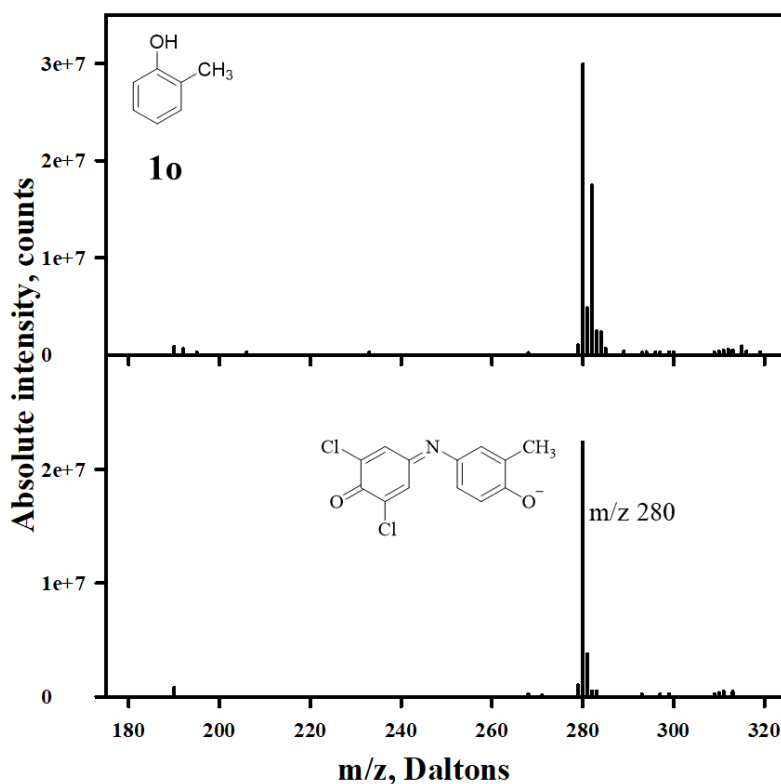


Figure 3.3. ESI mass spectra of products of *o*-cresol reaction with the Gibbs reagent. a) Gibbs product in buffer reaction, 5 minutes after mixing; b) mixture mass spectrum deconvoluted for the 2-chlorine isotope pattern.

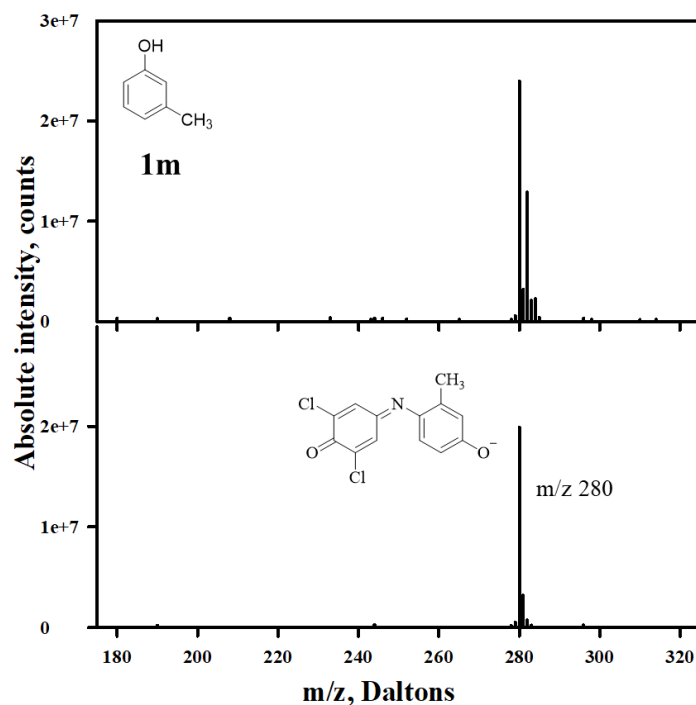


Figure 3.4. ESI mass spectra of products of *m*-cresol reaction with the Gibbs reagent. a) Gibbs product in buffer reaction, 5 minutes after mixing; b) mixture mass spectrum deconvoluted for the 2-chlorine isotope pattern

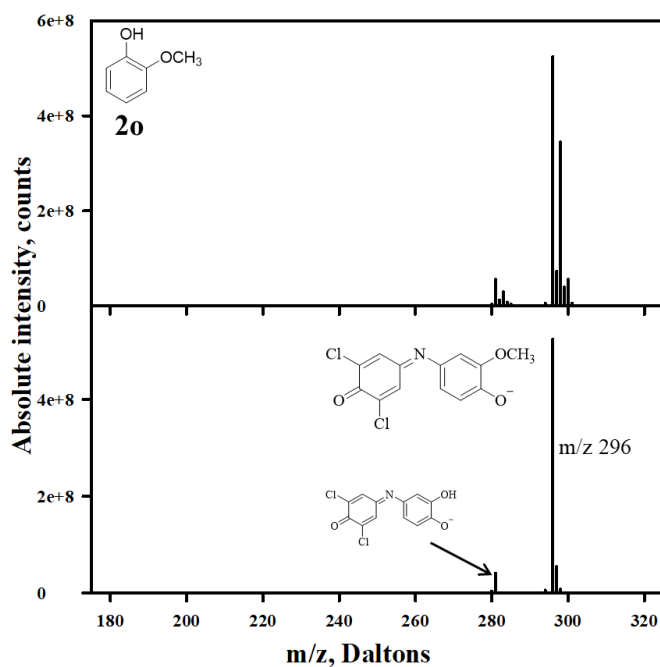


Figure 3.5. ESI mass spectra of products of *o*-methoxyphenol or guaiacol reaction with the Gibbs reagent. a) Gibbs product in buffer reaction, 5 minutes after mixing; b) mixture mass spectrum deconvoluted for the 2-chlorine

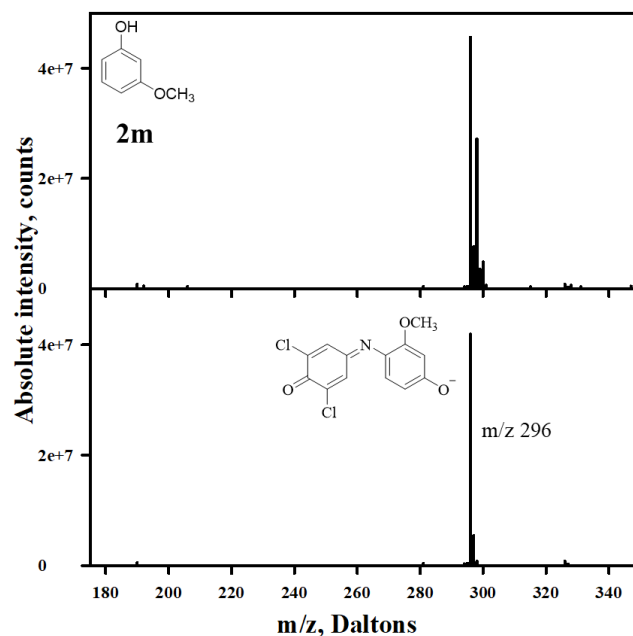


Figure 3.6. ESI mass spectra of products of *m*-methoxyphenol reaction with the Gibbs reagent. a) Gibbs product in buffer reaction, 5 minutes after mixing; b) mixture mass spectrum deconvoluted for the 2-chlorine isotope pattern

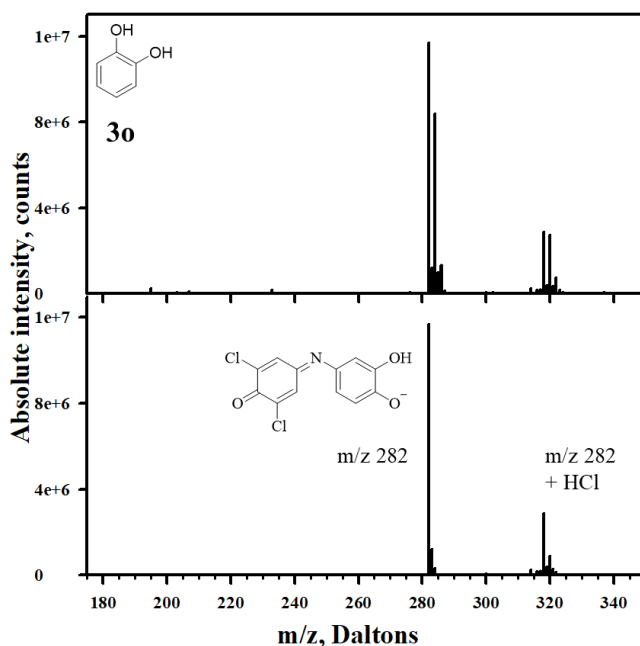


Figure 3.7. ESI mass spectra of products of catechol reaction with the Gibbs reagent. a) Gibbs product in buffer reaction, 5 minutes after mixing; b) mixture mass spectrum deconvoluted for the 2-chlorine isotope pattern

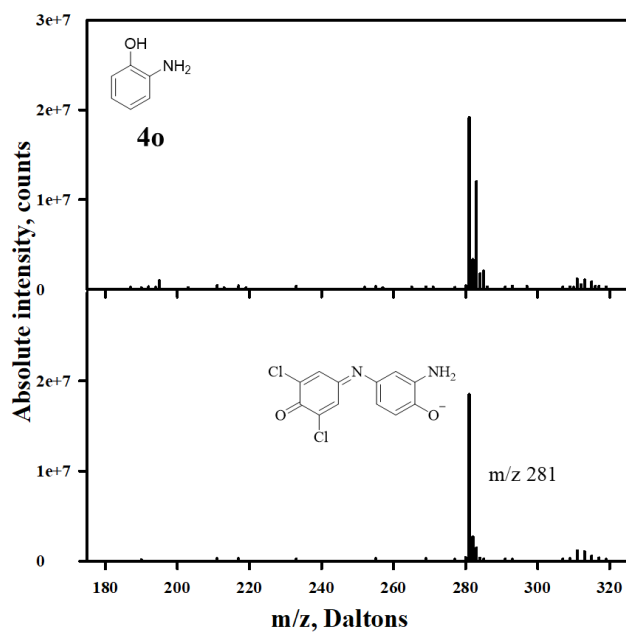


Figure 3.8. ESI mass spectra of products of *o*-aminophenol reaction with the Gibbs reagent. a) Gibbs product in buffer reaction, 5 minutes after mixing; b) mixture mass spectrum deconvoluted for the 2-chlorine isotope pattern

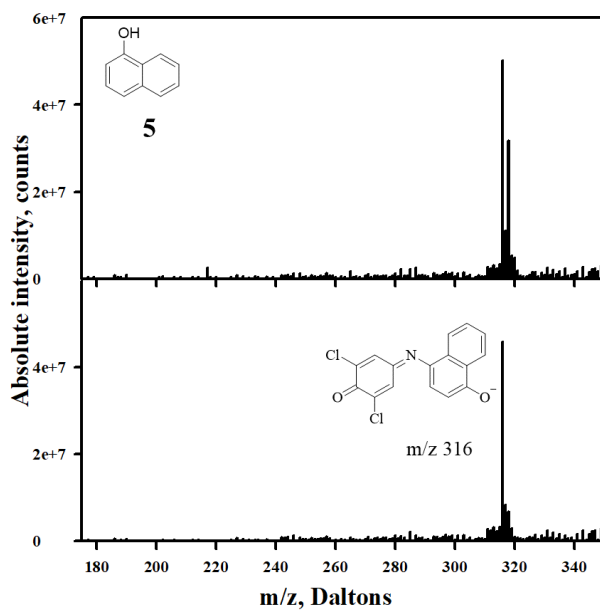


Figure 3.9. ESI mass spectra of products of 1-naphthol reaction with the Gibbs reagent. a) Gibbs product in buffer reaction, 5 minutes after mixing; b) mixture mass spectrum deconvoluted for the 2-chlorine isotope pattern

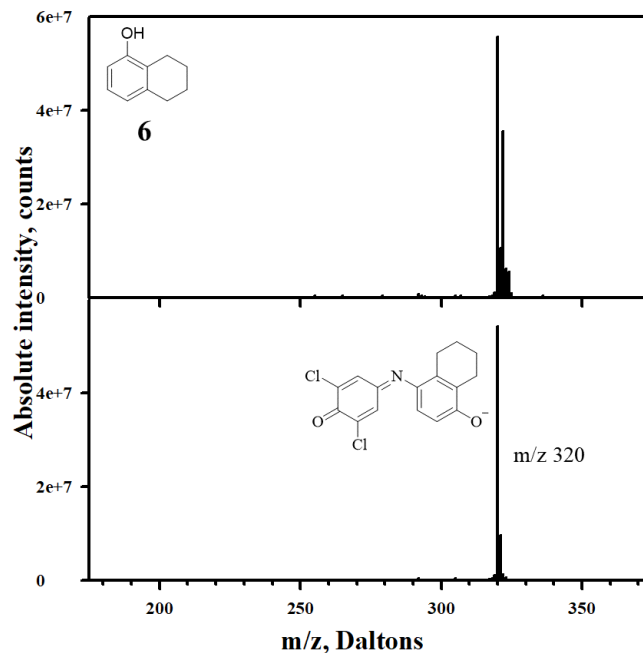


Figure 3.10. ESI mass spectra of products of 5,6,7,8-tetrahydro-1-naphthol reaction with the Gibbs reagent. a) Gibbs product in buffer reaction, 5 minutes after mixing; b) mixture mass spectrum deconvoluted for the 2-chlorine isotope pattern

While **1** – **6** all lack substitution in the *para*-position, it is also possible to detect Gibbs products for some *para*-substituted phenols,^{44, 45} as well, including *p*-chloro-, fluoro- and methoxyphenols (**7a-c**, respectively). For these substrates, the *para*-substituent is replaced to

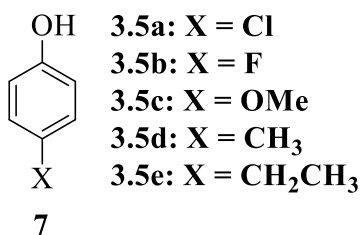


Figure 3.11. Structures of phenolic derivatives with *para*-substitution

form the same indophenol product as obtained with phenol (eq 1).⁴⁵ In addition, indophenol products are also observed with *p*-cresol (**7d**) and *p*-ethylphenol (**7e**) but in these cases, the indophenol products contain the substituent, indicating substitution at a non-*para* position.

Moreover, even in those systems where substitution occurs at the *para* position, additional products are observed that complicate the analysis. The mechanism of the reaction, including the reaction with *para*-substituted systems, is outside of the scope of this work, and will be described in future report.

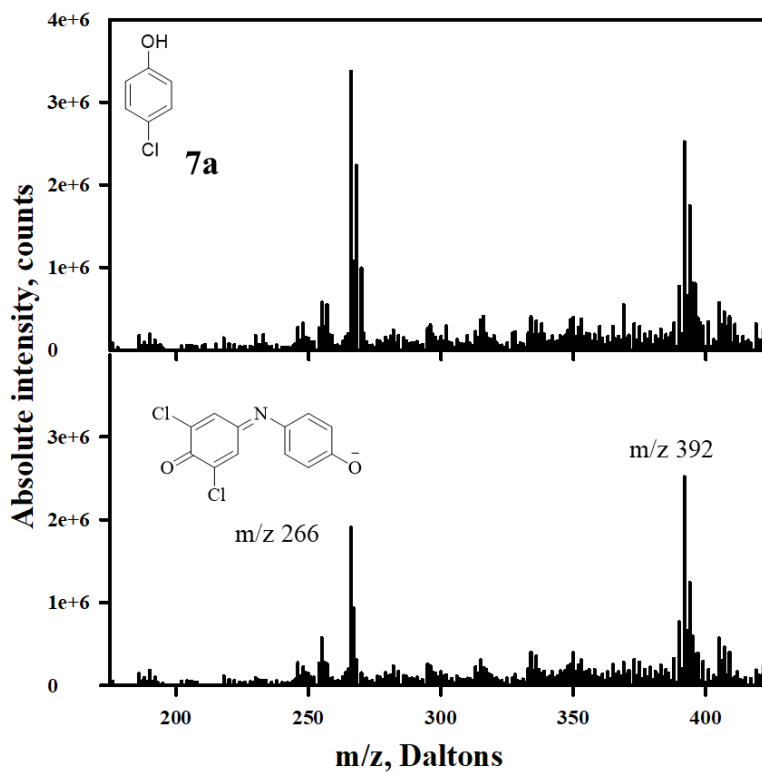


Figure 3.12. ESI mass spectra of products of *p*-chlorophenol reaction with the Gibbs reagent. a) Gibbs product in buffer reaction, 5 minutes after mixing; b) mixture mass spectrum deconvoluted for the 2-chlorine isotope pattern

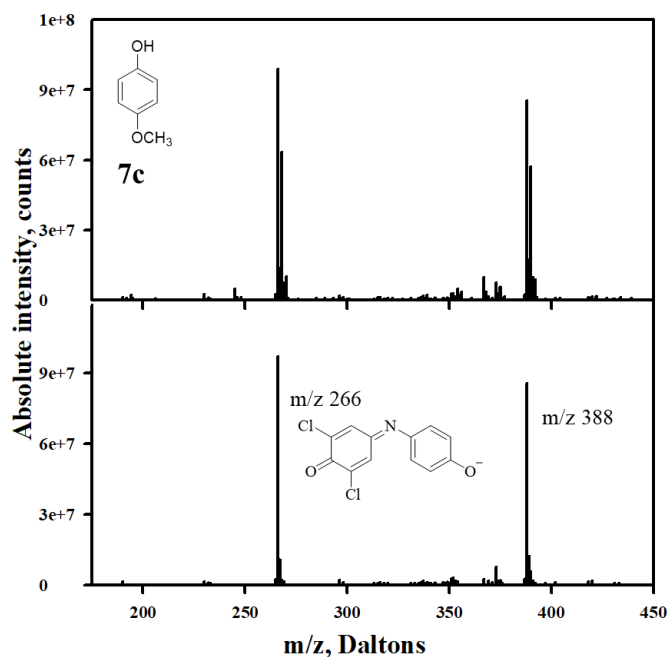


Figure 3.13. ESI mass spectra of products of *p*-methoxyphenol reaction with the Gibbs reagent. a) Gibbs product in buffer reaction, 5 minutes after mixing; b) mixture mass spectrum deconvoluted for the 2-chlorine isotope pattern

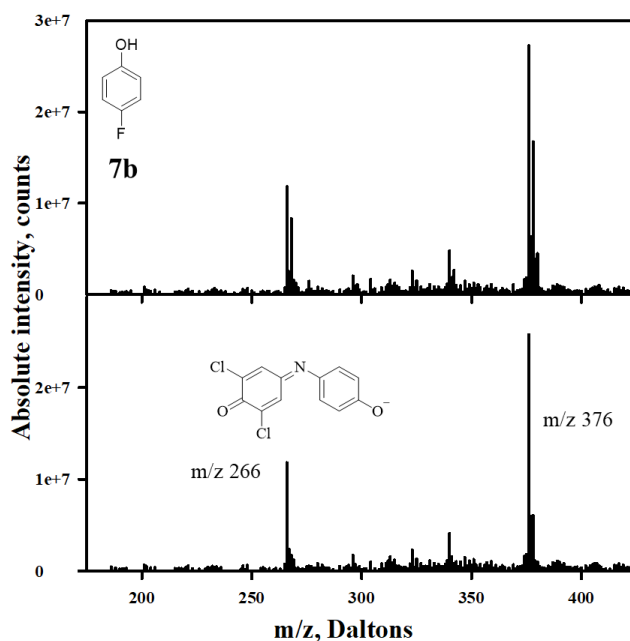


Figure 3.14. ESI mass spectra of products of *p*-fluorophenol reaction with the Gibbs reagent. a) Gibbs product in buffer reaction, 5 minutes after mixing; b) mixture mass spectrum deconvoluted for the 2-chlorine isotope pattern

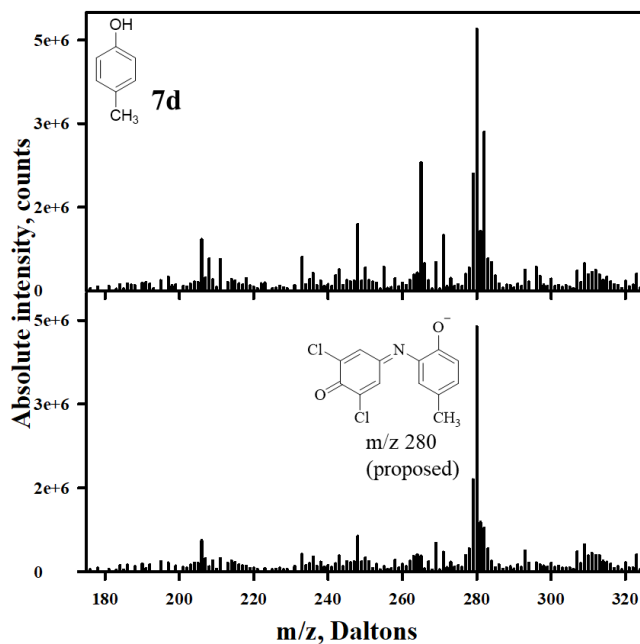


Figure 3.15. ESI mass spectra of products of *p*-cresol reaction with the Gibbs reagent. a) Gibbs product in buffer reaction, 5 minutes after mixing; b) mixture mass spectrum deconvoluted for the 2-chlorine isotope pattern

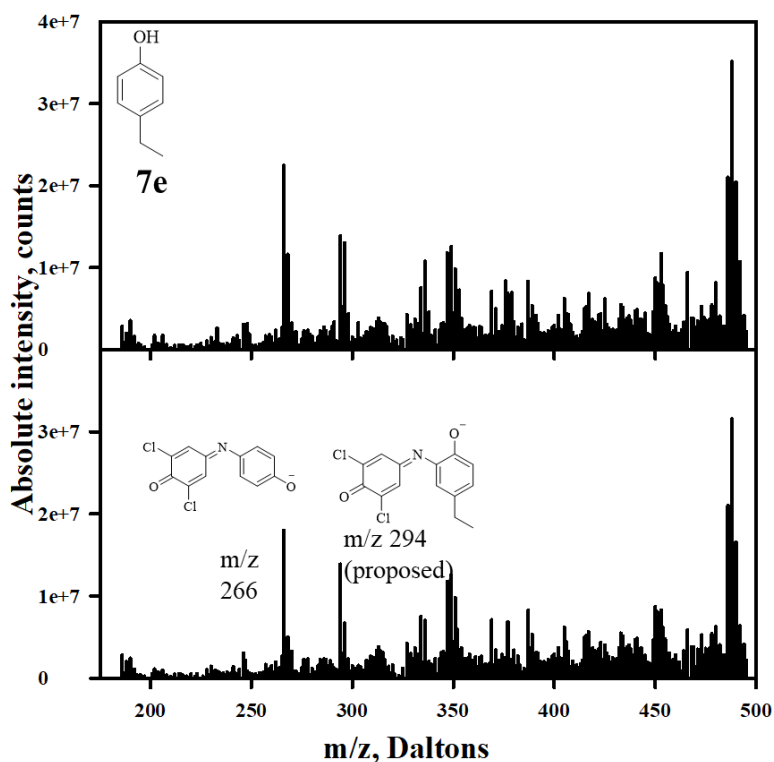


Figure 3.16. ESI mass spectra of products of *p*-ethylphenol reaction with the Gibbs reagent. a) Gibbs product in buffer reaction, 5 minutes after mixing; b) mixture mass spectrum deconvoluted for the 2-chlorine isotope pattern

3.3.3 Isomer distinction

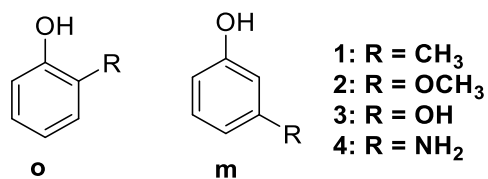


Figure 3.17. MS/MS of substituted phenols examined in this work

A limitation of the mass spectra of the indophenol products of the Gibbs reaction is that it cannot distinguish between isomeric phenols, which have the same mass-to-charge ratio. However, for most of the ions examined, the isomers can be distinguished on the basis of their

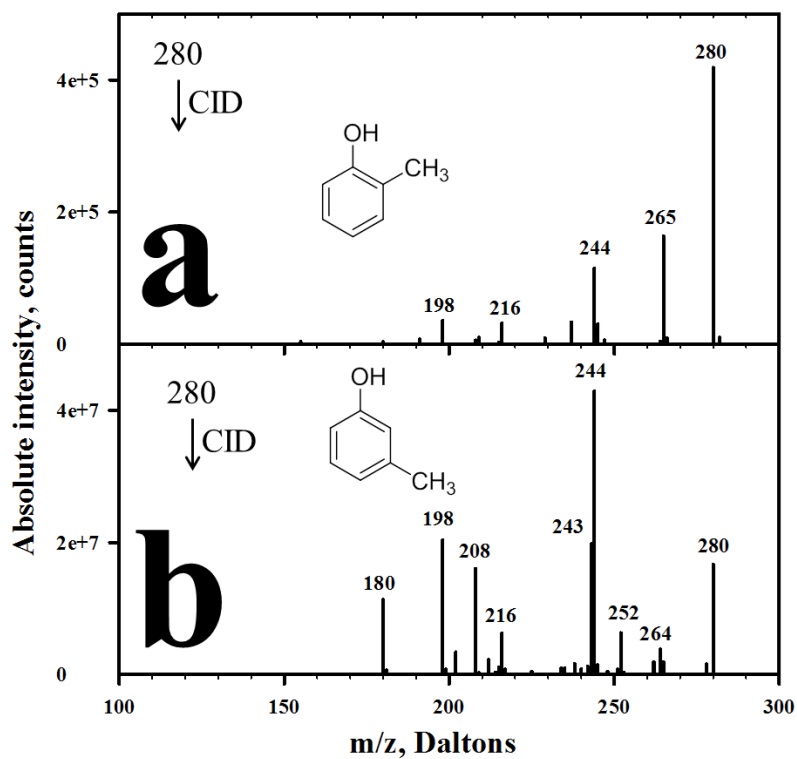


Figure 3.18. CID spectra of indophenols formed from a) *ortho*- and b) *meta*-cresol, with a normalized energy of 25%.

CID spectrum. For example, Figure 2 shows the CID spectra of the indophenols formed from *ortho*- (2a) and *meta*-cresol (2b). Significant differences are observed between the spectra, with methyl loss being a major dissociation pathway for the *ortho*-isomer, but not observed for *meta*, whereas *m/z* 252, 208 and 180 are exclusively observed for the *meta*-isomer. Although not all isomeric pairs show such dramatic differences (see Supporting Information), this shows that CID of the indophenols can be used to distinguish between isomeric phenols.

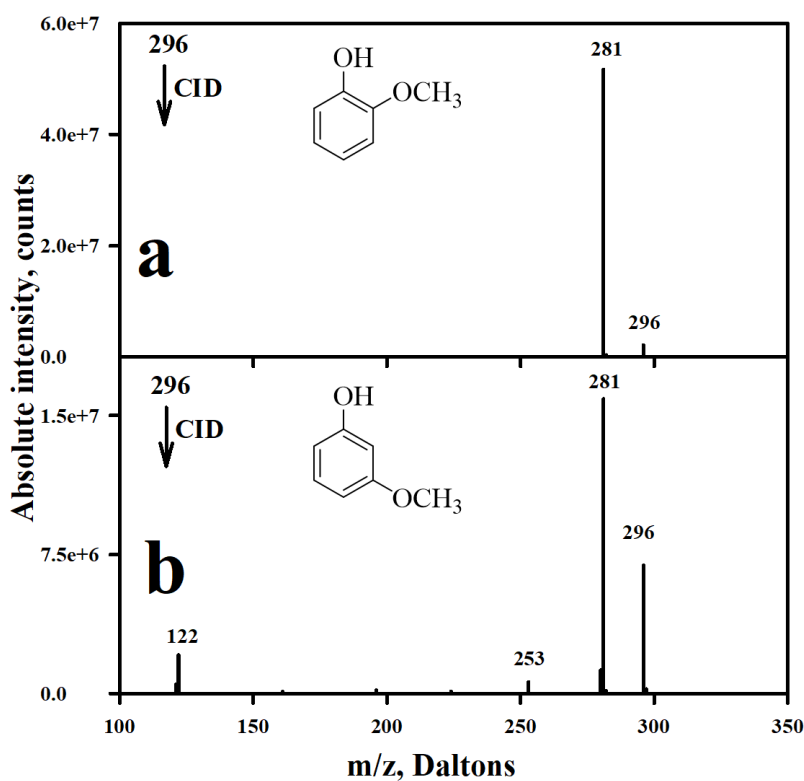


Figure 3.19. CID spectra of indophenols formed from a) *ortho*- and b) *meta*-methoxyphenol, with a normalized energy of 25%.

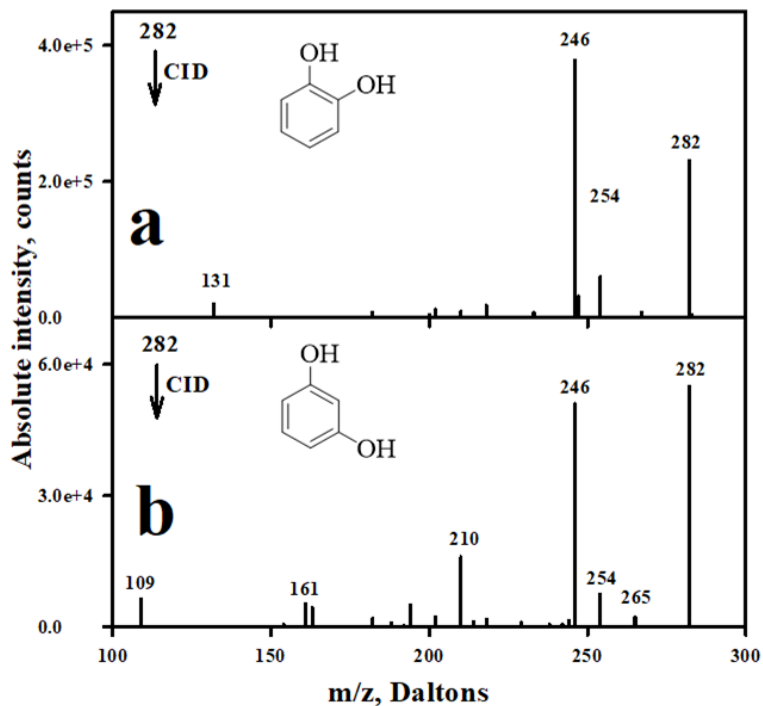


Figure 3.20. CID spectra of indophenols formed from a) catechol and b) resorcinol, with a normalized energy of 25%.

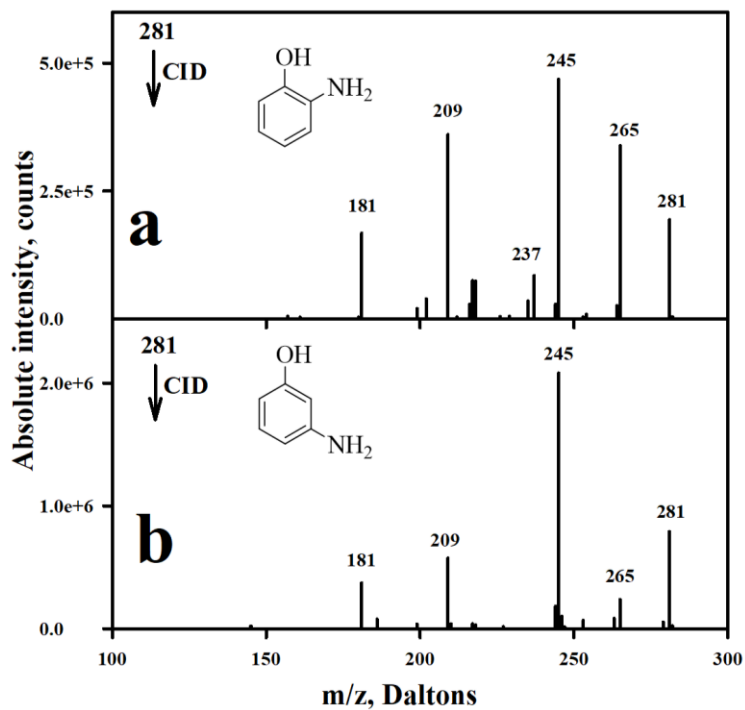


Figure 3.21. CID spectra of indophenols formed from a) *ortho*- and b) *meta*-aminophenol, with a normalized energy of 32%.

3.3.4 Mixture analysis and signal time dependence

One of the advantages of using mass spectrometry to detect the indophenol products of the Gibbs reaction is that it can be used for simultaneous detection of multiple phenol derivatives without separation. This is illustrated by the spectrum of 1:1 mixture of phenol and *o*-cresol (**1o**), each at 0.25 mmol/L concentration, shown in Figure 3. The presence of peaks at m/z 266 and m/z 280 in the deconvoluted mass spectrum indicate the presence of phenol and **1o**, respectively.

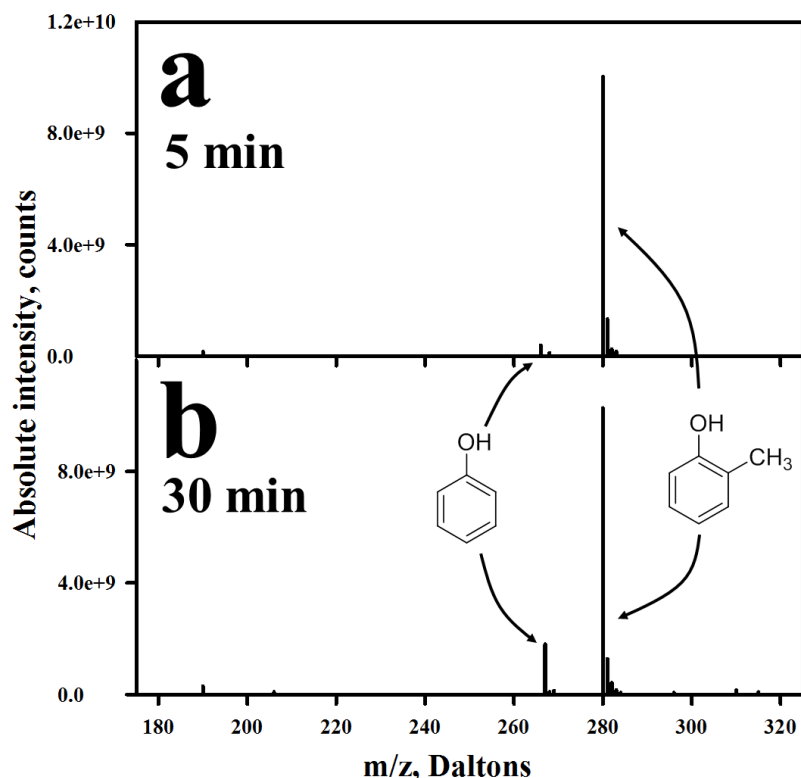


Figure 3.22. Deconvoluted ESI-mass spectrum of Gibbs products obtained from a 1:1 mixture of phenol and *o*-cresol, taken a) 5 minutes and b) 30 minutes after mixing. The spectrum in Figure 2a was taken 5 minutes after mixing the phenols with the Gibbs reagent.

Although the phenol and **1o** have equal concentrations, at 5 minutes the signal for the cresol is nearly 25 times larger than that for phenol. However, after 30 minutes, the absolute signal for phenol increases by nearly a factor of 5, whereas that for *o*-cresol increases by less than 5%, which

shows that under these buffer conditions, the reaction with *o*-cresol occurs much faster than that with phenol. The dependence of the rate of the Gibbs reaction on solvent/pH/substrate has been a subject of investigation since the original work of Gibbs in 1927.¹⁸

3.3.5 Sensitivity

To use this method for the quantitative detection of phenol, we have used *o*-cresol as an internal standard. Calibration curves for the ratio $I(m/z\ 266)/I(m/z\ 280)$ vs phenol concentration, for samples where the internal standard concentration is 3.0 $\mu\text{mol/L}$, at 5 min and 30 min post-mix are shown in Figure 4. Under the conditions used in this work, the reaction of the Gibbs reagent with *o*-cresol is faster than that with phenol, such that the relative amount of the Gibbs product for phenol, $m/z\ 266$, compared to the Gibbs product for phenol, $m/z\ 280$, at longer reaction time (~ 0.2) is larger than that at short reaction time (~ 0.05). Nonetheless, the ratio of phenol Gibbs product to *o*-cresol Gibbs product is essentially linear ($r^2 = 0.99$) over the range of phenol concentration from 1 - 50 $\mu\text{mol/L}$. Colorimetric detection of the phenols by using the Gibbs reaction typically have detection limits of approximately 1 $\mu\text{mol/L}$,^{19, 46} similar to what we find for phenol in this work. Alternatively, Aberici and co-workers have reported a detection limit near 0.1 $\mu\text{mol/L}$ or less for acetylated phenols when using trap-and-release membrane introduction mass spectrometry.¹¹

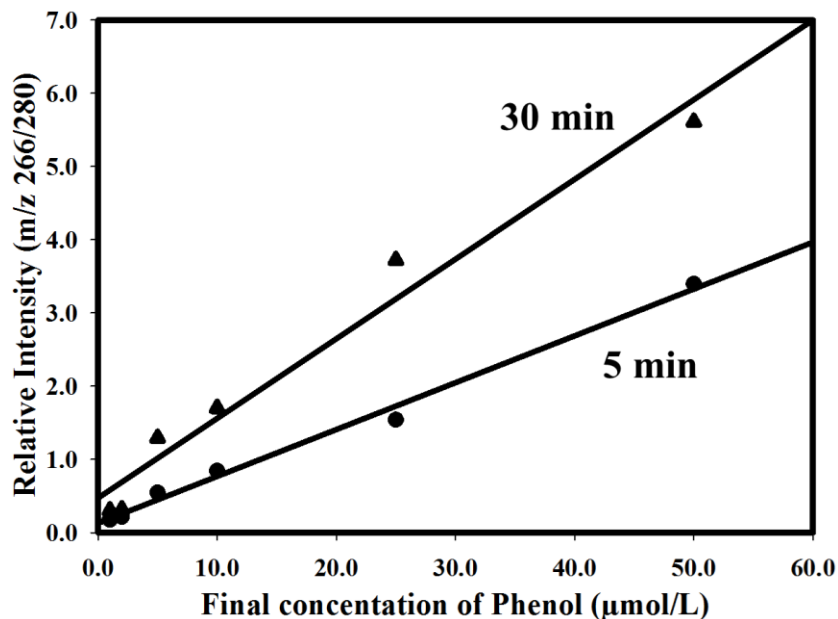


Figure 3.23. Relative intensities of phenol (m/z 266) and *o*-cresol (m/z 280) Gibbs products as a function of phenol concentration. The *o*-cresol is present at a concentration of 3 μmol/L.

3.3.6 Application: Analysis of “Hickory” and “Mesquite” Liquid Smoke

The mass spectrometric detection of Gibbs products can be used to analyze any sample that contains significant amounts of phenols. An example of this type of product is “liquid smoke,” a common additive used for flavoring⁴⁷ and preservation,⁴⁸ which consists of wood smoke condensates. Phenols make up approximately 1/3 of commercially available liquid smoke,⁴⁹ with guaiacol (**2o**), pyrocatechol (**3o**) and syringol (**8**) among the most important components.⁴⁹⁻⁵³ As an illustration of how this method can be used to analyze mixtures, we have carried out an analysis of two commercially-available liquid smoke products, sold by The Colgin Companies (Dallas, TX, www.colgin.com), a “Natural Hickory” and “Natural Mesquite” to determine the differences in phenolic composition.

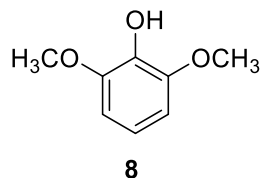


Figure 3.24. 2,6-Dimethoxyphenol or syringol is found in liquid smoke

The deconvoluted mass spectra for the hickory and mesquite flavors of liquid smoke upon reaction with the Gibbs reagent, taken 5 minutes after mixing, are shown in Figure 5. Gibbs products formed from guaiacol (m/z 296), pyrocatechol (m/z 282) and syringinol (m/z 326) are readily observed in both products, although the relative amounts are very different for the two flavorings. Additional signals in the spectrum near masses 349, 351 and 420 are unidentified products that are commonly observed in spectra of phenol-containing samples with Gibbs reagents. Based on the peak ratios and apparent isotope pattern, they likely contain multiple Gibbs reagent structures.

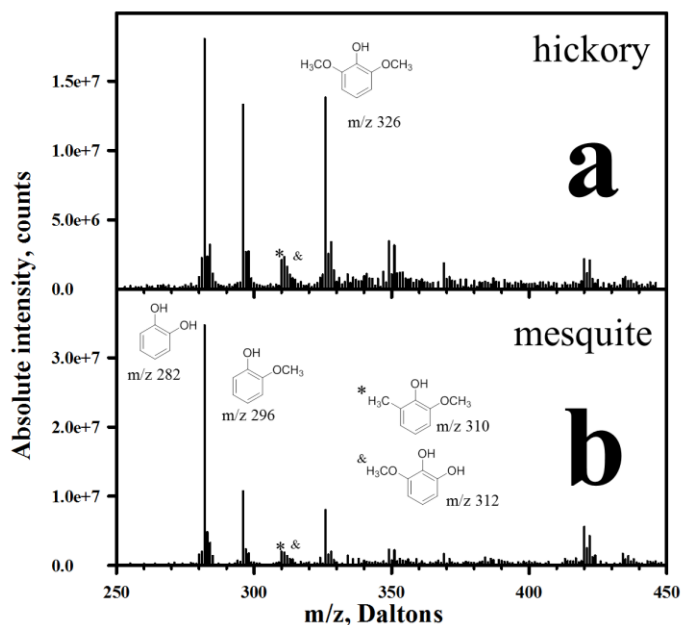


Figure 3.25. Deconvoluted mass spectrum of the Gibbs products obtained from analysis of a) Natural Hickory and b) Natural Mesquite flavors of colgin® brand liquid smoke.

For both samples, the Gibbs product for catechol (which could also contain resorcinol) is the most abundant. However, hickory flavor contains relatively higher amounts of the methoxy-substituted phenols, guaiacol and syringinol.

In an detailed analysis of Code 10-Poly full-strength liquid smoke, Montazeri et al.⁴⁹ found additional, less abundant products, including isomeric methoxymethylphenols and 3-methoxy-1,2-benzenediol. These appear to be present in the spectra in Figure 4, at m/z 310 and 312, respectively. However, in both spectra, there is a product at m/z 311 that is similar in abundance to those at m/z 310 and 312. The odd m/z value would require a nitrogen containing product, and could, in principle, be attributed to an amino-methoxyphenol. However, as with the products at m/z 349, 351 and 420, the m/z 311 product is observed in other samples we have examined, and therefore is likely a side-product formed from Gibbs reagent.

Assuming the reactions of hydroxy- and methoxyphenols with Gibbs reagents occur at approximately the same rates, then the relative intensities of the peaks in Figure 5 reflect the relative concentrations of the phenolic components. However, that assumption is not necessarily true, and proper relative and absolute quantification of the phenols in liquid smoke requires measurements with an internal standard and calibration. Similarly, control experiments are required to determine the products of the Gibbs reagent with *para*-substituted phenols present in liquid smoke.⁴⁹

3.4 Conclusions

While the Gibbs reagent has long been used as a phenolic assay, the use mass spectrometry to detect the indophenol product allows for a more specific determination of phenol composition. The relative yields of Gibbs products additionally allow for quantification of phenol components, by measuring intensity against an internal standard. Mass spectrometric analysis also allows for

investigation of the product structures, particularly for the reactions with *para*-substituted phenols, which can react either by direct substitution of the substituent, or at another site within the phenol, preserving the *para* substituent. Finally, the method is shown to work for the analysis of liquid smoke, and is therefore amenable for the analysis of wood-smoke condensates.

3.5 References

1. Arutchelvan, V.; Kanakasabai, V.; Nagarajan, S.; Muralikrishnan, V., Isolation and identification of novel high strength phenol degrading bacterial strains from phenol-formaldehyde resin manufacturing industrial wastewater. *Journal of Hazardous Materials* **2005**, *127* (1), 238-243.
2. Nollet, L. M. L., Determination of phenolic compounds in water. In *Handbook of Water Analysis*, 3rd ed.; Nollet, L. M. L.; Leen, S. P., Eds. CRC Press: Boca Raton, Fla, 2014; pp 613-646.
3. Yu, Y.-j.; Zhong, S.; Su, G.-y.; Liu, H.-l.; Dai, X.-l.; Wang, R.-j.; Cai, H.-x.; Yu, H.-x., Trace analysis of phenolic compounds in water by in situ acetylation coupled with purge and trap-GC/MS. *Anal. Methods* **2012**, *4*, 2156-2161.
4. Helaleh, M. I. H.; Fujii, S.; Korenaga, T., Column silylation method for determining endocrine disruptors from environmental water samples by solid phase micro-extraction. *Talanta* **2001**, *54* (6), 1039-1047.
5. Llompart, M.; Lourido, M.; Landin, P.; Garcia-Jares, C.; Cela, R., Optimization of a derivatization-solid-phase microextraction method for the analysis of thirty phenolic pollutants in water samples. *J. Chromatogr. A* **2002**, *963* (1-2), 137-148.
6. Lourenco, E. L. B.; Ferreira, A.; Pinto, E.; Yonamine, M.; Farsky, S. H. P., On-fiber derivatization of SPME extracts of phenol, hydroquinone and catechol with GC-MS detection. *Chromatographia* **2006**, *63* (3-4), 175-179.
7. Polo, M.; Llompart, M.; Garcia-Jares, C.; Gomez-Noya, G.; Bollain, M.-H.; Cela, R., Development of a solid-phase microextraction method for the analysis of phenolic flame retardants in water samples. *J. Chromatogr. A* **2006**, *1124* (1-2), 11-21.
8. Regueiro, J.; Becerril, E.; Garcia-Jares, C.; Llompart, M., Trace analysis of parabens, triclosan and related chlorophenols in water by headspace solid-phase microextraction with in situ derivatization and gas chromatography-tandem mass spectrometry. *J. Chromatogr. A* **2009**, *1216* (23), 4693-4702.

9. Schummer, C.; Groff, C.; Al Chami, J.; Jaber, F.; Millet, M., Analysis of phenols and nitrophenols in rainwater collected simultaneously on an urban and rural site in east of France. *Sci. Total Environ.* **2009**, *407* (21), 5637-5643.
10. Yu, Y.-J.; Liu, H.-L.; Dai, X.-L.; Cai, H.-X.; Li, C.-Y.; Yu, H.-X., Trace analysis of phenols and chlorophenols in water by in situ derivatization headspace solid-phase microextraction coupled with gas chromatography/mass spectrometry. *Fenxi Huaxue* **2010**, *38* (9), 1243-1248.
11. Sparrapan, R.; Eberlin, M. N.; Alberici, R. M., Quantitation of trace phenolic compounds in water by trap-and-release membrane introduction mass spectrometry after acetylation. *Rapid Commun. Mass Spectrom.* **2008**, *22* (24), 4105-4108.
12. Zhu, H.; Janusson, E.; Luo, J.; Piers, J.; Islam, F.; McGarvey, G. B.; Oliver, A. G.; Granot, O.; McIndoe, J. S., Phenol-selective mass spectrometric analysis of jet fuel. *Analyst* **2017**, *142* (17), 3278-3284.
13. Dumas, J.; Liebig, J., On the orcinol. *Chem. Zentralbl.* **1838**, *9* (44), 690-692.
14. Robiquet, Neue Beobachtungen uber das Orcin. *Ann. Pharm.* **1835**, *15*, 289-300.
15. Liebermann, C., Ueber die Einwirkung der salpetrigen Säure auf Phenole. *Berichte der deutschen chemischen Gesellschaft* **1874**, *7* (1), 247-250.
16. Liebermann, C., Ueber die aus aromatischen Oxyverbindungen und salpetriger Säure entstehenden Farbstoffe. *Berichte der deutschen chemischen Gesellschaft* **1874**, *7* (2), 1098-1102.
17. Liebermann, C., Ueber Orcein. *Berichte der deutschen chemischen Gesellschaft* **1875**, *8* (2), 1649-1651.
18. Gibbs, H. D., Phenol tests. IV. Velocity of indophenol formation-2,6-dibromobenzenoneindophenol. *J. Phys. Chem.* **1927**, *31*, 1053-81.
19. Gibbs, H. D., Phenol tests. III. The indophenol test. *J. Biol. Chem.* **1927**, *72*, 649-64.
20. Ettinger, M. B.; Ruchhoft, C. C., Determination of phenol and structurally related compounds by the Gibbs method. *Anal. Chem.* **1948**, *20*, 1191-6.
21. Mohler, E. F.; Jacob, L. N., Determination of Phenolic-Type Compounds in Water and Industrial Waste Waters Comparison of Analytical Methods. *Anal. Chem.* **1957**, *29* (9), 1369-1374.
22. Brooker, L. G. S.; Sprague, R. H., Color and constitution. IV. The absorption of Phenol Blue. *J. Am. Chem. Soc.* **1941**, *63*, 3214-15.

23. Gurupadayya, B. M.; Shankar, M. S.; Manohara, Y. N., Spectrophotometric methods for the estimation of butorphanol tartrate in bulk and pharmaceutical formulations. *Int. J. Chem. Sci.* **2007**, *5* (1), 109-116.
24. Ankita, M.; Gurupadayya, B. M.; Chandra, A., Colorimetric estimation of acenocoumarol in bulk and pharmaceutical formulations. *Asian J. Chem.* **2008**, *20* (7), 5001-5004.
25. Gowrisankar, D.; Sarsambi, P. S.; Raju, S. A., Development and validation of new spectrophotometric methods for the estimation of cefprozil in pure form and in pharmaceutical formulations. *J. Indian Counc. Chem.* **2008**, *25* (2), 106-108.
26. Bartzatt, R. L., Spectrophotometric and colorimetric methodology to detect and quantify hydrazide based chemotherapeutic drugs. *Environ. Sci.: Indian J.* **2010**, *5* (1), 86-91.
27. Patel, K.; Patel, C.; Panigrahi, B.; Parikh, A.; Patel, H., Development and validation of spectrophotometric methods for the estimation of mesalamine in tablet dosage forms. *J. Young Pharm* **2010**, *2* (3), 284-8.
28. Tuljarani, G.; Sankar, D. G.; Kadgpathi, P.; Suthakaran, R.; Satyanarayana, B., Quantitative determination of bisoprolol fumarate in bulk and pharmaceutical dosage forms by spectrophotometry. *Int. J. Chem. Sci.* **2010**, *8* (4), 2253-2258.
29. Chandan, R. S.; Vasudevan, M.; Deecaraman; Gurupadayya, B. M.; Indupriya, M., Spectrophotometric determination of lamotrigine using Gibb's and MBTH reagent in pharmaceutical dosage form. *J. Pharm. Res.* **2011**, *4* (6), 1813-1815.
30. Gousuddin, M.; Raju, S. A.; Sultanuddin; Manjunath, S., Development and validation of spectrophotometric methods for estimation of Formetrol bulk drug and its pharmaceutical dosage forms. *Int. J. Pharm. Pharm. Sci.* **2011**, *3* (3), 306-309.
31. Sowjanya, K.; Thejaswini, J. C.; Gurupadayya, B. M.; Indupriya, M., Spectrophotometric determination of Pregabalin using Gibb's and MBTH reagent in pharmaceutical dosage form. *Pharma Chem.* **2011**, *3* (1), 112-122.
32. Somisetty, V. S. R.; Bichala, P. K.; Rao, C. M. M. P.; Kirankumar, V., Development and validation of newer analytical methods for the estimation of deferasirox in bulk and in tablet dosage form by calorimetric method. *Int. J. Pharm. Pharm. Sci.* **2013**, *5* (Suppl. 3), 521-525.
33. Prabhu, P. P.; Das, P.; Kaneri, A.; Reddy, M. J., Simple spectrophotometric estimation of labetalol in bulk and marketed formulation. *Eur. J. Biomed. Pharm. Sci.* **2014**, *1* (2), 108-114.
34. Rajapandi, R.; Aswathy, S. R.; Sreedharran, B., Spectrophotometric method development and validation for estimation of enrofloxacin in pure and dosage forms. *World J. Pharm. Res.* **2016**, *5* (6), 1402-1410.

35. Jeong, H.-J.; Hwang, D.; Ahn, J. T.; Chun, J. Y.; Han, K.; Lee, W.-M.; Kwon, J.-K.; Lee, Y.-J.; Kang, B.-C., Development of a simple method for detecting capsaicinoids using Gibb's reagent in pepper. *Weon'ye Gwahag Gi'sulji* **2012**, *30* (3), 294-300.
36. Thompson, R. Q.; Chu, C.; Gent, R.; Gould, A. P.; Rios, L.; Vertigan, T. M., Visualizing Capsaicinoids: Colorimetric Analysis of Chili Peppers. *J. Chem. Educ.* **2012**, *89* (5), 610-612.
37. Ryu, W.-K.; Kim, H.-W.; Kim, G.-D.; Rhee, H.-I., Rapid determination of capsaicinoids by colorimetric method. *J. Food Drug Anal.* **2017**, *25* (4), 798-803.
38. Karimi, M.; Hassanshahian, M., Isolation and characterization of phenol degrading yeasts from wastewater in the coking plant of Zarand, Kerman. *Braz. J. Microbiol.* **2016**, *47* (1), 18-24.
39. Montazeri, N.; Oliveira, A. C. M.; Himelbloom, B. H.; Leigh, M. B.; Crapo, C. A., Chemical characterization of commercial liquid smoke products. *Food Sci. Nutr. (Hoboken, NJ, U. S.)* **2013**, *1* (1), 102-115.
40. Lowe, E. R.; Banks, C. E.; Compton, R. G., Indirect detection of substituted phenols and cannabis based on the electrochemical adaptation of the Gibbs reaction. *Analytical and Bioanalytical Chemistry* **2005**, *383* (3), 523-531.
41. Josephy, P. D.; Lenkinski, R. E., Reaction of Gibbs reagent (2,6-dichlorobenzoquinone-4-chloroimine) with the antioxidant BHA (3-tert-butyl-4-hydroxyanisole): isolation and identification of the major product. *J. Chromatogr.* **1984**, *294*, 375-9.
42. SDBS database.
43. Kang, D.; Ricci, F.; White, R. J.; Plaxco, K. W., Survey of Redox-Active Moieties for Application in Multiplexed Electrochemical Biosensors. *Analytical Chemistry* **2016**, *88* (21), 10452-10458.
44. Dacre, J. C., Nonspecificity of the Gibbs reaction. *Anal. Chem.* **1971**, *43* (4), 589-91.
45. Josephy, P. D.; Van Damme, A., Reaction of Gibbs reagent with para-substituted phenols. *Anal. Chem.* **1984**, *56* (4), 813-14.
46. Tulus, R.; Konyali, H., Spectrophotometric determination of some drugs by their phenolic groups. *Istanbul Univ. Eczacilik Fak. Mecm.* **1980**, *16*, 56-72.
47. Rozum, J. J., Smoke Flavor. In *Ingredients in Meat Products: Properties, Functionality and Applications*, Tarté, R., Ed. Springer New York: New York, NY, 2009; pp 211-226.
48. Lingbeck, J. M.; Cordero, P.; O'Bryan, C. A.; Johnson, M. G.; Ricke, S. C.; Crandall, P. G., Functionality of liquid smoke as an all-natural antimicrobial in food preservation. *Meat Science* **2014**, *97* (2), 197-206.

49. Montazeri, N.; Oliveira, A. C.; Himelbloom, B. H.; Crapo, C. A.; Leigh, M. B., Chemical characterization of commercial liquid smoke products. *Food Sci Nutr* **2013**, *1* (1), 102-15.
50. Budaraga, I. K.; Arnim; Marlida, Y.; Bulanin, U., Analysis of liquid smoke chemical components with GC MS from different raw materials variation production and pyrolysis temperature level. *Int. J. ChemTech Res.* **2016**, *9* (6), 694-708.
51. Simon, R.; de la Calle, B.; Palme, S.; Meier, D.; Anklam, E., Composition and analysis of liquid smoke flavouring primary products. *J. Sep. Sci.* **2005**, *28* (9-10), 871-882.
52. Wittkowski, R., Analysis of liquid smoke and smoked meat volatiles by headspace gas chromatography. In *Agriculture, Food Chemistry and the Consumer. Proceedings of the 5th European Conference on Food Chemistry (Vol. 2)*, INRA: Paris, FR, 1989; Vol. 2, pp 639-43.
53. Wittkowski, R.; Baltes, W.; Jennings, W. G., Analysis of liquid smoke and smoked meat volatiles by headspace gas chromatography. *Food Chem.* **1990**, *37* (2), 135-44.

CHAPTER 4. RAPID QUANTIFICATION OF PHENOLIC COMPOUNDS IN LIQUID SMOKE BY USING MASS SPECTROSCOPY

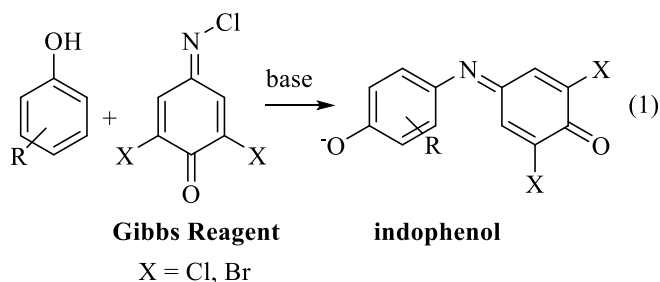
4.1 Introduction

Phenolic compounds in foods have been getting significant attention due to their antibacterial, antioxidant, antimutagenic, anticarcinogenic and antiviral activities.¹⁻⁸ Phenols are used in food products as preservatives,⁹ and for their organoleptic or sensory,^{10, 11} and texture characteristics.^{12, 13} Phenols also contribute to other sensory quality attributes, such as flavor, color or texture.¹⁴⁻¹⁹

Liquid smoke is a food additive with significant phenolic content.²⁰ Liquid smoke results from the liquid condensate obtained upon pyrolysis of the lignin or dry mass of wood, and contains a variety of phenolic compounds,^{16, 21} which, along with other organic compounds,²²⁻²⁴ give the liquid smoke its characteristic odor and color. In an early analysis, Baltes, *et al*, found that liquid smoke contains 0.2 – 2.9% phenol derivatives.²⁵ Phenol derivatives in liquid smoke have subsequently been characterized by using gas chromatography-mass spectrometry (GC-MS) analysis.^{16, 26-34}

In this work, we have carried out an analysis of phenols in commercial liquid smoke by using reaction with Gibbs reagent, 2,6-dichloro- or dibromo-4-(chloroimino)cyclohexa-2,5-dien-1-one (eq 1), to form indophenol (Gibbs reaction),^{35, 36} followed by analysis by using electrospray ionization mass spectrometry (ESI-MS). The advantage of this approach is that it gives ionized indophenols of the corresponding phenol derivatives in the reaction mixture.³⁷ Moreover, we can avoid any separation and/or solvent extraction steps before MS analysis. Finally, deconvolution of the mass spectra to account for the isotopic peaks of the indophenols removes signal from non-

phenolic products.³⁷⁻³⁹ With this analysis, we are able to determine and compare the phenolic compositions of hickory, mesquite, pecan and apple wood flavors of liquid smoke.



4.2 Materials and methods

4.2.1 Chemicals

Catechol, guaiacol, syringol, potassium hydrogenphosphate (KH_2PO_4), and Gibb's reagent were obtained from commercial sources, and used as received. Methanol solvent was "Reagent Grade" and used without further purification.

4.2.2 Samples

The liquid smoke samples were Colgin-brand liquid smoke, purchased as a "Colgin Assorted Liquid Smoke Gift Box 4.0 oz," (Figure 4.1) and used as received. It contains four different flavored liquid smokes – Hickory, Mesquite, Pecan, and Apple. Liquid smokes were used without any modification.



Figure 4.1. Commercially available four different flavored Colgin Assorted Liquid Smoke was examined in this work. The four different flavors are – (from left to right) Hickory, Mesquite, Apple and Pecan.

4.2.3 Analysis of Liquid Smoke

Analysis of liquid smoke was carried out by a small modification of previously described method (Chapter 3).³⁷⁻³⁹ In brief, 2 mL corresponding liquid sample was taken in 8 mL deionized water. 87 mg (0.5 mmol) of K_2HPO_4 was added into it. 50 μ L of 10 mmol/L of 5,6,7,8-tetrahydro-1-naphthol was added into the solution as an internal standard. 5.0 mL methanol having 500 μ L of 100 mmol/L Gibbs solution was prepared separately. These two solutions were mixed together and stirred at room temperature for 5 minutes. After the reaction time, 100 μ L of the solution was diluted to 2.0 mL in water-methanol solution (1:1), for ESI-MS analysis. Control experiments were done in each condition and the calculations for the compounds were done by subtracting corresponding values of the control from the liquid smoke sample experiments. The structures of phenol compounds were confirmed by MS/MS and MS^3 experiments and compared, if needed, with authenticate samples of corresponding compounds. 10 mL liquid smoke was taken for apple flavored Colgin Liquid Smoke to improve the signal intensity.

4.2.4 Calibration Curve

Calibration solutions were created by mixing 5 mL of a solution of Gibb's reagent in methanol (80 mmol/L) with 10 mL of an aqueous solution of potassium phosphate dibasic solution (50 mmol/L) that contains 30 μ L (60 mmol/L) of 5,6,7,8-tetrahydro-1-naphthol as internal standard. Specific volumes of methanol solutions of catechol, guaiacol, or syringol are added to get to the desired concentrations of those substrates. After mixing, the solutions were stirred at room temperature for the 5 minutes. 25 μ L of the reaction mixture was diluted to 2 mL in water-methanol solution (1:1) for ESI-MS analysis. The concentration of 5,6,7,8-tetrahydro-1-naphthol in the initial solution was chosen so to obtain a concentration of 0.20 mg/L (1.50 μ mol/L) in the final (electrosprayed) solution. Similarly, the concentration of phenols in the initial solution was chosen so to obtain a distribution of concentrations of the analytes.

4.2.5 Spectra collection

Electrospray ionization mass spectra were obtained on a commercial LCQ-DECA (Thermo Electron Corporation, San Jose, CA, USA) quadrupole ion trap mass spectrometer, equipped with electrospray ionization (ESI) source. Substrate solutions in a methanol:water mixture (1:1) and introduced into the source directly at a flow rate of 5 μ L/min. Electrospray and ion focusing conditions were varied so that maximize the signal of the ion of interest.

4.2.6 Spectral analysis

One important advantage of using the Gibbs reagent for derivatization is that the chlorine atoms make products containing the Gibbs reagent readily detectable by the isotopic pattern. Therefore, the spectra are deconvoluted using the isotope pattern for ions containing two chlorine atoms (1:0.648:0.105) to eliminate the peaks that cannot contain the Gibbs reagent, as described

previously. It is this ability to specifically detect phenoxides and eliminate non-Gibbs products that makes the Gibbs approach preferable to simple ESI-MS of the mixture.

4.3 Results

Guillen and co-workers reported GC-MS analyses of liquid smokes from a variety of sources, including aqueous liquid smokes from *Vitis vinifera* L shoot and *Fagus sylvatica* L wood,²⁷ aqueous smoke from *Thymus vulgaris* L plant,⁴⁰ liquid smoke flavoring obtained from *Salvia lavandulifolia*,³⁴ and aqueous oak smoke.³³ They found a wide range of phenolic components such as phenol, methoxyphenols, dimethoxyphenols, along with other types of compounds.^{14, 27, 33, 34, 40} Similar compounds have been identified in subsequent studies by other groups.^{20, 30} Generally, notable compounds present in liquid smokes include catechol, guaiacol, and syringol and their derivatives. In our previous study, we introduced the possibility of analysis of phenols in Hickory and Mesquite liquid smokes (Chapter 3).³⁷ In this work, we are quantitatively analyze phenol derivatives in commercial liquid smokes.

4.3.1 Identification of the phenols in liquid smokes

For the identification of major phenols, we started with colgin® Natural Hickory Liquid Smoke. Figure 4.2a and 4.2b show the full mass spectra and deconvoluted mass spectra when it reacts with Gibbs reagent having an internal standard (at m/z 320 due to THN, discussed below). In addition to internal standard peak, the most noteworthy Gibbs products at m/z 282, 296, and 326, which are corresponding to the indophenols formed from isomer of dihydroxybenzene, methoxyphenol, and dimethoxyphenol, respectively. There are other peaks under 10% of the base peak and we did not consider them for the analysis as not only due formation of minor products compares to the major indophenols but they also difficult to separate since the liquid smoke

contains hundreds of pyrolysis compounds.⁴⁰ In this work, we have focused on the analysis of the most significant product at m/z 282, 296 and 326, and do not consider the other products function.

The detail studies of initially mentioned indophenol peaks were studied, and the structure of the corresponding indophenols was determined by examining their tandem mass spectrometry and comparing them with those from authentic samples. For instance, dihydroxybenzene has three isomers – *ortho*-, *meta*-, and *para*- and they react with Gibbs reagent to form indophenols.

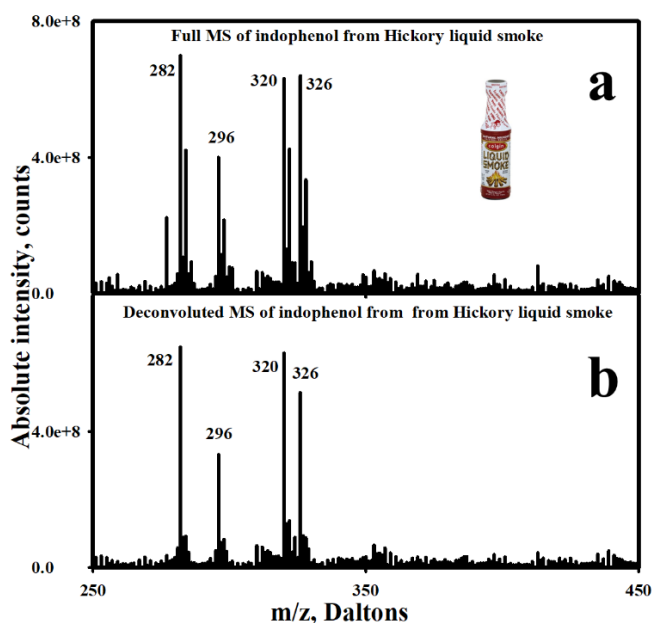


Figure 4.2. Full MS (top) and deconvoluted MS (bottom) of the Gibbs product of Hickory liquid some.

Figure 4.3 shows full MS and deconvoluted MS of indophenols formed when isomer of dihydroxybenzene react with Gibbs reagent. All three isomers form dominantly indophenol at m/z 282 in 5 minute reaction (Figure 4.3a – 4.3c). However, unlike catechol, additional peaks are observed for other two isomers. For instance, resorcinol gives many more indistinguishable products and hydroquinone forms additional but small peaks at m/z 312. In both cases, peak at m/z 349 forms due to the formation of dimer of Gibbs reagent. Moreover, unlike other isomers,

hydroquinone gives indophenol at m/z 266 which forms by substituting at *para*-position in longer reaction time (Figure 4.3d).

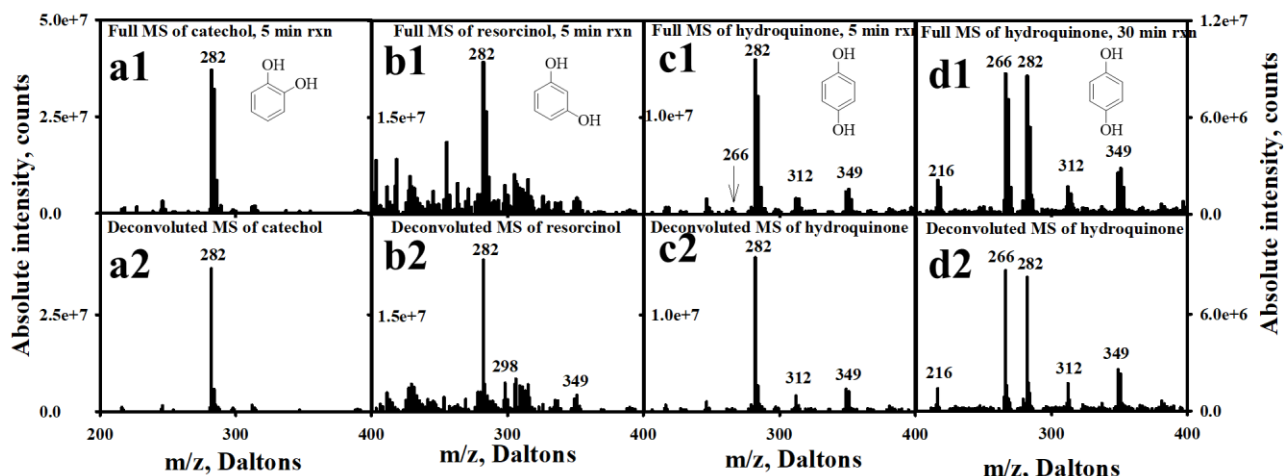


Figure 4.3. Full MS (top) and deconvoluted MS (bottom) of catechol, resorcinol, and hydroquinone, respectively. At 5 minute reaction hydroquinone gives peak at m/z 266, whereas it gives an additional peak at m/z 266 in longer reaction time.

The identification of between isomers was done by tandem mass spectroscopy. Figure 4.4 shows the tandem mass spectra of m/z 280 and 246 of Hickory and three isomers of dihydroxybenzene. MS/MS at 40% CID energy of 280 from catechol gives fragment ions more than 5% intensity of the base peak at m/z 218, 246, 254, and 282, whereas resorcinol gives at m/z 246, 267, 282 and hydroquinone forms at m/z 210, 218, 226, 238, 242, 246, 253, 254, 264, 266, 267, 282. Thus, the formation of m/z 267 may confirm the presence of resorcinol, whereas hydroquinone has its characteristic fragment peaks at m/z 210, 226, 238, 242, 253, 264, and 266. Since these distinctive peaks are low in intensity, we may use MS/MS/MS to distinguish between isomers. MS³ peaks at 40% CID energy from m/z 246 are at m/z 182, 200, 210, 218, and 246 for catechol, m/z 210, 217, 218, 246/247, and 325 for resorcinol, and m/z 210, 218 and 246 from hydroquinone. Here we can use m/z 182 for distinguishing indophenol form catechol than from other two isomers. Figure 4.4a1 and 4.4a2 are the MS/MS and MS³, respectively, of m/z 280 and

246 at similar condition. MS/MS gives fragments at m/z 218, 246, 282 and MS^3 gives at 210, 218, 246. These fragment ions match with those from catechol though the m/z 254 peak has intensity lower than 5% of the base peak. All the results are listed in Table 4.1.

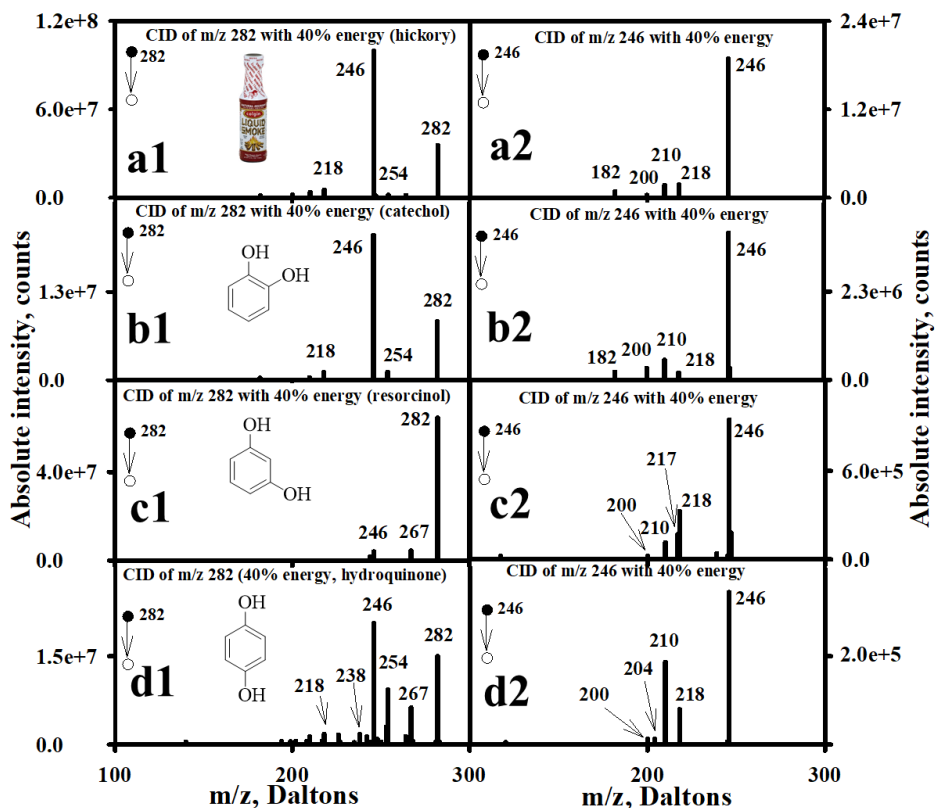


Figure 4.4. MS/MS of m/z 282 of indophenol from Hickory, *ortho*-, *meta*-, and *para*-hydroxyphenol, respectively, with CID energy of 45%.

The peak at m/z 296 is assigned to methoxyphenol. Figure 4.5 shows full MS and deconvoluted MS of the indophenol reaction formed by guaiacol (Figure 4.5a1 and 4.5a2), 3-methoxyphenol (Figure 4.5b1 and 4.5b2), and 4-methoxyphenol (Figure 4.5c1 and 4.5c2). m/z 296 product is formed by both 2-methoxyphenol and 3-methoxyphenol, whereas 4-methoxyphenol gives peak at m/z 266 and 388. The latter peak results from an additional adduct for the *para*-isomer (Chapter 3 and Chapter 7)³⁷ and indicates the presence of 4-methoxyphenol in the mixture.

The spectra from Hickory liquid smoke does not have any peak at m/z 388, indicating the absence of 4-methoxyphenol.

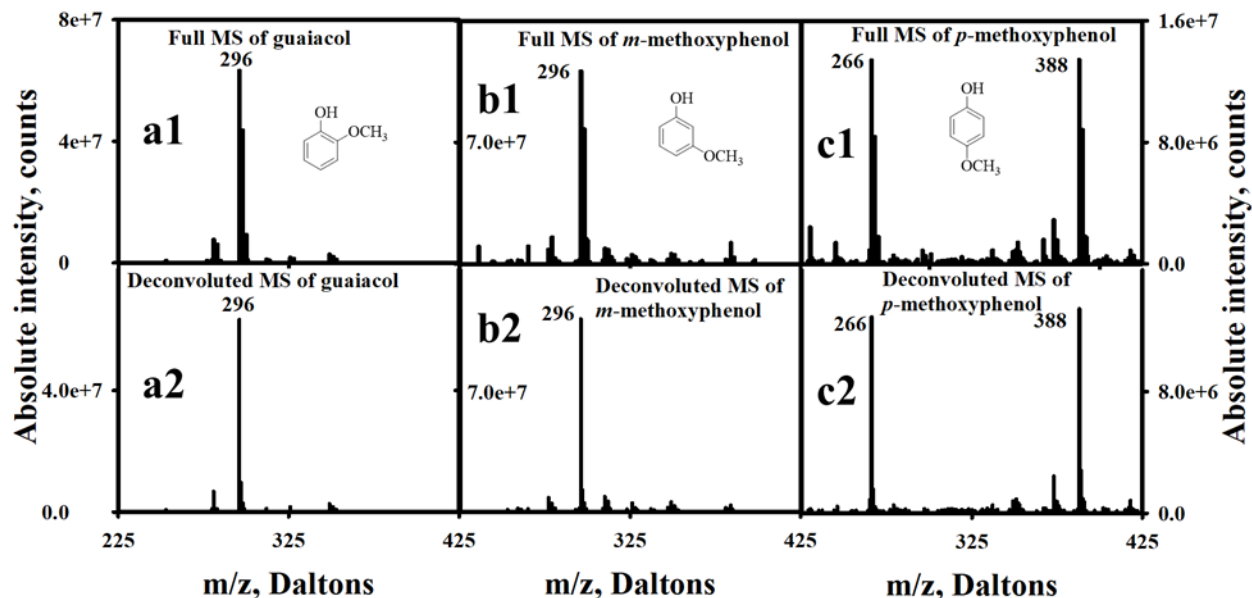


Figure 4.5. (From left to right) Full MS (top) and deconvoluted MS (bottom) of *ortho*-, *meta*-, and *para*-methoxyphenol, respectively. All of them give indophenol peak at m/z 296. In addition, *p*-methoxy phenol gives a characteristic peak among these isomers at m/z 388.

Indophenols forms at m/z 296 from Hickory liquid smoke and two methoxyphenol isomers are showing in Figure 4.6. CID having 32% energy is used in each case. Tandem mass of this ion from Hickory gives ions at m/z 296 and 281 with more than 5% intensity of the base peak. There are couple of peaks at m/z 158, 196, and 223 and 268 though their intensity is lower than 5%. Among the isomers, only *ortho*- gave fragment ions similar to what we have from Hickory. In addition of these peaks, *meta*-isomers gave additional fragment at m/z 122 Daltons. These results are summarized in Table 4.1. Thus, we presumably identified m/z 296 of Hickory due to the presence of *o*-methoxyphenol because of the absence of fragment at m/z 122 though we could not identify the formation of peaks at m/z 158, 196, and 223 and 268.

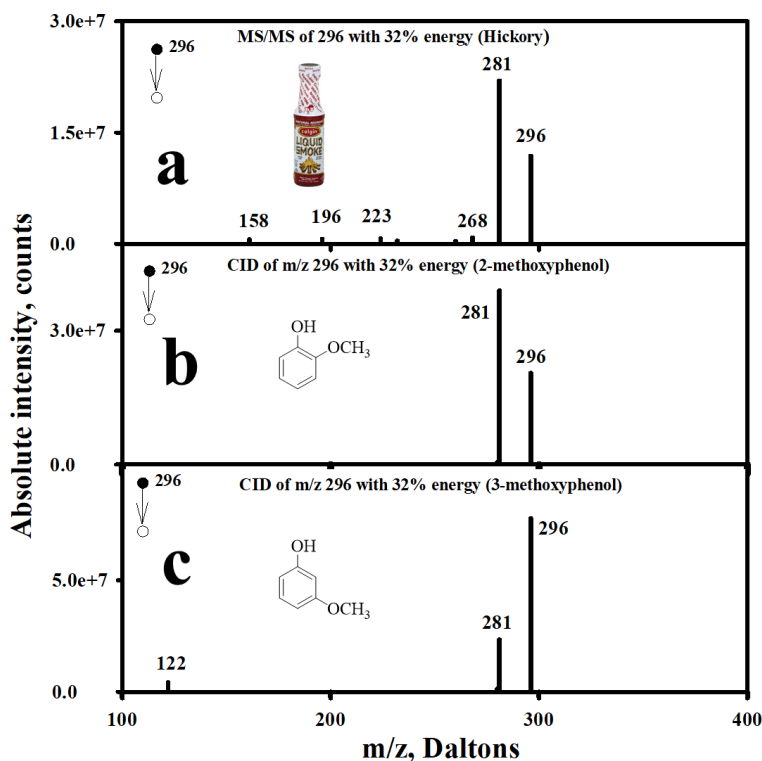


Figure 4.6. MS/MS of m/z 296 of indophenols formed by Hickory liquid smoke, *o*-, and *m*-methoxyphenol. CID energy of 32% is used for all experiments. *m*-isomer can be distinguished by the appearance of daughter ion at m/z 122.

The product at m/z 326 in Hickory liquid smoke is assigned to dimethoxyphenol. Figure 4.7 shows the full MS and deconvoluted MS of 2,6-dimethoxyphenol (a1 and a2), 2,3-dimethoxyphenol (b1 and b2), 2,5-dimethoxyphenol (c1 and c2), and 3,5-dimethoxyphenol (d1 and d2). All of them gave indophenols spectra at m/z 326 as base peak when reacted with the Gibbs reagent. In addition, there are few more minor peaks which were not important for this work.

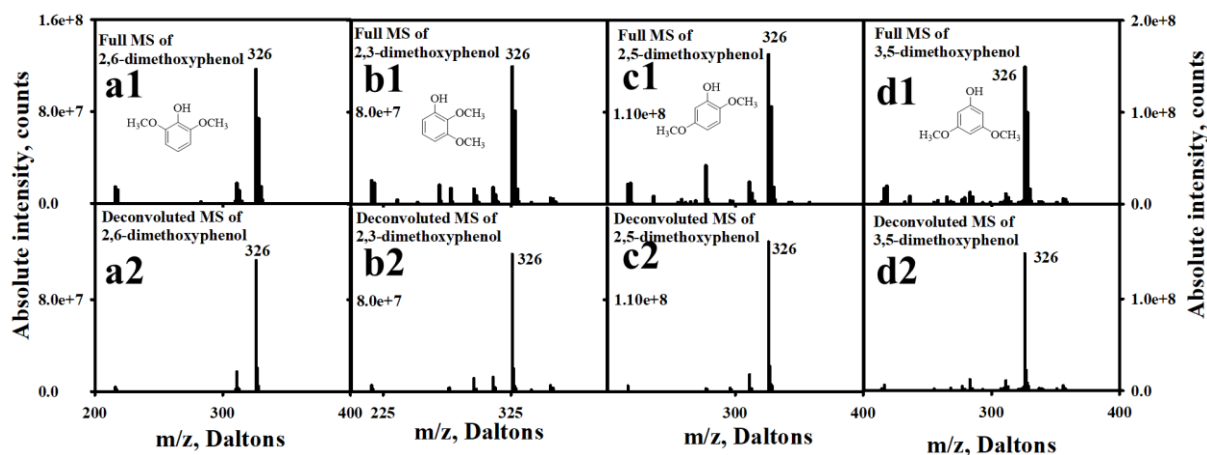


Figure 4.7. Full MS (top) and deconvoluted MS (bottom) of 2,6-, 2,3-, and 2,5-dimethoxyphenol, respectively.

Indophenol formation reactions for other two isomers, 2,4- and 3,4- dimethoxyphenols, are shown in Figure 4.8. In both cases, we observed complex reaction patterns. Both of them forms indophenols at m/z 296 by substituting at *para*-position and condensation product (CP) at m/z 488 (Chapter 7)³⁷ along with additional peaks. The product at m/z 414 from 3,4-dimethoxyphenol (Figure 4.9b1 and 4.9b2) is unknown and this could be due to the side reaction. In addition, we found minor indophenol m/z 326 only from the later isomer. This could be due to the *ortho*-substitution. In both cases, these phenols gave characteristic peaks at m/z 448 Daltons. Thus, the formation of this peak tells us about the presence of either of these two phenols. The spectra of Hickory liquid smoke do not contain a peak at m/z 488, indicating it does not have these compounds.

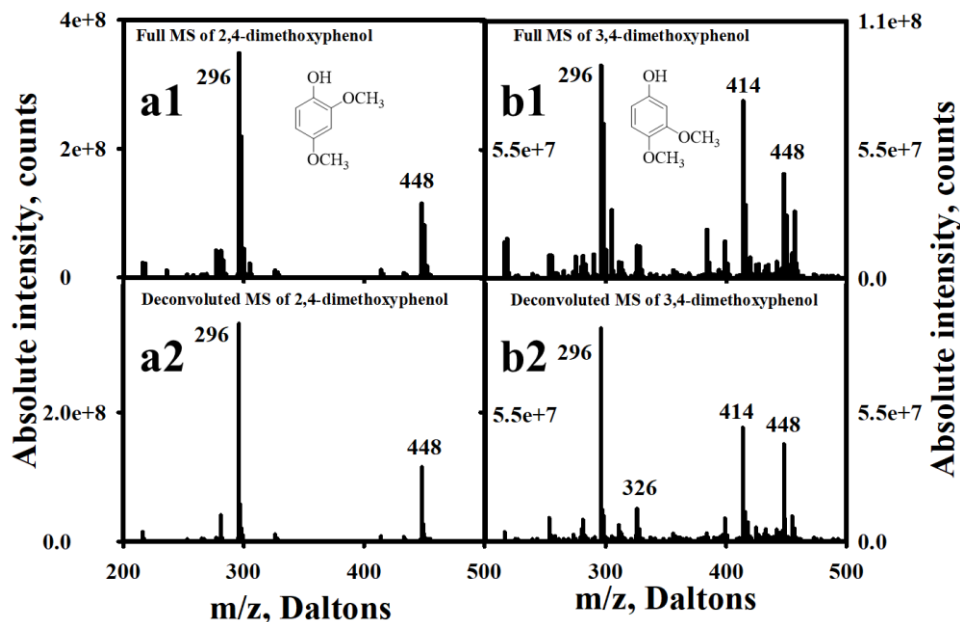


Figure 4.8. Full MS (top) and deconvoluted MS (bottom) of 2,4-, and 3,4-dimethoxyphenol, respectively.

By tandem mass spectrometry, it could be possible to distinguish between indophenols (m/z 326) formed by any of the other four dimethoxyphenols. Figure 4.9 shows results of MS/MS and MS³ experiments of this indophenols at 35% and 30% collision energy, respectively. In all cases, we only considered peaks having intensity more than 5% of the base peak of corresponding experiment. 2,6- and 2,5-dimethoxyphenol gave product ions at m/z 326 and m/z 311 with 35% collision energy (Figure 5.9b1 and 5.9d1, respectively), whereas 2,3- and 3,5-dimethoxyphenol gave additional fragments at m/z 296 for the 2,3-isomer and m/z 152, and m/z 283 for the 3,5-isomer (Figure 5.9c1 and 5.9e1). MS³ experiments helped to distinguish individual phenol from these pairs. For example, MS³ of 2,6-isomer gave fragments at 232, 260, 268, 283 and 296 Daltons (Figure 5.9b2). On the other hand, 189, 260, 268, 280, 282, 296 and 310 Daltons fragments were found when doing MS³ in the case of 2,5-dimethoxyphenol (Figure 5.9d2). Similarly, the 2,3- and 3,5-isomers were characterized by their MS/MS/MS signals. For instance, considering only more than 5% intensity of the base peak, 2,3-isomer gave a peak only at m/z 296, but with similar

conditions the 3,5-isomer gave a peak at m/z 283 and 310. Though both of them gave additional peaks at m/z 275 and 310 for the first case and m/z 268, 275 and 295 for later case, their intensities are less than 5% of the corresponding base peaks. These results are listed in Table 4.1. Thus, the isomers can be identified by using MS/MS and MS³ experiments.

MS/MS and MS³ in the case of Hickory gives ions at m/z 311 and 326 in MS/MS and m/z 232, 260, 268, 283, 296 and 311 in MS³ experiments, respectively (Figure 4.9a1 and 4.9a2, respectively). The formation of m/z 311 upon CID is the result from methyl loss, which is the most common fragment pathway upon dissociation for all of the isomers. But, the MS³ spectrum has characteristic peaks (m/z 232, 260, 268, 283, 296 and 311), with intensities that match those for the 2,6-dimethoxy isomer. In contrast, all other isomers give their distinguishable peaks in similar condition. For example, 2,3-dimethoxyphenol gives peak at m/z 296 in MS/MS experiment, 2,5-dimethoxyphenol gives 189, 280, 282, and 310 in MS³ experiment, and finally, 3,5-dimethoxyphenol gives peak at m/z 152 in its MS/MS experiment. Thus, comparing with all MS/MS and MS³ results we conclude the presence of syringol in Hickory liquid smoke as the results fairly match with only from this isomer.

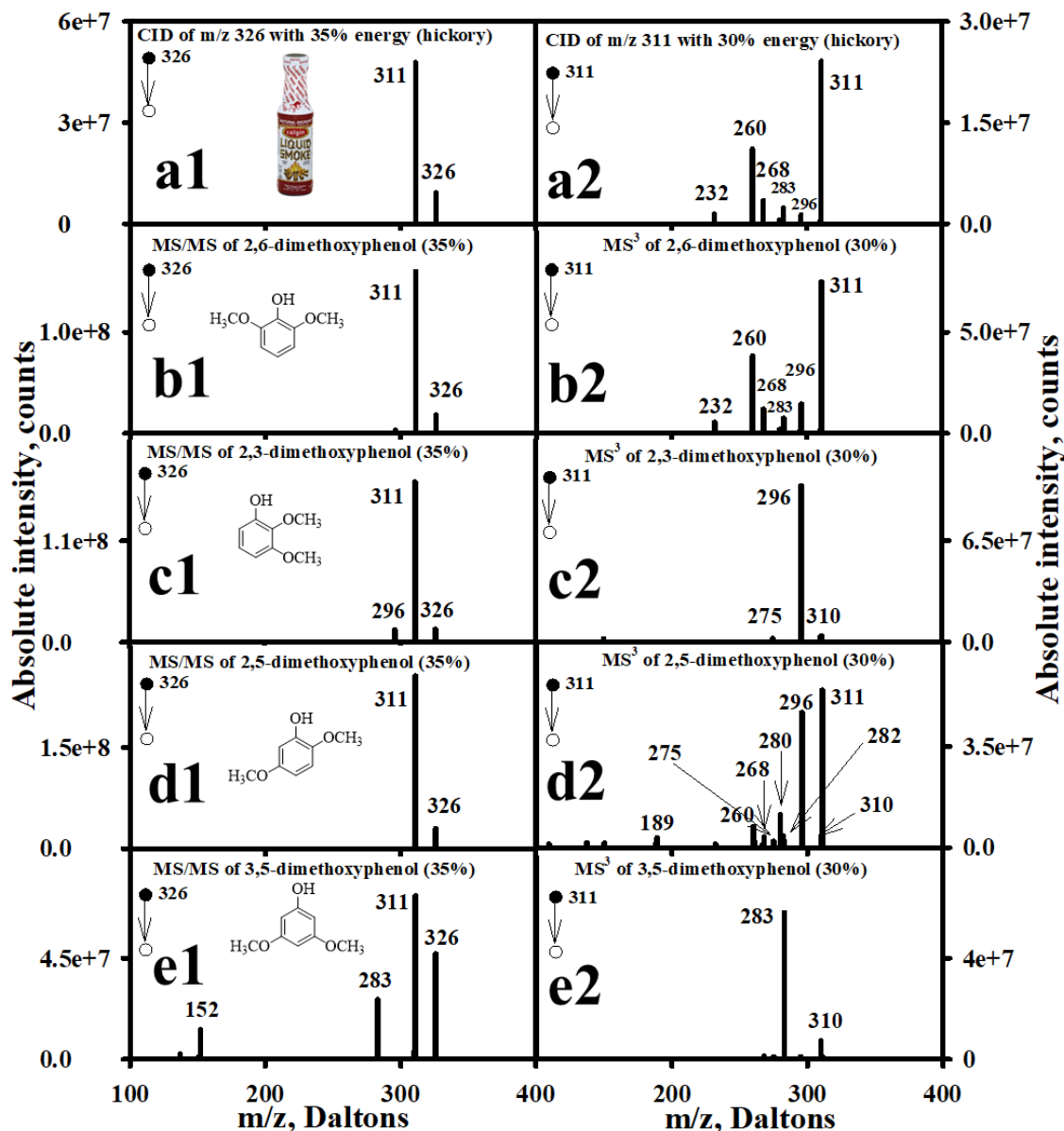


Figure 4.9. (From top to bottom) MS/MS (left) and MS/MS/MS (right) of indophenols formed from m/z 326 from Hickory, 2,6-, 2,3-, 2,5-, and 3,5-dimethoxyphenols, respectively. The collision energy for MS/MS is 35% and for MS³ is of 30%.

The other three liquid smokes were analyzed in the similar way. In case of apple wood analysis, 8 mL liquid smoke was taken for a 15 mL reaction mixture to improve signal intensity, whereas all other three cases only 2 mL sample was taken for same volume of reaction mixture. Figure 4.10 shows the full MS and deconvoluted MS of Mesquite (Figure 4.10a1 and 4.10a2),

Pecan (Figure 4.10b1 and 4.10b2), and Apple (Figure 4.10c1 and 4.10c2) liquid smokes having internal standard (THN, m/z 320). After deconvolution, we have significant peaks at m/z 282, 296 and 326. All other peaks have intensity of bellow 10% compare to the base peaks of the corresponding spectrum and unanalyzed as those are insignificant in this work.

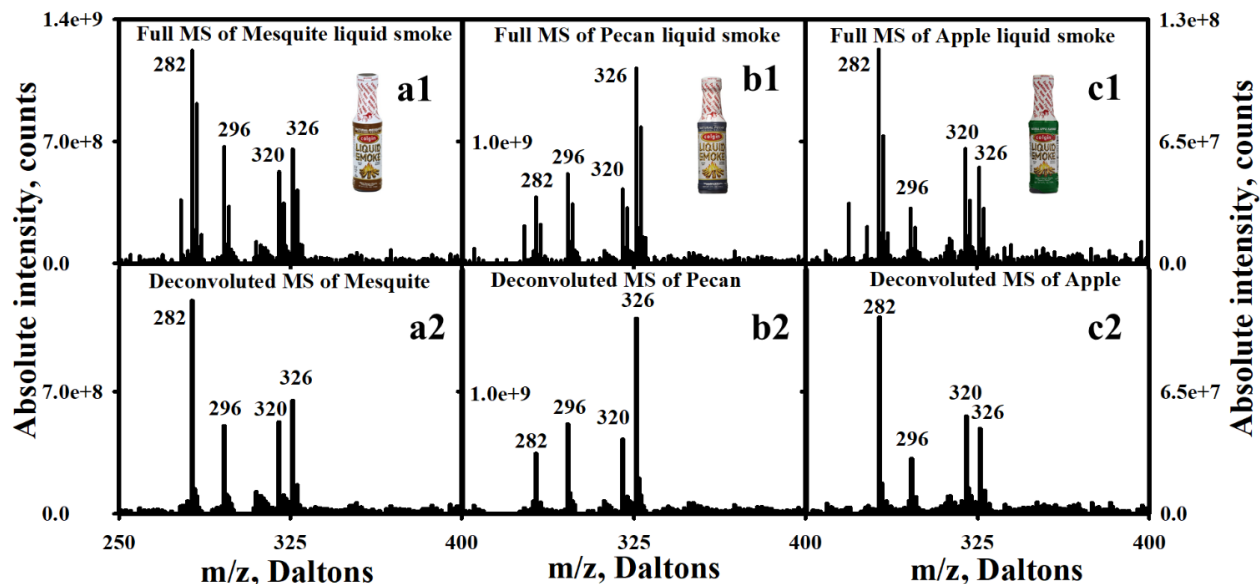


Figure 4.10. (From left to right) Full MS and deconvoluted MS of Mesquite, Pecan, and Apple liquid smokes, respectively.

Peaks of these liquid smokes also identified by comparing fragment ions with from authentic samples as before. In brief, Figure 4.11 shows MS² and MS³ of m/z 282 from these three different liquid smokes and, as before, we are considering peaks having intensity more than 5% of the base peak of the corresponding spectra. All three samples give peaks at m/z 246, 282 in MS² and 182, 210, 218, 246 in MS³. In addition, Pecan and Apple have fragment ions at m/z 218 in MS² experiment. We have found exactly same fragments in authentic indophenol from catechol experiment and other tow isomers gives different fragment ions. In addition of these ions, catechol gave more ions (m/z 218, 254 in MS² and m/z 200 in MS³) over 5% intensity. We had similar fragments in the liquid smoke samples though the intensities were lower than our threshold limit.

Based on the above findings, we can conclude the presence of catechol in all analyzed liquid smokes as all of them were missing all characteristic fragments for resorcinol and hydroquinone.

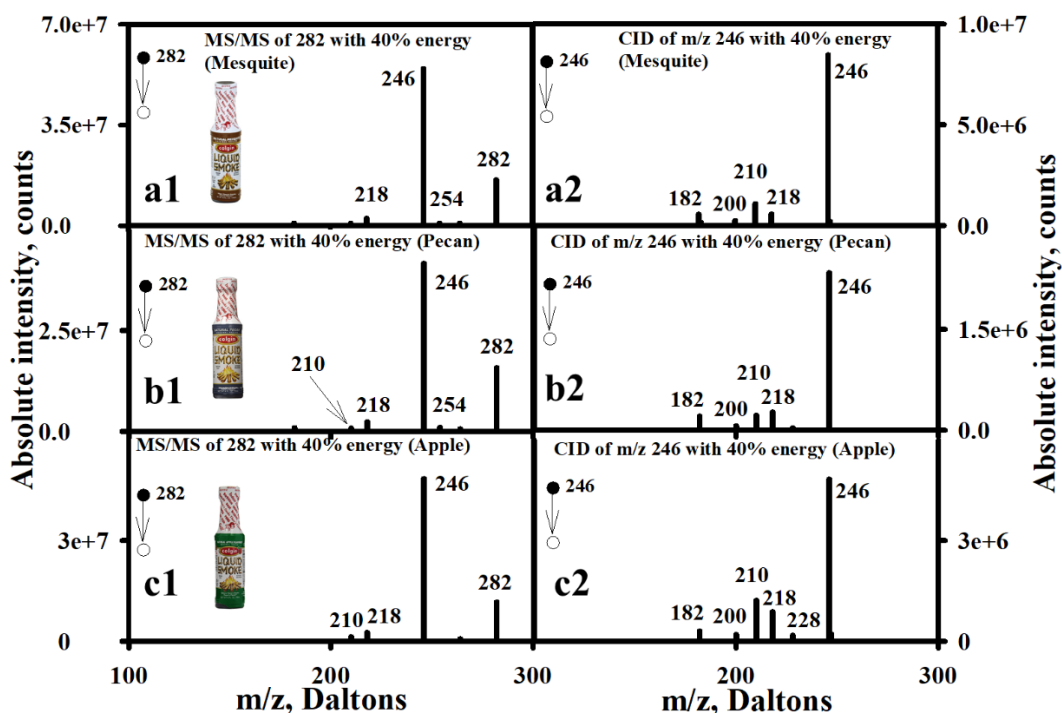


Figure 4.11. (From top to bottom) MS/MS (left) of m/z 282 (right) of Mesquite, Pecan, and Apple liquid smokes, respectively, at CID energy of 32%.

Figure 4.12 shows the 32% energy CID fragment ions from m/z 296 of Mesquite, Pecan, and Apple liquid smokes. All of them give ions at m/z 260, 281, 296 above our threshold level (Apple gives additional peak at m/z 268) along with more fragments with less than 5% intensity. The low intensity ions could form from the fragmentation of other untreated phenolic compounds. However, in all cases we did not see characteristic ion (m/z 122) for 3-methoxyphenol. Also, indophenol having m/z 388 Dalton is missing in the full MS and deconvoluted MS, which forms from 4-methoxyphenol. Thus, the formation of indophenol at m/z 296 in these three liquid smokes is due to the presence of guaiacol.

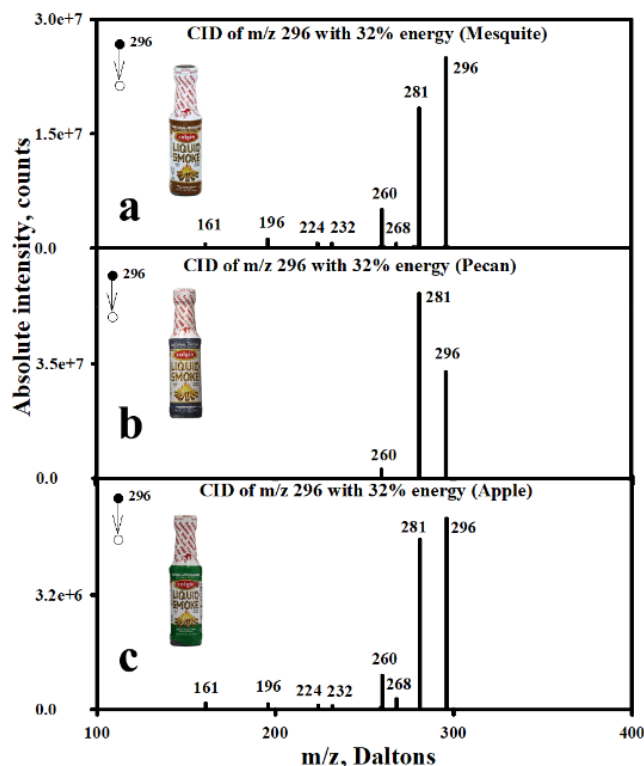


Figure 4.12. (Top to bottom) MS/MS of m/z 296 of Mesquite, Pecan, and Apple liquid smokes, respectively, at CID energy of 32%.

Similarly, MS² and MS³ of m/z 326 from these three liquid smokes are shown in Figure 4.13. m/z 311, 326 ions are formed in each of these liquid smokes in their MS² experiment with 35% energy and m/z 232, 260, 268, 283, 296, and 311 ions formed in MS³ with 30% energy. These fragmentation ions match exactly with what we had from the similar experiment of 2,6-dimethoxyphenol or syringol. In addition, the characteristic fragments for all other dimethoxy isomers are missing for the liquid smokes (m/z 296 in MS² for 2,3-dimethoxyphenol, m/z 189, 280, 282, 310 in MS³ of 2,5-dimethoxyphenol, and m/z 152 and 283 in MS² of 3,5-dimethoxyphenol). Finally, we did not see any formation of indophenols having m/z 488 which rules out the presence of *para*-substituted dimethoxyphenol. Thus, in all of them the peak at m/z 326 is due to the presence of indophenols formed by syringol.

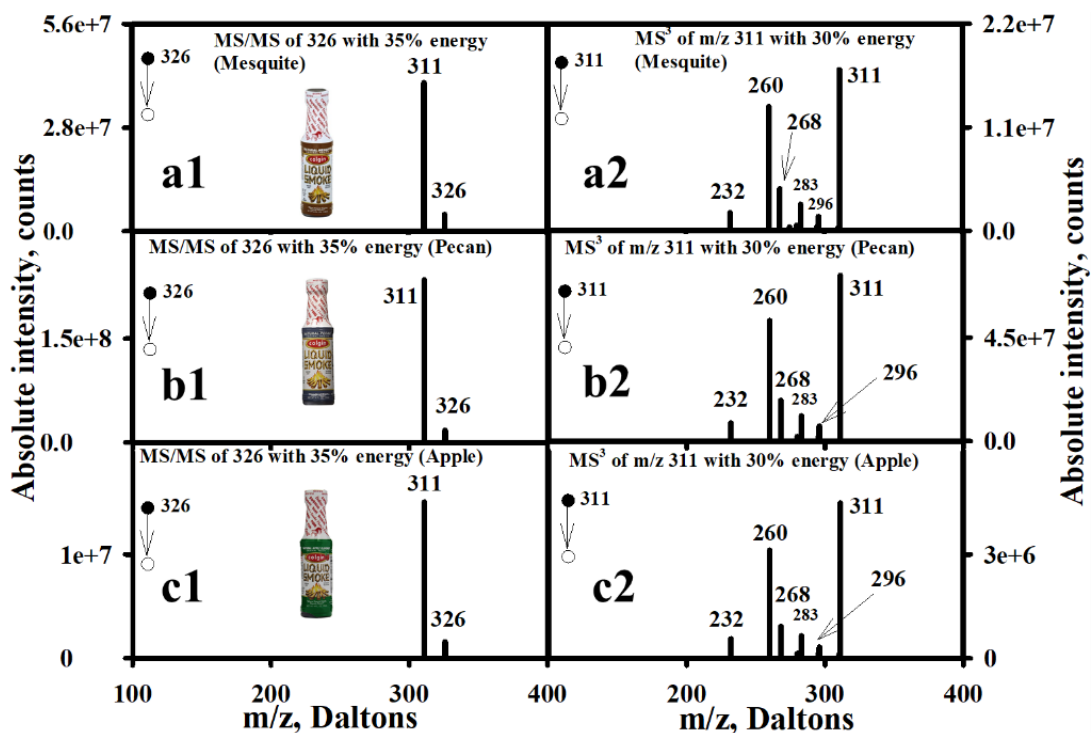


Figure 4.13. (From top to bottom) MS/MS (left) and MS³ (right) of indophenols formed at m/z 326 from Mesquite, Pecan, and apple liquid smokes, respectively.

Table 4.1. Tandem mass spectrometry of indophenols formed from the reaction of Gibbs reagent and dihydroxybenzene, methoxyphenol, and dimethoxyphenol isomers, and four different flavours of liquid smoke. CID fragmentation (peaks with intensity of more than 5% of the base peak).

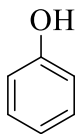
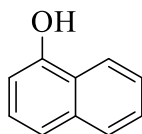
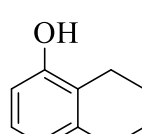
Reactant ion (m/z)	CID energy (%)	Fragment ions (m/z)
Catechol		
282	40	218, 246, 254, 282
246	40	182, 200, 210, 218, 246
Resorcinol		
282	40	246, 267, 282
246	40	210, 217, 218, 246, 247, 325
1,4-dihydroxybenzene		
282	40	210, 218, 226, 238, 242, 246, 253, 254, 264, 266, 267, 282
246	40	210, 218, 246
2-Methoxyphenol		
296	32	281, 296
3-Methoxyphenol		
296	32	122, 281, 296
2,6-dimethoxyphenol		
326	35	311, 326
311	30	232, 260, 268, 283, 296, 311
2,3-dimethoxyphenol		
326	35	296, 311, 326
311	30	296
2,5-dimethoxyphenol		
326	35	311, 326
311	30	189, 260, 268, 280, 282, 296, 310, 311
3,5-dimethoxyphenol		
326	35	152, 283, 311, 326
311	30	283, 310
Hickory		
282	40	218, 246, 282
246	40	210, 218, 246
296	32	281, 296
326	35	311, 326
311	30	232, 260, 268, 283, 296, 311
Mesquite		
282	40	246, 282
246	40	182, 210, 218, 246
296	32	260, 281, 296
326	35	311, 326
311	30	232, 260, 268, 283, 296, 311

Table 4.1 continued

Pecan		
280	40	218, 246, 282
246	40	182, 210, 218, 246
296	32	260, 281, 296
326	35	311, 326
311	30	232, 260, 268, 283, 296, 311
Apple		
282	40	218, 246, 282
246	40	182, 210, 218, 246
296	32	260, 268, 281, 296
326	35	311, 326
311	30	232, 260, 268, 283, 296, 311

4.3.2 Internal standard for the analysis

To quantify the concentration of phenols, we include an internal standard in the analysis. Though may have a variety of possibility as an internal standard, we started with the phenol (**1**), 1-naphthol (**2**) and 5,6,7,8-tetrahydro-1-naphthol (THN) (**3**) as it reacts with Gibbs reagent with about the same efficiency as do guaiacol and syringol, and the indophenol product has a mass that is adequately distinct from those of the substrates so to avoid any signal overlap. Figure 4.14 shows the full mass spectrum (4.14a) and deconvoluted mass spectrum (4.14b) of the Gibbs product from equimolar of these three compounds. Phenols forms indophenol at m/z 266, whereas indophenols from 1-naphthol and 5,6,7,8-tetrahydro-1-naphthol give peak at m/z 316 and 320, respectively. Though the reaction was carried out with an equimolar mixture of these three compounds, THN gives more intense (i.e., more sensitive) peak compare to other two and does not overlap with the analyte peaks. Thus, it was used as internal standard in this work.

**1****2****3**

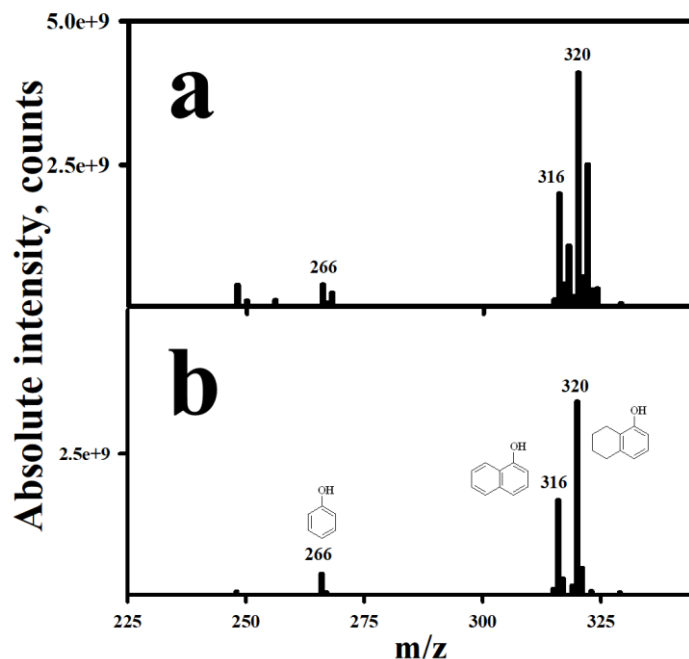


Figure 4.14. ESI mass spectra of products of phenol, 1-naphthol, and 5,6,7,8-tetrahydro-1-naphthol (THN) reaction with Gibbs reagent. a) phenol, 1-naphthol, and 5,6,7,8-tetrahydro-1-naphthol and Gibbs reagent mixture in buffer after 5 minutes; b) mixture mass spectrum deconvoluted for the $^{2}\text{-chlorine}$ isotope pattern.

4.3.3 Preparation of calibration curves

After selecting THN as an internal standard, we examined concentration range from 0.1 mg/L to 1 mg/L to find out optimum concentration given the expected substrate concentration in the liquid smoke analysis and found that 0.20 mg/L (1.5 $\mu\text{mol/L}$) final concentration (electrosprayed) gives optimum signal for the analysis of these four liquid smoke samples. Thus, this is the concentration that was used for making calibration curves and for analysis of liquid smoke samples.

To create the calibration curves, the ratio of the intensities of the M^- peak for the Gibbs product of the phenol analyte and the m/z 320 signal of the Gibbs product of the internal standard after 5 minutes of reaction is plotted against the known concentration of the analyte. For example, Figure 4.15a shows the calibration curve for catechol, obtained by plotting

I(m/z282)/I(m/z320) vs catechol concentration. The plot of the ratio of catechol Gibbs product to the internal standard Gibbs product is essentially linear ($r^2 = 0.99$) over the range of catechol concentration from 1.65 – 5.50 mg/L. Similarly, calibration curves for guaiacol and syringol have been found by plotting the ratios, I(m/z 296)/I(m/z 320) and I(m/z 326)/I(m/z 320), respectively vs concentration, as shown in Figures 4.3b and 4.3c. Again, the plots are essentially linear, with r^2 values > 0.99 , over the analyte concentration ranges of approximately 0.10 – 2.00 mg/L.

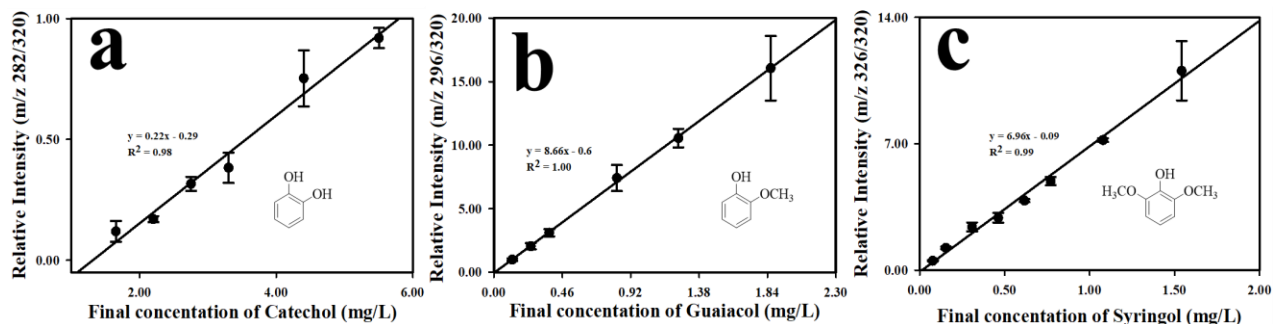


Figure 4.15. Calibration plots for Gibbs product formation compared to the internal standard for a) catechol, b) guaiacol and c) syringol obtained 5 minutes after mixing with the Gibbs reagent. The internal standard, 5,6,7,8-tetrahydro-1-naphthol, is present at a concentration of 0.20 mg/L.

4.3.4 Limit of detection (LOD) and limit of quantification (LOQ)

The limit of detection (LOD) and limit of quantification (LOQ) of catechol, guaiacol, and syringol were determined as following equations, respectively

$$LOD = \frac{3.3 \times \sigma}{S}$$

$$LOQ = \frac{10 \times \sigma}{S}$$

Table 4.2. Limit of detection (LOD) and limit of quantification (LOQ) of catechol, guaiacol, and syringol.

Compound	LOD (mg/L)	LOQ (mg/L)
Catechol	0.51	1.54
Guaiacol	0.11	0.33
Syringol	0.06	0.20

where σ is the standard deviation of the calibration curve and S is the slope of the curve.^{41, 42} The LOD and LOQ of catechol, guaiacol, and syringol with 95% confidence limit was calculated. Table 4.2 shows the findings of these compounds. Here, we can quantify as low as 1.54 mg/L of catechol, 0.33 mg/L of guaiacol, and 0.20 mg/L of syringol, respectively. As shown in Table 4.2, the limits of detection by this using method are all below 1 mg/L. The difference between the detection limits for catechol vs guaiacol and syringol can be attributed to the difference in reactivity due to the presence of the stronger electron donating groups for guaiacol and syringol (Chapter 3).³⁷

4.3.5 Quantification of Colgin Natural Liquid Smoke

Given the calibration curves shown in Figure 4.15, we can quantify the concentrations of the three analytes in a mixture, and our first analysis was applied to commercially available liquid smoke.

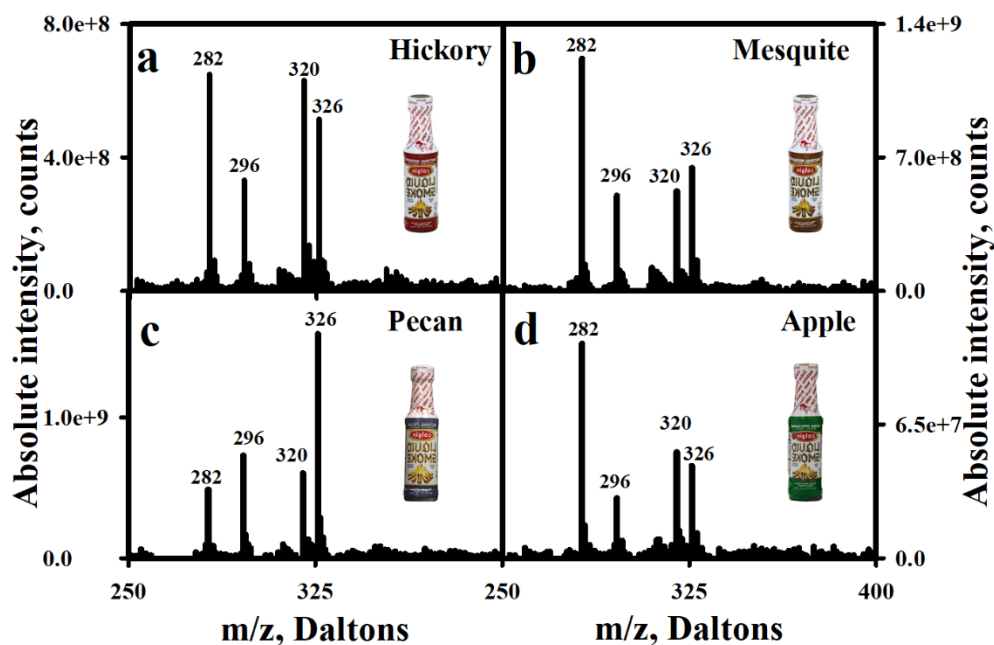


Figure 4.16. Deconvoluted ESI-mass spectra of Gibbs product obtained from Hickory (a), Mesquite (b), Pecan (c) and Apple (d) flavored “colgin® All Natural” liquid smokes obtained by mixing 0.2 mg/L (1.5 μ mol/L) 5,6,7,8-tetrahydro-1-naphthol as internal standard.

We have examined four different flavors of colgin® Natural Liquid Smoke (‘Hickory’, ‘Mesquite’, ‘Pecan’, and ‘Apple’). The deconvoluted ESI mass spectra of the samples containing added internal standard, after mixing with the Gibbs reagent, are showing in Figure 4.16. For all four samples, the significant peaks are observed at m/z 282, m/z 296, m/z 326 and m/z 320, which correspond to the Gibbs reaction products for catechol, guaiacol, syringol and THN, respectively. Differences among the intensities of the analyte peaks, relative to the intensity of that for THN, reflect differences in the phenolic composition of the different flavors of liquid smoke. For example, based on the ratios of m/z 282 to m/z 320, it can be seen that the hickory flavored liquid smoke has approximately twice as much catechol as the mesquite flavor. Similarly, the pecan flavor has much higher concentration of syringol, and slightly more guaiacol. The relative intensities of the applewood smoke suggest relatively more catechol. However, in this case the difference arises from the fact that four times as much analyte was required to obtain the signal

(while the concentration of internal standard was held constant). Therefore, compared to the other three samples, the relative ratios to the internal standard are 4 times smaller.

The absolute concentrations of the three phenols can be obtained by using the calibration curves in Figure 4.15, and the results are listed in Table 4.3, and are the average of 5 measurements.

Table 4.3. Concentration of catechol, guaiacol, and syringol in mg/L in four different flavored colgin® liquid some.

Compound	Pecan	Apple	Hickory	Mesquite
Catechol	2772.68 (83.69)	1486.47 (45.13)	3444.20 (140.81)	6728.43 (168.70)
Guaiacol	71.94 (2.68)	3.651 (0.17)	23.03 (2.65)	61.67 (3.55)
Syringol	209.42 (8.96)	20.90 (0.64)	91.42 (5.02)	94.78 (5.51)

The results show that catechol is the most abundant of the phenols in all four varieties, with concentrations on the order of multiple grams/liter. The other phenols are present in much lower concentrations (milligram/liter).

Reflecting the spectra in Figure 4.16, the mesquite flavor has the highest catechol concentration, of more than 6 g/L, whereas the pecan flavor has the greatest concentration of guaiacol and syringol. Applewood has the lowest concentrations for all of the phenolic components.

A comparison of the results is shown in the graph in Figure 4.17. The graph clearly shows the dramatic difference in the phenolic composition of the applewood flavored liquid smoke. Overall, mesquite has the highest total phenolic content, due to the large amount of catechol. In comparing flavors, mesquite has more catechol and guaiacol than hickory, but about the same amount of syringol. Pecan and mesquite have nearly the same amount of guaiacol, but pecan has

much more syringol and less catechol. Finally, hickory and pecan wood flavors have differences in all three phenols.

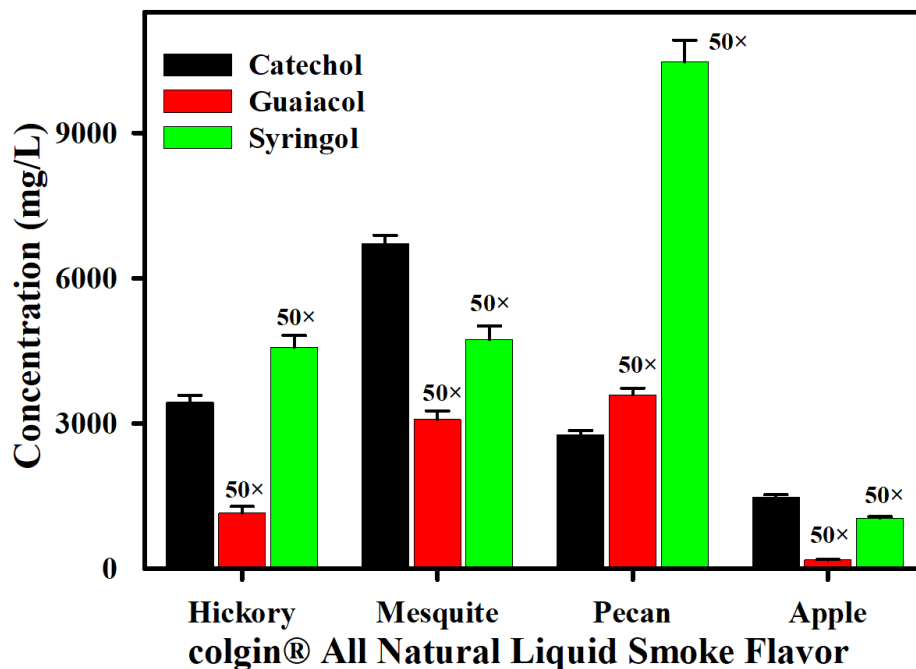


Figure 4.17. Comparison of the concentrations of catechol (black), guaiacol (red), and syringol (green) in mg/L in hickory, mesquite, pecan and apple flavored “Colgin All Natural” liquid smoke. For the better comparison, the concentration of guaiacol and syringol makes fifty times in the bar-chart.

4.4 Discussion

Different research groups reported the presence of high concentration of these three phenol derivatives in variety of commercial liquid smoke samples. Among them, *Soldera* and coworker reported their findings in twelve unknown commercial liquid smokes. She also found that catechol, guaiacol, and syringol were in the top three phenols in those sample.²⁹ To our knowledge, no work has been published of colgin® Natural Liquid Smoke flavored so far. Thus, it may not be an ideal comparison with the published data. Nonetheless, the catechol concentration of pecan (2772.68 ± 83.68 mg/L) and hickory (3444.20 ± 140.81 mg/L) flavored sample are close to that concentration

of sample S2 (3620 ± 55 mg/L); apple flavored (1486.47 ± 45.13 mg/L) has same of sample S1 (1326 ± 224 mg/L). Only the mesquite flavored (6728.43 ± 168.70 mg/L) has at least double the amount of catechol than the highest amount in those twelve sample. However, *Guillen, et al*, reported no presence of catechol in the dichloromethane extracted part of *Salvia lavandulifolia* flavored liquid smoke.³⁴

The syringol concentration of all four different flavored liquid smoke is lower than their reported values except S8 and S12 samples. The big difference in the amount of guaiacol. All of our guaiacol findings are one-third or lower than reported by *Soldera, et al*.²⁹

4.5 Conclusion

While conventional time consuming solvent extraction and spectroscopy has been used for the detection and quantification of phenol derivatives in liquid smoke, the use of the Gibbs reagent gives us indophenol when reacts with phenols followed by mass spectroscopic detection. In addition, the advantage of using deconvolution of mass spectra removes spectra contains only two chlorine atoms and removes all other spectra. Finally, using internal standard we generate calibration curves for the mostly present phenolic compounds, which is using to quantify phenolic compounds in the liquid smoke.

4.6 References

1. Estrada-Muñoz, R.; Boyle, E.; Marsden, J., Liquid smoke effects on *Escherichia coli* O157: H7, and its antioxidant properties in beef products. *Journal of food science* **1998**, *63* (1), 150-153.
2. Darmadji, P., Produksi Asap Rempah Cair dari Limbah Padat Rempah dengan Cara Pirolisa. *Agritech* **1999**, *19* (1999).
3. Guillen, M.; Cabo, N., Study of the effects of smoke flavourings on the oxidative stability of the lipids of pork adipose tissue by means of Fourier transform infrared spectroscopy. *Meat science* **2004**, *66* (3), 647-657.

4. Yuwanti, S., Asap cair sebagai pengawet alami pada bandeng presto (liquid smoke as a natural preservative on" bandeng presto). *Agritech* **2005**, *25* (2005).
5. Maga, J. A., *SMOKE IN FOOD PROCESSING*. CRC-Press: 1988.
6. Darmadji, P., Aktivitas antibakteri asap cair yang diproduksi dari bermacam-macam limbah pertanian. *Agritech* **1996**, *16* (1996).
7. Karseno, K.; Darmadji, P.; Rahayu, K., Daya hambat asap cair kayu karet terhadap bakteri pengkontaminan lateks dan ribbed smoke sheet. *Agritech* **2002**, *21* (1), 10-15.
8. Milly, P.; Toledo, R.; Chen, J., Evaluation of Liquid Smoke Treated Ready-to-Eat (RTE) Meat Products for Control of *Listeria innocua* M1. *Journal of food science* **2008**, *73* (4).
9. Hadiwiyoto, S.; Darmadji, P.; Purwasari, S. R., Perbandingan Pengasapan Panas dan Penggunaan Asap Cair pada Pengolahan Ikan; Tinjauan Kandungan Benzopiren, Fenol dan Sifat Organoleptik Ikan Asap. *Agritech* **2000**, *20* (1), 14-19.
10. Martinez, O.; Salmeron, J.; Guillen, M.; Casas, C., Texture profile analysis of meat products treated with commercial liquid smoke flavourings. *Food control* **2004**, *15* (6), 457-461.
11. Martinez, O.; Salmeron, J.; Guillen, M.; Casas, C., Textural and physicochemical changes in salmon (*Salmo salar*) treated with commercial liquid smoke flavourings. *Food Chemistry* **2007**, *100* (2), 498-503.
12. Gonulalan, Z.; Kose, A.; Yetim, H., Effects of liquid smoke on quality characteristics of Turkish standard smoked beef tongue. *Meat science* **2004**, *66* (1), 165-170.
13. Siskos, I.; Zotos, A.; Melidou, S.; Tsikritzi, R., The effect of liquid smoking of fillets of trout (*Salmo gairdnerii*) on sensory, microbiological and chemical changes during chilled storage. *Food Chemistry* **2007**, *101* (2), 458-464.
14. Guillén, M. D.; Ibargoitia, M. L., GC/MS analysis of lignin monomers, dimers and trimers in liquid smoke flavourings. *Journal of the Science of Food and Agriculture* **1999**, *79* (13), 1889-1903.
15. Naczk, M.; Shahidi, F., *Food Phenolics, sources, chemistry, effects applications*. Technomic Publishing: 1995.
16. Montazeri, N.; Oliveira, A.; Himelbloom, B. H.; Leigh, M. B.; Crapo, C. A., Chemical characterization of commercial liquid smoke products. *Food science & nutrition* **2013**, *1* (1), 102-115.
17. Varlet, V.; Serot, T.; Prost, C., Smoke flavoring technology in seafood. *Handbook of seafood and seafood products analysis* **2010**, 233-254.

18. Clifford, M.; Tang, S.; Eyo, A., Smoking of foods. *Process Biochemistry* **1980**, *15* (5), 8-+.
19. Maga, J. A., The flavor chemistry of wood smoke. *Food Reviews International* **1987**, *3* (1-2), 139-183.
20. Montazeri, N.; Oliveira, A. C.; Himelbloom, B. H.; Leigh, M. B.; Crapo, C. A., Chemical characterization of commercial liquid smoke products. *Food science & nutrition* **2013**, *1* (1), 102-115.
21. Sikorski, Z. E., *Seafood: Resources, nutritional composition, and preservation*. CRC press: 1990.
22. Kim, K.; Kurata, T.; Fujimaki, M., Identification of flavor constituents in carbonyl, non-carbonyl neutral and basic fractions of aqueous smoke condensates. *Agricultural and Biological Chemistry* **1974**, *38* (1), 53-63.
23. Underwood, G. L., High browning liquid smoke composition and method of making a high browning liquid smoke composition. Google Patents: 1992.
24. Toledo¹, R. T., Wood smoke components and functional properties. *Smoked seafood safety* **2007**, 55.
25. Baltes, W.; Wittkowski, R.; Sochtig, I.; Block, H.; Toth, L., The Quality of Foods and Beverages” Vol. 2, “Chemistry and Technology. Academic Press New York: 1981.
26. Hadanu, R.; Apituley, D. A. N., Volatile Compounds Detected in Coconut Shell Liquid Smoke through Pyrolysis at a Fractioning Temperature of 350-420 °C. *Makara Journal of Science* **2016**, 95-100.
27. Guillén, M. D.; Ibargoitia, M. L., Volatile components of aqueous liquid smokes from *Vitis vinifera* L shoots and *Fagus sylvatica* L wood. *Journal of the Science of Food and Agriculture* **1996**, *72* (1), 104-110.
28. SCHWANKE, S. K.; IKINS, W. G.; BREWER, M. S., Phenol compounds identified in selected liquid smokes. *Journal of Food Lipids* **1995**, *2* (4), 239-247.
29. Soldera, S.; Sebastianutto, N.; Bortolomeazzi, R., Composition of phenolic compounds and antioxidant activity of commercial aqueous smoke flavorings. *Journal of agricultural and food chemistry* **2008**, *56* (8), 2727-2734.
30. Simon, R.; de la Calle, B.; Palme, S.; Meier, D.; Anklam, E., Composition and analysis of liquid smoke flavouring primary products. *Journal of separation science* **2005**, *28* (9-10), 871-882.
31. Guillén, M. D.; Manzanos, M. J.; Ibargoitia, M. L., Carbohydrate and nitrogenated compounds in liquid smoke flavorings. *Journal of agricultural and food chemistry* **2001**, *49* (5), 2395-2403.

32. Guillén, M. D.; Ibargoitia, M. L., New components with potential antioxidant and organoleptic properties, detected for the first time in liquid smoke flavoring preparations. *Journal of Agricultural and Food Chemistry* **1998**, *46* (4), 1276-1285.
33. Guillén, M. a. D.; Manzanos, M. a. J., Study of the volatile composition of an aqueous oak smoke preparation. *Food Chemistry* **2002**, *79* (3), 283-292.
34. Guillén, M. D.; Manzanos, M. J., Extractable components of the aerial parts of *Salvia lavandulifolia* and composition of the liquid smoke flavoring obtained from them. *Journal of agricultural and food chemistry* **1999**, *47* (8), 3016-3027.
35. Ettinger, M.; Ruchhoft, C., Determination of Phenol and Structurally Related Compounds by Gibbs Method. *Analytical Chemistry* **1948**, *20* (12), 1191-1196.
36. Mohler, E. F.; Jacob, L. N., Determination of Phenolic-Type Compounds in Water and Industrial Waste Waters Comparison of Analytical Methods. *Analytical Chemistry* **1957**, *29* (9), 1369-1374.
37. Mistry, S.; Wenthold, P. G., Mass spectrometric detection of the Gibbs reaction for phenol analysis. *Journal of Mass Spectrometry* **2018**.
38. Mistry, S.; Wenthold, P. In *Mass spectroscopic analysis of phenol derivatives by Gibbs reaction*, ABSTRACTS OF PAPERS OF THE AMERICAN CHEMICAL SOCIETY, AMER CHEMICAL SOC 1155 16TH ST, NW, WASHINGTON, DC 20036 USA: 2019.
39. Wenthold, P. G.; Mistry, S., Methods of detecting chemicals. Google Patents: 2019.
40. Guillén, M. D.; Manzanos, M. J., Smoke and liquid smoke. Study of an aqueous smoke flavouring from the aromatic plant *Thymus vulgaris* L. *Journal of the Science of Food and Agriculture* **1999**, *79* (10), 1267-1274.
41. Chen, Y.; Mao, P.; Wang, D., Quantitation of Intact Proteins in Human Plasma Using Top-Down Parallel Reaction Monitoring-MS. *Analytical chemistry* **2018**.
42. Guideline, I. H. T. In *Validation of analytical procedures: text and methodology Q2 (R1)*, International Conference on Harmonization, Geneva, Switzerland, 2005; pp 11-12.

CHAPTER 5. HOW SMOKEY THE WHISKEY IS: A QUANTITATIVE APPROACH ON CHEMISTRY ASPECT

5.1 Introduction

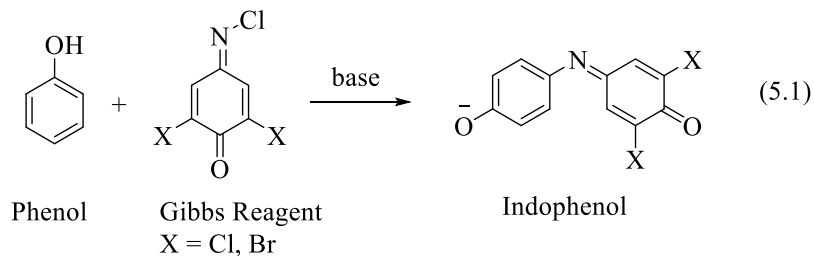
Phenolic compounds are a significant part of the aroma of foodstuffs and alcoholic beverages. For instance, it is known that the presence of phenolic compounds is high in roasted and smoked products.¹⁻³ Alcoholic beverages, beers, wines, and matured, distilled spirits also contain those type of compounds.^{4,5} In particular, phenolic compounds are partly responsible for the aroma and the smokiness in Scotch whiskies.¹ The phenolic compounds in whiskies originate from various sources including yeast. During fermentation a great number of different compounds of this type are synthesized by the yeast or are formed as cleavage products.^{6,7} The formation of these phenolic is influenced by the kind of yeast and the fermentation temperature, which effects the taste and flavor of the final product, whiskey. Another profound effect on the aroma and taste of alcoholic beverages is the distillation in the second production stage. The new compounds formed during distillation and the pyrolysis steps have their own individual effects on the aroma.⁶ A third important factor that can modify the aroma is maturing. Some new aroma compounds are formed and others are consumed in chemical reactions during the ageing process.⁸⁻¹⁰ The notable phenolic compounds produced in the above mentioned steps are phenol, cresol, guaiacol, syringol, and eugenol^{1,6,11-15} and the concentration of these species is between 2 ppm to 54 ppm in total. The source of particularly strong, smokey and bitter flavors and aromas found within whiskey depends on the type of phenols present and their amount.

Several methods have been used for the determination and quantification of phenols in whiskies. Masuda, et al. used column and paper chromatography, ultraviolet absorption spectroscopy, and gas chromatography to analyze phenolic aromatic hydrocarbons in different

commercial whiskies.¹⁶ Later on, a few articles were reported on the analysis of whiskey and wine samples by HPLC using a reversed phase C₁₈ column, and phenols were monitored over a range of wavelengths from 250 to 390 nm.^{17, 18} A couple of the limitations of detecting phenols by using this approach is the short absorption range for hundreds of compounds, and the absorption peaks are not very sensitive to substituent groups and isomers of phenol.^{19, 20} In addition, although HPLC is useful for determining phenols it requires a lot of time, money, effort, and equipment. Thus, it may not be an efficient technique in the quality control to processed a large quantity of product samples quickly.^{21, 22} Another requirement of this technique is to have an enormous number of standards to compare with, and it needs a separation step.²³ On the other hand, LC-MS has been used for the analysis of phenolic compounds in whiskey for many years.²⁴⁻²⁶ For instance, atmospheric-pressure photoionization (APPI) LC-MS was used to analyzed different components, including phenols, in whiskey to avoid using ionization by ESI and APCI of relatively nonpolar compounds.²⁴ In addition, Heller, et al. reported using capillary electrophoresis along with LC-MS to study phenolic aldehydes in a whiskey sample.²⁷

Chromatography is commonly used with derivatization techniques to separate free phenols from their isomers. In addition, derivatization of phenols also has an improved sensitivity in detection. For instance, Lehtonen used gas chromatography-mass spectroscopy (GC-MS) to analyze phenols in whiskies after derivatization by 2,4-dinitrophenyl to ethers.^{1, 28} Detection of phenols by derivatization with 2,6-dichloro- or dibromo-4-(chloroimino)cyclohexa-2,5-dien-1-one (Gibbs reagent) to indophenol (eq. 5.1) has been known as a standard technique for a long time.²⁹⁻³² An important feature of the formation of indophenols is the robust color and, thus, it is a common practice to use spectrophotometry to analyze phenols.^{21, 33-46} Though spectrophotometry has been used to detect Gibbs products, it carries a major limitation – the absorption peak is not

very sensitive to substitution of phenol. Thus, it may not be capable of distinguishing between individual substituted phenols.^{21, 22} Therefore, an additional separation step is required for the detection of specific phenol derivatives. However, we may improve the specificity of the Gibbs product by using mass spectrometry (MS) (Chapter 3).²³



Herein, we describe the detection of the Gibbs product in four different commercial Scotch whiskies containing phenols by using simple electrospray-ionization mass spectrometry (ESI-MS). ESI-MS is useful due to the natural anionic characteristics of indophenols. In addition, the great advantage of using MS for the detection of indophenols is that it readily distinguishes between different types of substituted phenols. In this work, we report ESI-MS for indophenols obtained in the Gibbs reaction of simple substituted phenol from Tomintoul, Johnnie Walker, Laphroaig, and Gordo Graham's whiskies and show the quantity of the mostly present components and their effect on taste, flavor, and aroma. The approach of using the Gibbs reagent to form indophenols from phenols in whiskies provides an alternative to previously reported derivatization methods, such as ether formation from phenols in whiskies,^{1, 6, 28} acetylation of the phenols in water sample⁴⁷ or conversion to the imidazolium ether of phenols in jet fuel.⁴⁸ Addition of an internal standard, 5,6,7,8-tetrahydro-1-naphthol (THN), concentrations of the mainly present phenols in the whiskies are readily obtained. In addition, an important advantage of this approach is that because it has characteristic isotopic patterns, non-phenolic components can be removed by deconvolution. In this work, we report ESI-

MS spectra for indophenols obtained from the Gibbs reaction of phenol derivatives present in four different commercial whiskies and show the simultaneous quantification of multiple compounds in them. With this analysis we are able to determine and compare the composition of phenols in them and their contribution in the taste, smokey, and aroma to the whiskies.

5.2 Materials and methods

5.2.1 Chemicals

o-Cresol, guaiacol, syringol, *p*-ethylphenol, phenol, 2-aminophenol, potassium hydrogenphosphate, and Gibb's reagent were obtained from commercial sources and used as received. Absolute ethanol and methanol were "Reagent Grade" and used without further purification. Deionized water was used for the experiment.

5.2.2 Scotch Whiskey Samples

Four different brands of scotch whiskey were purchased from local liquor store and analyzed as received. These are Tomintoul 10 years Scotch Whisky (The Tomintoul Distillery Company Ltd., Ballindalloch, Banffshire, Speyside, Scotland); Johnnie Walker Double Black Blended Scotch Whisky (John Walker & Sons, Kilmarnock, Scotland); Laphroaig Aged 10 Years Islay Single Malt Scotch Whisky (D. JOHNSTON & CO., Laphroaig Distillery, Isle of Islay, Scotland); and Gordon Graham's Black Bottle Blended Scotch Whiskey (Gordon Graham & Co Ltd., Scotland (Figure 5.1).



Figure 5.1. Four different brands of whiskey: (from left to right) Tomintoul 10 years aged; Johnnie Walker Double Black Blended Scotch Whiskey; Laphroaig Islay Single Malt Scotch Whiskey, 10 years aged; and Gordon Graham's Black Bottle Blended Scotch whiskey.

5.2.3 Calibration Curve

10 mmol/L of 5,6,7,8-tetrahydro-1-naphthol, 500 mmol/L of Gibbs reagent (2,6-dichloroquinone-4-chloroimide); and 20 mmol/L of each of *o*-cresol, guaiacol, and syringol were prepared in methanol as standards. Experiments were carried out by adding the required amount of solvent to get final solutions with the desired concentrations.

For calibration reactions, samples were prepared by mixing 100 μ L of Gibbs solution (500 mmol/L) into 10 mL of ethanol with 10 mL of an aqueous solution of potassium phosphate dibasic solution (87 mg, 0.5 mmol) contains 50 μ L (20 mmol/L) methanol solution of 5,6,7,8-tetrahydro-1-naphthole as internal standard and specific volume of methanol solution of any of *o*-cresol, guaiacol, or syringol to get desire concentrations of them. After mixing, the solutions were stirred at room temperature for the 5 minutes, after which 100 μ L of the reaction mixture was diluted to 2.0 mL in water-methanol solution (1:1) for ESI-MS analysis. The concentration of 5,6,7,8-tetrahydro-1-naphthol in the initial solution was chosen so to obtain a concentration of 0.20 mg/L (1.25 μ mole/L) in the final (electrosprayed) solution. Similarly, the concentration of phenols in the initial solution was chosen so to obtain final concentrations of 0.11, 0.22, 0.24, 0.54, and 1.10 mg/L (1.0, 2.0, 2.25, 5.0, 10.0 mmol/L, respectively) of *o*-cresol; 0.03, 0.06, 0.12, 0.25, 0.62, 1.24 mg/L (0.25, 0.50, 1.00, 2.00, 5.00, and 10.00 mmol/L, respectively) of guaiacol; and 0.04, 0.08,

0.15, 0.31, 0.46, and 0.77 mg/L (0.25, 0.50, 1.00, 2.00, 3.00, and 5.00 mmol/L, respectively) of syringol in the final concentration. The regression analysis was done in excel.

5.2.4 Analysis of Whiskey

The analysis of whiskey was carried out by modifying the procedure described previously (Chapter 3 and Chapter 4).^{23, 49, 50} In brief, 87 mg (0.5 mmol) of potassium phosphate dibasic was dissolved in 10.0 mL of the corresponding whiskey and 50 μ L of 10 mmol/L of 5,6,7,8-tetrahydro-1-naphthol was added into the solution as an internal standard. In another portion of 10.0 mL of the same whiskey, 100 μ L of 500 mmol/L Gibbs solution was added. These two solutions were mixed and stirred at room temperature for 5 minutes. After the specific time, 100 μ L of the solution was diluted to 2.0 mL in water-methanol solution (1:1), for ESI-MS analysis. Control experiments were done in each condition and the calculations for the compounds were done by subtracting corresponding values of the control from the whiskey sample experiments. The structures of phenol compounds were confirmed by MS/MS and MS³ experiments and compared, if needed, with authenticate samples of corresponding compounds.

5.2.5 Spectra collection

Electrospray ionization mass spectra were obtained on a commercial LCQ-DECA (Thermo Electron Corporation, San Jose, CA, USA) quadrupole ion trap mass spectrometer, equipped with electrospray ionization (ESI) source. Substrate solutions in a methanol:water mixture (1:1) and introduced into the source directly at a flow rate of 5 μ L/min. Electrospray and ion focusing conditions were varied so that it maximized the signal of the ion of interest.

5.2.6 Spectral analysis

Important advantages of using the Gibbs reagent for derivatization are: (i) the indophenol product is readily ionized and (ii) it can be easily detectable by the isotopic pattern. Therefore, no sample preparation or purification is required for the analysis of the indophenol by ESI-MS. Moreover, the deconvolution of the isotopic pattern for ions containing two chlorine atoms (1:0.648:0.105) can eliminate the peaks that do not contain the Gibbs reagent.²³

5.3 Results

5.3.1 Identification of the phenols in whiskey

We start with one of the smokiest commercial whiskeys, Laphroaig Islay Single Malt Scotch Whiskey (LISMSW), Aged 10 Years (third of Figure 5.1). Figure 5.2a shows the full mass spectra of the Gibbs product of this whiskey including internal standard at m/z 320 (due to the formation of indophenol from 5,6,7,8-tetrahydro-1-naphthol). Figure 5.2b is the deconvoluted product of it. In addition to the internal standard peak (m/z 320), the most noteworthy peaks are m/z 280, 281, 294, 296, 326 and 329. Among these peaks, m/z 280, 296 and 326 are correspond to the indophenols formed from isomers of cresol, methoxyphenol, and dimethoxyphenol, respectively. Among the other peaks, m/z 281 and 294 could be due to the indophenols formed from isomer of aminophenol and ethylphenol or dimethylphenol, respectively. But we could not get any phenol related structure for m/z 329. In this work, we have focused on the analysis of the most significant product at m/z 280, 296 and 326, and do not consider the other products function.

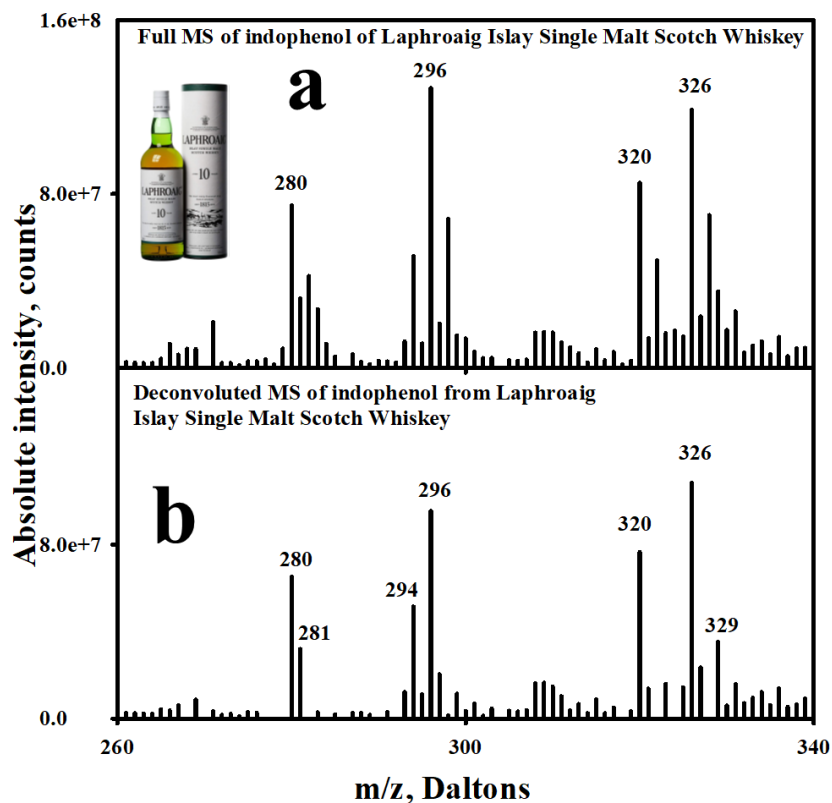


Figure 5.2. Full MS (top) and deconvoluted MS (bottom) of the Gibbs product of Laphroaig Islay Single Malt Scotch Whiskey, Aged 10 Years.

The peak at m/z 280 likely corresponds to the indophenol forms from cresol. The full MS and deconvoluted MS of indophenols from three isomers of cresol (*o*-, *m*- and *p*-) are shown in Figure 5.3. All three isomers give indophenols having m/z 280. Among these three, *ortho*- and *meta*-isomers form exclusively indophenols, while *para*-isomer gives a dominating indophenol peak with low signals of significant number of other products. By using deconvolution, we are able to get almost only m/z 280 for *ortho*- and *meta*-isomers, whereas deconvolution process could not eliminate all of the other peaks for *p*-cresol.

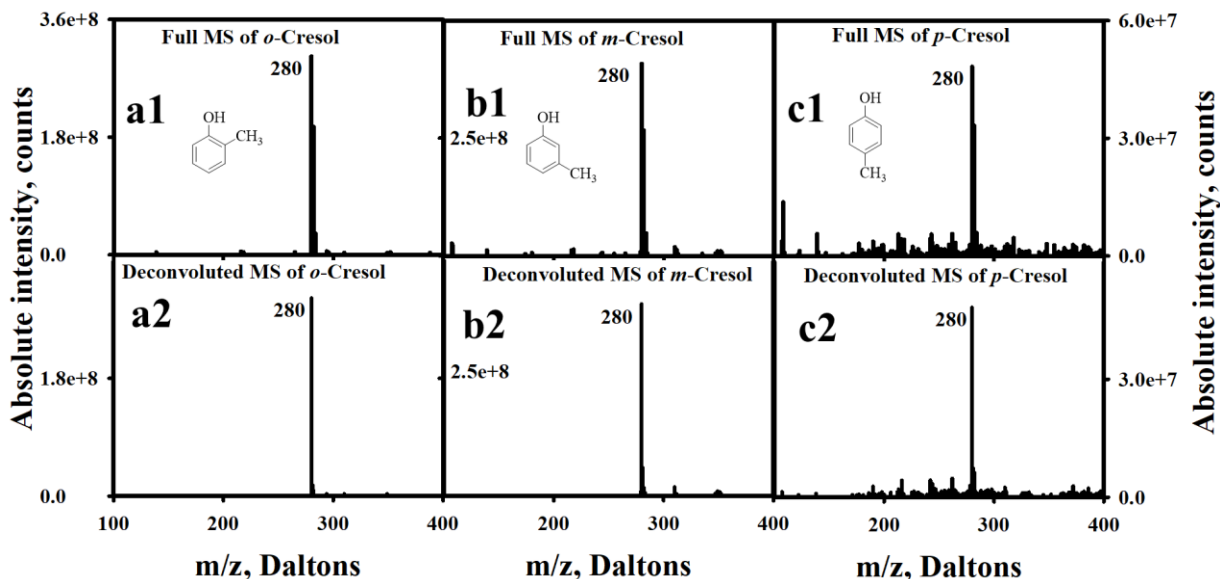


Figure 5.3. Full MS (top) and deconvoluted MS (bottom) of *ortho*-, *meta*-, and *para*-cresol, respectively.

The MS/MS with 45% collision induced dissociation (CID) energy of m/z 280 (indophenols) from Laphroaig and three cresol isomers are shown in Figure 5.4. and Table 5.1 lists the peaks equal to or above 5% of the base peak. Significant signals above that intensity of the base peaks from *o*-cresol are m/z 208, m/z 244, m/z 265 and m/z 280 (Figure 5.4b). Similarly, Figure 5.4c and 5.4d are from *m*-cresol, and *p*-cresol, respectively. With the same CID energy, *m*-cresol gave peaks at m/z 180, 198, 202, 208, 212, 216, 243, 244, 252, 264, 265, 278 and 280 Daltons and *p*-cresol gave peaks at m/z 180, 198, 202, 208, 216, 242, 243, 244, 250, 252, 264 and 280 Daltons. Among these three isomers, only *ortho*-isomer fragments gave the least number of product ions upon dissociation. On the other hand, Figure 5.4a shows fragments of indophenol of m/z 280 for Laphroaig with 45% of CID energy. MS/MS of m/z 280 gave fragment ions of more than 5% intensity of the base peak including not only m/z 208, 244, 265, and 280. In addition, there is a product ion peak at m/z 180 though below 5% intensity. The presence of m/z 208, 244, 265, and 280 product ions match with what we have from *o*-cresol of same experimental condition.

However, the presence of m/z 180 product ion implies the existence of *m*-cresol and/or *p*-cresol. However, in both cases, two characteristic product peaks at m/z 198 and 243 (Figure 5.4c and 5.4d) are missing in Laphroaig spectra (Figure 5.4a, Table 5.1). For the above discussion, we can conclude that the Laphroaig's peak at m/z 280 is mostly due to the formation of indophenol of *o*-cresol and there could be a little (< 5%) presence of either *m*-cresol, *p*-cresol, or a mixture of both.

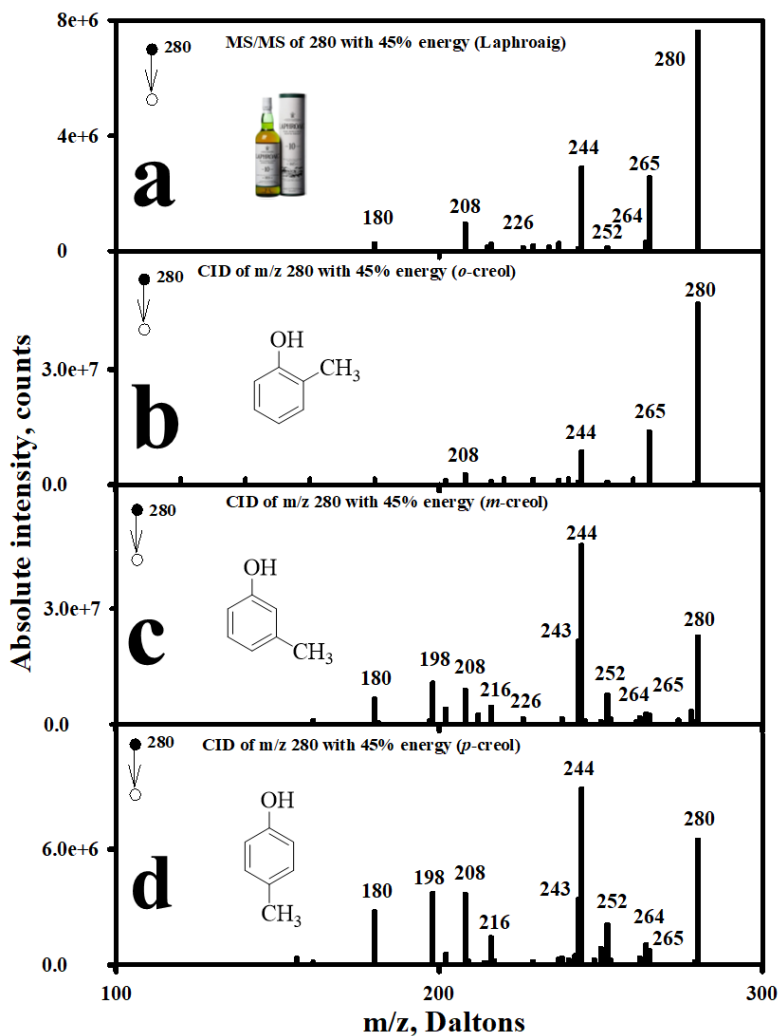


Figure 5.4. (From top to bottom) MS/MS of m/z 280 of indophenol from Laphroaig, *o*-cresol, *m*-cresol, *p*-cresol with CID energy of 45%.

The peak at m/z 296 is assigned to methoxyphenol. Figure 5.5a1, Figure 5.5b1, and Figure 5.5c1 are the full MS and Figure 5.5a2, Figure 5.5b2, and Figure 5.5c2 are the corresponding deconvoluted MS of 2-methoxyphenol (guaiacol), 3-methoxyphenol, and 4-methoxyphenol, respectively. 2-Methoxyphenol and 3-methoxyphenol gave indophenols at m/z 296 Daltons, whereas 4-methoxyphenol gives peak at m/z 266 and 388. The peak at m/z 388 results from an additional adduct for the *para*-isomer (Chapter 7) and indicates the presence of *p*-methoxyphenol in the matrix. The spectrum from Laphroaig does not have any peak at m/z 388, indicating that *p*-methoxyphenol is not present.

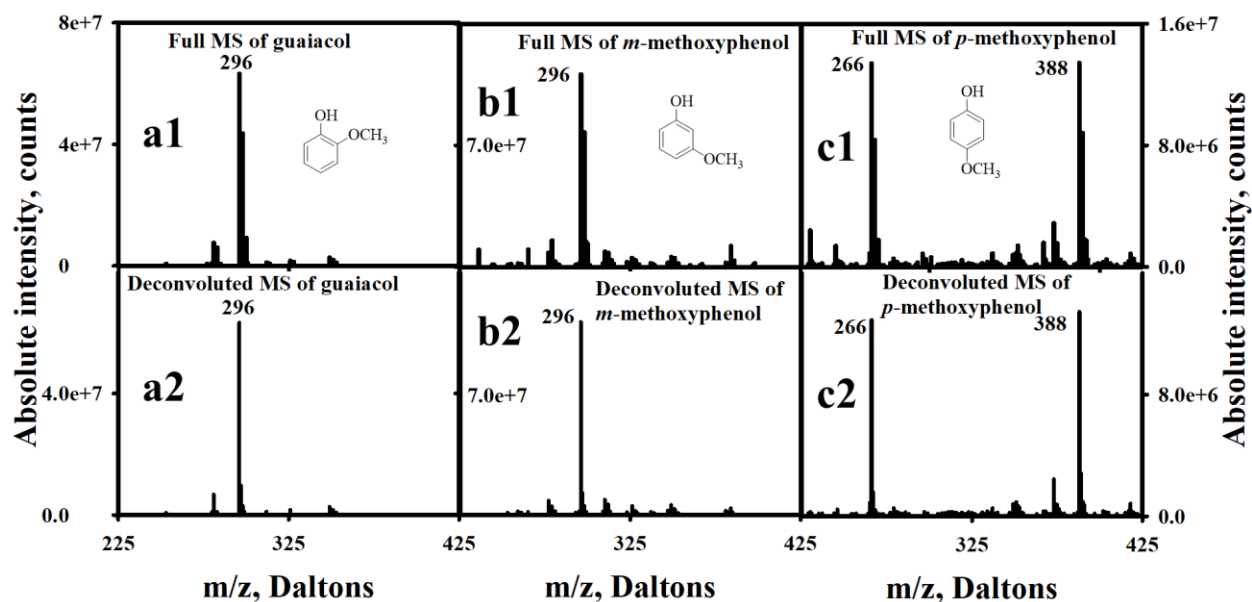


Figure 5.5. (From top to bottom) Full MS (top) and deconvoluted MS (bottom) of *ortho*-, *meta*-, and *para*-methoxyphenol, respectively. The first two isomers give indophenol peak at m/z 296 and *p*-methoxyphenol gives a characteristic peak among these isomers at m/z 388 along with another indophenol at m/z 266.

Figure 5.6 shows the tandem mass spectrometry of m/z 296 from Laphroaig and two methoxyphenol isomers. CID having 32% energy is used in every case. Tandem mass of this ion from Laphroaig gives fragment ions at m/z 296 and 281 with more than 5% intensity of the base

peak. There are couple of peaks at m/z 258 and 260 though the intensity is less than 5% of the base peak. On the other hand, *ortho*-isomer gave product ions having more than 5% intensity of the base peak which were m/z 296 and 281 Daltons, whereas the *meta*- and *para*-isomers gave an additional fragment at m/z 122 Daltons. These results are summarized in Table 5.1. Though we could not identify the formation of peaks at m/z 258 and 260, by comparing CID ions of authentic methoxyphenol isomers with the fragments of m/z 296 from Laphroaig whiskey reactions, we can conclude the presence of guaiacol in it since it is missing peak at m/z 122.

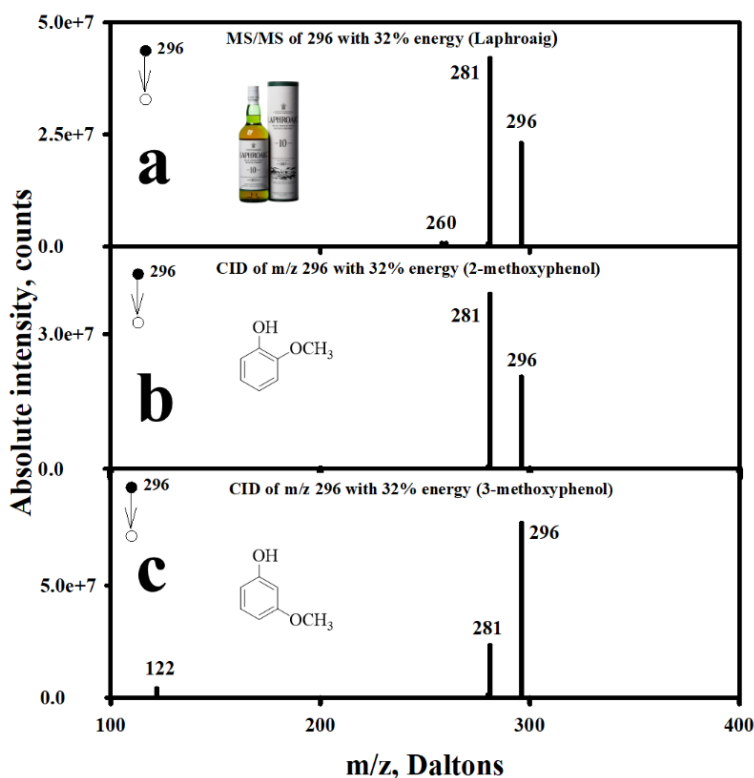


Figure 5.6. (From top to bottom) MS/MS of m/z 296 of indophenols formed by Laphroaig, *o*-, and *m*-methoxyphenol. CID energy of 32% is used for all experiments. *m*-isomer can be distinguished by the appearance of daughter ion at m/z 122.

The product at m/z 326 in the Laphroaig is assigned to dimethoxyphenol. Figure 5.7 shows the full MS and deconvoluted MS of 2,6-dimethoxyphenol (a1 and a2, respectively), 2,3-

dimethoxyphenol (b1 and b2, respectively), 2,5-dimethoxyphenol (c1 and c2, respectively), and 3,5-dimethoxyphenol (d1 and d2, respectively). All of them gave indophenols spectra at m/z 326 as base peak when reacted with the Gibbs reagent. In addition, there are few more unidentified small peaks.

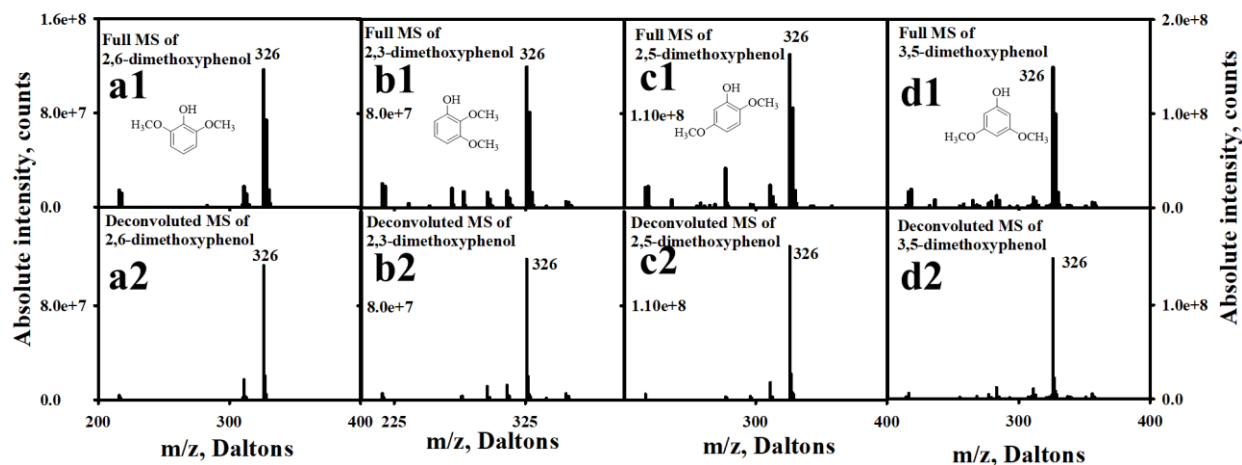


Figure 5.7. (From left to right) Full MS (top) and deconvoluted MS (bottom) of 2,6-, 2,3-, and 2,5-dimethoxyphenol, respectively.

In the case of other two isomers, 2,4- and 3,4- dimethoxyphenol, we observed complex reaction patterns (Figure 5.8). For instance, the first isomer gives mostly peak at m/z 296 and m/z 448. However, 3,4-dimethoxyphenol gives additional products at m/z 326 and 414. In both cases, the base signal was m/z 296, which is believed to be the formation of indophenol by replacement of the methoxy group at the *para*-position (Chapter 7).²³ Interestingly, both of these phenols also gave characteristic peaks at m/z 448 Daltons. Thus, the presence of this peak tells us about the presence of either of these two phenols. The spectrum of Laphroaig does not contain a peak at m/z 488, indicating it does not have these compounds.

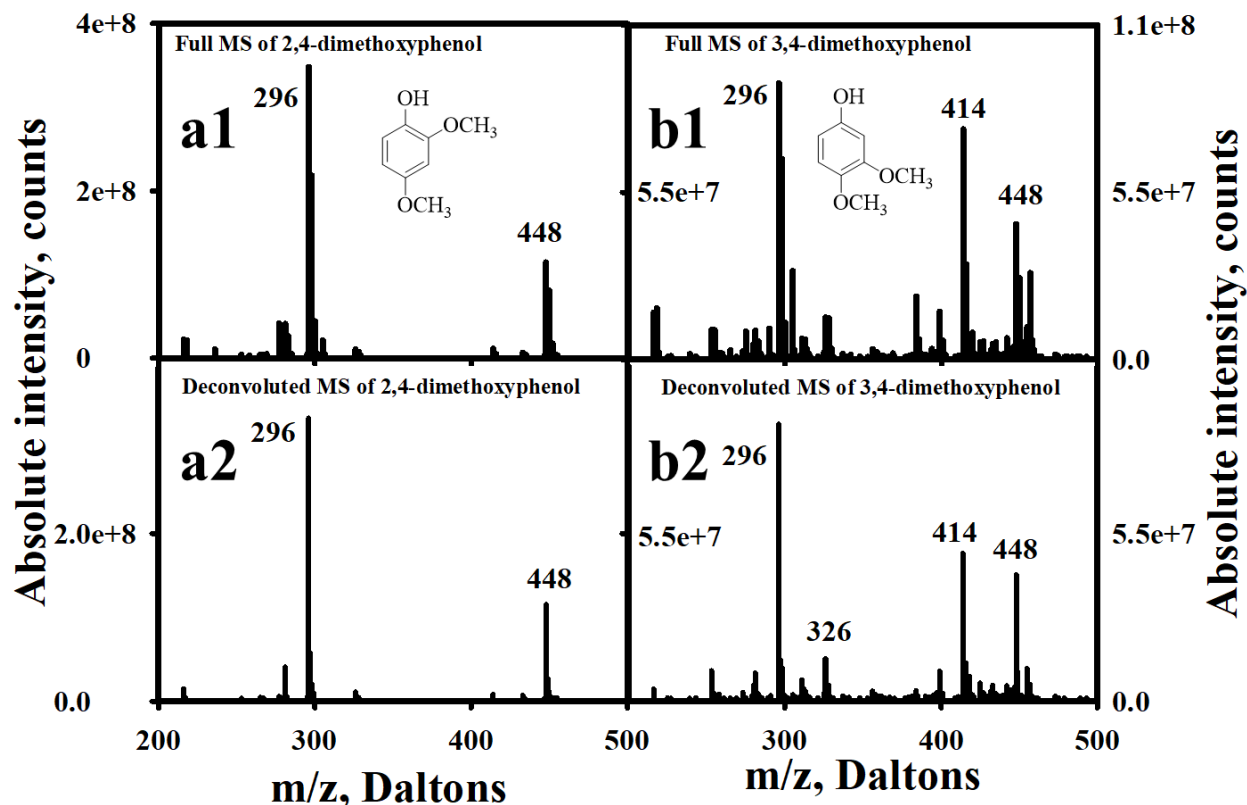


Figure 5.8. Full MS (top) and deconvoluted MS (bottom) of 3,5-, 2,4-, and 3,4-dimethoxyphenol, respectively.

By tandem mass spectrometry, it could be possible to distinguish between indophenols (m/z 326) formed by any of the other four dimethoxyphenols. Figure 5.9 shows the MS/MS (with 35% CID energy) and MS³ (with 30% CID energy) of indophenols from Laphroaig, and authentic samples of 2,6-, 2,3-, 2,5-, and 3,5-dimethoxyphenol. 2,6- and 2,5-dimethoxyphenol gave product ions at m/z 326 and m/z 311 with 35% collision energy (Figure 5.9b1 and 5.9d1, respectively), whereas 2,3- and 3,5-dimethoxyphenol gave additional fragments at m/z 296 for the 2,3-isomer and m/z 152, and m/z 283 for the 3,5-isomer (Figure 5.9c1 and 5.9e1). MS³ experiments helped to distinguish individual phenol from these pairs. For example, MS³ of 2,6-isomer gave fragments at 232, 260, 268, 283 and 296 Daltons (Figure 5.9b2). On the other hand, 189, 260, 268, 280, 282, 296 and 310 Daltons fragments were found when doing MS³ in the case of 2,5-dimethoxyphenol

(Figure 5.9d2). Similarly, the 2,3- and 3,5-isomers were characterized by their MS/MS/MS signals. For instance, considering only more than 5% intensity of the base peak, 2,3-isomer gave a peak only at m/z 296, but with similar conditions the 3,5-isomer gave a peak at m/z 283 and 310. Though both of them gave additional peaks at m/z 275 and 310 for the first case and m/z 268, 275 and 295 for later case, their intensities are less than 5% of the corresponding base peaks. These results are listed in Table 5.1. Thus, the isomers can be identified by using MS/MS and MS³ experiments.

Figure 5.9a1 and 5.9a2 are the MS² and MS³ of m/z 326 and m/z 311, respectively, from the indophenol formed from Laphroaig whiskey. The only product observed upon CID of m/z 326 is m/z 311, resulting from methyl loss, and is the most common fragment pathway upon dissociation for all of the isomers. However, the MS³ spectrum has characteristic peaks at m/z 232, 260, 268, 283 and 296, with intensities that match those for the 2,6-dimethoxy isomer. Although many similar products are observed upon MS³ of 2,5-dimethoxyphenol, the intensities in the Laphroaig spectra are inconsistent with what was found for that isomer. Thus, the fragmentation patterns from Laphroaig exactly matched with those of 2,6-dimethoxyphenol (syringol), and we conclude the peak at m/z 326 was due to the presence of syringol in this whiskey.

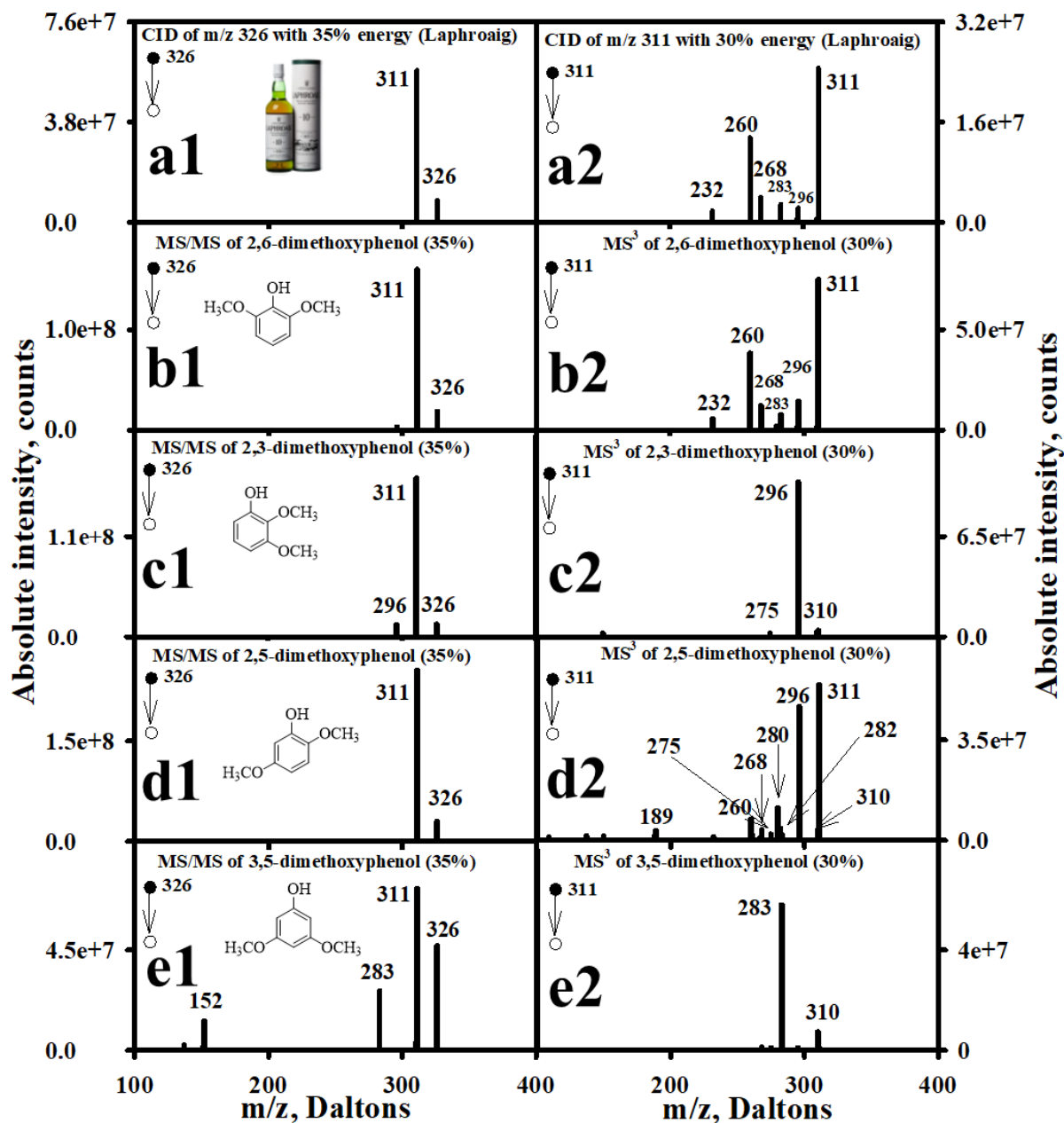


Figure 5.9. (From top to bottom) MS/MS (left) and MS/MS/MS (right) of indophenols formed from 2,6-, 2,3-, 2,5-, and 3,5-dimethoxyphenols, respectively. The collision energy for MS/MS is 35% and for MS³ is of 30%.

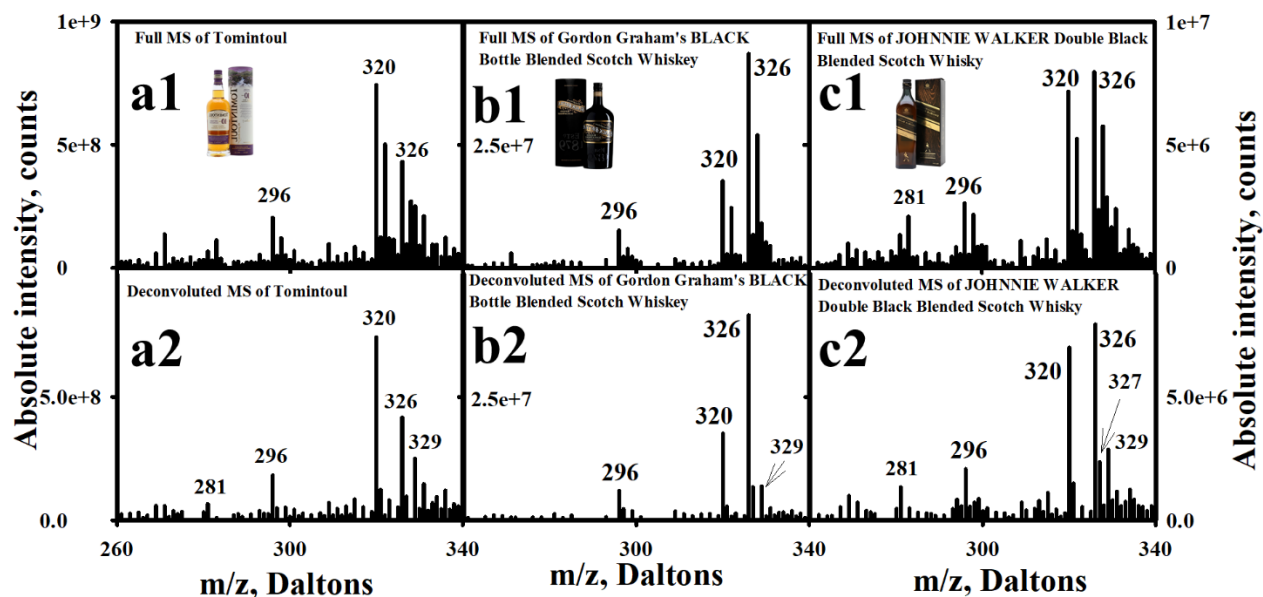


Figure 5.10. (From left to right) Full MS (top) and deconvoluted MS (bottom) of Tomintoul Scotch Whiskey, Gordon Graham's Black Bottle Blended Scotch whiskey and Johnnie Walker Double Black Blended Scotch Whiskey, respectively.

The other three whiskeys were analyzed by using the same approach, and the full MS and deconvoluted MS are shown in Figure 5.10. The Tomintoul whiskey forms significant peaks are m/z 281, 296, 326 and 329 (Fig. 5.10a1 and 5.10a2). Gordon Graham's Black Bottle Blended Scotch Whiskey gives significant peaks at m/z 296, 326 and 329 (Figure 5.10b1 and 5.10b2). Finally, Johnne Walker Double Black Blended Scotch Whiskey gives peaks at m/z 281, 296, 326, 327, and 329 (Figure 5.10c1 and 5.10c2). Among these peaks only m/z 296 and 326 were identified as methoxyphenol and dimethoxyphenols. Other peaks were unidentifiable due to either low signal intensity or could appear due to the isotopic peaks. In all three cases, internal standard gives peak at m/z 320.

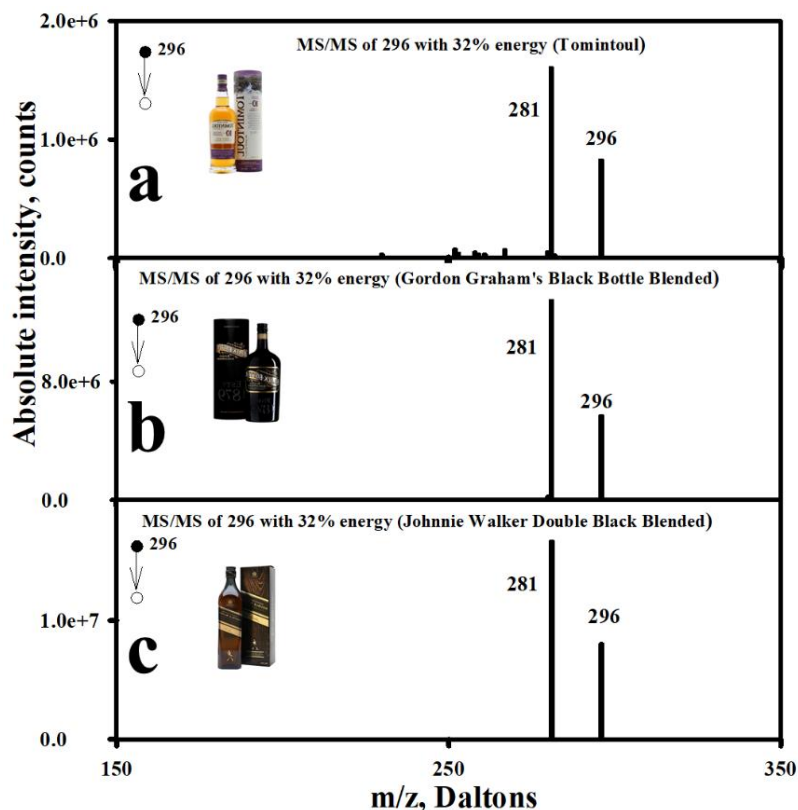


Figure 5.11. (From top to bottom) MS/MS of m/z 296 of Tomintoul Scotch Whiskey, Gordon Graham's Black Bottle Blended Scotch whiskey and Johnnie Walker Double Black Blended Scotch Whiskey, respectively, at CID energy of 32%.

Figure 5.11 shows the CID of the whiskey indophenols at m/z 296 with 32% energy of other three whiskeys (Figure 5.11a, 5.11b and 5.11c for Tomintoul, Gordon Graham's Black Bottle Blended, and Johnnie Walker Double Black Blended Whiskey, respectively). In all cases, we got fragment ions peaks at m/z 281 and 296 (Table 5.1), which indicates the structure of guaiacol. Similarly, MS/MS of m/z 326 formed from other three whiskeys are shown in Figure 5.12a1, 5.12b1, and 5.12c1 and MS³s of m/z 311 are shown in Figure 5.12a2, 5.12b2, and 5.12c2. Considering more than 5% intensity of the base peak, in MS/MS and MS³ experiments all of them gives fragment ions at m/z 311 and 326, and 232, 260, 268, 283, 296 and 311, respectively (Table 5.1). Thus, in all of them the peak at m/z 326 is due to the presence of indophenols formed by syringol.

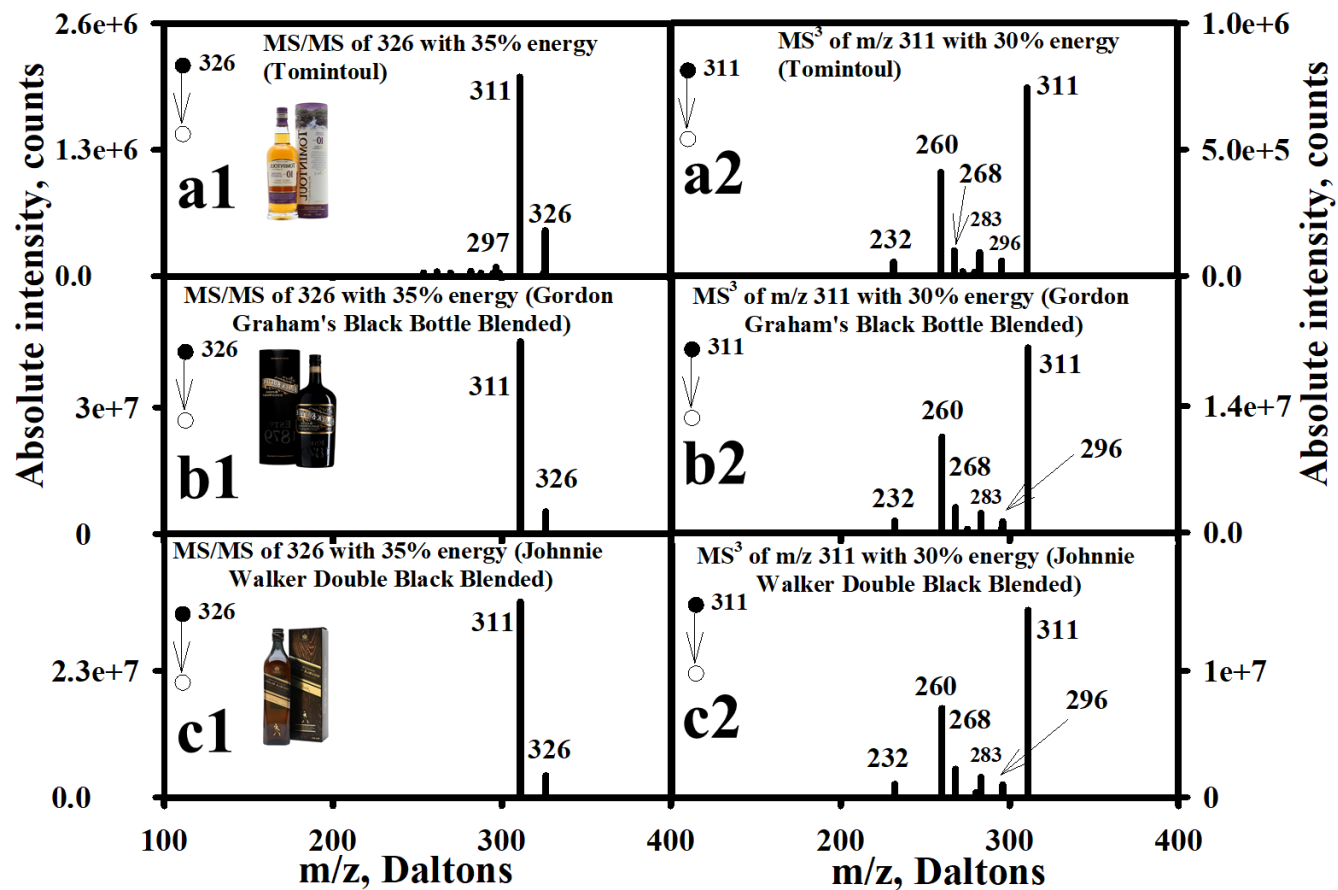


Figure 5.12. (From top to bottom) MS/MS (left) and MS³ (right) of indophenols at m/z 326 from Tomintoul, Gordon Graham's Black Bottle Blended, and Johnnie Walker Double Black Blended whiskeys, respectively.

Table 5.1. Tandem mass spectrometry of indophenols formed from the reaction of Gibbs reagent and cresol, methoxyphenol, and dimethoxyphenol isomers, and four different brands of whiskey. CID fragmentation (peaks with intensity of more than 5% of the base peak).

Reactant ion (m/z)	CID energy (%)	Fragment ions (m/z)
	<i>o</i>-Cresol	
280	45	208, 244, 265, 280
	<i>m</i>-Cresol	
280	45	180, 198, 202, 208, 212, 216, 243, 244, 252, 264, 265, 278, 280
	<i>p</i>-Cresol	
280	45	180, 198, 202, 208, 216, 242, 243, 244, 250, 252, 264, 280
	2-Methoxyphenol	
296	32	281, 296
	3-Methoxyphenol	
296	32	122, 281, 296
	2,6-dimethoxyphenol	
326	35	311, 326
311	30	232, 260, 268, 283, 296, 311
	2,3-dimethoxyphenol	
326	35	296, 311, 326
311	30	296
	2,5-dimethoxyphenol	
326	35	311, 326
311	30	189, 260, 268, 280, 282, 296, 310, 311
	3,5-dimethoxyphenol	
326	35	152, 283, 311, 326
311	30	283, 310
	<i>Lephroaige</i>	
280	45	208, 244, 265, 280
296	32	281, 296
326	35	311, 326
311	30	232, 260, 268, 283, 296, 311
	Tomintoul	
296	32	281, 296
326	35	311, 326
311	30	232, 260, 268, 283, 296, 311
	Black Bottle Blended Scotch Whiskey	
296	32	281, 296
326	35	311, 326
311	30	232, 260, 268, 283, 296, 311

Table 5.1 continued

Johnnie Walker Black Label Whiskey		
296	32	281, 296
326	35	311, 326
311	30	232, 260, 268, 283, 296, 311

5.3.2 Preparation of calibration curves

Using an internal standard, we made calibration curves for *o*-cresol, guaiacol, and syringol. Previously, our lab showed that 5,6,7,8-tetrahydro-1-naphthol (THN) gave a better intensity in the Gibbs reaction (Chapter 3), so it was used as an internal standard for the quantification of phenols.²³ Herein, we used 1.25 $\mu\text{mol/L}$ or 0.2 mg/L THN for five minutes reactions to form the calibration curves by varying the concentration of either *o*-cresol, guaiacol, or syringol. Figure 5.13a shows the calibration curve of *o*-cresol by plotting $I(m/z\ 280)/I(m/z\ 320)$ vs *o*-cresol concentrations. The ratio of the *o*-cresol Gibbs product to the internal standard Gibbs product is linear ($r^2 = 0.99$) over the range of 0.11 – 1.40 mg/L *o*-cresol. Similarly, the calibration curves are made for guaiacol (Figure 5.13b) and syringol (Figure 5.13c) by plotting $I(m/z\ 296)/I(m/z\ 320)$ vs guaiacol concentrations and $I(m/z\ 326)/I(m/z\ 320)$ vs syringol concentrations, respectively. The ratios of guaiacol and syringol Gibbs products to internal standard Gibbs product are linear ($r^2 = 0.99$ for guaiacol, and $r^2 = 0.99$ for syringol) over the range of 0.29 to 1.50 mg/L for guaiacol and 0.04 to 1.00 mg/L for syringol concentrations.

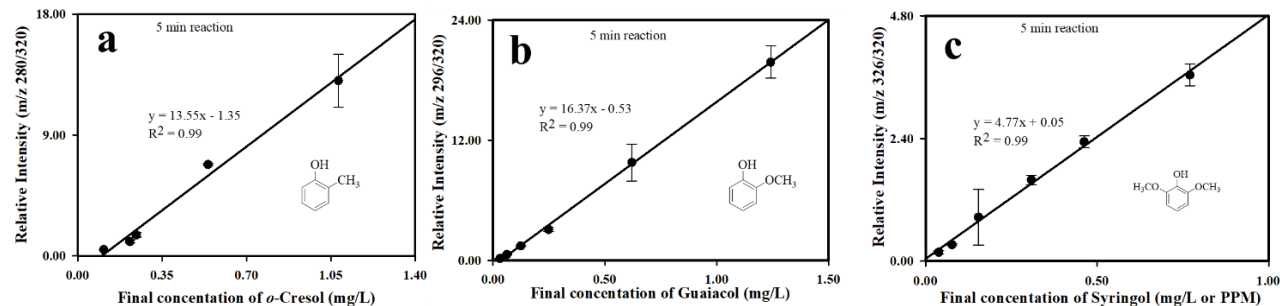


Figure 5.13. Relative intensities of each of *o*-cresol (m/z 280) (a), guaiacol (m/z 296) (b), syringol (m/z 326) (c) to 5,6,7,8-tetrahydro-1-naphthol (m/z 320) Gibbs products as a function of concentration of the compounds. The 5,6,7,8-tetrahydro-1-naphthol is present at a concentration of 1.25 μ mole/L or 0.20 mg/L.

5.3.3 Limit of quantification (LOQ)

The limit of detection (LOD), and limit of quantification (LOQ) of *o*-cresol, guaiacol, and syringol were determined using the following equations, respectively:

$$LOD = \frac{3.3 \times \sigma}{S}$$

$$LOQ = \frac{10 \times \sigma}{S}$$

where σ is the standard deviation of the calibration curve and S is the slope of the curve.^{51, 52} The LOD and LOQ of *o*-cresol, guaiacol, and syringol with 95% confidence limit were calculated. In our previous article, we have shown that the electron donating group containing phenols reacts with the Gibbs reagent faster than the others.²³ The LOD and LOQ of *o*-cresol, guaiacol, and syringol supports our previous claim. Here, we can quantify as low as 0.11 mg/L of *o*-cresol, 0.03 mg/L of guaiacol, and 0.04 mg/L of syringol (Table 5.2). In addition, the lower of quantifications were 0.34 mg/L, 0.09 mg/L, and 0.13 mg/L for *o*-cresol, guaiacol, and syringol, respectively (Table 5.2).

Table 5.2. Limit of detection and limit of quantification of catechol, guaiacol, and syringol.

Compound	LOD (mg/L)	LOQ (mg/L)
<i>o</i> -Cresol	0.11	0.34
Guaiacol	0.03	0.09
Syringol	0.04	0.13

5.3.4 Quantification of Phenols in Whiskeys

Quantification of the above three compounds in commercial whiskey samples (Figure 5.1) were carried out using the internal standard, 5,6,7,8-tetrahydro-1-naphthol (THN). The signal of the Gibbs product of the corresponding molecule was used for quantification by comparing it with the corresponding calibration curves. Table 5.3 shows the concentration of phenols in four different whiskeys in mg/L. These results were calculated by averaging of at least five sets of experiments and showing the most detectable compounds in all four- scotch whiskeys. The noticeable compounds were *o*-cresol, guaiacol, and syringol. Among these three compounds, *o*-cresol was found only in Laphroaig whiskey and the other two compounds were seen in all four whiskeys. All of these compounds were found on a milligram scale. Among these four whiskeys, Laphroaig contains the most phenolic compounds with 3.48 mg/L (± 0.03 mg/L) of *o*-cresol, 2.25 mg/L (± 0.02 mg/L) of guaiacol, and 6.82 mg/L (± 0.08 mg/L) of syringol. The second highest phenols are in Gordon Graham Black Bottle Blended (GGBBB) scotch whiskey with 1.24 mg/L (± 0.02 mg/L) of guaiacol and 11.86 mg/L (± 0.36 mg/L) of syringol. The other two brands contain least and approximately same amount of phenols. 0.87 mg/L (± 0.01 mg/L) of guaiacol and 3.76 mg/L (± 0.20 mg/L) of syringol were present in Johnnie Walker Double Black (JWDB) scotch whiskey, whereas 0.92 mg/L (± 0.01 mg/L) and 2.24 mg/L (± 0.01 mg/L) of guaiacol and syringol, respectively, were found in Tomintoul 10 years scotch whiskey. Among these three phenols, syringol was present in

the highest concentration in all types of whiskeys. These results are shown in Table 5.3 and Figure 5.16 as bar a chart.

Table 5.3. Concentration of *o*-cresol, guaiacol, and syringol in Johnnie Walker Double Black, Tomintoul, Laphroaig, and Gordon Graham Black Bottle Blended Whiskey in mg/L (or ppm).

Whiskey	<i>o</i> -Cresol (mg/L)	SD (mg/L)	Guaiacol (mg/L)	SD (mg/L)	Syringol (mg/L)	SD (mg/L)
Johnnie Walker Double Black	<LOD	-	0.87	0.01	3.76	0.20
Tomintoul 10 years Whiskey	<LOD	-	0.92	0.01	2.24	0.01
Laphroaig Whiskey	3.48	0.03	2.25	0.02	6.82	0.08
Gordon Graham Black Bottle Blended	<LOD	-	1.24	0.02	11.86	0.36

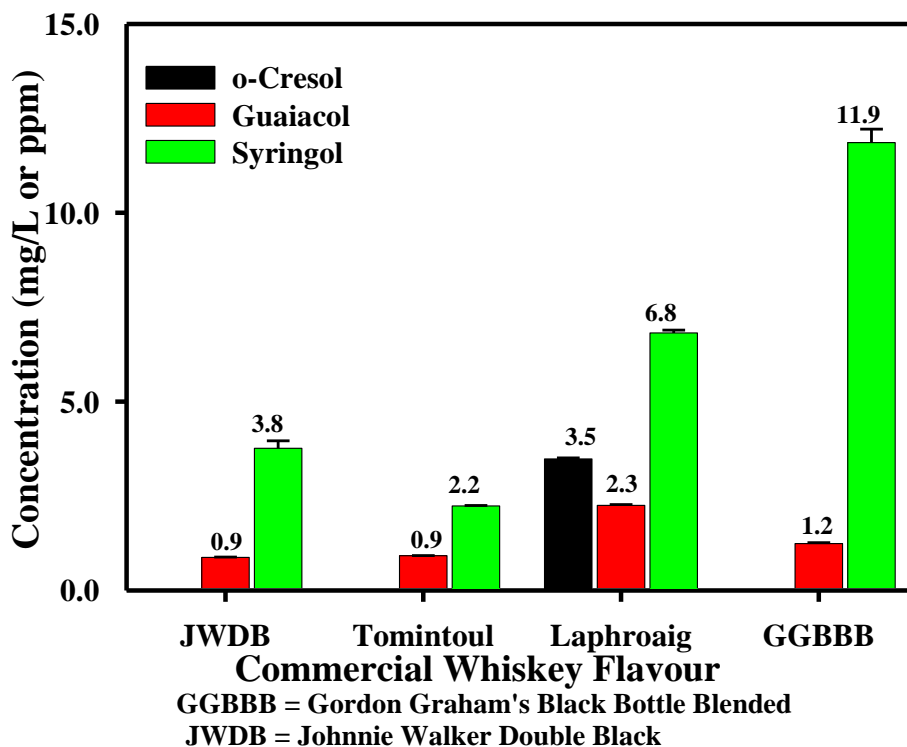


Figure 5.14. Amount of different phenols in all four different whiskeys. Laphroaig contains all three phenols: *o*-cresol, guaiacol, and syringol, whereas other three whiskeys contain only guaiacol and syringol.

5.4 Discussion

A number of phenol derivatives have been identified in different brands of whiskey, though the constituents and quantities vary in brands, location, malt number, and age.^{1, 6, 9, 11, 13-17, 53-57} According to Lehtonen, the most prevalent phenols in commercial whiskey are phenol, *o*-cresol, guaiacol, and eugenol.^{1, 13-15, 53} In addition, the presence of syringol in whiskey was reported by Harrison and Priest,¹¹ MacNamara, *et al*,¹² and Cullere, *et al*.⁵⁸ There are multiple ways to get these phenols in whiskey.¹² In those processes, not only these compounds but also a variety of phenols can come to the whiskey. The specific type of phenols and their quantities varies from one batch to another.

In the barley-malting process, the introduction of peat smoke is known as ‘Peating’. ‘Peating’ contributes to the characteristic peaty flavor of many Scotch malt whiskies. The peaty (or phenolic) characteristic is very distinctive and easily identified and described as the level of ‘peatiness - that is, the phenolic character of the finished product determined by the amount of peat smoke adsorbed by the barley. In the whiskey industry, the concentration of phenols is reported in parts per million (ppm). The higher the ppm, the peatier and smokier the taste of the drink.¹³ A lightly peated malt contains 1 – 5 ppm total phenol, whereas 5 – 15 ppm of total phenols contained is known as medium peated, and finally, heavily peated malt contains total phenols of 15 – 50 ppm.^{59, 60} On the other hand, Lee, *et al*,¹⁴ used Quantitative Descriptive Analysis (QDA) as an important sensory analysis technique which allows communication of data on flavor characters in a specific product. She found that, for an example, guaiacol is generally described as evoking a smokey taste (39%). Also, it was characterized as rubbery (15%) and medicinal (19%) and it could possibly be related to knowledge of the malt peating process. Moreover, it was reported that the heavily-peated malt whiskies mostly contain guaiacol, phenol, cresol, and eugenol.^{1, 61}

Different research groups have used a variety of techniques to measure the concentration of different phenols including *o*-cresol, guaiacol, and syringol. For instance, Lehtonen¹ studied a variety of whiskies originating in different countries and reported as an average concentration of volatile phenols. The notable compounds he reported for Scotland Scotch whiskies were phenol (0.12 mg/L), *o*-cresol (0.09 mg/L), guaiacol (0.08 mg/L). Masuda, et al,¹⁶ reported the presence of syringol (2,6-dihydroxyphenol) (1 µg/L), guaiacol (2-methoxyphenol) (1 µg/L), phenol (6 µg/L) and other compounds. Lee, et al,⁶² reported the presence of guaiacol (burnt smokey) concentration in whiskey as high as 27 mg/L. Thus, concentrations of phenolic compounds are different not only in different brands of whiskies but also one batch of whiskey from one particular brand may differ in phenolic concentration from another batch of the same type. The whiskeys examined in the work were chosen for being smokey.

Based on the manufacturing procedure, there are three types of whiskies- blended whiskey, grain whiskey, and malt whiskey. Blended whiskey is made up via the mixing of grain whiskey and single malt whiskey. Grain whiskey is made from a mash consisting of different grains. The common grains used for this type of whiskey are mostly barley, wheat and corn. It is produced via continuous distillation in a column still. The final type is malt whiskey which is made from malted barley. Its distillation takes place in copper pot stills, following by maturation in oak barrels. Johnnie Walker Double Black is a Scottish blended whiskey.^{25, 63} Guaiacol and cresol are formed from roasted barley and are responsible for the unique taste of whiskey.²⁵ Thus, they are expected to be present in Johnnie Walker Double Black whiskey. Although we detected guaiacol in a significant amount (0.87±0.01 mg/L), we did not see any presence of cresol. The other compound we found was 2,6-dimethoxyphenol (syringol) with a concentration of 3.76±0.20 mg/L. Relatively

higher amounts of guaiacol makes its smokey taste,⁶⁴ and syringol creates the characteristic aroma of Johnnie Walker Double Black scotch whiskey.

Tomintoul whiskey is a Scottish whiskey and is made by the use to peat from Tomintoul. Tomintoul peat is similar to Islay peat and this whiskey is similar peaty of Mackinlay whiskey.⁶⁵ Both of these whiskies were classified as light, medium-sweet, lot peat, with flora, malty notes and fruity, spicy, honey hints. The phenolic concentration of Tomintoul whiskey has not been reported previously.⁶⁵ However, one report was published on the volatile phenols of the peat of Islay by using Curie point pyrolysis. According to that report, the concentration of the compounds in peat smoke were phenol (1.03 ± 0.02 mg/L), guaiacol (0.45 ± 0.06 mg/L), *m*- or *p*-cresol (0.58 ± 0.02 mg/L), *o*-cresol (0.58 ± 0.03 mg/L), 4-methylguaiacol (0.23 ± 0.02 mg/L), 4-ethylphenol (0.55 ± 0.05 mg/L), 4-ethyl guaiacol (0.10 ± 0.00 mg/L).⁶⁵ Since peat used for firing is an important source of phenols in whiskey, we may use it to compare our findings. In our experiments, only guaiacol and syringol were found in Tomintoul whiskey. The guaiacol level was 0.92 ± 0.01 mg/L which is nine times higher than what was reported by Pryde, *et al.*⁶⁵ The extra guaiacol could be added to the whiskey in the aging process. In addition, we found the syringol concentration of 2.24 ± 0.01 mg/L in this whiskey. Harrison, *et al.*,¹¹ examined the presence of phenols in peat of different geographical locations including Tomintoul and reported the presence of guaiacol and syringol, as lignin derivatives, as a ratio to phenol and it was as much as 0.30 in the Tomintoul.¹¹ This report is an evidence of the source of syringol from Tomintoul peat, but it may be difficult to compare the amount of it. Our analysis did not show the presence of *m*- or *p*-cresol, phenol and other reported compounds. This could be due to the limitation of our technique using ion-trap MS and/or the slower kinetics of the Gibbs reaction with those compounds. However, even upon running the reaction for a longer time (30 minutes), we did not see any peak corresponding to those compounds

(data not shown). Interestingly, the total phenolic compounds present in Mackinlay whiskey is 3.48 ± 0.18 mg/L,⁶⁶ which is close to our finding value in Tomintoul whiskey.

Wishart used 0 to 4 scale to classify smokiness of whiskey having 0 is for ‘not present’, 1 for ‘low hints’, 2 for ‘medium notes’, 3 for ‘definite notes’ and finally 4 for ‘pronounced’ in his book named “*Whisky Classified: Choosing Single Malts by Flavour*”.⁶⁷ In that book, he pointed out Tomintoul 10 years aged whiskey as ‘low hints’ smokey, and no medicinal taste.⁶⁷ The findings of low guaiacol level in our experiment supports the low smokey property of this whiskey. Also, the absence of *o*-cresol justified its medicinal taste of ‘not present’.

Though Gordon Graham Black Bottle Blended (GGBBB) is a blended whiskey like Johnnie Walker Double Black, it is more peaty whiskey than the latter. The higher smokiness property comes from the presence of 40% more guaiacol (1.24 ± 0.02 mg/L) than the latter whiskey. Also, its smokey aroma is due to the significantly higher presence of syringol (11.86 ± 0.36 mg/L). We have not found any reference to the amount of phenols in GGBBB whiskey.

Laphroaig Single Islay Malt (LSIM) is an Islay scotch whiskey. It epitomizes smokey, peaty whiskey.⁶⁷ In 1996, Withers, et al.⁵⁶ found that both the mature and new distillate of Laphroaig were one of the heavily-peated whiskies. In his book about whiskey distillery, named “*Raw Spirit – In Search of the Perfect Dram*,” Iaian Banks mentioned the ten-years-old of Laphroaig as one of the flagships among the peat whiskeys. He also mentioned that it was “busted with smells straight out of the cabinet”.⁶⁸ Wishart⁶⁹ made a ‘Single Malt Whisky Flavor Map’ based on their taste, smokiness, and aroma and described Laphroaig ten-years-old whiskey as having a smokey, medicinal, dry smoke pepperiness. Moreover, he described Laphroaig as ‘pronounced smokey’ (smokey: 4), ‘pronounced medicinal taste’ (medicinal: 4) in his book.⁶⁷

Finally, peatiness of Laphroaig whiskey was correlated with phenol, cresols, and guaiacols, which are derived from peat smoke, and a peaty characteristic is also associated with eugenol, which is oak-derived. The medicinal quality of whiskeys is correlated with *o*-cresol.⁷⁰ All of the above claims were supported by our finding reported in Table 5.3. Among the four whiskies, only Laphroaig had medicinal property due to the presence of a high amount of *o*-cresol (3.48 ± 0.03 mg/L). The ‘pronounced smokey’ property was due to the highest amount of guaiacol (2.25 ± 0.02 mg/L) among the four whiskies, which was at least twice as much as any other brand. Finally, the smokey aroma was due to the 6.82 mg/L (± 0.08) of syringol, which was almost half the amount in GGBBB whiskey and more than twice as much as the other two. The whiskey’s total phenolic concentration contributes to its distinctive characteristics and separates it from other tested brands.

5.5 Conclusion

While conventional time consuming and expensive solvent extraction, GC-MS, or LC-MS and insensitive colorimetry have been used for the detection and quantification of phenols in whiskies, we used the Gibbs reaction to derivatize followed by MS analysis of those compounds in four different brands of whiskies within few minutes. Though the Gibbs reaction cannot derivatized all phenols present in whisky to corresponding indophenols, this technique was successful detected and quantified the major phenolic compounds in them. In addition, the isotopic deconvolution of mass spectra confirmed the presence of corresponding indophenols having at least two chlorine atoms. Finally, by using internal standard we were able to quantify *o*-cresol, guaiacol and syringol in whiskies and our findings are comparable with previously reported.

5.6 References

1. Lehtonen, M., Phenols in whisky. *Chromatographia* **1982**, *16* (1), 201-203.
2. Luten, J. B.; Ritskes, J. M.; Weseman, J. M., Determination of phenol, guaiacol and 4-methylguaiacol in wood smoke and smoked fish-products by gas-liquid chromatography. *Zeitschrift für Lebensmittel-Untersuchung und Forschung* **1979**, *168* (4), 289-292.
3. Tressl, R.; Grünewald, K. G.; Köppler, H.; Silwar, R., Flüchtige Phenole in Röstkaffees verschiedener Sorten. I. *Zeitschrift für Lebensmittel-Untersuchung und Forschung* **1978**, *167* (2), 108-110.
4. Etievant, P. X., Volatile phenol determination in wine. *Journal of Agricultural and Food Chemistry* **1981**, *29* (1), 65-67.
5. Nishimura, K.; Masuda, M., Minor constituents of whisky fusel oils. 1. Basic, phenolic and lactonic compounds. *Journal of Food Science* **1971**, *36* (5), 819-822.
6. Lehtonen, M.; Suomalainen, H., analytical profile of some whisky brands. *Process biochemistry* **1979**.
7. Suomalainen, H.; Lehtonen, M., The production of aroma compounds by yeast. *Journal of the Institute of Brewing* **1979**, *85* (3), 149-156.
8. MacNamara, K.; Van Wyk, C.; Brunerie, P.; Augustyn, O.; Rapp, A., Flavour components of whiskey. III. ageing changes in the low-volatility fraction. *South African Journal of Enology and Viticulture* **2001**, *22* (2), 82-92.
9. MacNamara, K.; Brunerie, P.; Squarcia, F.; Rozenblum, A., Investigation of flavour compounds in whiskey spent lees. In *Developments in Food Science*, Elsevier: 1995; Vol. 37, pp 1753-1766.
10. Kosar, K. R., *Whiskey: A global history*. Reaktion Books: 2010.
11. Harrison, B. M.; Priest, F. G., Composition of Peats Used in the Preparation of Malt for Scotch Whisky Production □ Influence of Geographical Source and Extraction Depth. *Journal of agricultural and food chemistry* **2009**, *57* (6), 2385-2391.
12. MacNamara, K.; Dabrowska, D.; Baden, M.; Helle, N., Advances in the ageing chemistry of distilled spirits matured in oak barrels. **2011**.
13. Hübner, K., Torf, lass nach. *Chemie in unserer Zeit* **2015**, *49* (3), 159-163.
14. Lee, K. Y. M.; Paterson, A.; Piggott, J. R.; Richardson, G. D., Perception of whisky flavour reference compounds by Scottish distillers. *Journal of the Institute of Brewing* **2000**, *106* (4), 203-208.

15. Morales, M.; Benitez, B.; Troncoso, A., Accelerated aging of wine vinegars with oak chips: evaluation of wood flavour compounds. *Food Chemistry* **2004**, *88* (2), 305-315.
16. MASUDA, Y.; MORI, K.; HIROHATA, T.; KURATSUNE, M., CARCINOGENESIS IN THE ESOPHAGUS. *GANN Japanese Journal of Cancer Research* **1966**, *57* (5), 549-557.
17. Goldberg, D. M.; Hoffman, B.; Yang, J.; Soleas, G. J., Phenolic constituents, furans, and total antioxidant status of distilled spirits. *Journal of agricultural and food chemistry* **1999**, *47* (10), 3978-3985.
18. Goldberg, D. M.; Soleas, G. J., [12] Analysis of antioxidant wine polyphenols by high-performance liquid chromatography. In *Methods in enzymology*, Elsevier: 1999; Vol. 299, pp 122-137.
19. Łabudzińska, A.; Gorczyńska, K., The UV difference spectra as a characteristic feature of phenols and aromatic amines. *Journal of molecular structure* **1995**, *349*, 469-472.
20. Hemmateenejad, B.; Akhond, M.; Samari, F., A comparative study between PCR and PLS in simultaneous spectrophotometric determination of diphenylamine, aniline, and phenol: effect of wavelength selection. *Spectrochimica Acta Part A: Molecular and Biomolecular Spectroscopy* **2007**, *67* (3-4), 958-965.
21. Ryu, W.-K.; Kim, H.-W.; Kim, G.-D.; Rhee, H.-I., Rapid determination of capsaicinoids by colorimetric method. *journal of food and drug analysis* **2017**, *25* (4), 798-803.
22. Montazeri, N.; Oliveira, A. C.; Himelbloom, B. H.; Leigh, M. B.; Crapo, C. A., Chemical characterization of commercial liquid smoke products. *Food science & nutrition* **2013**, *1* (1), 102-115.
23. Mistry, S.; Wenthold, P. G., Mass spectrometric detection of the Gibbs reaction for phenol analysis. *Journal of Mass Spectrometry* **2018**.
24. TechnologyInc., S., Atmospheric Pressure Photoionization (APPI) for LC-MS: Analysis of Lipids. *LC GC NORTH AMERICA* **2005**, *23* (9), 29.
25. Wiśniewska, P.; Dymerski, T.; Wardencki, W.; Namieśnik, J., Chemical composition analysis and authentication of whisky. *Journal of the Science of Food and Agriculture* **2015**, *95* (11), 2159-2166.
26. Sharpe, F.; Chappell, C., An introduction to mass spectrometry and its application in the analysis of beer, wine, whisky and food. *Journal of the Institute of Brewing* **1990**, *96* (6), 381-393.
27. Heller, M.; Vitali, L.; Oliveira, M. A. L.; Costa, A. C. O.; Micke, G. A., A rapid sample screening method for authenticity control of whiskey using capillary electrophoresis with online preconcentration. *Journal of agricultural and food chemistry* **2011**, *59* (13), 6882-6888.

28. Lehtonen, M., Gas chromatographic determination of phenols as 2, 4-dinitrophenyl ethers using glass capillary columns and an electron-capture detector. *Journal of Chromatography A* **1980**, 202 (3), 413-421.
29. Gibbs, H. D., Phenol Tests. IV. A Study of the Velocity of Indophenol Formation 2, 6-Dibromobenzenoneindophenol. *The Journal of Physical Chemistry* **1927**, 31 (7), 1053-1081.
30. Gibbs, H. D., Phenol tests III. The indophenol test. *Journal of biological chemistry* **1927**, 72 (2), 649-664.
31. Ettinger, M.; Ruchhoft, C., Determination of Phenol and Structurally Related Compounds by Gibbs Method. *Analytical Chemistry* **1948**, 20 (12), 1191-1196.
32. Mohler, E. F.; Jacob, L. N., Determination of Phenolic-Type Compounds in Water and Industrial Waste Waters Comparison of Analytical Methods. *Analytical Chemistry* **1957**, 29 (9), 1369-1374.
33. BM, G.; SHANKAR, S., SPECTROPHOTOMETRIC METHODS FOR THE ESTIMATION OF BUTORPHANOL TARTARATE IN BULK AND PHARMACEUTICAL FORMULATIONS.
34. Ankita, M.; Gurupadayya, B.; Chandra, A., Colorimetric estimation of acenocoumarol in bulk and pharmaceutical formulations. *Asian Journal of Chemistry* **2008**, 20 (7), 5001.
35. Gowrisankar, D.; Sarsambi, P. S.; Raju, S., Development and validation of new spectrophotometric methods for the estimation of cefprozil in pure form and in pharmaceutical formulations. *J Indian Counc Chem* **2008**, 25, 106-8.
36. Bartzatt, R., Spectrophotometric and colorimetric methodology to detect and quantify hydrazide based chemotherapeutic drugs. *Environmental Science: An Indian Journal* **2010**, 5 (1), 86.
37. Patel, K.; Patel, C.; Panigrahi, B.; Parikh, A.; Patel, H., Development and validation of spectrophotometric methods for the estimation of mesalamine in tablet dosage forms. *Journal of young pharmacists: JYP* **2010**, 2 (3), 284.
38. Tuljarani, G.; Sankar, D. G.; Kadgapathi, P.; Suthakaran, R.; Satyanarayana, B., Quantitative determination of bisoprolol fumarate in bulk and pharmaceutical dosage forms by spectrophotometry. *International Journal Of Chemical Sciences* **2010**, 8 (4), 2253-2258.
39. Chandan, R.; Vasudevan, M.; Deecaraman, B.; Indupriya, M., Spectrophotometric determination of lamotrigine using Gibb's and MBTH reagent in pharmaceutical dosage form. *Journal of Pharmacy Research* **2011**, 4 (6), 1813-1815.

40. Gousuddin, M.; Raju, S. A.; Sultanuddin, M. S., Development and validation of spectrophotometric methods for estimation of formoterol bulk drug and its pharmaceutical dosage forms. *International Journal of Pharmacy and Pharmaceutical Sciences* **2011**, *3*, 300-309.
41. Sowjanya, K.; Thejaswini, J.; Gurupadayya, B.; Indupriya, M., Spectrophotometric determination of pregabalin using Gibb's and MBTH reagent in pharmaceutical dosage form. *Der Pharma Chemica* **2011**, *3* (1), 112-122.
42. Somisetty, V.; Bichala, P. K.; Rao, C.; Kirankumar, V., Development and validation of newer analytical methods for the estimation of deferasirox in bulk and in tablet dosage form by calorimetric method. *International Journal of Pharmacy and Pharmaceutical Sciences* **2013**, *5* (3), 521-525.
43. Rajapandi, R.; Aswathy, S.; Sreedharan, B., Spectrophotometric method development and validation for estimation of enrofloxacin in pure and dosage forms. *World J. Pharm. Res* **2016**, *5* (6), 1402-10.
44. Jeong, H.-J.; Hwang, D.-Y.; Ahn, J.-T.; Chun, J.-Y.; Han, K.-E.; Lee, W.-M.; Kwon, J.-K.; Lee, Y.-J.; Kang, B.-C., Development of a simple method for detecting capsaicinoids using Gibb's reagent in pepper. *Horticultural Science & Technology* **2012**, *30* (3), 294-300.
45. Thompson, R. Q.; Chu, C.; Gent, R.; Gould, A. P.; Rios, L.; Vertigan, T. M., Visualizing capsaicinoids: colorimetric analysis of chili peppers. *Journal of Chemical Education* **2012**, *89* (5), 610-612.
46. Karimi, M.; Hassanshahian, M., Isolation and characterization of phenol degrading yeasts from wastewater in the coking plant of Zarand, Kerman. *brazilian journal of microbiology* **2016**, *47* (1), 18-24.
47. Sparrapan, R.; Eberlin, M. N.; Alberici, R. M., Quantitation of trace phenolic compounds in water by trap-and-release membrane introduction mass spectrometry after acetylation. *Rapid Communications in Mass Spectrometry: An International Journal Devoted to the Rapid Dissemination of Up-to-the-Minute Research in Mass Spectrometry* **2008**, *22* (24), 4105-4108.
48. Zhu, H.; Janusson, E.; Luo, J.; Piers, J.; Islam, F.; McGarvey, G. B.; Oliver, A. G.; Granot, O.; McIndoe, J. S., Phenol-selective mass spectrometric analysis of jet fuel. *Analyst* **2017**, *142* (17), 3278-3284.
49. Mistry, S.; Wenthold, P. In *Mass spectroscopic analysis of phenol derivatives by Gibbs reaction*, ABSTRACTS OF PAPERS OF THE AMERICAN CHEMICAL SOCIETY, AMER CHEMICAL SOC 1155 16TH ST, NW, WASHINGTON, DC 20036 USA: 2019.
50. Wenthold, P. G.; Mistry, S., Methods of detecting chemicals. Google Patents: 2019.

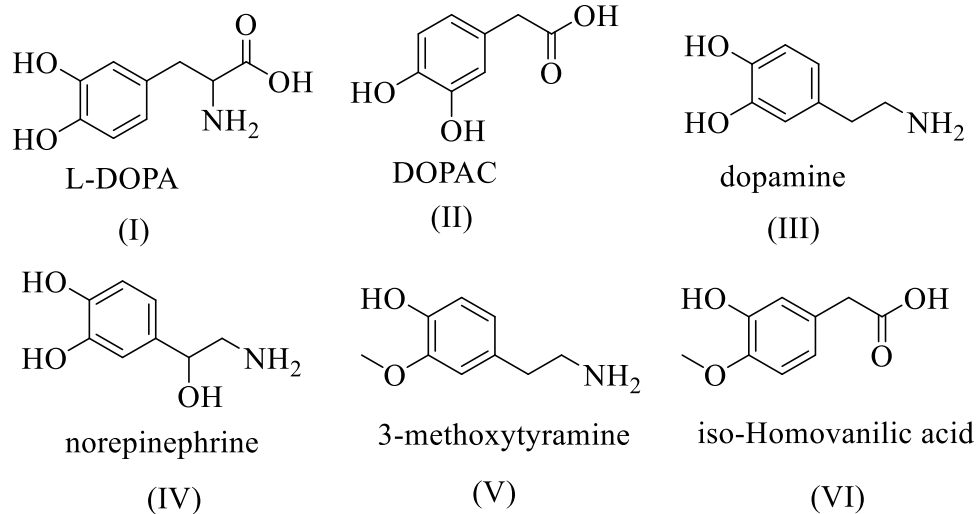
51. Chen, Y.; Mao, P.; Wang, D., Quantitation of Intact Proteins in Human Plasma Using Top-Down Parallel Reaction Monitoring-MS. *Analytical chemistry* **2018**.
52. Guideline, I. H. T. In *Validation of analytical procedures: text and methodology Q2 (R1)*, International Conference on Harmonization, Geneva, Switzerland, 2005; pp 11-12.
53. Zhang, P.; Littlejohn, D., Modification of an ultraviolet spectrophotometric method for the determination of trace amounts of phenols with iodine monobromide. *Analyst* **1993**, *118* (8), 1065-1069.
54. Braus, H.; Miller, F., Composition of Whisky-Steam-Volatile Phenols of Fusel Oil. *Journal of the Association of Official Agricultural Chemists* **1958**, *41* (1), 141-144.
55. Aoshima, H.; Tsunoue, H.; Koda, H.; Kiso, Y., Aging of whiskey increases 1, 1-diphenyl-2-picrylhydrazyl radical scavenging activity. *Journal of agricultural and food chemistry* **2004**, *52* (16), 5240-5244.
56. Withers, S.; Piggott, J.; Conner, J.; Paterson, A., Peaty characteristic of Scotch malt whisky. *SPECIAL PUBLICATION-ROYAL SOCIETY OF CHEMISTRY* **1996**, *197*, 354-360.
57. Hossain, S. J.; Aoshima, H.; Koda, H.; Kiso, Y., Potentiation of the ionotropic GABA receptor response by whiskey fragrance. *Journal of agricultural and food chemistry* **2002**, *50* (23), 6828-6834.
58. Culleré, L.; Escudero, A.; Cacho, J.; Ferreira, V., Gas chromatography– olfactometry and chemical quantitative study of the aroma of six premium quality Spanish aged red wines. *Journal of Agricultural and Food Chemistry* **2004**, *52* (6), 1653-1660.
59. Bathgate, G.; Taylor, A., THE QUALITATIVE AND QUANTITATIVE MEASUREMENT OF PEAT SMOKE ON DISTILLER'S MALT. *Journal of the Institute of Brewing* **1977**, *83* (3), 163-168.
60. Bathgate, G.; Cook, R., Malting of barley for Scotch whiskies. *The Science and Technology of Whiskies* **1989**, 19-63.
61. SWAN, J.; HOWIE, D., Current Developments in Malting. *Brewing and Distilling (Aviemore Proceedings), Institute of Brewing, London* **1983**, 129.
62. Lee, K. Y. M.; Paterson, A.; Piggott, J. R.; Richardson, G. D., Origins of flavour in whiskies and a revised flavour wheel: a review. *Journal of the Institute of Brewing* **2001**, *107* (5), 287-313.
63. Jacques, K. A.; Lyons, T. P.; Kelsall, D. R., *The alcohol textbook: a reference for the beverage, fuel and industrial alcohol industries*. Nottingham University Press: 2003.
64. Sun, Z. Accelerated seasoning of Manuka and Oak Wood chips destined for wine and spirit flavour. Auckland University of Technology, 2013.

65. Pryde, J.; Conner, J.; Jack, F.; Lancaster, M.; Meek, L.; Owen, C.; Paterson, R.; Steele, G.; Strang, F.; Woods, J., Sensory and Chemical Analysis of 'Shackleton's' Mackinlay Scotch Whisky. *Journal of the Institute of Brewing* **2011**, *117* (2), 156-165.
66. Taylor, A. J.; Mottram, D. S., *Flavour science: recent developments*. Elsevier: 1997.
67. Wishart, D., *Whisky Classified: Choosing Single Malts by Flavour*. Pavilion: 2006.
68. Banks, I., *Raw spirit: In search of the perfect dram*. Random House: 2013.
69. Wishart, D., The flavour of whisky. *Significance* **2009**, *6* (1), 20-26.
70. Miller, G. H., Malting. In *Whisky Science*, Springer: 2019; pp 83-119.

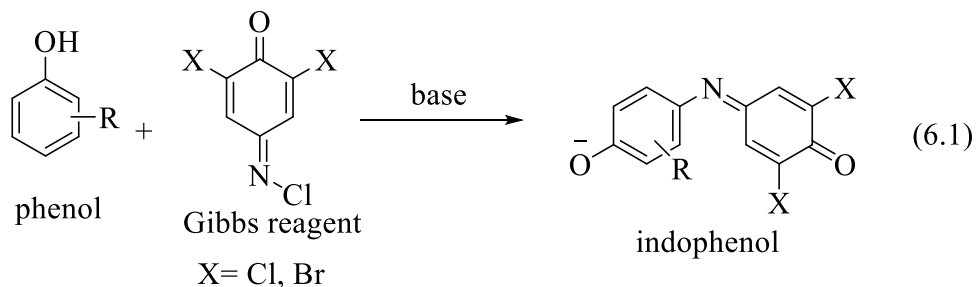
CHAPTER 6. MASS SPECTROSCOPIC ANALYSIS OF L-DOPA NEUROTRANSMITTER AND IT'S METABOLITES BY USING GIBBS REACTION

6.1 Introduction

Neurotransmitters such as L-3,4-dihydroxyphenylalanine (levodopa, or L-DOPA) (I), 3,4-dihydroxyphenylacetic acid (DOPAC) (II), dopamine (III), 4-(2-amino-1-hydroxyethyl)benzene-1,2-diol (norepinephrine) (IV), 3-methoxytyramine (3-MT) (V) and 2-(3-hydroxy-4-methoxyphenyl)acetic acid (*iso*-homovanillic acid) (VI) have been attracting substantial interest for a long time due their multiple functions in biological system and their use as drugs.^{1, 2} For instance, in the clinical treatment of Parkinson's disease (PD), a neurodegenerative disorder, L-dopa is widely used to improve motor functions.³⁻⁵ In addition, L-Dopa is the precursor of dopamine and it converts to dopamine in the central nervous system, which is responsible for the dopamine-responsive dystonia.⁵ This dopamine converts to many other neurotransmitters in the presence of enzymes. For instance, dopamine converts to norepinephrine by dopamine β -monooxygenase inside neurotransmitter vesicles,⁶ to 3-methoxytyramine by the enzyme catechol-*O*-methyl transferase (COMT),⁷ and to 3,4-dihydroxyphenylacetic acid (DOPAC) by monoamino oxidase (MAO).^{8, 9} The last compound of this series, *iso*-homovanillic acid (VI), is formed in the metabolism of catecholamines by catechol-*O*-methyltransferase (COMT) and it is found in the urine of human patients having neural crest tumors and those receiving L-DOPA for PD.¹⁰ Due to the substantial interest of these neurotransmitters, numerous methods have been published for their analysis in serum and urine samples.



Currently used techniques for the analysis of these compounds are spectrophotometry,^{3, 4, 10-12} flow injection analysis,^{13, 14} HPLC,¹⁵⁻²¹ gas chromatography,^{22, 23} mass spectroscopy (MS),²⁴⁻²⁶ electrochemical methods,^{1, 27-38} and separation technique such as capillary electrophoresis.³⁹⁻⁴¹ All of these methods have either lack of sensitivity, specificity, low detection limit, long analysis time, and/or simplicity for routine analysis. Derivatization is a common practice to improve sensitivity of these compounds.⁴² The common techniques of phenol derivatizations are (i) conversion to a colored compound by reaction with an amine and a suitable oxidant (oxidative coupling),⁴³⁻⁴⁵ (ii) formation of an azo dye,⁴⁶ and (iii) formation of a colored metal complex.⁴⁷ Among these three derivatization methods, the most commonly used technique is to convert phenols into a colored compound by reaction with 2,6-dihalobenzoquinone-4-chloroimine (Gibbs reagent) and a suitable base before their analysis using a visible spectrophotometer (eq 1).^{48, 49} Moreover, the introduction of electrospray mass spectrometry (ESI-MS) to analyze indophenols may increase specificity and low detection limit within short period of time.



Herein, we describe the detection of Gibbs products, indophenols, formed from these neurotransmitters after reaction with Gibbs reagent, by using simple electrospray-ionization mass spectrometry (ESI-MS) as the naturally anionic indophenols are readily detected by ESI-MS. In addition, a significant benefit of using mass spectrometry for the detection of the Gibbs product is that we can easily distinguish between substituted phenols by using tandem mass spectroscopy. In this work, we report the formation of indophenol after reaction of these neurotransmitters with Gibbs reagent followed by ESI-MS analysis as an alternative method for the detection and simultaneous quantification.

6.2 Experiment

6.2.1 Chemicals

L-3,4-dihydroxyphenylalanine or levodopa (L-DOPA), dopamine, norepinephrine (noradrenaline), 3,4-dihydroxyphenylacetic acid (DOPAC), 3-methoxytyramine (3-TM), iso-Homovanillic acid (iso-HVA), 5,6,7,8-tetrahydro-1-naphthol (THN) and Gibb's reagent were obtained from commercial sources and used as received. Methanol was "Reagent Grade" and used without further purification. Deionized water was used for the experiment.

6.2.2 Stock solution

10 mmol/L stock solutions of L-DOPA, dopamine, norepinephrine, DOPAC, 3-MT, *iso*-HAV and THN were prepared in methanol. Gibbs reagent (500 mmol/L) and potassium phosphate dibasic (K_2HPO_4) (2 mol/L) solutions were prepared in methanol and water, respectively. Fresh solutions were prepared every week and stored in refrigerator.

6.2.3 Sample preparation – general procedures

The reaction was done by modifying our previously reported procedure.^{42, 50, 51} In brief, samples were prepared by mixing 2 mL of Gibbs reagent in 5 mL methanol with 155 μ L of K_2HPO_4 , 25 μ L of THN, and required volume of the analyte in deionized water to make total volume of 5 mL. The reaction mixture was stirred at room temperature for 5 minutes. 200 μ L of reaction mixture was dissolved in 4 mL water-methanol (1:1) solution for MS analysis.

6.2.4 L-DOPA methyl ester formation

A sample of 0.2 mmol (40 mg) of L-Dopa was dissolved in 5 mL methanol and cooled to 0°C. 200 μ L thionyl chloride ($SOCl_2$) was added dropwise and brought to room temperature. The solution was refluxed for an hour and cooled to room temperature. The solvent was removed by reduced pressure and the formed methyl ester was used without purification.

6.2.5 Spectra collection

Electrospray ionization mass spectra was obtained on a commercial LCQ-DECA (Thermo Electron Corporation, San Jose, CA, USA) quadrupole ion trap mass spectrometer, equipped with electrospray ionization (ESI) source. Substrate solutions were made in a methanol:water mixture

(1:1) and introduced into the source directly at a flow rate of 10 $\mu\text{L}/\text{min}$. Electrospray and ion focusing conditions were varied to maximize the signal of the ion of interest.

6.2.6 Spectral analysis

One important advantage of using the Gibbs reagent for derivatization is that the chlorine atoms make products containing the Gibbs reagent readily detectable by the isotopic pattern. Therefore, the spectra are deconvoluted using the isotope pattern for ions containing two chlorine atoms (1:0.648:0.105) to eliminate the peaks that cannot contain the Gibbs reagent by Microsoft Excel. It is this ability to specifically detect phenoxides and eliminate non-Gibbs products that makes the Gibbs approach preferable to simple ESI-MS of the mixture. The spectra were regenerated by using Sigmaplot 11.0.

6.3 Results

6.3.1 L-Dopa

L-DOPA does not form indophenol when mixed with Gibbs reagent in buffer solution. We tried different reaction conditions by changing the ratio of reactants, pH of the solution and buffer system, but no product was observed. This is probably due to the formation of zwitterion by the amine and acid groups. Thus, protecting either of the amine or acid groups may prevent the formation of zwitterion. The amine was protected by *tert*-butyloxycarbonyl (boc) group. The conversion was poor due to the poor solubility of L-dopa in aprotic solvents. However, the protection of the acid group by esterification was successful and almost the entire acid was converted to ester (eq 6.2). Figure 6.1 shows the full mass spectrum of the L-DOPA methyl ester (L-Dopa-OCH₃) reaction mixture in positive ionization (+ESI). The spectrum is dominated by the peak at m/z 212. This is due to L-Dopa-OCH₃. We did not see any peak at m/z 198 [L-Dopa + H]⁺.

This is because of the conversion of L-Dopa to methyl ester. However, there are few more peaks at m/z 152 and 192 and we did not characterize them. The L-Dopa-methyl ester formed in this reaction was used for the Gibbs reaction without purification.

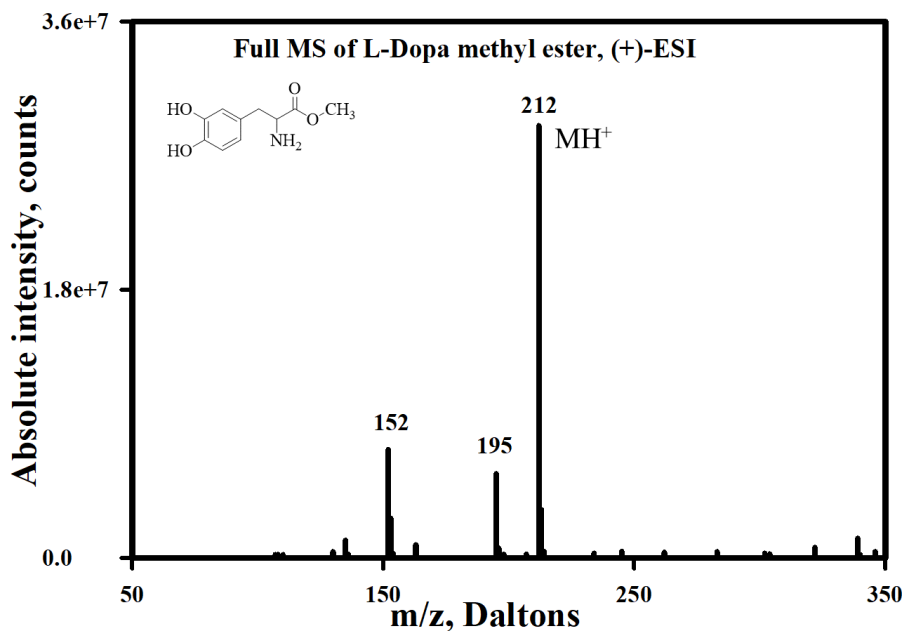
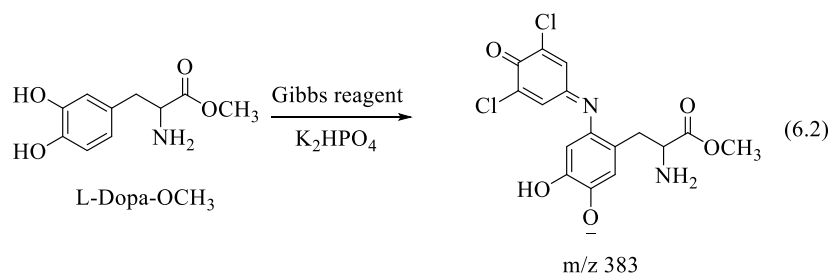


Figure 6.1. Full MS of L-DOPA methyl ester

Figure 6.2 shows full mass spectra (6.2a) and deconvoluted mass spectra (6.2b) in negative ionization of the reaction mixture of the L-Dopa-OCH₃ with Gibbs reagent after a five minute reaction. The spectra are dominated by the peak m/z 383. Thus, mass spectroscopic analysis of indophenol of L-dopa methyl ester is a viable technique for the analysis of this neurotransmitter and this is the characteristic peak of L-Dopa-OMe analysis. The other notable peaks are at m/z

280, 352, 400, and 417. Though we know from our previous work that the peak at m/z 280 is due to the indophenol formed by cresol (Chapter 3),⁴² we could not identify the mechanism of the formation of this product in this reaction. The peak at m/z 352 is from the dimer of the Gibbs reagent. Finally, the structures of the other two products were unknown.

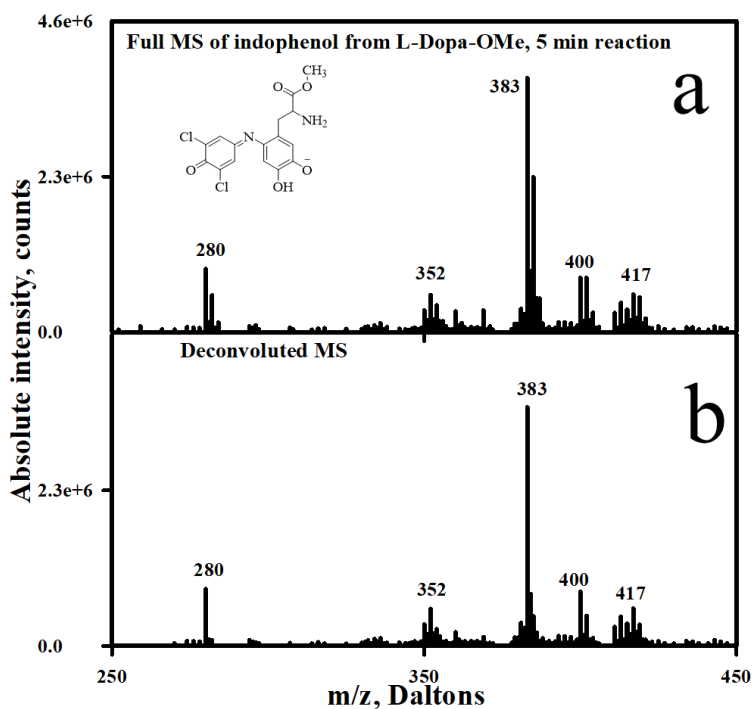


Figure 6.2. (a) Full MS and (b) deconvoluted MS of the Gibbs products from L-DOPA-methyl ester.

6.3.2 *iso*-Homovanillic acid (*iso*-HVA)

The reaction of *iso*-homovanillic acid (*iso*-HVA) with Gibbs reagent gives two indophenol products with m/z 354 and 310 (eq 6.3). The first product forms when *iso*-HVA directly adds with Gibbs reagent without any loss of side chain, specifically the carboxylic group, whereas the other indophenol has mass lower by 44 Dalton than the previous product. This is believed to happen because of the loss of CO_2 at the carboxylic acid side chain of *iso*-HAV either before or after

formation of indophenol. Figure 6.3a shows the Full MS after a 5 minutes reaction and 6.3b shows the deconvoluted spectra. In addition of these two peaks, there is another product at m/z 295. We could not identify the structure of this product. The base peak is due to the decarboxylated indophenol at m/z 310 and it does not overlap with any other peaks of the reaction mixture. Thus, the formation of m/z 310 is a characteristic peak for *iso*-HVA, along with m/z 354.

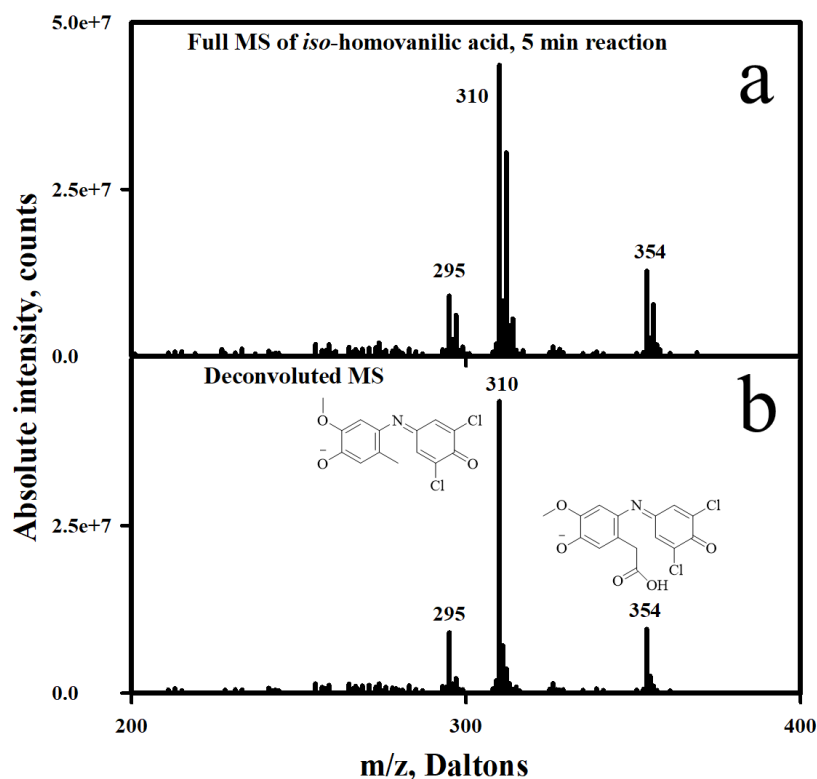
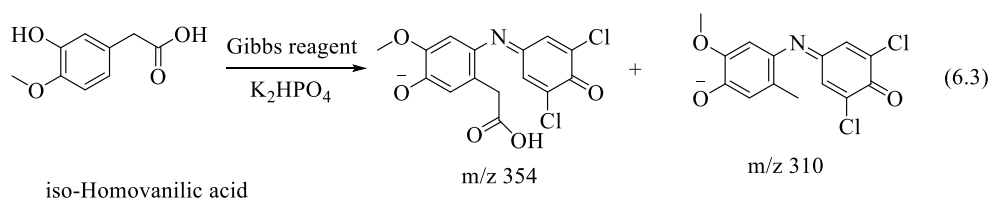


Figure 6.3. (a) Full MS and (b) deconvoluted MS of the Gibbs products from *iso*-Homovanillic acid.

6.3.3 Dopamine

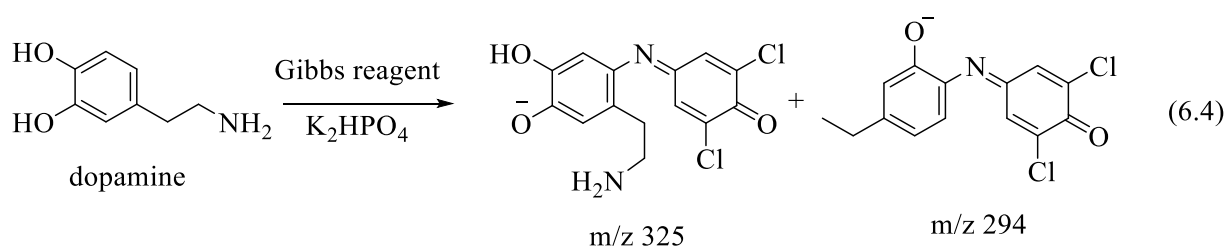


Figure 6.4 shows the full mass spectrum (6.4a) and deconvoluted mass spectrum (6.4b) of the Gibbs products from the reaction of dopamine (eq 6.4). The spectra show the main indophenol product at m/z 325 Dalton. There is a small product at m/z 294. This is probably due to the formation of ethyl group containing indophenol (Chapter 3). This indophenol may form when the substitution occurs by replacing hydroxy group at ortho position followed by a removal of ammonia (NH_3). No other significantly relative product was seen. Thus, this peak may be used as the characteristic peak for dopamine.

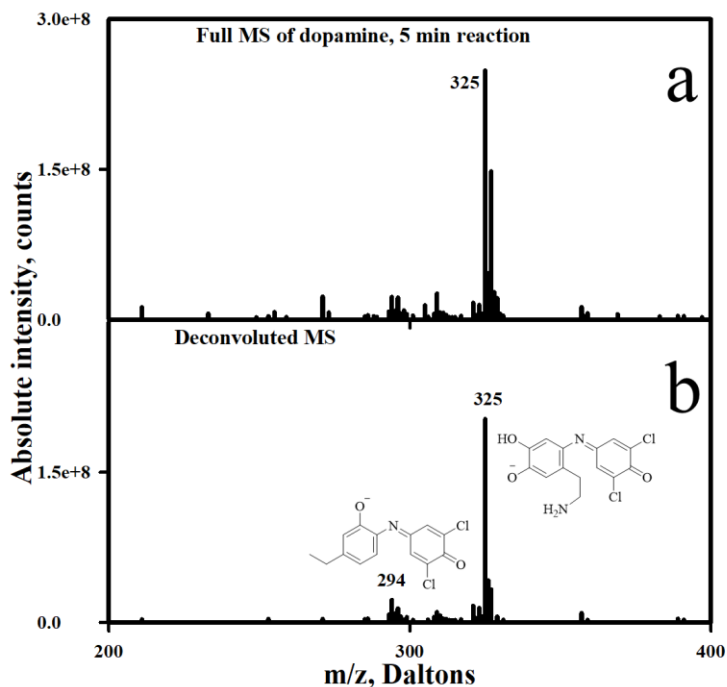


Figure 6.4. (a) Full MS and (b) deconvoluted MS of the Gibbs products from dopamine. Dopamine gives only indophenol at m/z 325.

6.3.4 3,4-Dihydroxyphenylacetic acid (DOPAC)

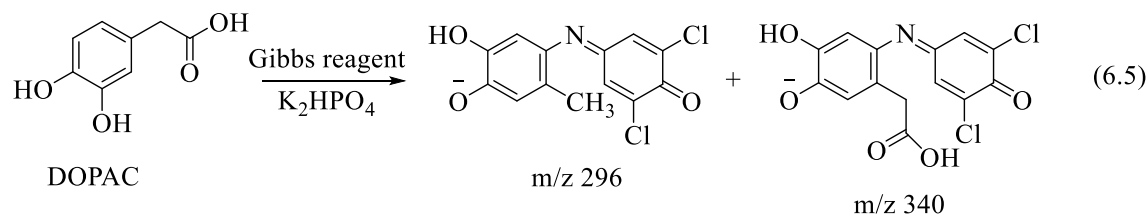


Figure 6.5 shows the full mass spectra (Figure 6.5a) and deconvoluted mass spectra (Figure 6.5b) of the Gibbs product of 3,4-dihydroxyphenylacetic acid (DOPAC). m/z 340 is due to the formation of expected indophenol of DOPAC. However, the base peak is m/z 296 which forms after decarboxylate. Though m/z 296 is the base peak for DOPAC, dimethoxyphenols (Chapter 4 and Chapter 5) also forms indophenols at m/z 296. Thus, we may use m/z 296 as the characteristic peak for the identification of this compound along with m/z 340.

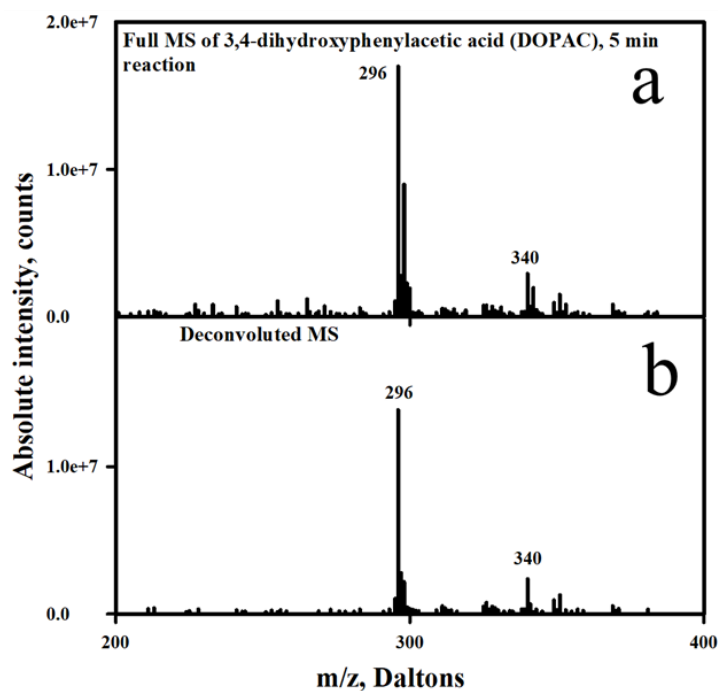
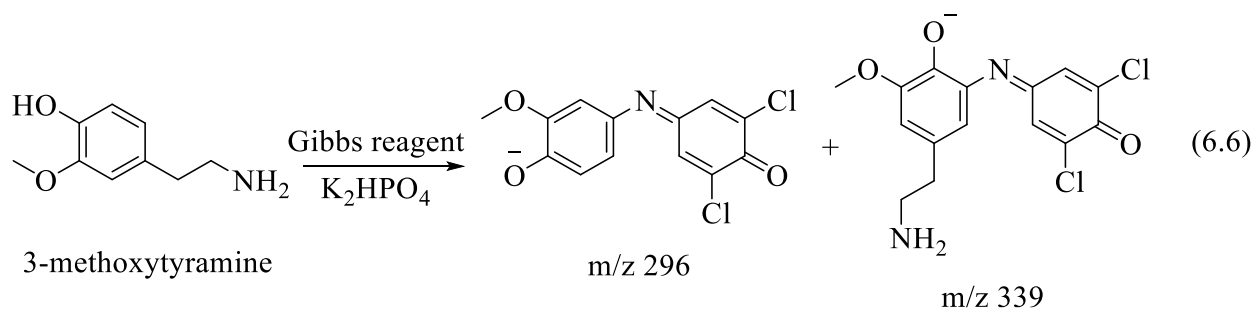


Figure 6.5. (a) Full MS and (b) deconvoluted MS of the Gibbs products from DOPAC.

6.3.5 3-Methoxytyramine (3-MT)



In the case of 3-methoxytyramine (3-MT), we have indophenols at m/z 339 and 296 (eq 6.6 and Figure 6.6). The first product is believed to form due to substitution at ortho position and the later due to the replacement of substituent at *para*-postion.⁴² Unfortunately, the *para*-substituted product may not be used for analyzing this compound identification peak as couple of other discussed neurotransmitters also gave the same indophenol. However, formation of m/z 296 along with m/z 339 can be used to identify 3-MT.

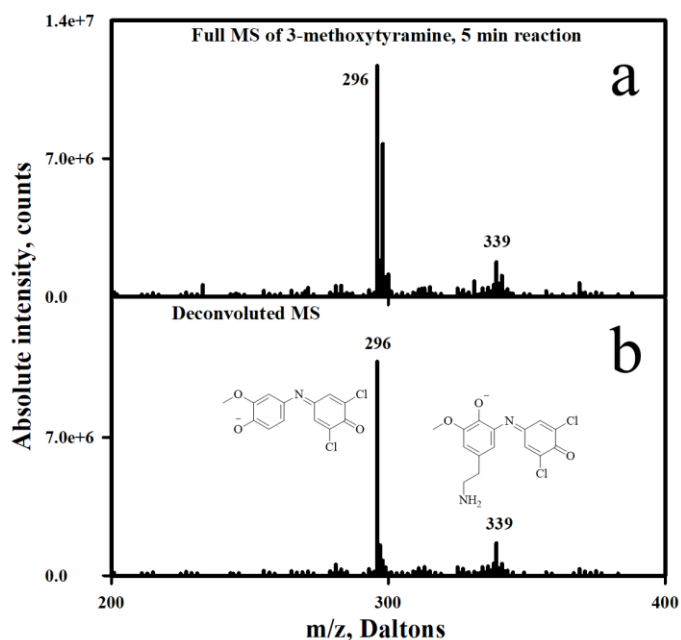
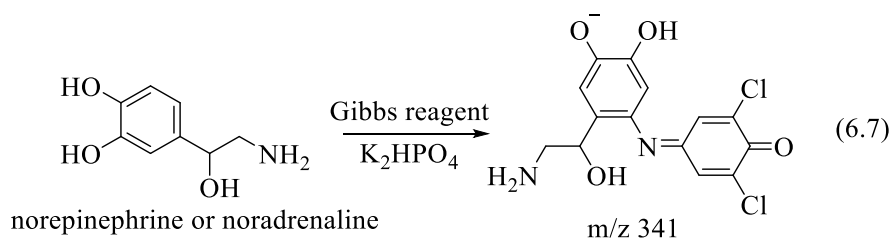


Figure 6.6. (a) Full MS and (b) deconvoluted MS of the Gibbs products from 3-methoxytyramine.

6.3.6 Norepinephrine (noradrenaline)



Finally, norepinephrine or noradrenaline gives indophenol at m/z 341 and 311 (eq 6.7). The mass spectra are shown in following figures (Fig. 6.7a for full MS and 6.7b for deconvoluted MS). The only significant indophenol formed here is at m/z 341 and we did not see any loss of ammonia (NH_3). Here also we could not identify the structure of m/z 311. The peak at m/z 341 Dalton can be used as characteristic peak for the analysis of noradrenaline.

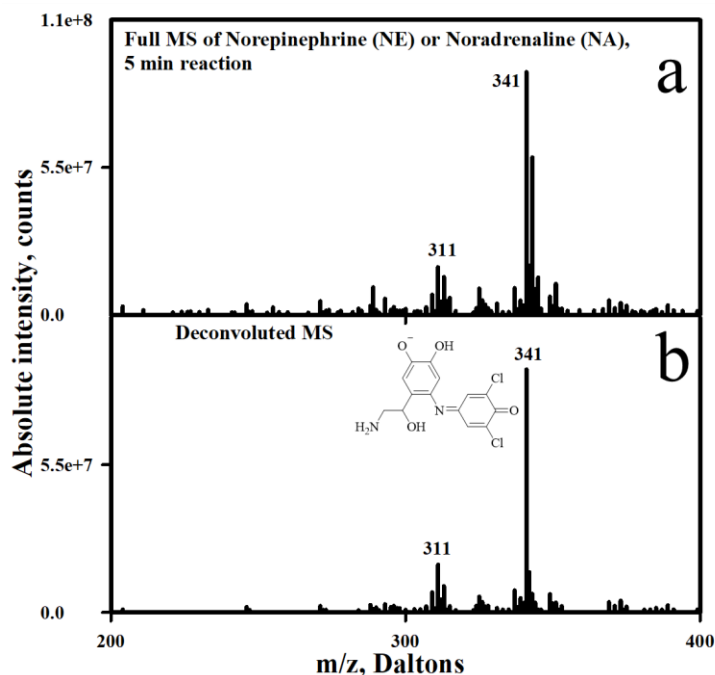


Figure 6.7. (a) Full MS and (b) deconvoluted MS of the Gibbs products from norepinephrine or noradrenaline.

6.4 Discussion

Though few of the analyzed neurotransmitters gave multiple indophenols, each of them had a characteristic peak regardless of the dominant product. In some cases, the dominant product can be used as a characteristic peak. For instance, m/z 310 for *iso*-homovanillic acid. On the other hand, there were few analytes where the dominant peaks and characteristic peak were different. Examples of this type are DOPAC and 3-MT. Both of these compounds form major product at m/z 296, but the characteristic peaks are different, at m/z 340 and m/z 339 for DOPAC and 3-MT, respectively. We saw only one indophenol product in each of the other three analytes. Thus, we may use m/z 383, 310, 325, 340, 339 and 341 Dalton for the identification of L-Dopa (methyl ester), *iso*-HVA, dopamine, DOPAC, 3-MT, and norepinephrine, respectively. This result is shown in the following in Table 6.1. In addition, there is a scope to optimized the reaction conditions to improve intensity of the characteristic peak of these neurotransmitters.

Table 6.1. Indophenol peak analysis of L-Dopa and it's metabolites

Analyte	Indophenol peaks	Dominated peak	Characteristic peak
L-Dopa-methyl ester	383	383	383
<i>iso</i> -Homovanillic acid (<i>iso</i> -HVA)	310, 354	310	310
Dopamine	325	325	325
3,4-Dihydroxyphenylacetic acid (DOPAC)	296, 340	296	340
3-Methoxytyramine (3-MT)	296, 339	296	339
Norepinephrine (noradrenaline)	341	341	341

6.5 Conclusion

Though spectrophotometry has been used in the analysis of L-DOPA metabolites even in biological samples by Gibbs reaction, we have shown that introduction of mass spectrometry would be a better alternative for these types of analysis. ESI-MS is capable of distinguishing between the different neurotransmitters. Finally, L-Dopa, which is unreactive with the Gibbs reagent, gives Gibbs reaction after esterification and can be analyzed using ESI-MS.

6.6 References

1. Baron, R.; Zayats, M.; Willner, I., Dopamine-, L-DOPA-, adrenaline-, and noradrenaline-induced growth of Au nanoparticles: assays for the detection of neurotransmitters and of tyrosinase activity. *Analytical chemistry* **2005**, *77* (6), 1566-1571.
2. Klegeris, A.; Korkina, L. G.; Greenfield, S. A., Autoxidation of dopamine: a comparison of luminescent and spectrophotometric detection in basic solutions. *Free radical biology and medicine* **1995**, *18* (2), 215-222.
3. Helaleh, M. I.; Rahman, N.; Abu-Nameh, E. S., Use of cerium (IV) nitrate in the spectrophotometric determination of levodopa and methyl dopa in the pure form and pharmaceutical preparations. *Analytical sciences* **1997**, *13* (6), 1007-1010.
4. Nagaraja, P.; Murthy, K. S.; Rangappa, K.; Gowda, N. M., Spectrophotometric methods for the determination of certain catecholamine derivatives in pharmaceutical preparations. *Talanta* **1998**, *46* (1), 39-44.
5. Pulikkalpara, H.; Kurup, R.; Mathew, P. J.; Baby, S., Levodopa in *Mucuna pruriens* and its degradation. *Scientific reports* **2015**, *5*, 11078.
6. Musacchio, J. M., Enzymes involved in the biosynthesis and degradation of catecholamines. In *Biochemistry of Biogenic Amines*, Springer: 1975; pp 1-35.
7. Khan, M. Z.; Nawaz, W., The emerging roles of human trace amines and human trace amine-associated receptors (hTAARs) in central nervous system. *Biomedicine & pharmacotherapy= Biomedecine & pharmacotherapie* **2016**, *83*, 439-449.
8. ROFFLER-TARLOV, S.; Sharman, D.; Tegerdine, P., 3, 4-Dihydroxyphenylacetic acid and 4-hydroxy-3-methoxyphenylacetic acid in the mouse striatum: a reflection of intra- and extra-neuronal metabolism of dopamine? *British journal of pharmacology* **1971**, *42* (3), 343-351.

9. Desvignes, C.; Bert, L.; Vinet, L.; Denoroy, L.; Renaud, B.; Lambás-Señas, L., Evidence that the neuronal nitric oxide synthase inhibitor 7-nitroindazole inhibits monoamine oxidase in the rat: in vivo effects on extracellular striatal dopamine and 3, 4-dihydroxyphenylacetic acid. *Neuroscience letters* **1999**, *261* (3), 175-178.
10. Comoy, E.; Bohuon, C., Iso-homovanillic acid determination in human urine. *Clinica Chimica Acta* **1971**, *35* (2), 369-375.
11. Dalmaz, Y.; Peyrin, L., Rapid procedure for chromatographic isolation of DOPA, DOPAC, epinephrine, norepinephrine and dopamine from a single urinary sample at endogenous levels. *Journal of Chromatography B: Biomedical Sciences and Applications* **1978**, *145* (1), 11-27.
12. Sorouraddin, M.; Manzoori, J.; Kargarzadeh, E.; Shabani, A. H., Spectrophotometric determination of some catecholamine drugs using sodium bismuthate. *Journal of pharmaceutical and biomedical analysis* **1998**, *18* (4-5), 877-881.
13. Hasan, B. A.; Khalaf, K. D.; De La Guardia, M., Flow analysis-spectrophotometric determination of l-dopa in pharmaceutical formulations by reaction with p-aminophenol. *Talanta* **1995**, *42* (4), 627-633.
14. Marcolino-Junior, L. H.; Teixeira, M. F.; Pereira, A. V.; Fatibello-Filho, O., Flow injection determination of levodopa in tablets using a solid-phase reactor containing lead (IV) dioxide immobilized. *Journal of pharmaceutical and biomedical analysis* **2001**, *25* (3-4), 393-398.
15. Tolokan, A.; Klebovich, I.; Balogh-Nemes, K.; Horvai, G., Automated determination of levodopa and carbidopa in plasma by high-performance liquid chromatography-electrochemical detection using an on-line flow injection analysis sample pretreatment unit. *Journal of Chromatography B: Biomedical Sciences and Applications* **1997**, *698* (1-2), 201-207.
16. Doležalová, M.; Tkaczykova, M., Direct high-performance liquid chromatographic determination of the enantiomeric purity of levodopa and methyl dopa: comparison with pharmacopoeial polarimetric methods. *Journal of pharmaceutical and biomedical analysis* **1999**, *19* (3-4), 555-567.
17. Siddhuraju, P.; Becker, K., Rapid reversed-phase high performance liquid chromatographic method for the quantification of L-Dopa (L-3, 4-dihydroxyphenylalanine), non-methylated and methylated tetrahydroisoquinoline compounds from Mucuna beans. *Food chemistry* **2001**, *72* (3), 389-394.
18. Schieffer, G. W., Reversed-phase high-performance liquid chromatographic investigation of levodopa preparations II: levodopa determination. *Journal of pharmaceutical sciences* **1979**, *68* (10), 1299-1301.
19. Lucero, M. T.; Farrington, H.; Gilly, W. F., Quantification of L-dopa and dopamine in squid ink: implications for chemoreception. *The Biological Bulletin* **1994**, *187* (1), 55-63.

20. Wagner, J.; Vitali, P.; Palfreyman, M. G.; Zraika, M.; Huot, S., Simultaneous determination of 3, 4-dihydroxyphenylalanine, 5-hydroxytryptophan, dopamine, 4-hydroxy-3-methoxyphenylalanine, norepinephrine, 3, 4-dihydroxyphenylacetic acid, homovanillic acid, serotonin, and 5-hydroxyindoleacetic acid in rat cerebrospinal fluid and brain by high-performance liquid chromatography with electrochemical detection. *Journal of neurochemistry* **1982**, *38* (5), 1241-1254.
21. Shoup, R. E.; Kissinger, P. T., Determination of urinary normetanephrine, metanephrine, and 3-methoxytyramine by liquid chromatography, with amperometric detection. *Clinical chemistry* **1977**, *23* (7), 1268-1274.
22. Hansson, C.; Agrup, G.; Rorsman, H.; Rosengren, A.-M.; Rosengren, E.; Edholm, L.-E., Analysis of cysteinyl-dopa, dopa, dopamine, noradrenaline and adrenaline in serum and urine using high-performance liquid chromatography and electrochemical detection. *Journal of Chromatography B: Biomedical Sciences and Applications* **1979**, *162* (1), 7-22.
23. Szopa, J.; Wilczyński, G.; Fiehn, O.; Wenczel, A.; Willmitzer, L., Identification and quantification of catecholamines in potato plants (*Solanum tuberosum*) by GC-MS. *Phytochemistry* **2001**, *58* (2), 315-320.
24. Carrera, V.; Sabater, E.; Vilanova, E.; Sogorb, M. A., A simple and rapid HPLC-MS method for the simultaneous determination of epinephrine, norepinephrine, dopamine and 5-hydroxytryptamine: Application to the secretion of bovine chromaffin cell cultures. *Journal of Chromatography B* **2007**, *847* (2), 88-94.
25. Twentyman, J. M.; Cradic, K. W.; Singh, R. J.; Grebe, S. K., Ionic cross talk can lead to overestimation of 3-methoxytyramine during quantification of metanephrines by mass spectrometry. *Clinical chemistry* **2012**, *58* (7), 1156-1158.
26. Narasimhachari, N.; Leiner, K.; Brown, C., The simultaneous determination by selected ion monitoring of the levels of homovanillic, isohomovanillic, 3, 4-dihydroxyphenylacetic and 3-methoxy-4-hydroxymandelic acids in single biological samples. *Clinica Chimica Acta* **1975**, *62* (2), 245-253.
27. Chen, R.-S.; Huang, W.-H.; Tong, H.; Wang, Z.-L.; Cheng, J.-K., Carbon fiber nanoelectrodes modified by single-walled carbon nanotubes. *Analytical chemistry* **2003**, *75* (22), 6341-6345.
28. Raj, C. R.; Okajima, T.; Ohsaka, T., Gold nanoparticle arrays for the voltammetric sensing of dopamine. *Journal of Electroanalytical Chemistry* **2003**, *543* (2), 127-133.
29. Huang, T.; Yang, L.; Gitzen, J.; Kissinger, P. T.; Vreeke, M.; Heller, A., Detection of basal acetylcholine in rat brain microdialysate. *Journal of Chromatography B: Biomedical Sciences and Applications* **1995**, *670* (2), 323-327.
30. Liu, T.; Li, M.; Li, Q., Electroanalysis of dopamine at a gold electrode modified with N-acetylcysteine self-assembled monolayer. *Talanta* **2004**, *63* (4), 1053-1059.

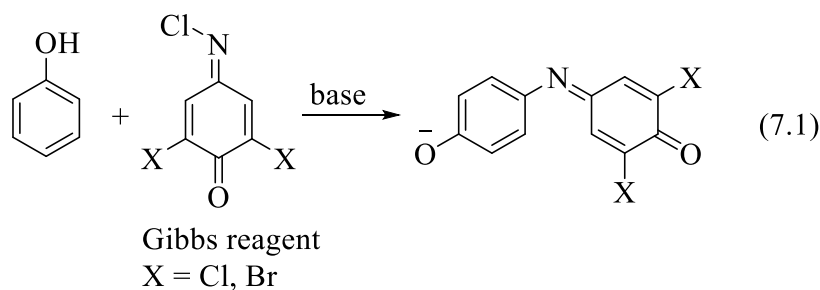
31. Raj, C. R.; Ohsaka, T., Electroanalysis of ascorbate and dopamine at a gold electrode modified with a positively charged self-assembled monolayer. *Journal of Electroanalytical Chemistry* **2001**, 496 (1-2), 44-49.
32. Wiedemann, D. J.; Kawagoe, K. T.; Kennedy, R. T.; Ciolkowski, E. L.; Wightman, R. M., Strategies for low detection limit measurements with cyclic voltammetry. *Analytical chemistry* **1991**, 63 (24), 2965-2970.
33. Kawagoe, K. T.; Zimmerman, J. B.; Wightman, R. M., Principles of voltammetry and microelectrode surface states. *Journal of neuroscience methods* **1993**, 48 (3), 225-240.
34. Viswanathan, S.; Liao, W.-C.; Huang, C.-C.; Hsu, W.-L.; Ho, J.-a. A., Rapid analysis of L-dopa in urine samples using gold nanoelectrode ensembles. *Talanta* **2007**, 74 (2), 229-234.
35. Lahav, M.; Shipway, A. N.; Willner, I., Au-nanoparticle–bis-bipyridinium cyclophane superstructures: assembly, characterization and sensoric applications. *Journal of the Chemical Society, Perkin Transactions 2* **1999**, (9), 1925-1931.
36. Kharitonov, A. B.; Shipway, A. N.; Willner, I., An Au nanoparticle/bisbipyridinium cyclophane-functionalized ion-sensitive field-effect transistor for the sensing of adrenaline. *Analytical chemistry* **1999**, 71 (23), 5441-5443.
37. Dai, M.; Sun, L.; Chao, L.; Tan, Y.; Fu, Y.; Chen, C.; Xie, Q., Immobilization of enzymes by electrochemical and chemical oxidative polymerization of L-DOPA to fabricate amperometric biosensors and biofuel cells. *ACS applied materials & interfaces* **2015**, 7 (20), 10843-10852.
38. Sanati, A. L.; Faridbod, F.; Ganjali, M. R., Synergic effect of graphene quantum dots and room temperature ionic liquid for the fabrication of highly sensitive voltammetric sensor for levodopa determination in the presence of serotonin. *Journal of Molecular Liquids* **2017**, 241, 316-320.
39. Britz-Mckibbin, P.; Wong, J.; Chen, D. D., Analysis of epinephrine from fifteen different dental anesthetic formulations by capillary electrophoresis. *Journal of Chromatography A* **1999**, 853 (1-2), 535-540.
40. Swanek, F. D.; Chen, G.; Ewing, A. G., Identification of multiple compartments of dopamine in a single cell by CE with scanning electrochemical detection. *Analytical Chemistry* **1996**, 68 (22), 3912-3916.
41. Moini, M.; Schultz, C. L.; Mahmood, H., CE/electrospray ionization-MS analysis of underivatized d/l-amino acids and several small neurotransmitters at attomole levels through the use of 18-crown-6-tetracarboxylic acid as a complexation reagent/background electrolyte. *Analytical chemistry* **2003**, 75 (22), 6282-6287.
42. Mistry, S.; Wenthold, P. G., Mass spectrometric detection of the Gibbs reaction for phenol analysis. *Journal of Mass Spectrometry* **2018**.

43. Singleton, V. L.; Orthofer, R.; Lamuela-Raventós, R. M., [14] Analysis of total phenols and other oxidation substrates and antioxidants by means of folin-ciocalteu reagent. In *Methods in enzymology*, Elsevier: 1999; Vol. 299, pp 152-178.
44. Hay, A. S., Polymerization by oxidative coupling. II. Oxidation of 2, 6-disubstituted phenols. *Journal of Polymer Science* **1962**, 58 (166), 581-591.
45. Dewar, M. J.; Nakaya, T., Oxidative coupling of phenols. *Journal of the American Chemical Society* **1968**, 90 (25), 7134-7135.
46. Whitlock, L. R.; Siggia, S.; Smola, J. E., Spectrophotometric analysis of phenols and of sulfonates by formation of an azo dye. *Analytical Chemistry* **1972**, 44 (3), 532-536.
47. Menek, N.; Topçu, S.; Uçar, M., Voltammetric and spectrophotometric studies of 2-(5-bromo-2-pyridylazo)-5-diethylamino) phenol copper (II) complex. *Analytical letters* **2001**, 34 (10), 1733-1740.
48. Gibbs, H. D., Phenol Tests. IV. A Study of the Velocity of Indophenol Formation 2, 6-Dibromobenzenoneindophenol. *The Journal of Physical Chemistry* **1927**, 31 (7), 1053-1081.
49. Gibbs, H. D., Phenol tests III. The indophenol test. *Journal of biological chemistry* **1927**, 72 (2), 649-664.
50. Wenthold, P. G.; Mistry, S., Methods of detecting chemicals. Google Patents: 2019.
51. Mistry, S.; Wenthold, P. In *Mass spectroscopic analysis of phenol derivatives by Gibbs reaction*, ABSTRACTS OF PAPERS OF THE AMERICAN CHEMICAL SOCIETY, AMER CHEMICAL SOC 1155 16TH ST, NW, WASHINGTON, DC 20036 USA: 2019.

CHAPTER 7. SPECIFICITY OF *PARA*-SUBSTITUTED PHENOLS IN GIBBS REACTION

7.1 Introduction

The Gibbs reaction is a longstanding assay used for the detection of phenols.¹⁻¹⁷ In the presence of base and the “Gibbs reagent,” (2,6-dibromo- or 2,6-dichloro-4-(chloroimino)cyclohexa-2,5-dien-1-one), phenols are converted to highly colored indophenols (eq 7.1). Total phenol content can consequently be determined by using spectrophotometry.



Early studies of the Gibbs reaction of substituted phenols focused on those without substitution in the *para*-position.^{1,2,18} However, Dacre¹⁹ and Josephy and Van Damme²⁰ ultimately showed that the Gibbs reaction occurs with a wide variety of *para*-substituted phenols, in addition to those without *para*-substitution, and that the indophenol is formed by displacing the *para* substituent.²⁰ Consequently, while the Gibbs reagent is useful for the detection of total phenolic content, it lacks specificity in terms of reactivity. Moreover, because the absorption wavelengths of the substituted indophenols are not highly sensitive to phenol substitution, the Gibbs method is not specific in colorimetric detection, either.

In a recent study, we described an approach for the detection of Gibbs indophenol products by using electrospray ionization- mass spectrometry (ESI-MS), which allows for simple differentiation of phenols with different substituents according to their mass-to-charge ratio. It was shown that this approach is essentially as sensitive as the colorimetric approach, but provides detection specificity. In the course of that work, it was shown that, as reported by Dacre¹⁹ and

Josephy and Van Damme,²⁰ positive Gibbs tests are obtained for a wide range of *para*-substituted phenols, and that, in most cases, substitution occurs by displacement of the *para*-substituent. Herein, we describe a more detailed study of the Gibbs reaction of *para*-substituted phenols, as assayed by using ESI-MS. An advantage of use MS for detection of this process is that it is readily possible to determine the site of substitution, without requiring chemical isolation. In this work, we confirm the results of Josephy and Van Damme²⁰ showing it is possible to displace the *para*-substituents in reaction with the Gibbs reagent, leading to the formation of the same indophenol formed in the reaction with phenol (eq 7.1) However, in select cases (particularly, with alkyl substitution), the substituent is not displaced, and the substitution appears to occur at the *ortho* position to form a short-lived *iso*-indophenol. Moreover, we show that, even in cases where substitution occurs at the *para* position, there is generally an additional unique second-phenol-addition product, which conveniently can be used from an analytical perspective to distinguish *para*-substituted phenols from the unsubstituted versions.

7.2 Experimental

7.2.1 Chemicals

4-Fluorophenol, 4-chlorophenol, 4-bromophenol, 4-methoxyphenol, p-cresol, 4-ethylphenol, 4-aminophenol, 1,4-dihydroxybenzene, 4-nitrophenol, 4-hydroxybenzaldehyde, 4-hydroxybenzotrile and 2,6-dichlorobenzoquinone-4-chloroimine (Gibbs reagent) were obtained from commercial sources and used as received. Ethyl acetate, hexane and methanol were “Reagent Grade” and used without further purification. Deionized water was used for the experiments.

7.2.2 Sample preparation

105 mg (0.5 mmole) of Gibbs reagent and 112 mg (1 mmole) *p*-fluorophenol were dissolved in 10 mL methanol and added into a 10 mL water solution of 87 mg (0.5 mmol) K_2HPO_4 at room temperature. The whole reaction mixture was stirred at room temperature for 5 minutes. 25 μL of the reaction mixture was dissolved in 2 mL water-methanol (1:1) solution for ESI-MS analysis.

7.2.3 Purification of the Gibbs product

Only the Gibbs products with *p*-fluorophenol were isolated. In brief, after the 5 minutes reaction, 1 g NH_4Cl and 20 mL ethyl acetate was added into the reaction mixture and shaken vigorously. The organic layer was separated, washed with 10 mL brine ($\times 2$), dried by MgSO_4 and filtered. Finally, the solvent was removed below 30°C under reduced pressure and silica slurry was prepared for column chromatography. The silica slurry was loaded into a 12-inch-long silica column and 10% ethyl acetate in hexane was to isolate the compounds initially. Selected collections were combined and dries to make another silica slurry and used about 10-inch silica column and 10% ethyl acetate in hexane to separate compounds.

7.2.4 Spectra collection

Electrospray ionization mass spectra were obtained on a commercial LCQ-DECA (Thermo Electron Corporation, San Jose, CA, USA) quadrupole ion trap mass spectrometer, equipped with ESI source, operating in negative ion mode. Substrate solutions were in methanol: water mixture (1:1) and introduced into the source directly at a flow rate of 5 $\mu\text{L}/\text{min}$. Electrospray and ion focusing conditions were varied to maximize the signal of the ion of interest.

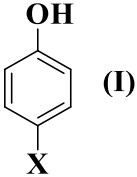
7.2.5 Spectral analysis

The advantages of using Gibbs reagent for derivatization are the readily ionizable product, indophenol, and it can be easily detectable by the isotopic pattern. Therefore, no sample preparation and purification are required for the analysis of the indophenol by ESI-MS. Moreover, the deconvolution of the isotopic pattern for ions containing two chlorine atoms (1:0.648:0.105) can eliminate the peaks that do not contain the Gibbs reagent²¹⁻²³. We used Microsoft Excel for the analysis of the MS data and for the deconvolution of two chlorine atoms. The MS spectra were plotted by using Sigma Plot 11.

7.3 Results

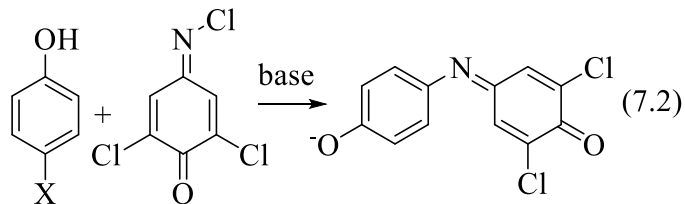
In the previous work,²¹ we reported positive Gibbs reactions with *para*-substituted phenols **1c, d, f, g, i**. The substituents range from halogens to alkyl groups, and therefore have a wide variety of electronic and chemical properties.

Table 7.1. List of *para*-substituted phenols that were analyzed

	
a: X = NH₂	b: X = OH c: X = CH₃ d: X = C₂H₅ e: X = OC₆H₅
f: X = F g: X = Cl h: X = Br i: X = OCH₃ j: X = OC₂H₅ k: X = OCH₂CH₂CH₃ l: X = OCH₂CH₂CH₂CH₃	m: X = NO₂ n: X = CHO o: X = CN p: X = COOH q: X = CH₂CH₂CH₃

In this work, we have added phenols to get all phenols listed in Table 7.1 (**1a – q**). The results can be broken down into four classes of reactions. Although all substrates give a mixture of products, the phenols with amine substituted (**1a**) gives indophenol by substituted at the *para*-position. In the second class, phenols (X = hydroxy, methyl, ethyl, phenoxy), **1b-e**, may react without any substitution of X and give products that include the substituent, indicating that the reaction occurs at a different site within the phenol. In the following group (**1f – k**), phenols contain halogen (F, Cl, and Br) or alkoxy (methoxy, ethoxy, propoxy, and butoxy) substituted react to give indophenols that result from the substitutions of X (eq 7.2) and an additional product. The fourth group does not substitute at the *para*-position and does not give additional product. The four reactions are addressed separately below. In every case, the upper figure is the full MS and the lower one is the deconvolution of the corresponding full MS.

7.3.1 Direct substitution of X



Reaction of 4-aminophenol (**1a**) with Gibbs reagent for 5 minutes does not give any indophenol of m/z 266, which is the indophenol product observed in the reaction with phenol (eq 7.1) and would result from replacing the amino group (Figure 7.1a). We also did not see any peak at m/z 281, which might form by *ortho*-substitution. But the spectra show peaks of unknown compounds at m/z 318, 336, and 386.

When we observed reaction after 30 minutes, it gave product resulting from the replacement of amine group ($-NH_2$) at *para*-position (m/z 266) according to eq. 7.2 (Figure 7.1b1 and 7.1b2). In the latter case, as the shorter reaction, we did not see any formation of *ortho*-substituted indophenol. Like previous observation, the reaction gave few peaks having unknown structures (at m/z 279, 318, 336, and 386).

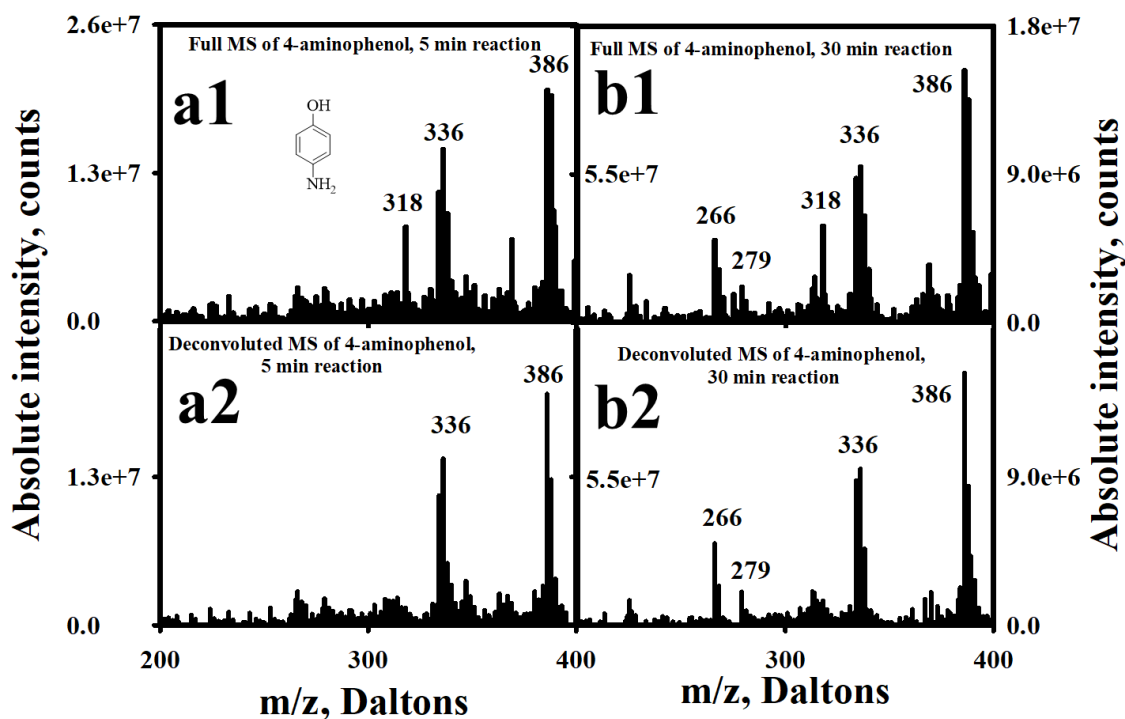


Figure 7.1. The Gibbs reaction of 4-aminophenol after (a) 5 minute and (b) 30-minute reaction. a1 is the full MS and a2 is corresponding deconvoluted MS. After 5-minute reaction, 4-aminophenol gives no substitution product and no condensation product. The peak formed at ortho-substitution (at m/z 281) is also missing. However, after 30-minute reaction, it gives only substitution product at m/z 266 (b1 and b2). The peak formed by ortho-substitution (at m/z 281) is also missing even after 30-minute reaction.

7.3.2 Substitution at ortho position

p-Methylphenol (*p*-cresol), *p*-ethylphenol, hydroquinone (*p*-hydroxyphenol) and *p*-phenoxyphenol are belong in this group. We can divide this group into two subgroups – (i) compound gives absolutely no substitution at *para*-position and (ii) compounds give both substitution at *para*-position and *ortho*-position. The first subgroup contains only *p*-cresol. When this compound reacts with Gibbs reagent, only a product with m/z 280 formed (Figure 7.2). This indophenol formed while the new bond formed at presumably the *ortho*-position of *p*-cresol and keeping methyl substituent ($-CH_3$) at *para*-position. Unlike in the previous cases, we did not see the direct replacement at *para*-position. Here, we propose that reacts at *ortho*-position as the bond formation at *para*-position would give m/z 266. The *meta*-substituted product has not been

reported. We did not see any peak at m/z 266 even at longer time reaction (data not shown). However, Josephy and Damme reported the formation of indophenol for this reaction.²⁴ In that case, the mass of the indophenol should be 266 instead of 280. Previously, Pallagi, *et al.* mentioned about the formation of indophenol at *ortho*-position²⁵ and thus the structure might be as in eq. 7.3.

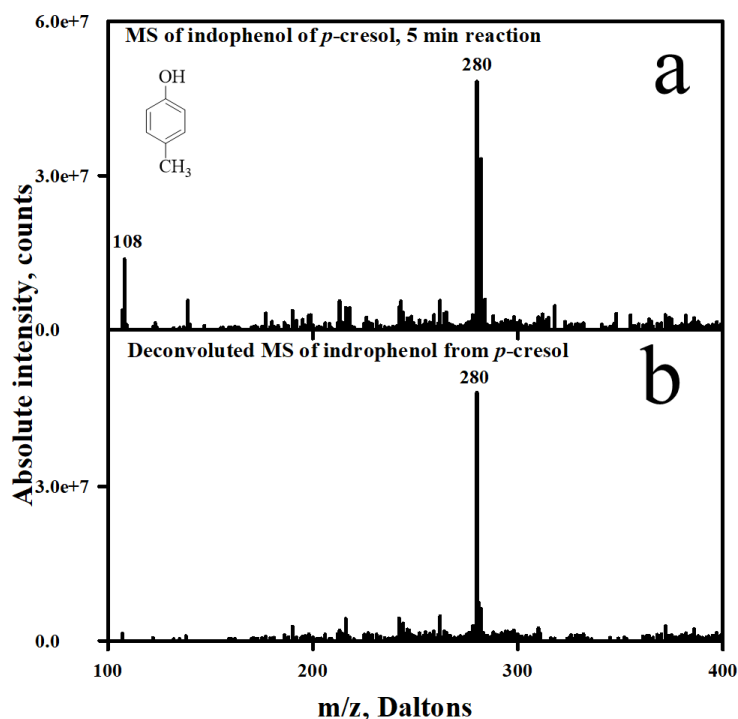
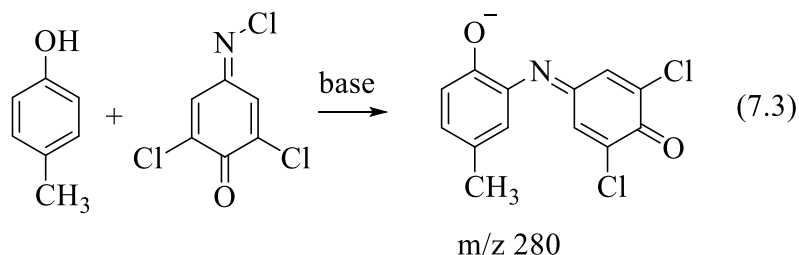


Figure 7.2. The Gibbs products of 4-methylphenol or *p*-cresol after 5 minute reaction. (a) is the Full MS of the reaction solution and (b) is the deconvoluted MS. 4-Methylphenol gives neither the substitution product nor the condensation product. It is proposed that the peak at m/z 280 is formed from the substitution of *ortho*-position instead of *para*-substitution.

The other subgroup contains -OH, -C₂H₅ and -OC₆H₅ at the *para*-position. Hydroquinone and *para*-ethylphenol give corresponding *ortho*-substituted indophenol at *m/z* 282 and *m/z* 294, respectively, in the 5 minute reactions (Figure 7.3a1, 7.3a2 for hydroxyquinone and Figure 7.4a1 and 7.4a2 for *p*-ethylphenol). However, in longer reaction time (30 minute), both give indophenol at *m/z* 266 after replacing groups at *para*-position (Figure 7.3b1, 7.3b2 for hydroxyquinone and Figure 7.4b1 and 7.4b2 for *p*-ethylphenol).

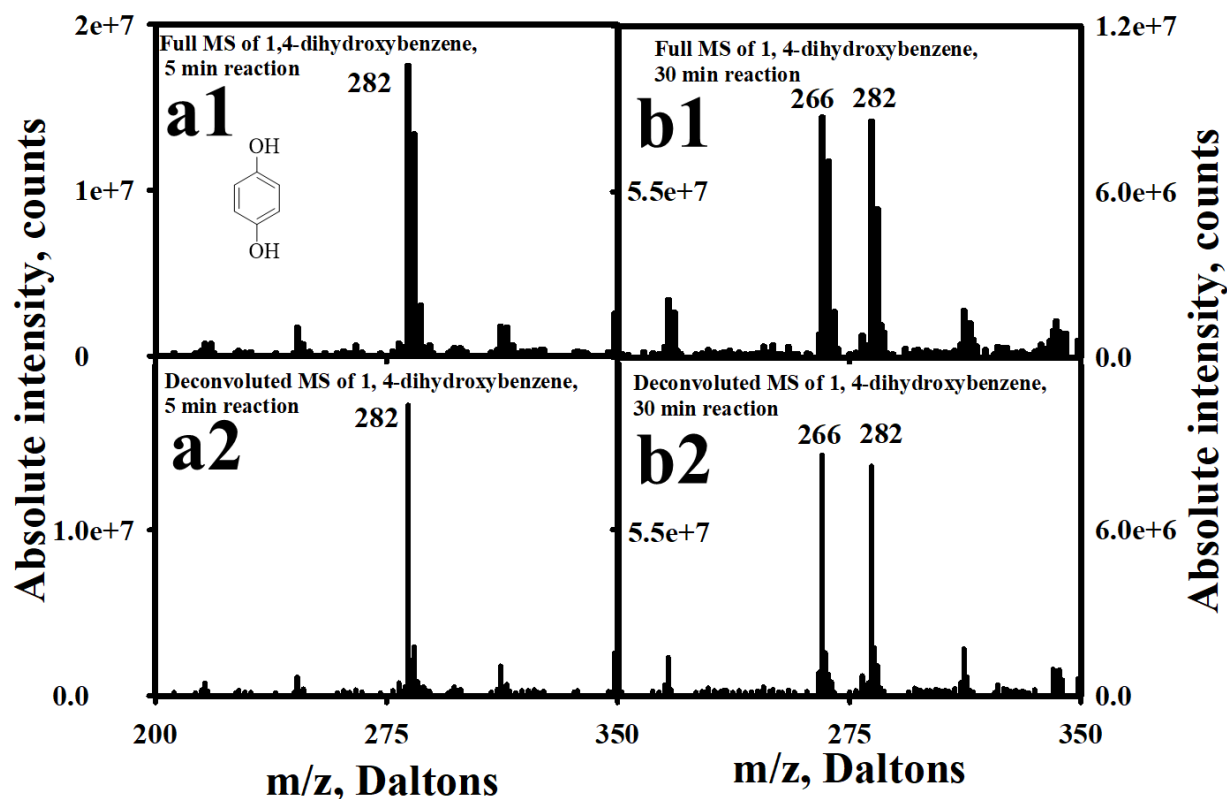


Figure 7.3. The Gibbs products of hydroxyquinone after 5 minute reaction (a1 and a2) and 30 minute reaction (b1 and b2). Only *ortho*-substituted product forms after 5 minutes and both *ortho*- and *para*-substituted products form in longer reaction time.

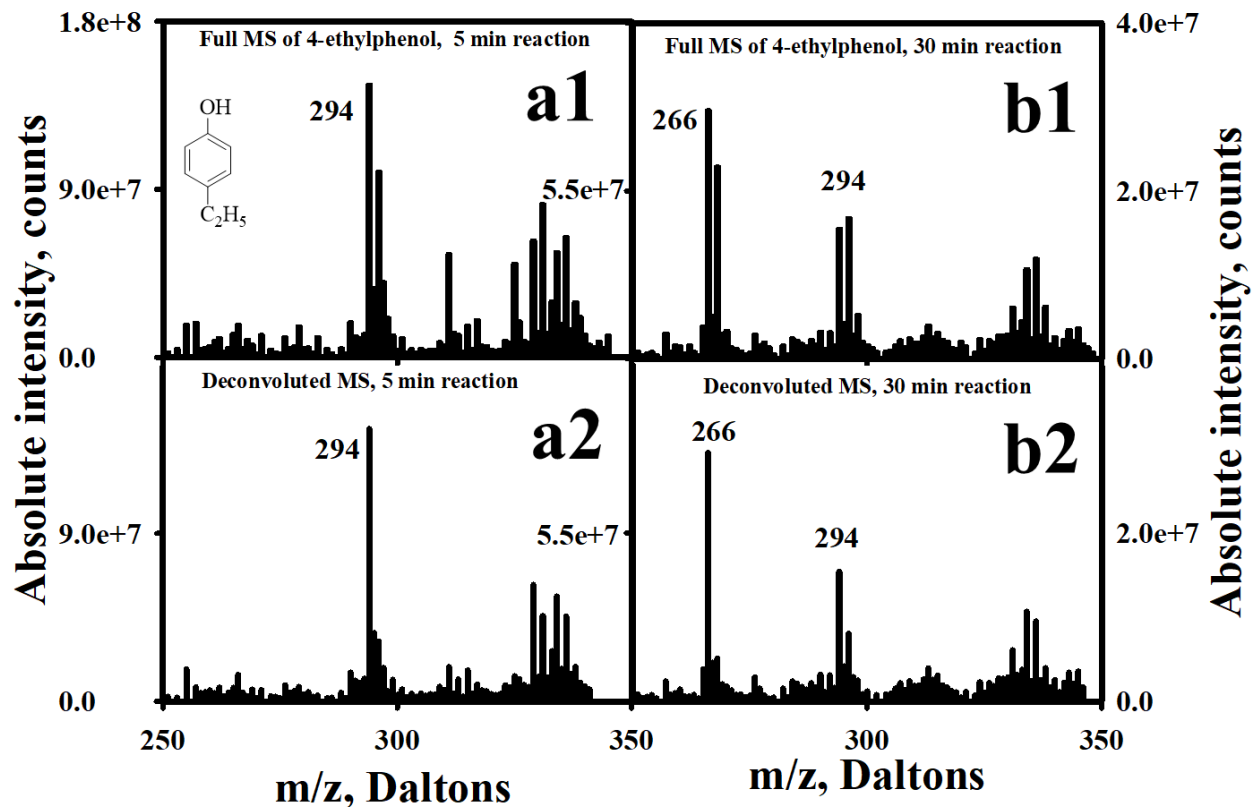


Figure 7.4. The Gibbs products of *p*-ethylphenol after 5 minute reaction (a1 and a2) and 30 minute reaction (b1 and b2). Only *ortho*-substituted product forms after 5 minutes and both *ortho*- and *para*-substituted products form in longer reaction time.

The last compound of this group is *p*-phenoxyphenol. Figure 7.5 shows the full MS and deconvoluted MS of the Gibbs product of this compound after 5 minute reaction. Both *ortho*- and *para*-substituted indophenols form in 5 minutes and we did not see any change in longer reaction time.

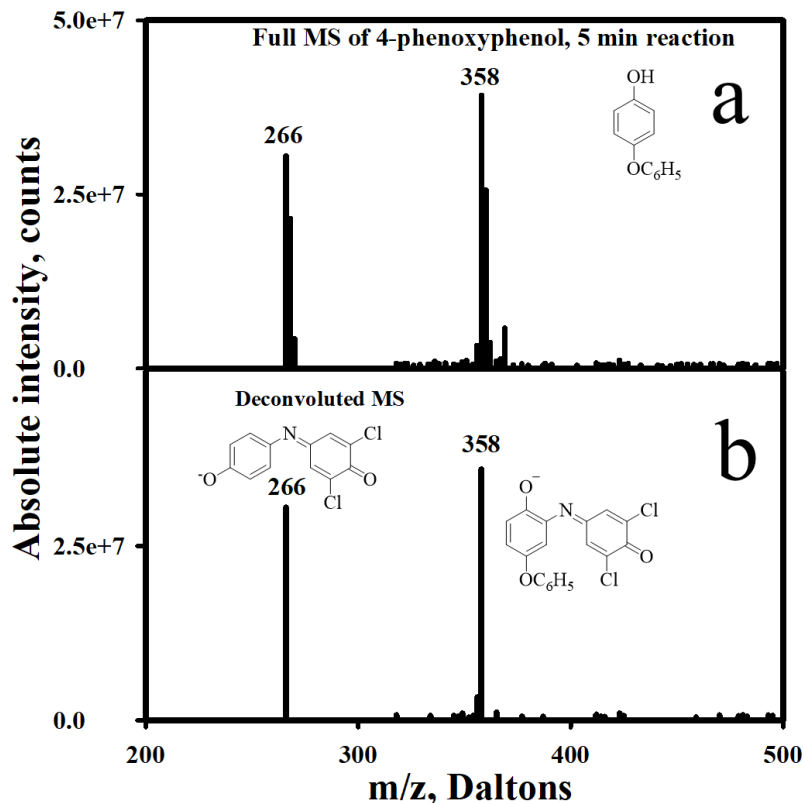


Figure 7.5. The Gibbs products of *p*-phenoxyphenol after 5 minute reaction. (a) is the Full MS of the reaction solution and (b) is the deconvoluted MS. 4-phenoxyphenol gives *ortho*-substituted indophenol at m/z 266 and *para*-substituted indophenol at m/z of 358.

7.3.3 Substitution and second addition of X

Phenols having fluorine, chlorine, bromine, methoxy, ethoxy, *n*-propoxy, and *n*-butoxy groups at *para*-position (**1f-l**) belong in this class. These compounds give indophenol at m/z 266 by replacing substituents at *para*-position. In addition, these compounds give another product at higher mass than the indophenol. In every case, we saw the second product has mass of one corresponding phenol more than the first indophenol. The mass of the second product can be calculated by subtracting two hydrogen atoms from indophenol and adding corresponding phenol (m/z 266 + M – 2). Since it forms by the condensation of indophenol and a phenol molecule, we are calling it condensation product (**CP**). The formation of condensation product is shown in eq. 7.4. For instance, Figure 7.6 shows the full MS and deconvoluted MS of the products when 4-

fluorophenol reacts with Gibbs reagent. It forms both indophenol at m/z 266 and **CP** product at m/z 376.

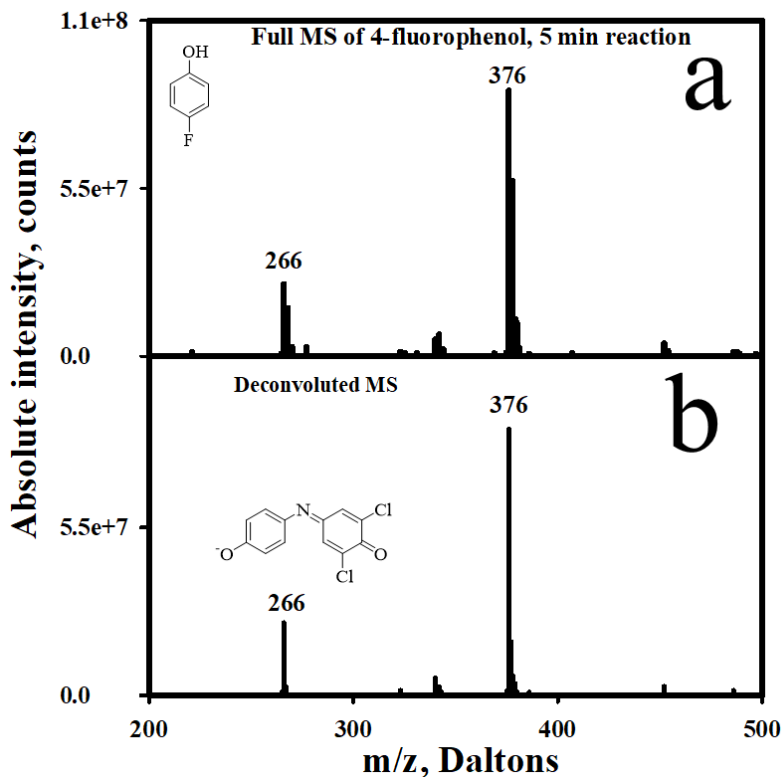
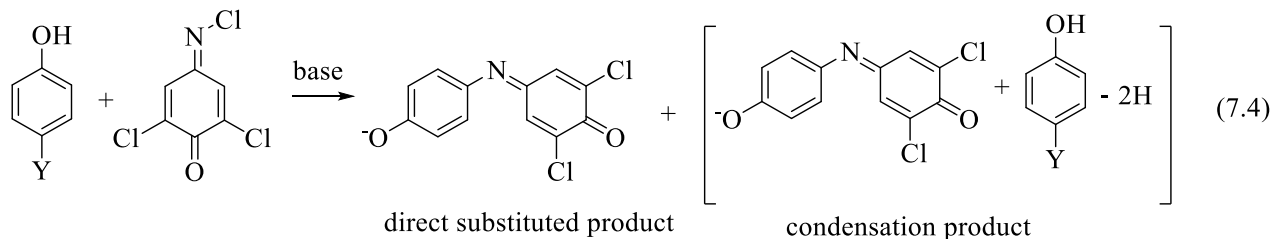


Figure 7.6. The Gibbs products of 4-fluorophenol after 5 minutes reaction. (a) is the Full MS of the reaction solution and (b) is the deconvoluted MS. 4-fluorophenol gives both substituted product, indophenol, at m/z 266 and an adduct at m/z 376.

Similarly, all other phenols in this group gave indophenol at m/z 266 by substituting at *para*-position and a condensation product. For example, the **CP** products of *p*-chlorophenol, *p*-bromophenol, *p*-methoxyphenol, *p*-ethoxyphenol, 4-*n*-propoxyphenol, and 4-*n*-butoxyphenol are

at m/z 292, 436, 388, 402, 416, and 430, respectively. These are shown in following figures (Figure 7.7 to Figure 7.12). Interestingly, for halogen containing substituents, with decreasing electronegativity or increasing the length of side chain result lower **CP** amount. In nucleophilic aromatic substitution leaving group stability apparently plays a crucial role in the reaction kinetics.²⁶

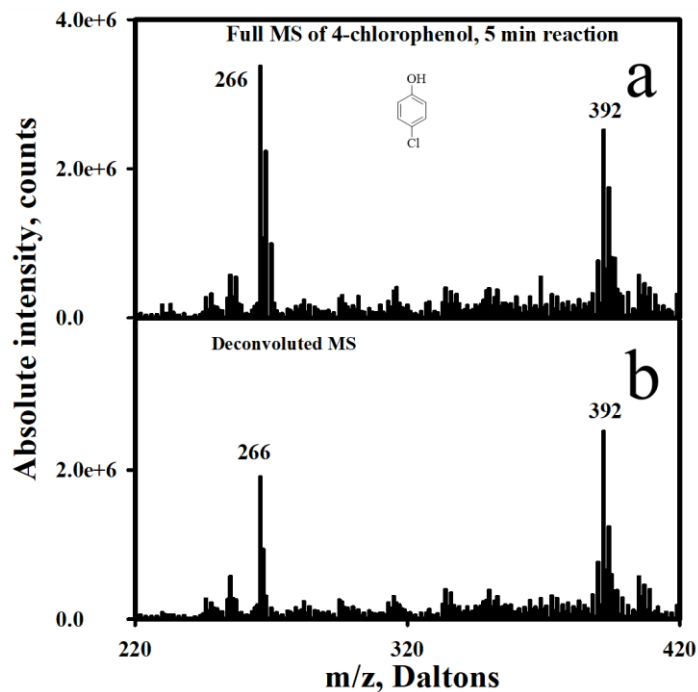


Figure 7.7. The Gibbs products of 4-chlorophenol after 5 minutes reaction. (a) is the Full MS and (b) is the deconvoluted MS. 4-chlorophenol gives both substituted product, indophenol, at m/z 266 and an adduct at m/z 392.

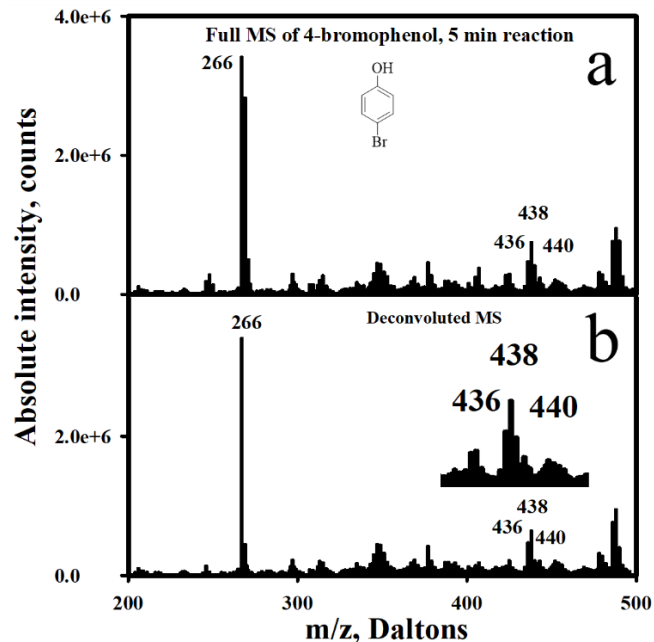


Figure 7.8. The Gibbs products of 4-bromophenol after 5 minutes reaction. (a) is the Full MS and (b) is the deconvoluted MS. 4-bromophenol gives both substituted product, indophenol, at m/z 266 and an adduct at m/z 436.

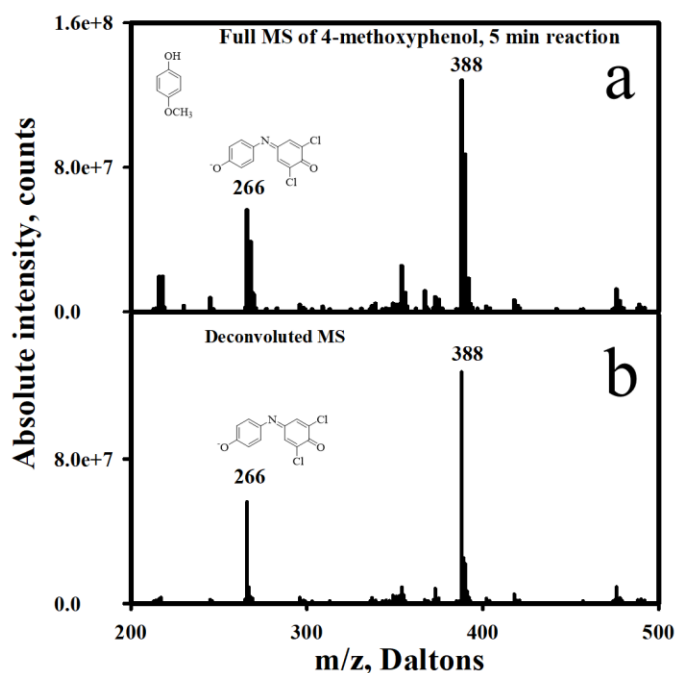


Figure 7.9. The Gibbs products of 4-methoxyphenol after 5 minutes reaction. (a) is the Full MS and (b) is the deconvoluted MS. 4-methoxyphenol gives both substituted product, indophenol, at m/z 266 and an adduct at m/z 388.

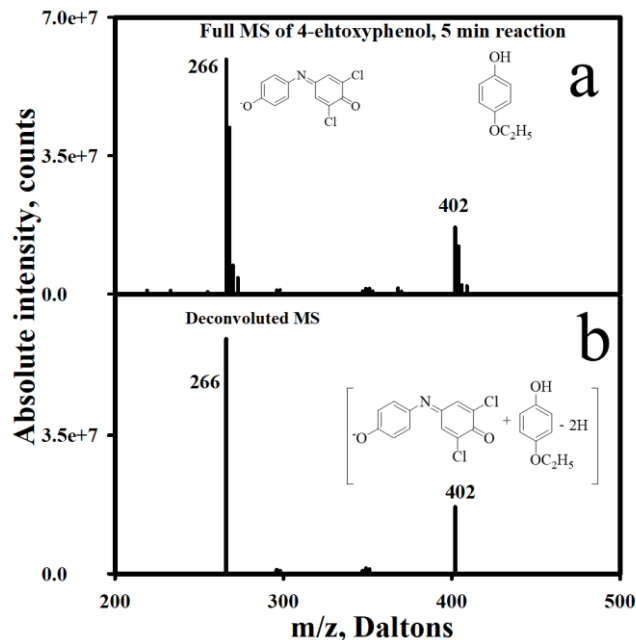


Figure 7.10. The Gibbs products of 4-ethoxyphenol after 5 minutes reaction. (a) is the Full MS and (b) is the deconvoluted MS. 4-ethoxyphenol gives both substituted product, indophenol, at m/z 266 and an adduct at m/z 402.

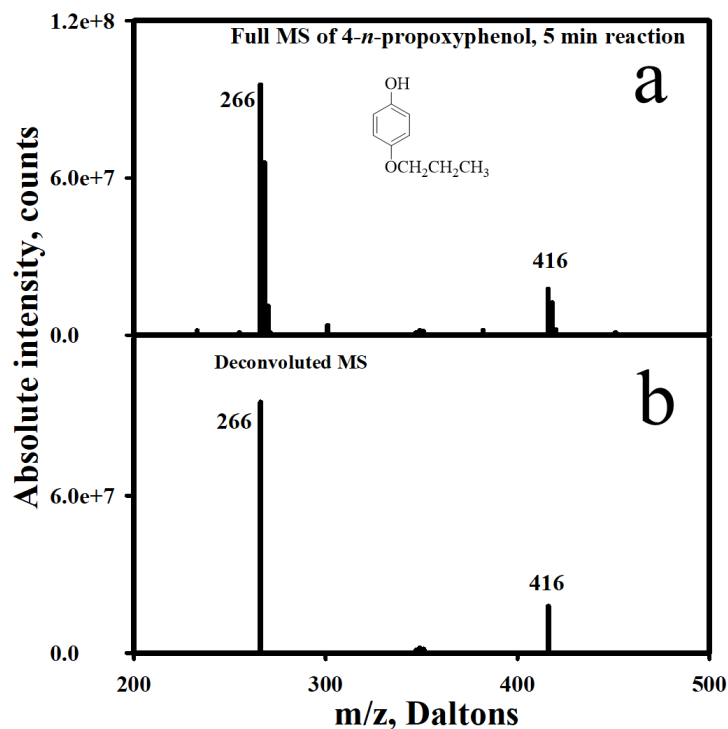


Figure 7.11. The Gibbs products of 4-n-propoxyphenol after 5 minutes reaction. (a) is the Full MS and (b) is the deconvoluted MS. 4-n-propoxyphenol gives both substituted product, indophenol, at m/z 266 and an adduct at m/z 416.

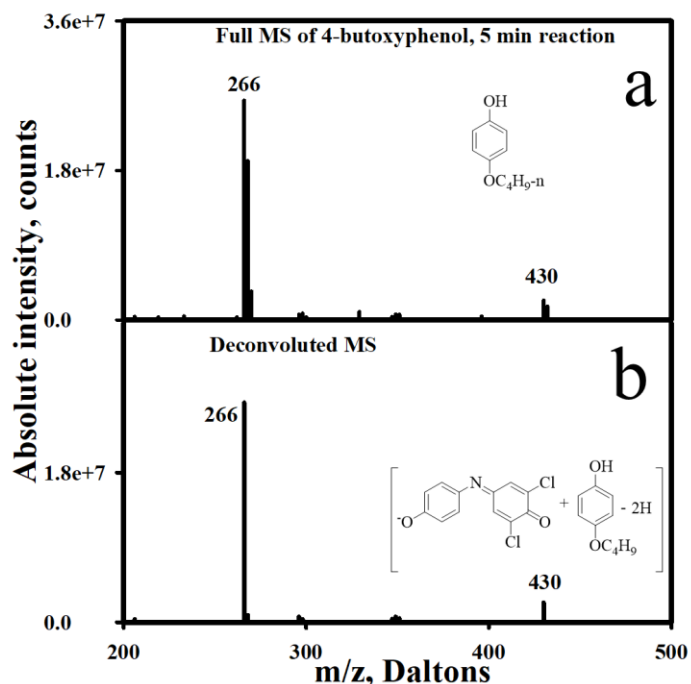
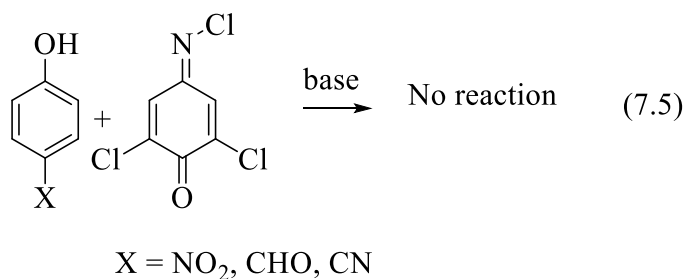


Figure 7.12. The Gibbs products of 4-*n*-butoxyphenol after 5 minutes reaction. (a) is the Full MS and (b) is the deconvoluted MS. 4-*n*-butoxyphenol gives both substituted product, indophenol, at m/z 266 and an adduct at m/z 430.

7.3.4 No reaction

We also tested few other substituents (X = -NO₂, -CHO, -CN, -COOH, -CH₂CH₂CH₃) (**1m-q**) at *para*-position in this reaction and did not see any Gibbs product even in longer reaction time (data not shown). Interestingly, unlike F, and Cl these electron-withdrawing groups did not give any product. Non reactivity of this class of compounds is also reported by Josephy.^{24, 27}



7.3.5 Structure of the condensation product (CP)

Though the reaction of 4-fluorophenol with Gibbs reagent was done on a large scale, we found that the condensation product (CP) is short lived as it breaks down within two to three weeks at room temperature, whereas the indophenol is stable. We were able to purify 23 mg of CP along with indophenol after doing column chromatography with increasing gradient of ethyl acetate in hexane from 1% to 30% (Figure 7.13). Both compounds gave single spot in thin layer chromatography (TLC) where the mobile phase was 30% ethyl acetate in hexane. In addition, we got a single compound at m/z 376 in negative electron spray mass spectrometry ((-) ESI-MS) for CP and m/z 266 for indophenol in same condition. The Figure 7.14 shows the full MS (top) and deconvoluted MS (bottom) of the CP shows that compound was fairly pure. However, in the ^1H -NMR and ^{13}C -NMR we did not see any signal except for the solvent peaks. This could be due to the presence of different isomers and/or the formation of polymers. We tried experiments to get crystals from it. The solvent compositions were dichloromethane-hexane, ethyl acetate-hexane, ethyl acetate-pet ether, methanol-hexane, ethyl acetate-pentane. Unfortunately, none of these cases yielded even a single crystal. This could be due to the formation diastereomers. Other possibilities could be the formation polymer over time and/or decomposition before the formation of crystal.

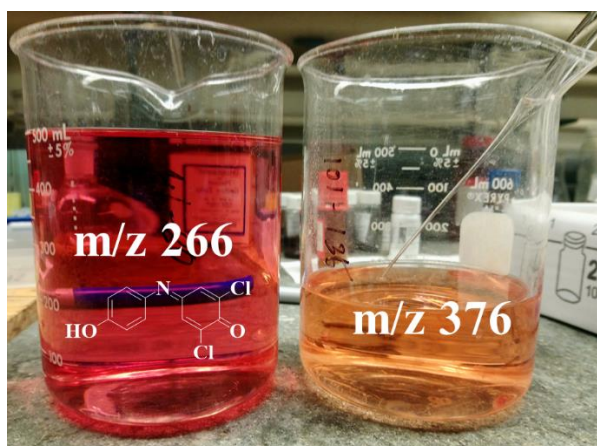


Figure 7.13. Solution of pure indophenol (m/z 266) and pure condensation product (m/z 376) in ethyl acetate. Indophenol gives brown colored solution, whereas condensation product gives orange colored solution in ethyl acetate.

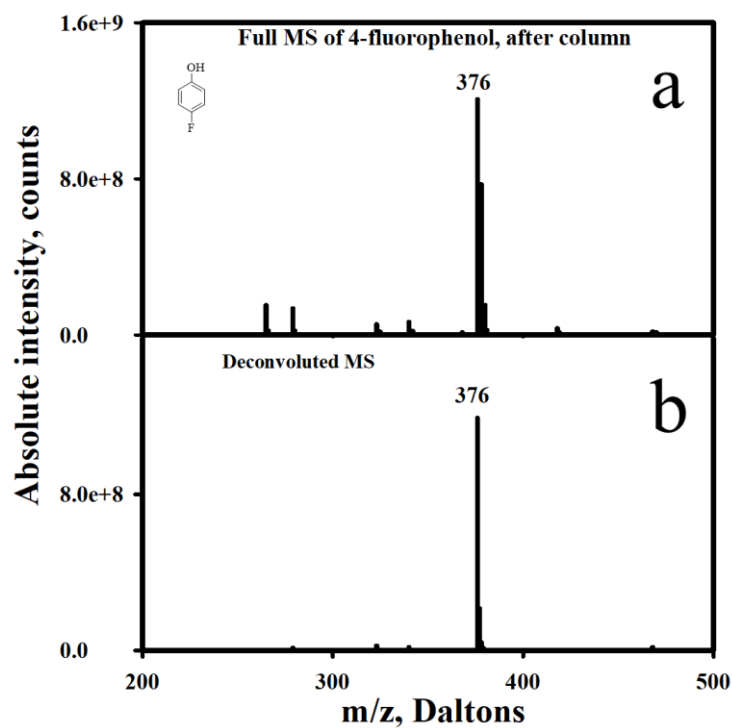


Figure 7.14. The Gibbs products of 4-fluorophenol after separation of the second product. (a) is the Full MS of the reaction solution and (b) is the deconvoluted MS.

On the other hand, we had nice crystal for indophenol and the crystal structure is shown in Figure 7.15.

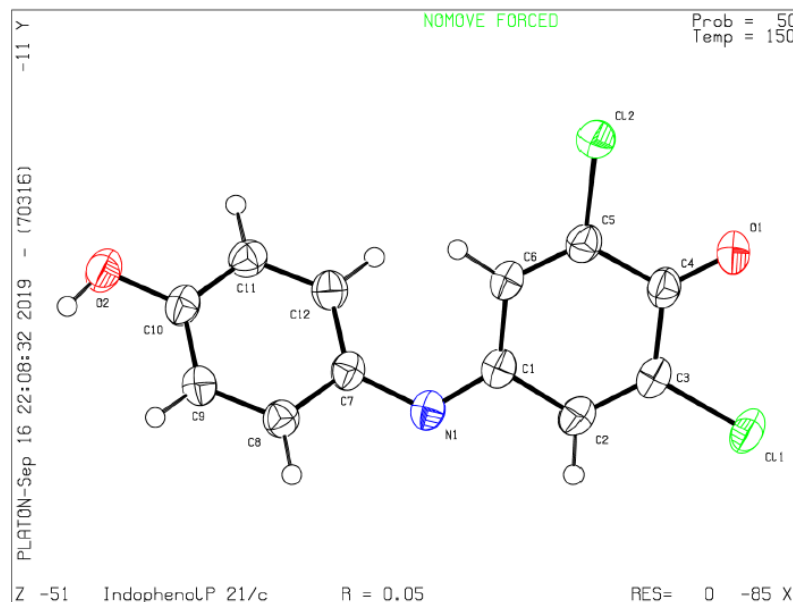


Figure 7.15. Crystal structure of indophenol

7.4 Conclusion

While the Gibbs reagent has long been used as a phenolic assay by spectrophotometry, it could not distinguish *para*-substituted phenols from their corresponding *ortho*- and *meta*-isomers. ESI-MS allowed us to distinguish *para*-substituted phenols from other isomers. In addition, we have shown that few *para*-substituted phenols give indophenols by replacing the groups at *para*-position. Few other compounds gave additional condensation products. The third class of compounds gave indophenol while retaining the substituent at *para*-position. We propose that substitution occurs at the *ortho*-position. Finally, there are a few more compounds where we have not seen any indophenol formation.

7.5 References

1. Gibbs, H. D., Phenol tests. IV. Velocity of indophenol formation-2,6-dibromobenzenoneindophenol. *J. Phys. Chem.* **1927**, *31*, 1053-81.
2. Gibbs, H. D., Phenol tests. III. The indophenol test. *J. Biol. Chem.* **1927**, *72*, 649-64.

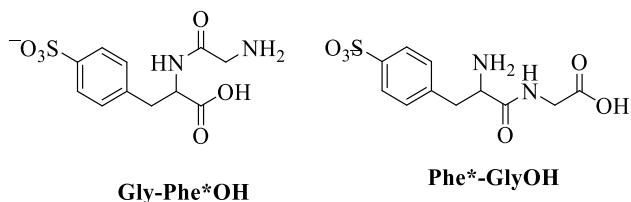
3. Parke, D.; Williams, R., Studies in detoxication. 81. The metabolism of halogenobenzenes:(a) Penta-and hexa-chlorobenzenes.(b) Further observations on 1: 3: 5-trichlorobenzene. *Biochemical journal* **1960**, *74* (1), 5.
4. Ettinger, M.; Ruchhofs, C., Determination of Phenol and Structurally Related Compounds by Gibbs Method. *Analytical Chemistry* **1948**, *20* (12), 1191-1196.
5. Davidson, V.; Keane, J.; Nolan, T. In *The chemical constituents of lichens found in Ireland-Lecanora gangaleoides-Part 3-the constitution of gangaleoidin*, Sci. Proc. Roy. Dublin Soc, 1943; pp 143-163.
6. Beshgetoor, A. W.; Greene, L. M.; Stenger, V. A., Determining Phenols in Dilute Solutions. Notes on the Gibbs Method. *Industrial & Engineering Chemistry Analytical Edition* **1944**, *16* (11), 694-696.
7. Calam, C.; Clutterbuck, P.; Oxford, A.; Raistrick, H., Studies on the biochemistry of micro-organisms: 74. The molecular constitution of geodin and erdin, two chlorine-containing metabolic products of *Aspergillus terreus* Thom. Part 3. Possible structural formulae for geodin and erdin. *Biochemical Journal* **1947**, *41* (3), 458.
8. Barton, D.; Scott, A., 363. The constitutions of geodin and erdin. *Journal of the Chemical Society (Resumed)* **1958**, 1767-1772.
9. Raistrick, H., Bakerian Lecture: A region of biosynthesis. *Proceedings of the Royal Society of London. Series A. Mathematical and Physical Sciences* **1949**, *199* (1057), 141-168.
10. Mahon, J.; Chapman, R., Butylated Hydroxyanisole in Lard and Shortening Control Analysis. *Analytical Chemistry* **1951**, *23* (8), 1120-1123.
11. Birkinshaw, J.; Raistrick, H.; Ross, D.; Stickings, C., Studies in the biochemistry of micro-organisms. 85. Cyclopolic and cyclopaldic acids, metabolic products of *Penicillium cyclopium* Westling. *Biochemical Journal* **1952**, *50* (5), 610.
12. Dacre, J.; Denz, F.; Kennedy, T., The metabolism of butylated hydroxyanisole in the rabbit. *Biochemical Journal* **1956**, *64* (4), 777.
13. Kuramoto, S.; Jenness, R.; Coulter, S., The oxidation of vanillin by unheated milk. *Journal of Dairy Science* **1957**, *40* (2), 187-191.
14. Birkinshaw, J.; Chaplen, P.; Lahoz-Oliver, R., Studies in the biochemistry of micro-organisms. 102. Quadrilineatin (1: 2-diformyl-5-hydroxy-3-methoxy-4-methylbenzene), a metabolic product of *Aspergillus quadrilineatus* Thom & Raper. *Biochemical Journal* **1957**, *67* (1), 155.
15. Dacre, J., The metabolism of 3: 5-di-tert.-butyl-4-hydroxytoluene and 3: 5-di-tert.-butyl-4-hydroxybenzoic acid in the rabbit. *Biochemical Journal* **1961**, *78* (4), 758.

16. Thoss, V.; Baird, M. S.; Lock, M. A.; Courty, P. V., Quantifying the phenolic content of freshwaters using simple assays with different underlying reaction mechanisms. *Journal of Environmental Monitoring* **2002**, *4* (2), 270-275.
17. Lykken, L.; Treseder, R.; Zahn, V., Colorimetric Determination of Phenols. Application to Petroleum and Allied Products. *Industrial & Engineering Chemistry Analytical Edition* **1946**, *18* (2), 103-109.
18. Baylis, J. R., Improved method for phenol determinations. *J. - Am. Water Works Assoc.* **1928**, *19*, 597-604.
19. Dacre, J. C., Nonspecificity of the Gibbs reaction. *Anal. Chem.* **1971**, *43* (4), 589-91.
20. Josephy, P. D.; Van Damme, A., Reaction of Gibbs reagent with para-substituted phenols. *Anal. Chem.* **1984**, *56* (4), 813-14.
21. Mistry, S.; Wenthold, P. G., Mass spectrometric detection of the Gibbs reaction for phenol analysis. *Journal of Mass Spectrometry* **2018**.
22. Wenthold, P. G.; Mistry, S., Methods of detecting chemicals. Google Patents: 2019.
23. Mistry, S.; Wenthold, P. In *Mass spectroscopic analysis of phenol derivatives by Gibbs reaction*, ABSTRACTS OF PAPERS OF THE AMERICAN CHEMICAL SOCIETY, AMER CHEMICAL SOC 1155 16TH ST, NW, WASHINGTON, DC 20036 USA: 2019.
24. Josephy, P. D.; Van Damme, A., Reaction of Gibbs reagent with para-substituted phenols. *Analytical chemistry* **1984**, *56* (4), 813-814.
25. Pallagi, I.; Toro, A.; Farkas, O., Mechanism of the Gibbs Reaction. 3. Indophenol Formation via Radical Electrophilic Aromatic Substitution (SREAr) on Phenols. *The Journal of Organic Chemistry* **1994**, *59* (22), 6543-6557.
26. Carey, F. A.; Sundberg, R. J., *Advanced organic chemistry: part A: structure and mechanisms*. Springer Science & Business Media: 2007.
27. Josephy, P. D.; Lenkinski, R. E., Reaction of Gibbs reagent (2, 6-dichlorobenzoquinone 4-chloroimine) with the antioxidant BHA (3-tert.-butyl 4-hydroxyanisole): isolation and identification of the major product. *Journal of Chromatography A* **1984**, *294*, 375-379.
28. Quintana, M.; Didion, C.; Dalton, H., Colorimetric method for a rapid detection of oxygenated aromatic biotransformation products. *Biotechnology techniques* **1997**, *11* (8), 585-587.

CHAPTER 8. FRAGMENTATION MECHANISM OF PROLINE CONTAINING DIPEPTIDES

8.1 Introduction

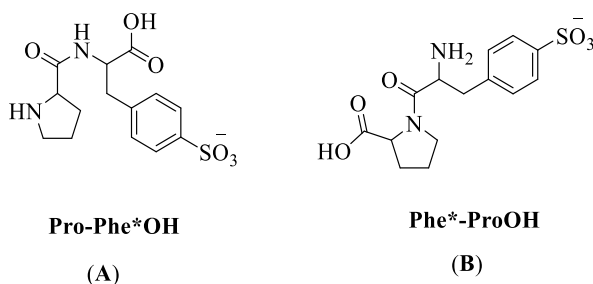
Mass spectrometry (MS) has been used for sequencing proteins and peptides for decades because of its ability for rapid, accurate analysis.^{1,2} In addition, tandem mass spectrometry (MSⁿ) is an important tool for differentiating isobaric ions and determining their sequence. Thus, it is common to use a mass spectral library to identify unknown protein fragments. For instance, mass spectrometry can be used to sequence the C- and N-terminus of a peptide by matching the results with known b- and y-type ions in a library.³⁻⁷ A better understanding by MS is required for b-



ions from peptides to improve peptide sequencing algorithms and the current models for peptide fragmentation because those ions are common and stable.⁸ To better understand the b₂ ion structures and their formation mechanisms, several experimental and theoretical studies have been carried out.⁹⁻²⁸ In previous work, we examined the fragmentation of dipeptides that contains phenylaniline with a sulfonated tag in the benzene ring (PheSO₃⁻ or Phe*) connected with glycine (Gly) to form Phe*GlyOH and GlyPhe*OH dipeptides. These two dipeptides were anionic which are different from the protonated ions used in other studies. The advantages of using anions is that the sulfonate charge is more stable than a carboxylic acid. Also, the charge is localized, and the canonical structures can be predicted.²⁹ Thus, the fragmentations of our anionic dipeptides were similar to previously studied protonated dipeptides containing histidine (His)³⁰⁻³⁴ or arginine

(Arg)^{20, 21, 28, 35} which have basic side chains with a localized positive charge. We reported that the dipeptides fragmented after rearranging to a common structure³⁶ which was similar to previously reported ArgGly and other dipeptides. However, in that study we showed that not only is a ‘mobile proton’ involved in the dissociation process to form a b₂ ion but also a ‘back bone hydrogen atom’.^{8, 36-39}

In this study, we have focused on a dipeptide with a proline residue. Proline occupies a unique position among the twenty amino acids. For instance, it imposes strong restraints on the conformation of a peptide chain due to the α -nitrogen atom being part of the rigid pyrrolidine ring. Additionally, the nitrogen atom forms secondary amide bond to the preceding amino acid.^{40, 41} Furthermore, when proline is present inside an α -helix, proline prevents the amide nitrogen of its C-terminal neighbor from making a hydrogen bond with a carbonyl in the preceding turn.⁴² Proline can also introduce heterogeneity when bonded with another amino acid, such as phenylalanine, in proteins and peptides.⁴³ Finally, it is known that peptides containing proline exhibit very distinct fragmentation upon CID because of its high basicity.^{44, 45} A wide variety of collision conditions have been studied on protonated peptides having a proline residue.⁴⁶⁻⁴⁸ However, no studies of proline peptides with remote charges have been reported.



Here, we have used mass spectrometry to examine the fragmentation of dipeptides that include *para*-sulfonated phenyl alanine (PheSO₃⁻ or Phe*) connected with proline (Pro) to form

ProPhe*OH (A) and Phe*ProOH (B) dipeptides. These dipeptides are similar to Phe*GlyOH and GlyPhe*OH with respect to charge such that the dipeptide backbone has a canonical structure and is not protonated.

8.2 Experimental

8.2.1 Mass spectrometric analysis

Mass spectrometric analysis was carried out as written in our previous work.³⁶ In brief, LCQ-DECA (Thermo Electron Corporation, San Jose, CA) quadrupole ion trap mass spectrometer, equipped with an electrospray ionization (ESI) source was used for the analysis. Methanol:water mixture (1:1) was used to dissolve samples and introduced into the source at a flow rate of 5 μ l/min. For the ion of interest, electrospray and ion focusing conditions were adjusted to maximize the signals. MSⁿ experiments with mass-selected ions in the cell were carried out for the ion dissociations. Helium buffer was used as the collision target. $q_z = 0.250$ was set as isolation window for the CID of the reaction ions. Also, to avoid off-resonance excitation a mass-width sufficient was used. In the cell, the energy of collision-induced dissociation (CID) is reflected in the “normalized collision energy,” which ranges from 0 – 100%.

8.2.2 Computational methods

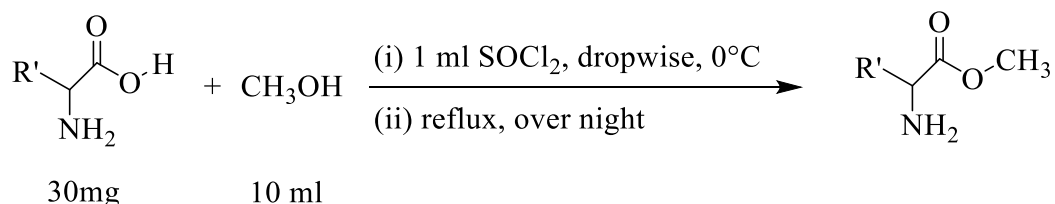
Geometries and electronic energies were calculated at the B3LYP/6-31+G* level of theory. Low-energy conformations were initially identified by using the Monte Carlo multiple minimum search method, with the Merck molecular force field (MMFF) as implemented in ChemAxon’s MarvinSketch ver. 19.20.0,⁴⁹ and unique conformations were used as starting points in B3LYP optimizations. Single point energies for selected optimized structures were

carried out at the MP2/6-311+G** level of theory in order to obtain a better description of van der Waals interactions and charge polarization. Energies are not corrected for zero-point energies or thermal energy contributions. B3LYP calculations were carried out using QCHEM ver 4.0.⁵⁰

8.2.3 Synthesis of amino acid esters

Amino acid esters were synthesized by modifying published articles.^{36, 51, 52} In brief, 30 mg amino acid was dissolved in 10 mL methanol and cooled to 0° C. 500 µL of SOCl₂ was added dropwise into the cold amino acid solution. Finally, the solution was warmed to room temperature and was refluxed overnight to get desired product (Scheme 1). The prepared esters were analyzed without further purification.

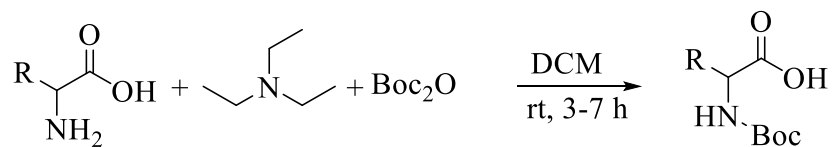
Scheme 1



8.2.4 Synthesis of Boc protected amino acid

The procedure reported by Jahani F, et al. was modified to get better yield for our case.⁵³ Briefly, 0.1 mmol amino acid sample was taken in a 50 mL round bottle flask with 10 mL DCM. 0.2 mmol (2 equivalent) triethylamine was added dropwise and 0.11 mmol (1.1 equivalent) di-*tert*-butyl dicarbonate was added into it and the reaction mixture was stirred for 3 – 7 hours at room temperature (Scheme 2). The reaction was monitored by TLC and was stopped once all the reactant had disappeared. The solvent was removed by evaporation and the mixture was used without further purification.

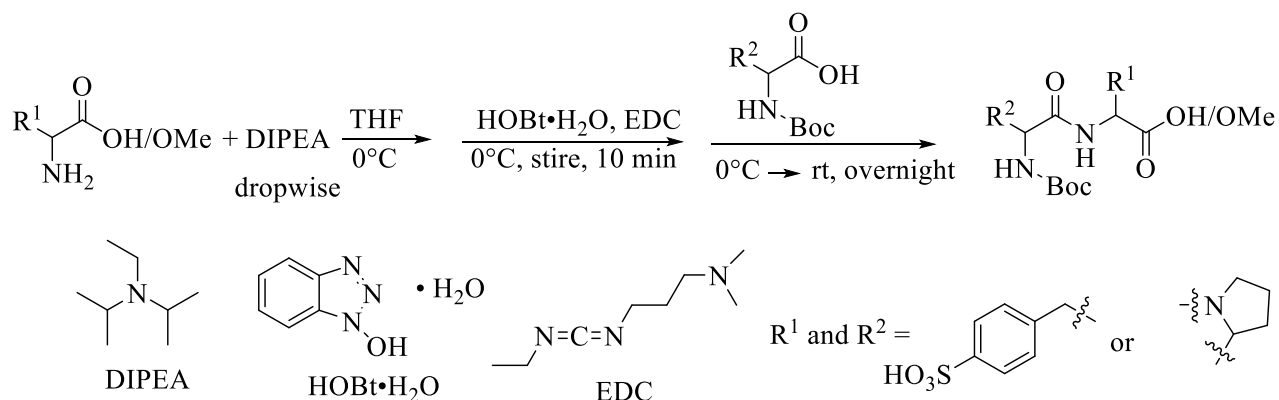
Scheme 2



8.2.5 Synthesis of Pro-Phe*OH and Phe*-ProOH dipeptides and their methyl ester

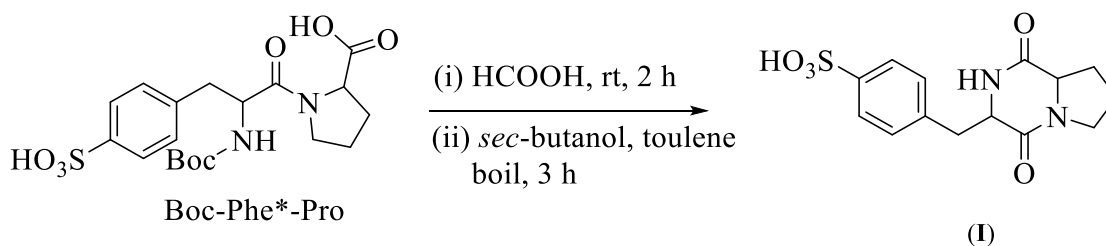
0.1 mmol of corresponding Boc-amino acid (Boc-R^1) was dissolved in 10 mL tetrahydrofuran (THF) at 0°C and 100 μL N,N -diisopropylethylamine was added dropwise into it. Hydroxybenzotriazole (HOBt) (46 mg, 3 equivalent) and 1-ethyl-3-(3-dimethylaminopropyl)-carbodiimide (EDC) (47 mg, 3 equivalent) were added into the solution mixture and stirred at 0°C for 5 minutes. Finally, 0.1 mmol amino acid (or its methyl ester derivatives) (R^2) was added into it and was brought to room temperature. The reaction mixture was stirred at room temperature for overnight to get the dipeptide. After stirring for overnight, the excess THF was evaporated under vacuum. Formation of the dipeptide product ($\text{BocR}^1\text{-R}^2\text{OH}$ and $\text{BocR}^1\text{-R}^2\text{OMe}$) was confirmed by mass spectrometry. The Boc group was removed by dissolving the product in excess trifluoroacetic acid (TFA) in toluene or methylene dichloride (DCM) for 20 min, followed by evaporation of the TFA and toluene (or DCM) under vacuum, resulting in formation of the desired product. The ester, $\text{R}^1\text{-R}^2\text{OMe}$, can be hydrolyzed to $\text{R}^1\text{-R}^2\text{OH}$ by treating their aqueous solution with concentrated sulfuric acid. The synthesis of GlyPhe*OMe is shown in Scheme 3 as an illustration.

Scheme 3



8.2.6 Synthesis of Diketopiperazine

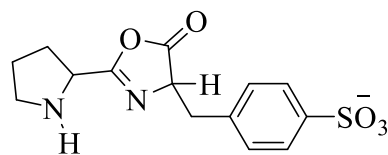
The synthesis of diketopiperazine (**I**) was carried out by following approach previously published.⁵⁴ In brief, 10 ml formic acid (98%) was added into a 50 mg of Boc-Phe*Pro containing solution and the solution was stirred at room temperature for 2 hours. Unreacted formic acid was removed under vacuum. The crude product formed was dissolved in 15 ml of *sec*-butyl alcohol and 10 ml of toluene. This solution was boiled for about three hours and fresh butanol was added to maintain the solvent level. The solution was cooled to 0° C after boiling off solvent to 5 ml. The final product was obtained by filtration.



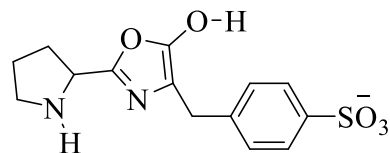
8.2.7 Synthesis of oxazolone (from ProPhe*)

The approach previously published by Uraguchi, et al, was used for the syntheses of the oxazolones.⁵⁵ In briefly, the solution containing 10 umol of Boc-ProPhe*OH and 15 umol of 1, 3,-Dicyclohexylcarbodiimide (DCC) were dissolved in 10 ml of dichloromethane. The solution

was stirred at room temperature for 3 hr. Excess solvent was removed in vacuum and the resulting crude product was dissolved in 3 ml TFA to produce ProPhe*-oxazolone (**II**) and oxazolone-enol (**III**).



oxazolone
II



oxazolone-enol
III

8.3 Result

8.3.1 Formation of Phe*-ProOH and Pro-Phe*OH

Figure 8.1 shows the full MS of the reaction mixture of sulfonate containing phenylalanine (Phe*) and proline (Pro) dipeptide. The top spectrum (Figure 8.1a) is Phe*-Pro having Boc on Phe to protect the amine group of phenylalanine. The bottom figure (Figure 8.1b) shows the product after deprotection. The major peak in the top spectrum is m/z 441 due to formation of Phe*(Boc)-Pro. Other significant minor peaks are m/z 344 due to Boc protected phenylalanine (Phe*-Boc), and m/z 244 from unreacted phenylalanine (Phe*). The base peak in the bottom spectra is due to the formation of Phe*-Pro (m/z 341) from Phe*(Boc)-Pro. There is also some unreacted Phe*(Boc)-Pro and Phe*. However, in both cases the targeted products are dominating.

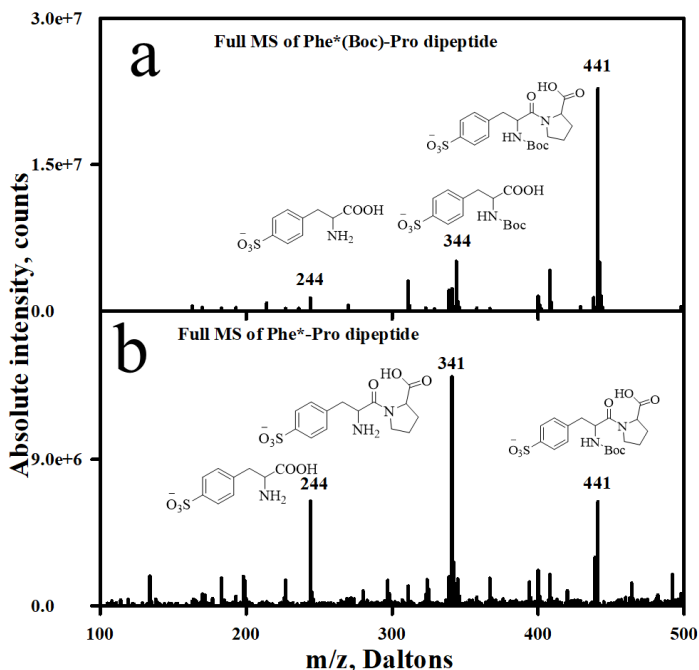


Figure 8.1. Dipeptide formed by phenylalanine with sulfonated tag and proline (Phe*-Pro). (a) dipeptide having 'Boc' as protecting group (Phe*(Boc)-ProOH), whereas (b) is after deprotected (Phe*-ProOH).

Figure 8.2a shows the full mass spectrum of the reaction mixture of dipeptides of proline having a Boc protecting group (Pro-Boc) and sulfonated phenylalanine (Phe*), and Figure 8.2b shows the deprotected Pro-Phe* dipeptide reaction mixture. The top spectrum is dominated by the targeted compound although there is a small amount of unreacted sulfonated phenylalanine present (Phe*, m/z 244). However, the bottom spectrum is dominated by Pro-Phe* at m/z 341. Similar to previous compounds, Pro(Boc)-Phe* and Pro-Phe* are also dominant here.

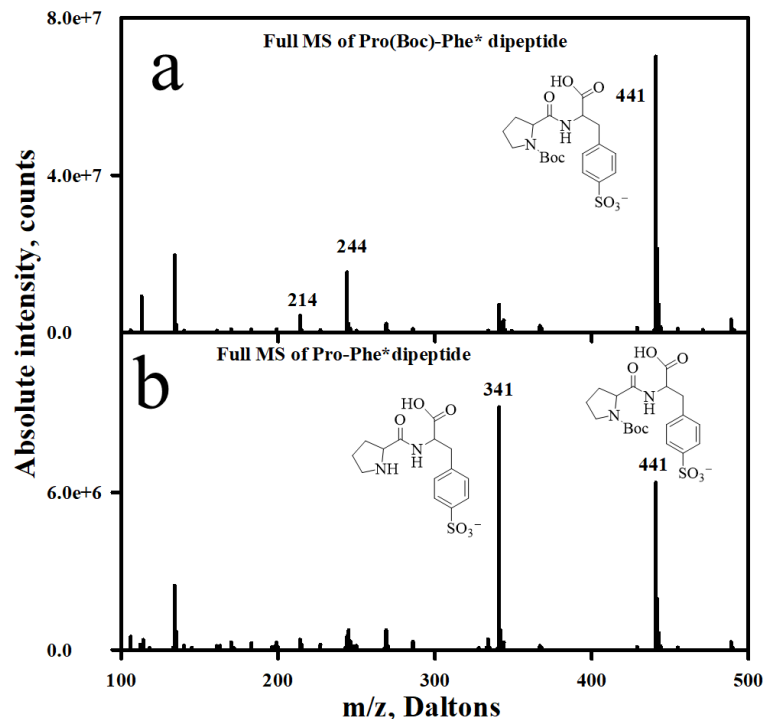


Figure 8.2. Dipeptide formed by proline and phenylalanine with sulfonated tag (Pro-Phe*). (a) dipeptide having ‘Boc’ as protecting group (Pro(Boc)-Phe*), whereas (b) is after deprotected (Pro-Phe*).

8.3.2 Analysis of Phe*-ProOH and Pro-Phe*OH

Figure 8.3 shows the MS/MS mass spectra of Phe*ProOH and ProPhe*OH dipeptides (m/z 341) with 35% collision energy. Both of the peptides gave the same fragmentation ions with similar intensity. The primary fragmentation products are m/z 324 (M-NH₃), m/z 323 (M-H₂O), m/z 297 (M-CO₂), and m/z 244 (M-C₅ONH₇, net loss of proline – H₂O). The additional peaks (i.e., products) can be attributed to secondary fragmentation of the primary products. Formation of the same fragment results from Phe*ProOH and ProPhe*OH dipeptides indicates a rearrangement to a common structure occurred before fragmentation. A similar type of rearrangement of Arg-Gly and Gly-Arg dipeptides was reported by O’Hair and co-workers in 2003,²⁰ and more recently with Phe-Gly and Gly-Phe.³⁶ Thus, the ProPhe*OH and Phe*ProOH rearrangement process is similar to those reported before, and a proton transfer is involved within the dipeptide to form zwitterionic

structures. Figure 8.4 shows the proposed mechanism for the rearrangement, with a zwitterionic structure rearranging to form a common cyclic anhydride intermediate. It is expected that any of these structures of this figure can dissociate to give fragment products by following lowest energy pathway.⁵⁶

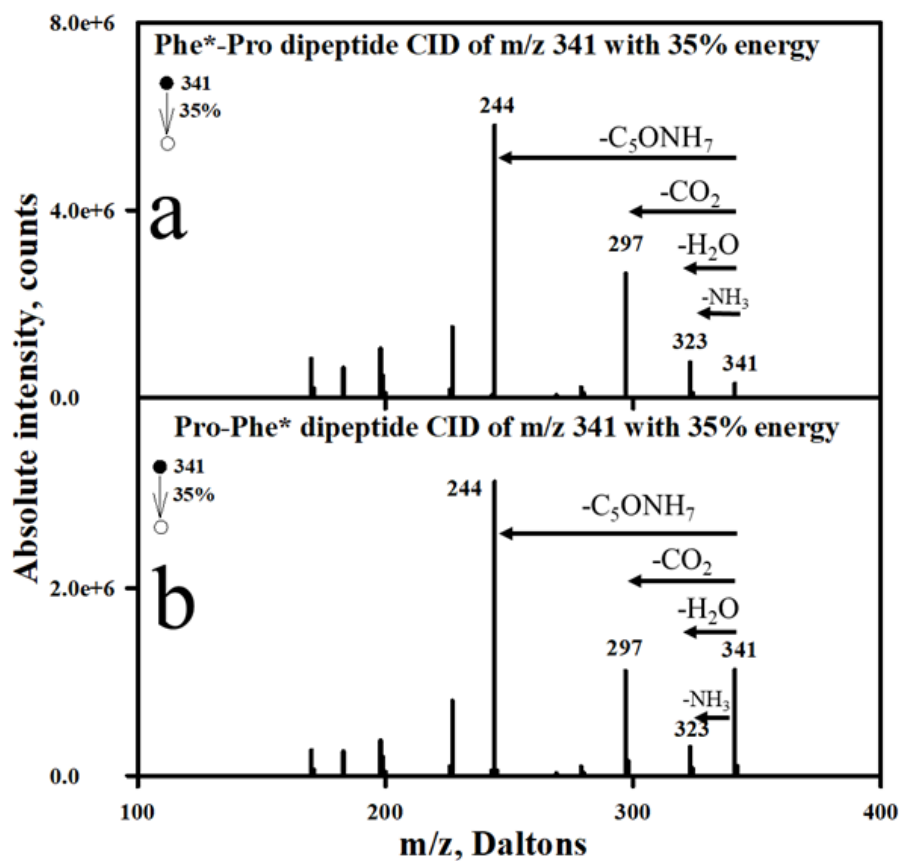


Figure 8.3. MS/MS mass spectra for Full MS of the reaction mixtures of (a) Phe*-Pro dipeptide and (b) Pro-Phe*

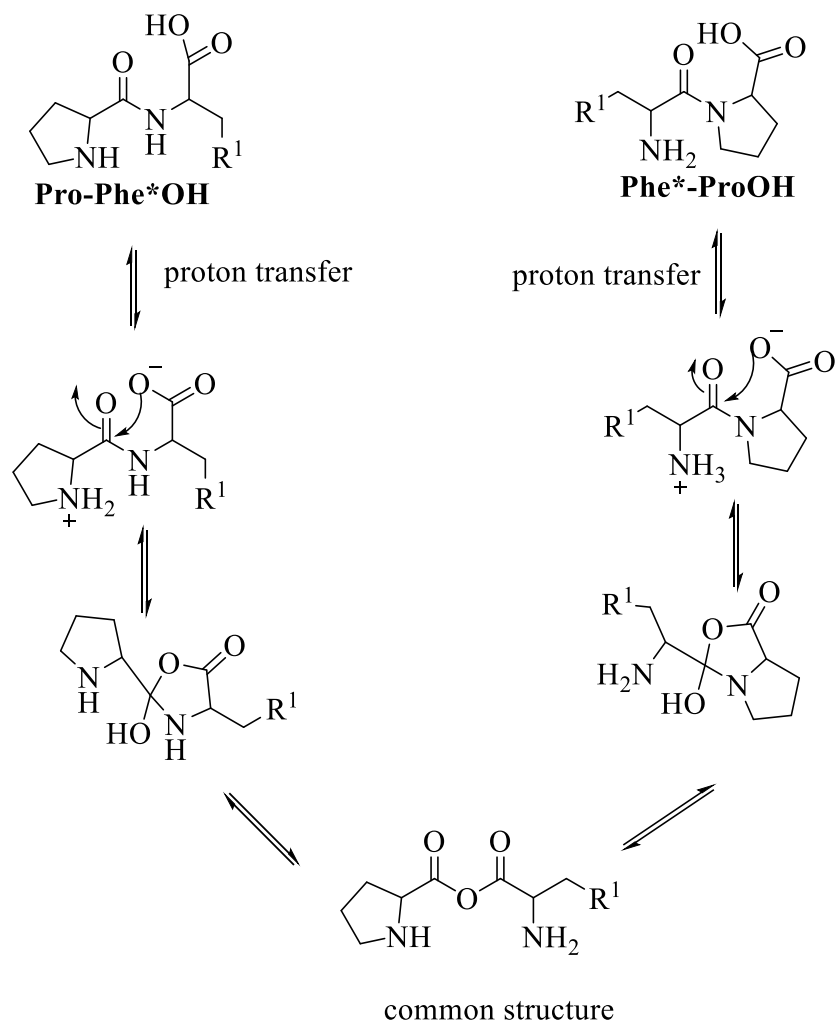


Figure 8.4. Proposed mechanism for formation of common structure from ProPhe*OH and Phe*ProOH. Both of the dipeptides rearranged to a common structure before fragmentation.

8.3.3 Analysis of Phe*ProOMe and ProPhe*OMe

The rearrangement mechanism is supported by the analysis of dipeptide methyl esters, as the methylation at the C-terminus carboxylic acid inhibits the rearrangement reaction by blocking the initial proton transfer step of Phe*ProOH and ProPhe*OH.²⁰ Figure 8.5 shows the CID spectra of the methyl esters of these two dipeptides. The CID spectra of Phe*ProOCH₃ and ProPheOCH₃ are significantly different in both identities of the products and the intensities. Even though both of them are giving products of m/z 323 ($M - \text{CH}_3\text{OH}$), m/z 295 ($M - \text{CH}_3\text{OH} - \text{CO}$), and m/z 170,

the relative intensities are very different. For instance, the b_2 ion (m/z 323, $M - \text{CH}_3\text{OH}$) is the base peak upon CID of Phe*ProOMe, whereas it is not the base peak upon CID of ProPhe*OMe. Moreover, peaks at m/z 171, m/z 225, m/z 251, m/z 266, and m/z 338 are observed solely on CID of Phe*ProOMe spectra, whereas m/z 197, m/z 241, m/z 279, and m/z 306 are observed solely on CID of ProPhe*OMe spectra.

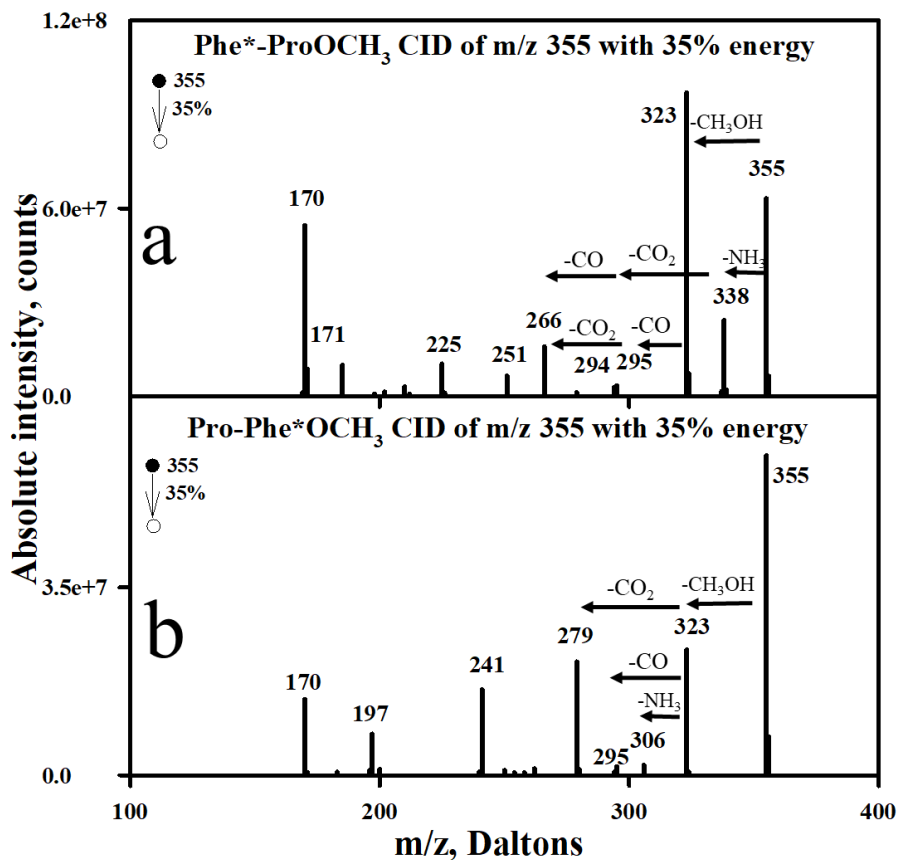


Figure 8.5. a) CID of Phe*ProOCH₃ and b) ProPhe*OCH₃ with 35% energy. Formation of methyl esters block the rearrangement of the dipeptides

Although b_2 ions formed from peptides are significant in peptide sequencing,³⁶ the methyl esters of the dipeptides is of equal importance because they are not dependent on the substitution at the carboxyl end.

Figure 8.6 shows the CID spectra of b_2 ions (m/z 323) obtained from Phe*ProOMe (8.6a) and from ProPhe*OMe (8.6b). The MS^3 of these two esters are also different. This reveals that the different isomers are giving different products without going through a common structure.

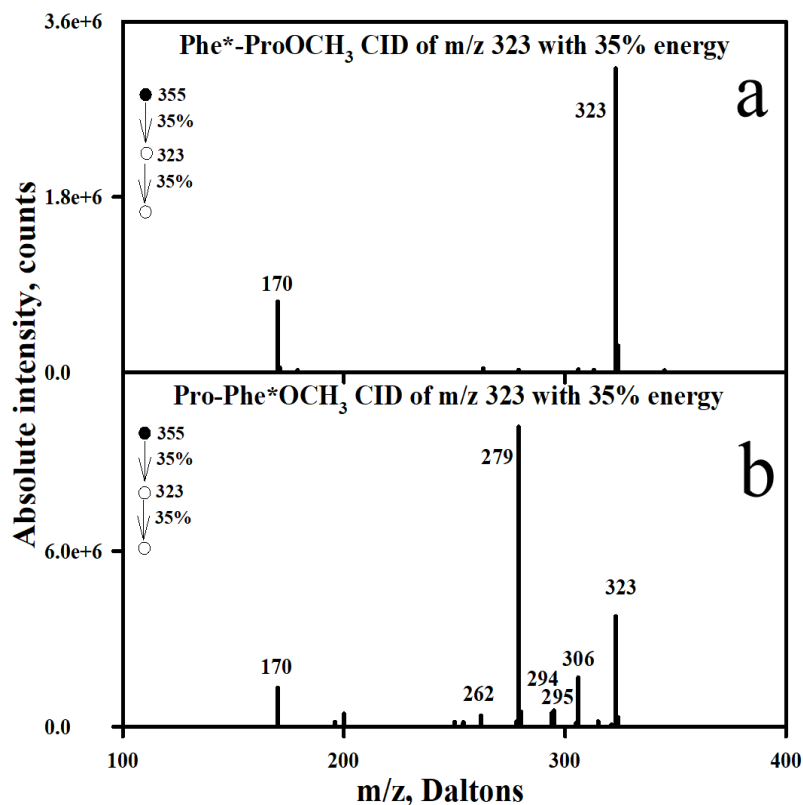


Figure 8.6. CID of b_2 ions from dipeptides methyl ester. (a) is MS^3 spectra of Phe*ProOCH₃ and (b) is MS^3 spectra of ProPhe*OCH₃. The different isomers give different products in MS^3 , which reveals that the isomers fragment without going through a common structure.

8.3.4 Comparison to Authentic Diketopiperazine and Oxazolones

The possible structures of the b_2 ions are diketopiperazine and oxazolones.^{20, 36} Thus, to determine the b_2 ion structure, the CID spectra of them are compared with the authentic diketopiperazine and oxazolone. The CIDs with 35% energy of authentic diketopiperazine (from Phe*Pro) and oxazolone (from Pro-Phe*) are showing in Figure 8.7.

Comparison of fragmentation between the b_2 ions from Phe*ProOCH₃ and Pro-Phe*OCH₃ (Figure 8.6) and the authentic samples of Phe*Pro diketopiperazine and Pro-Phe* oxazolone (Figure 8.7) reveals an agreement. For instance, m/z 170 fragment ions form from the CID of both b_2 ions from Phe*-ProOMe and Phe*Pro diketopiperazine though the intensities are not same. Therefore, the CID spectra of the b_2 ion obtained from Phe*ProOMe is consistent with that for diketopiperazine.

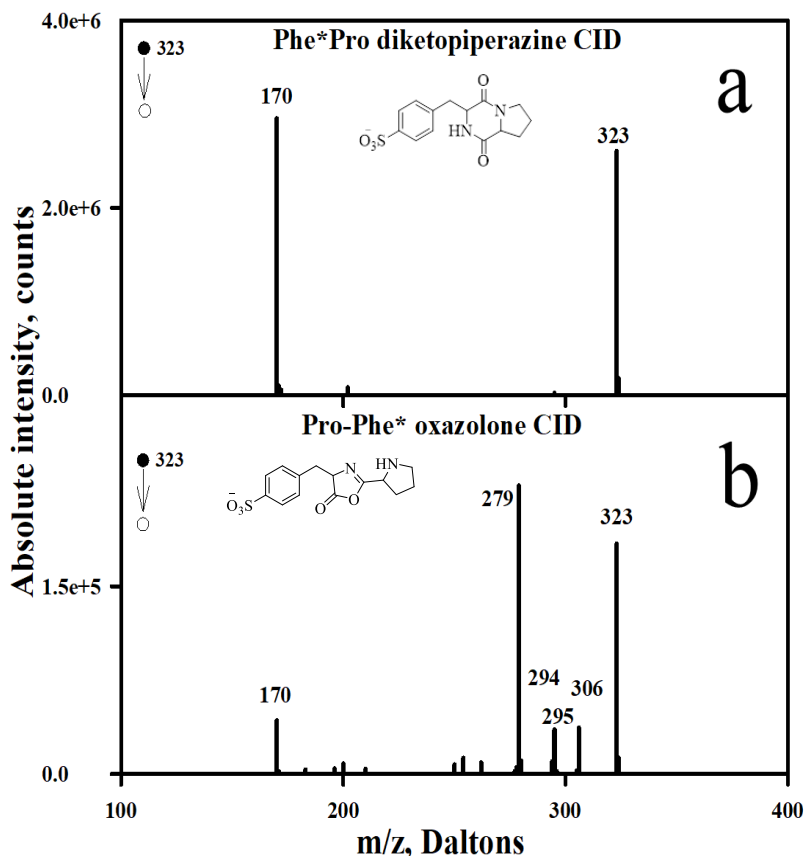


Figure 8.7. CID spectra of authentic structures of m/z 323 ions derived from the dipeptide (a) diketopiperazine is from Phe*Pro and (b) oxazolone is from Pro-Phe*.

On the other hand, the CID spectra of b_2 spectra from ProPhe*OMe agrees very well with that for oxazolone prepared from ProPhe*OH. The peaks present in Figure 8.6b exactly match with the peaks in Figure 8.7b. However, there are a few additional peaks in the later spectra with

very low intensity, and the relative intensity of m/z 323 (b_2 ions) does not match. Based on the above-discussed results, we can conclude that the b_2 ion from ProPhe*OMe is mostly the expected oxazolone.

8.3.5 Deuterium labelling

Additional insight into the products structure of b_2 ion may be found by deuterium labelling experiment. 50:50 D_2O and CH_3OD solution was used to execute of H/D exchange of two labile protons of Phe*ProOH and ProPhe*OH. Formation of m/z 343 is due to the exchange of two labile protons with deuterium atoms. Upon CID, both of the ions give b_2 ion with m/z 323 ($M - D_2O$), m/z 324 ($M - DOH$), and m/z 325 ($M - H_2O$). The formation of m/z 323 indicates the carboxylic OD takes one deuterium to form D_2O , whereas one H atom is added to the carboxyl OD to form DOH. This observation depicts that there are two different options for transferring protons, which is shown in Figure 8.9 for deuterium labelling of ProPhe*OH.

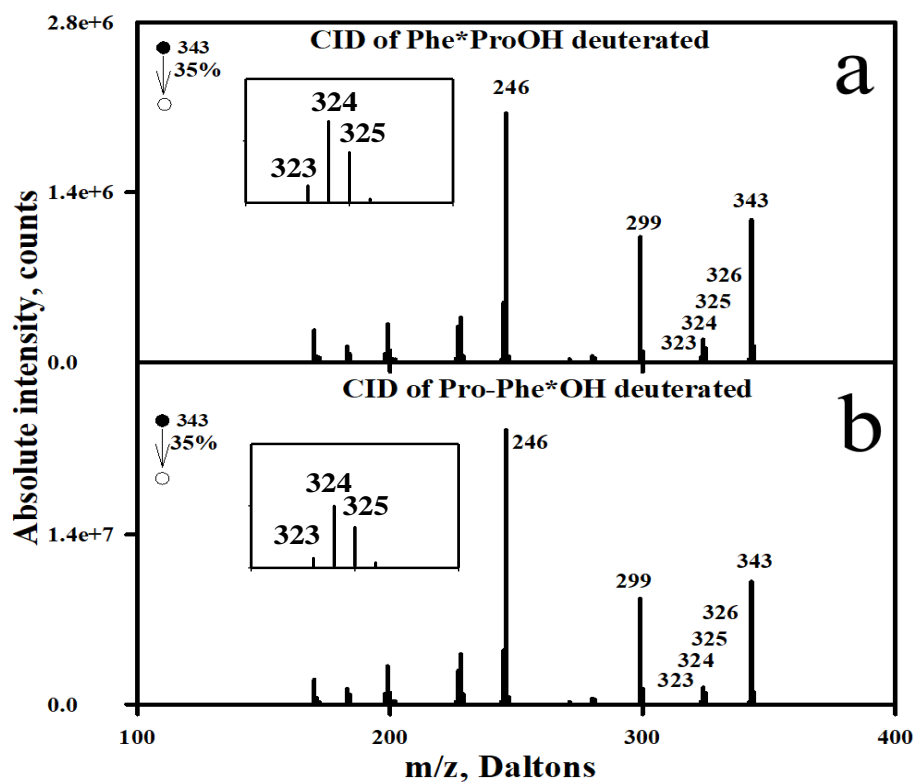


Figure 8.8. MS/MS spectra of deuterated a) Phe*ProOH and b) ProPhe*OH. The removal of D₂O (formation of m/z 323, M – D₂O) and DOH (formation of m/z 324, M – DOH) depict that there are two different options for transferring protons.

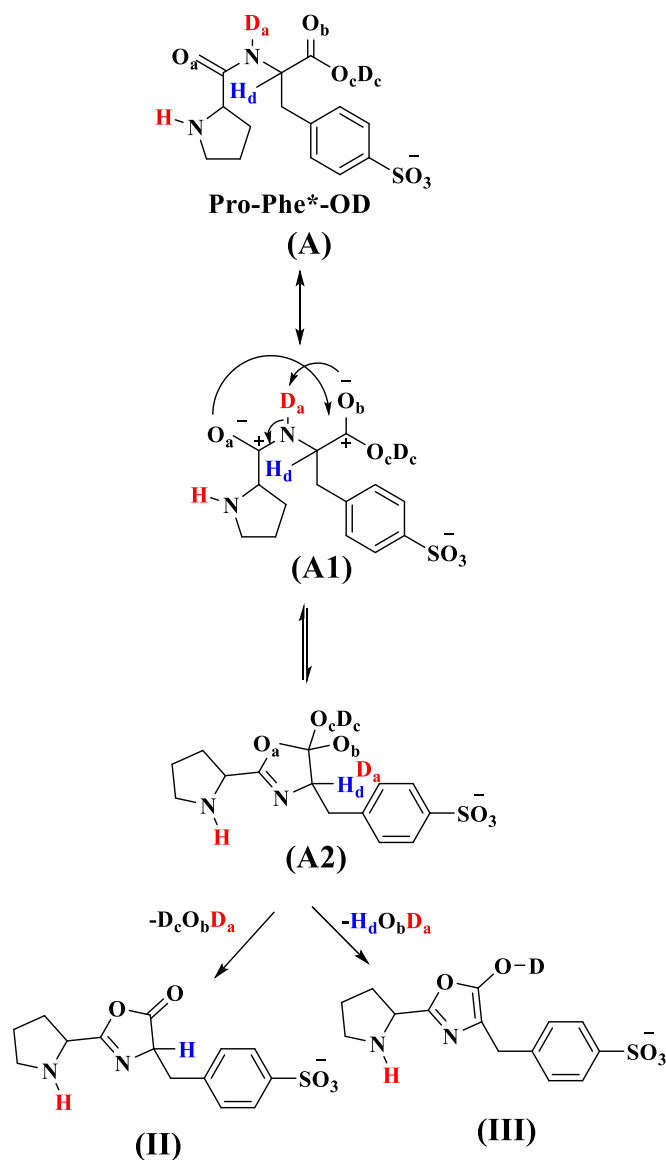


Figure 8.9. Proton transfer mechanism for the b_2 ion formation from ProPhe*OH

The transfer of two labile protons are shown in Figure 8.9 by deuterium labelling of ProPhe*OH. Initially, the labile protons are exchanged by deuterium shown in **A** (Pro-Phe*-OD). Five-membered ring formed through the removal of deuterium atom (D_a) from nitrogen atom to carbonyl oxygen (O_b) followed by the attack of oxygen (O_a) on carbonyl carbon to give five membered intermediate structure, **A2**. The oxazolone, **II**, may form by the removal of $D_cO_bD_a$,

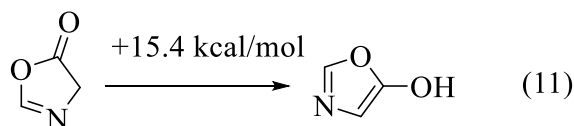
whereas oxazolone-enol, **III**, formed by the removal of H_dO_bD_a. Our previous work on Gly-Phe dipeptide³⁶ supports the oxazolone and oxazolone-enol formation mechanism.

The relative energies of possible isomeric b₂ ion structures obtained from Phe*-Pro and Pro-Phe* are shown in Table 8.1. the most stable product is predicted to be the diketopiperazine (**I**). Oxazolone b₂ ions **II** and **III** are calculated to be 25.2 and 72.8 kcal/mol higher in energy, respectively. This relative energies of the diketopiperazine and oxazolones are consistent with what was published previously.^{30, 31, 36, 57}

Table 8.1. Calculated Relative Energies of b₂ ions in kcal/mol at B3LYP/6-31+G* optimized geometries.

Ion	MP2/6-31+G*
Pro-Phe* Oxazolone-enol (III)	72.8
Pro-Phe* Oxazolone (II)	25.2
(Phe*-Pro) Diketopiperazine (I)	0

Aside from diketopiperazine, the lowest energy structure is predicted to be the oxazolone (**II**) at the B3LYP/6-31+G* level of theory (Figure 8.9). The stability of the oxazolone (**II**) structure for the Pro-Phe* b₂ can be attributed to a favorable hydrogen bond interaction between the N-H and the sulfonate group, as shown in Figure 8.10. Whereas, oxazolone-enol (**III**) structure for the Pro-Phe* b₂ ion is linear and lack of formation of hydrogen bond between sulfonate group and any between O-H and N-H. All the optimized geometry for b₂ ions is shown in Figure 8.10.



Previously, our lab found that the simple oxazolone is computed to be 15.4 kcal/mol lower in energy than hydroxyoxazole at the MP2/6-31+G*//B3LYP/6-31+G* level of theory (eq 11).³⁶

The stability of keto form over the enol supports our findings. Moreover, the stabilization of b2 ion by intramolecular hydrogen bonding was previously observed for His-Pro,⁵⁷ and in our studies we have found that the hydrogen bonding preferentially stabilizes the diketopiperazine structure by almost 73 kcal/mol.

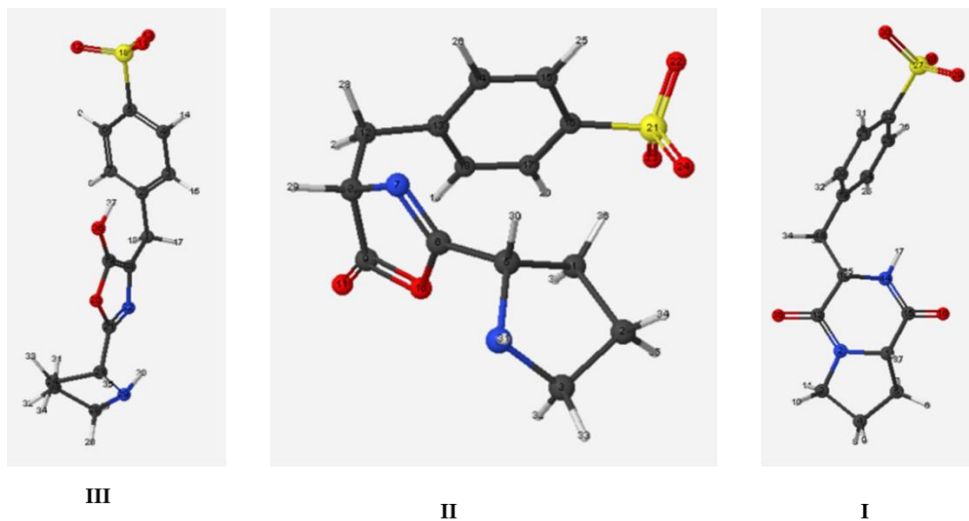


Figure 8.10. Lowest energy structures of possible b2 ion structures.

8.4 Conclusion

Collision induced dissociation (CID) was used to study the Phe*Pro and ProPhe* dipeptides to form sequence specific ions such as b2 ions. This b2 ion is typically formed by protonated dipeptides. However, the exceptionality of our study is that dipeptides have a localized anionic charge on the phenyl ring of phenylalanine; thus, the studied site is unaffected by the remote charge. In this study, we have found that not only is the ‘mobile proton’ involved in the dissociation process, but also the ‘backbone hydrogen’ is involved in forming b2 ions, which is similar to our previous studies. Finally, this study also supports our previous claim that modified amino acids can be used to find out the effect of the peptide structure and the effect on the products.

8.5 References

1. Aebersold, R.; Mann, M., Mass spectrometry-based proteomics. *Nature* **2003**, *422* (6928), 198.
2. Hunt, D. F.; Yates, J. R.; Shabanowitz, J.; Winston, S.; Hauer, C. R., Protein sequencing by tandem mass spectrometry. *Proceedings of the National Academy of Sciences* **1986**, *83* (17), 6233-6237.
3. Ahmed, F. E., Utility of mass spectrometry for proteome analysis: part I. Conceptual and experimental approaches. *Expert review of proteomics* **2008**, *5* (6), 841-864.
4. Brodbelt, J. S., Ion activation methods for peptides and proteins. *Analytical chemistry* **2015**, *88* (1), 30-51.
5. Hunt, D. F.; Shabanowitz, J.; Bai, D. L., Peptide sequence analysis by electron transfer dissociation mass spectrometry: a web-based tutorial. *Journal of the American Society for Mass Spectrometry* **2015**, *26* (7), 1256-1258.
6. Medzihradzky, K. F.; Chalkley, R. J., Lessons in de novo peptide sequencing by tandem mass spectrometry. *Mass spectrometry reviews* **2015**, *34* (1), 43-63.
7. Seidler, J.; Zinn, N.; Boehm, M. E.; Lehmann, W. D., De novo sequencing of peptides by MS/MS. *Proteomics* **2010**, *10* (4), 634-649.
8. Wysocki, V. H.; Tsaprailis, G.; Smith, L. L.; Brechi, L. A., Mobile and localized protons: a framework for understanding peptide dissociation. *Journal of Mass Spectrometry* **2000**, *35* (12), 1399-1406.
9. Yalcin, T.; Khouw, C.; Csizmadia, I. G.; Peterson, M. R.; Harrison, A. G., Why are B ions stable species in peptide spectra? *Journal of the American Society for Mass Spectrometry* **1995**, *6* (12), 1165-1174.
10. Ambihapathy, K.; Yalcin, T.; Leung, H. W.; Harrison, A. G., Pathways to immonium ions in the fragmentation of protonated peptides. *Journal of Mass Spectrometry* **1997**, *32* (2), 209-215.
11. Bowie, J. H.; Brinkworth, C. S.; Dua, S., Collision-induced fragmentations of the (M-H)⁻ parent anions of underivatized peptides: An aid to structure determination and some unusual negative ion cleavages. *Mass Spectrometry Reviews* **2002**, *21* (2), 87-107.
12. Bythell, B. J.; Knapp-Mohammady, M.; Paizs, B.; Harrison, A. G., Effect of the His residue on the cyclization of b ions. *Journal of the American Society for Mass Spectrometry* **2010**, *21* (8), 1352-1363.
13. Chen, X.; Tirado, M.; Steill, J. D.; Oomens, J.; Polfer, N. C., Cyclic peptide as reference system for b ion structural analysis in the gas phase. *Journal of Mass Spectrometry* **2011**, *46* (10), 1011-1015.

14. Harrison, A. G., To b or not to b: the ongoing saga of peptide b ions. *Mass spectrometry reviews* **2009**, 28 (4), 640-654.
15. Rodriguez, C. F.; Shoeib, T.; Chu, I. K.; Siu, K. M.; Hopkinson, A. C., Comparison between protonation, lithiation, and argentination of 5-oxazolones: A study of a key intermediate in gas-phase peptide sequencing. *The Journal of Physical Chemistry A* **2000**, 104 (22), 5335-5342.
16. Bythell, B. J.; Dain, R. P.; Curtice, S. S.; Oomens, J.; Steill, J. D.; Groenewold, G. S.; Paizs, B.; Van Stipdonk, M. J., Structure of $[M+H-H_2O]^+$ from protonated tetraglycine revealed by tandem mass spectrometry and IRMPD spectroscopy. *The Journal of Physical Chemistry A* **2010**, 114 (15), 5076-5082.
17. Chen, X.; Yu, L.; Steill, J. D.; Oomens, J.; Polfer, N. C., Effect of peptide fragment size on the propensity of cyclization in collision-induced dissociation: oligoglycine b₂– b₈. *Journal of the American Chemical Society* **2009**, 131 (51), 18272-18282.
18. Chu, I. K.; Shoeib, T.; Guo, X.; Rodriguez, C. F.; Lau, T.-C.; Hopkinson, A. C.; Siu, K. M., Characterization of the product ions from the collision-induced dissociation of argentinated peptides. *Journal of the American Society for Mass Spectrometry* **2001**, 12 (2), 163-175.
19. Grewal, R. N.; El Aribi, H.; Harrison, A. G.; Siu, K. M.; Hopkinson, A. C., Fragmentation of protonated tripeptides: the proline effect revisited. *The Journal of Physical Chemistry B* **2004**, 108 (15), 4899-4908.
20. Farrugia, J. M.; Richard, A., Involvement of salt bridges in a novel gas phase rearrangement of protonated arginine-containing dipeptides which precedes fragmentation. *International Journal of Mass Spectrometry* **2003**, 222 (1-3), 229-242.
21. Farrugia, J. M.; Richard, A.; Reid, G. E., Do all b₂ ions have oxazolone structures? Multistage mass spectrometry and ab initio studies on protonated N-acyl amino acid methyl ester model systems. *International Journal of Mass Spectrometry* **2001**, 210, 71-87.
22. Forbes, M. W.; Jockusch, R. A.; Young, A. B.; Harrison, A. G., Fragmentation of protonated dipeptides containing arginine. Effect of activation method. *Journal of the American Society for Mass Spectrometry* **2007**, 18 (11), 1959-1966.
23. Harrison, A. G., Cyclization of peptide b₉ ions. *Journal of the American Society for Mass Spectrometry* **2009**, 20 (12), 2248-2253.
24. Knapp-Mohammady, M.; Young, A. B.; Paizs, B.; Harrison, A. G., Fragmentation of doubly-protonated Pro-His-Xaa tripeptides: Formation of b₂²⁺ ions. *Journal of the American Society for Mass Spectrometry* **2009**, 20 (11), 2135-2143.

25. Nold, M. J.; Wesdemiotis, C.; Yalcin, T.; Harrison, A. G., Amide bond dissociation in protonated peptides. Structures of the N-terminal ionic and neutral fragments. *International Journal of Mass Spectrometry and Ion Processes* **1997**, *164* (1-2), 137-153.
26. Wysocki, V. H.; Resing, K. A.; Zhang, Q.; Cheng, G., Mass spectrometry of peptides and proteins. *Methods* **2005**, *35* (3), 211-222.
27. Yoon, S. H.; Chamot-Rooke, J.; Perkins, B. R.; Hilderbrand, A. E.; Poutsma, J. C.; Wysocki, V. H., IRMPD spectroscopy shows that AGG forms an oxazolone b₂⁺ ion. *Journal of the American Chemical Society* **2008**, *130* (52), 17644-17645.
28. Zou, S.; Oomens, J.; Polfer, N. C., Competition between diketopiperazine and oxazolone formation in water loss products from protonated ArgGly and GlyArg. *International Journal of Mass Spectrometry* **2012**, *316*, 12-17.
29. Koirala, D.; Kodithuwakkuge, S. R.; Wenthold, P. G., Mass spectrometric study of the decomposition pathways of canonical amino acids and α -lactones in the gas phase. *Journal of Physical Organic Chemistry* **2015**, *28* (10), 635-644.
30. Farrugia, J. M.; Taverner, T.; Richard, A., Side-chain involvement in the fragmentation reactions of the protonated methyl esters of histidine and its peptides. *International Journal of Mass Spectrometry* **2001**, *209* (2-3), 99-112.
31. Perkins, B. R.; Chamot-Rooke, J.; Yoon, S. H.; Gucinski, A. C.; Somogyi, A.; Wysocki, V. H., Evidence of diketopiperazine and oxazolone structures for HA b₂⁺ ion. *Journal of the American Chemical Society* **2009**, *131* (48), 17528-17529.
32. Gucinski, A. C.; Chamot-Rooke, J.; Nicol, E.; Somogyi, Á.; Wysocki, V. H., Structural influences on preferential oxazolone versus diketopiperazine b₂⁺ ion formation for histidine analogue-containing peptides. *The Journal of Physical Chemistry A* **2012**, *116* (17), 4296-4304.
33. Dunbar, R. C.; Steill, J. D.; Polfer, N. C.; Oomens, J., Gas-phase infrared spectroscopy of the protonated dipeptides H⁺ PheAla and H⁺ AlaPhe compared to condensed-phase results. *International Journal of Mass Spectrometry* **2009**, *283* (1-3), 77-84.
34. Tsaprailis, G.; Nair, H.; Zhong, W.; Kuppanan, K.; Futrell, J. H.; Wysocki, V. H., A mechanistic investigation of the enhanced cleavage at histidine in the gas-phase dissociation of protonated peptides. *Analytical chemistry* **2004**, *76* (7), 2083-2094.
35. Tsaprailis, G.; Somogyi, A.; Nikolaev, E. N.; Wysocki, V. H., Refining the model for selective cleavage at acidic residues in arginine-containing protonated peptides. *International Journal of Mass Spectrometry* **2000**, *195*, 467-479.
36. Koirala, D.; Mistry, S.; Wenthold, P. G., Participation of CH Protons in the Dissociation of a Proton Deficient Dipeptide. *Journal of The American Society for Mass Spectrometry* **2017**, *28* (7), 1313-1323.

37. Boyd, R.; Somogyi, Á., The mobile proton hypothesis in fragmentation of protonated peptides: a perspective. *Journal of the American Society for Mass Spectrometry* **2010**, *21* (8), 1275-1278.
38. Dongré, A. R.; Jones, J. L.; Somogyi, Á.; Wysocki, V. H., Influence of peptide composition, gas-phase basicity, and chemical modification on fragmentation efficiency: Evidence for the mobile proton model. *Journal of the American Chemical Society* **1996**, *118* (35), 8365-8374.
39. Wysocki, V. H.; Cheng, G.; Zhang, Q.; Hermann, K.; Beardsley, R. L.; Hilderbrand, A. E., Peptide fragmentation overview. Wiley Online Library: 2006; pp 279-300.
40. Vanhoof, G.; Goossens, F.; De Meester, I.; Hendriks, D.; Scharpe, S., Proline motifs in peptides and their biological processing. *The FASEB Journal* **1995**, *9* (9), 736-744.
41. MacArthur, M. W.; Thornton, J. M., Influence of proline residues on protein conformation. *Journal of molecular biology* **1991**, *218* (2), 397-412.
42. Barlow, D.; Thornton, J., Helix geometry in proteins. *Journal of molecular biology* **1988**, *201* (3), 601-619.
43. Fischer, G.; Heins, J.; Barth, A., The conformation around the peptide bond between the P1-and P2-positions is important for catalytic activity of some proline-specific proteases. *Biochimica et Biophysica Acta (BBA)-Protein Structure and Molecular Enzymology* **1983**, *742* (3), 452-462.
44. Vaisar, T.; Urban, J., Probing proline effect in CID of protonated peptides. *Journal of Mass Spectrometry* **1996**, *31* (10), 1185-1187.
45. Schwartz, B. L.; Bursey, M. M., Some proline substituent effects in the tandem mass spectrum of protonated pentaalanine. *Biological mass spectrometry* **1992**, *21* (2), 92-96.
46. Martin, S. A.; Biemann, K., A comparison of keV atom bombardment mass spectra of peptides obtained with a two-sector mass spectrometer with those from a four-sector tandem mass spectrometer. *International journal of mass spectrometry and ion processes* **1987**, *78*, 213-228.
47. Loo, J. A.; Edmonds, C. G.; Smith, R. D., Primary sequence information from intact proteins by electrospray ionization tandem mass spectrometry. *Science* **1990**, *248* (4952), 201-204.
48. Smith, R. D.; Loo, J. A.; Barinaga, C. J.; Edmonds, C. G.; Udseth, H. R., Collisional activation and collision-activated dissociation of large multiply charged polypeptides and proteins produced by electrospray ionization. *Journal of the American Society for Mass Spectrometry* **1990**, *1* (1), 53-65.
49. Csizmadia, P., MarvinSketch and MarvinView: molecule applets for the World Wide Web. **1999**.

50. Kong, J.; White, C. A.; Krylov, A. I.; Sherrill, D.; Adamson, R. D.; Furlani, T. R.; Lee, M. S.; Lee, A. M.; Gwaltney, S. R.; Adams, T. R., Q-Chem 2.0: a high-performance ab initio electronic structure program package. *Journal of Computational Chemistry* **2000**, *21* (16), 1532-1548.
51. Vicente, A. I.; Caio, J. M.; Sardinha, J.; Moiteiro, C.; Delgado, R.; Félix, V., Evaluation of the binding ability of tetraaza [2] arene [2] triazine receptors anchoring l-alanine units for aromatic carboxylate anions. *Tetrahedron* **2012**, *68* (2), 670-680.
52. Da Costa, C. F.; Pinheiro, A. C.; De Almeida, M. V.; Lourenço, M. C.; De Souza, M. V., Synthesis and antitubercular activity of novel amino acid derivatives. *Chemical biology & drug design* **2012**, *79* (2), 216-222.
53. Jahani, F.; Tajbakhsh, M.; Golchoubian, H.; Khaksar, S., Guanidine hydrochloride as an organocatalyst for N-Boc protection of amino groups. *Tetrahedron letters* **2011**, *52* (12), 1260-1264.
54. Nitecki, D. E.; Halpern, B.; Westley, J. W., Simple route to sterically pure dioxopiperazines. *J. Org. Chem.* **1968**, *33* (2), 864-6.
55. Uraguchi, D.; Asai, Y.; Ooi, T., Site-directed asymmetric quaternization of a peptide backbone at a C-terminal azlactone. *Angew. Chem., Int. Ed.* **2009**, *48* (4), 733-737.
56. Hauptert, L. J.; Poutsma, J. C.; Wenthold, P. G., The Curtin–Hammett Principle in Mass Spectrometry. *Accounts of chemical research* **2009**, *42* (10), 1480-1488.
57. Gucinski, A. C.; Chamot-Rooke, J.; Steinmetz, V.; Somogyi, A. r. d.; Wysocki, V. H., Influence of N-terminal residue composition on the structure of proline-containing b2+ ions. *The Journal of Physical Chemistry A* **2013**, *117* (6), 1291-1298.

VITA

Sabyasachy (Babu) Mistry was born in December 1980 to Nil Ratan Mistry and Sandhya Rani Samaddar in Morrelgonj, Bangladesh. He joined University of Dhaka for undergraduate degree (B.Sc.) in Chemistry and master's degree (M.S.) in Organic Chemistry. After finishing his master's, he was an instructor for few years at Stamford University Bangladesh, Dhaka. He started his graduate school at Purdue University in Fall 2014 and joined the Wenthold group. In 2017, he got married to Amity Saha, who is a Graduate student in Hospitality & Tourism Management (HTM) at Purdue University, and now they are expecting a baby girl at anytime between late November and early December (name: Krittika Opola Mistry). In his spare time, he loves to spend time with his family.

PUBLICATIONS



© American Society for Mass Spectrometry, 2017



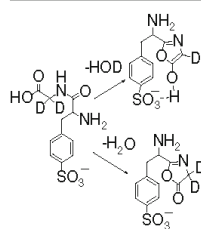
J. Am. Soc. Mass Spectrom. (2017) 28:1313–1323
DOI: 10.1007/s13361-017-1662-7

FOCUS: BIO-ION CHEMISTRY: INTERACTIONS OF BIOLOGICAL IONS
WITH IONS, MOLECULES, SURFACES, ELECTRONS, AND LIGHT: RESEARCH ARTICLE

Participation of C-H Protons in the Dissociation of a Proton Deficient Dipeptide

Damodar Koirala, Sabyasachy Mistry, Paul G. Wenthold

Department of Chemistry, Purdue University, 560 Oval Drive, West Lafayette, IN 47906, USA



Abstract. The dissociation of anionic dipeptides Phe*Gly and GlyPhe*, where Phe* refers to sulfonated phenyl alanine, has been investigated by using ion trap mass spectrometry. The dipeptides undergo collision-induced dissociation (CID) to give the same products, indicating that they rearrange to a common structure before dissociation. The rearrangement does not occur with the dipeptide methyl esters. The structures of the b_2 ions were investigated to determine the effect that having a remote, anionic site has on product formation. Comparison with the CID spectra for authentic structures shows that the b_2 ion obtained from GlyPhe* has predominantly a diketopiperazine structure. The CID spectra for the Phe*Gly b_2 ion and the authentic oxazolone are similar, but differences in intensity suggest a two-component mixture.

Isotopic labeling studies are consistent with the formation of two products, with one resulting from loss of a non-mobile proton on the Gly α -carbon. The results are attributed to the formation of an oxazole and oxazolone enol product. Electronic structure calculations predict that the enol structure of the Phe*Gly b_2 ion is lower in energy than the keto version due to intramolecular hydrogen bonding with the sulfonate group.

Keywords: Dipeptide dissociation, b_2 Ions, Charge remote fragmentation, Canonical structures, Diketopiperazine, Oxazolone

Received: 17 November 2016/Revised: 13 March 2017/Accepted: 14 March 2017/Published Online: 20 April 2017

Introduction

The significance of amino acids and peptides to the world around us, and to life itself, cannot be overstated, and, therefore, it is not surprising that their structures, properties, and reactivity are exceptionally well-characterized, largely due to the capabilities of mass spectrometry and electrospray ionization [1]. The ability for rapid, accurate analysis of proteins and peptides by mass spectrometry has had a major impact on the field of proteomics, and allows for the study of the structures and functions of large proteins in complex biological system.

One of the most important features of using mass spectrometry to identify proteins and peptides in proteomics is the ability to use tandem mass spectrometry (MS^n) to differentiate isobaric ions and for sequence determination. Therefore, whereas

libraries of mass spectra can be used to identify known proteins, amino acid sequences in unknown proteins can be determined by de novo analysis of ionic fragments. In particular, fragments observed in peptide dissociation, especially b- and y-type sequence ions resulting from fragmentation of amide bonds, can be used to determine the sequence from the C- and N-terminus [2–8].

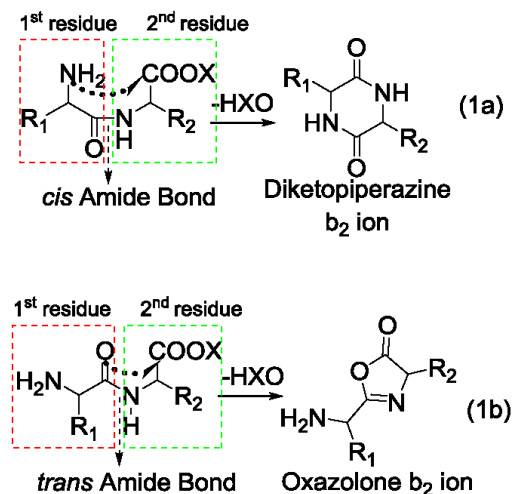
Products obtained upon dissociation of protonated peptides have generally been explained in terms of the “mobile proton theory” [9–12]. The model assumes that protons, initially localized on the most basic sites (N-terminus and the side chains of basic amino acid residues) of protonated peptides, can be transferred to the less basic of sites upon activation, including the various peptide linkages, thereby producing a heterogeneous population of protonated peptides [9, 10, 12]. The mobile proton model provides a quantitative framework such that if the peptide sequence and number of protons are known, one can predict the general appearance of the fragmentation spectrum [12]. Although the mobile proton model is not intended to model the full peptide fragmentation spectrum quantitatively, it successfully accounts for common dissociation, including aforementioned b- and y-type ions [13–15].

Electronic supplementary material The online version of this article (doi:10.1007/s13361-017-1662-7) contains supplementary material, which is available to authorized users.

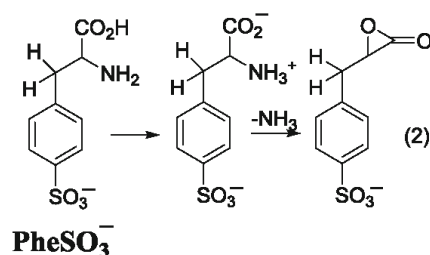
Correspondence to: Paul Wenthold; e-mail: pgw@purdue.edu

Because peptide b ions are common, stable, species in peptide fragmentation [16], a better understanding of how they are formed can improve peptide sequencing algorithms and the current models for peptide fragmentation [9]. Consequently, several theoretical and experimental studies have been carried out in recent years to better understand the structures of b ions and the mechanism of their formation [16–35]. In this work, we use dipeptides with backbone charges to investigate the formation of b₂ ions for canonical structures.

Many structures have been proposed for b₂ ions [12]. Initially, an acylium ion was thought to be the major b₂ ion structure, but it was later discovered to be thermodynamically less stable than its isomeric cyclic structures [32]. Of the structures proposed for b₂ ions, the most common are protonated diketopiperazines and protonated oxazolones [28, 35–49]. Six-membered cyclic diketopiperazine is formed when the N-terminal amino group acts as a nucleophile and attacks at the carbonyl carbon of second amino acid residue. In contrast, a five-membered cyclic oxazolone is formed when the N-terminal carbonyl oxygen acts as a nucleophile and attacks at the carbonyl carbon of second amino acid residue. Which ion forms is mainly determined by the structure of the peptide (Equation 1). A *cis* conformation of the first amide bond favors diketopiperazine because it facilitates the nucleophilic attack by amino group of N-terminal amino acid (Equation 1a), whereas a *trans* conformation of the first amide bond favors oxazolone (Equation 1b) because it facilitates the nucleophilic attack by carbonyl oxygen of N-terminal amino acid [13, 45–48, 50, 51]. Although diketopiperazine structures are generally lower in energy [47], the oxazolone structures result for *trans* amides because the barrier for the formation is lower than the barrier for *cis-trans* isomerization.



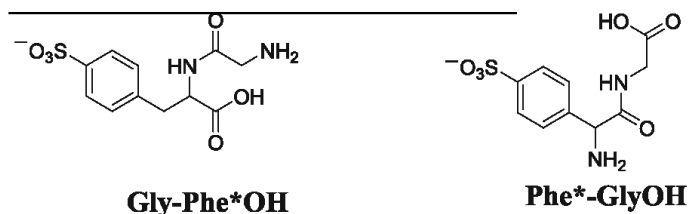
The nature of the charge on peptides also plays an important role in the dissociation mechanism. Mass spectrometry studies of peptide and peptide's dissociation usually involve the use of protonated [13] or metallated [36, 52] peptides, often multiply charged depending on the number of basic sites. Therefore, the excess positive charge allows for facile intramolecular proton transfer that does not require, *inter alia*, formation of salt-bridges or other forms of charge separation. In a recent study, we reported the formation and dissociation of sulfonated phenylalanine, **PheSO₃⁻**, an anionic amino acid where the charge is isolated from the α-amino acid moiety by a phenyl spacer [53]. The ion dissociates only by loss of NH₃ to make a product assigned to be an α-lactone (Equation 2) [54]. The proposed mechanism involves proton transfer within the canonical amino acid to form a zwitterionic intermediate, which dissociates by intramolecular substitution to make the lactone (Equation 2), and therefore nominally illustrates the potential of mobile electron within anionic systems as well. However, an important feature of all these reactions is that although energetically unfavorable proton transfer can occur in these reactions upon activation, it is still generally limited to protons on heteroatom positions, such as amines, amide nitrogen, or carboxyl groups.



In this work, we have used mass spectrometry to examine the dissociation of dipeptides that include **PheSO₃⁻**, namely GlyPhe*OH and Phe*GlyOH, where Phe* refers to sulfonated Phe, **PheSO₃⁻**. Unlike protonated and metallated ions, these dipeptides are anionic and hence proton deficient. However, because the sulfonate charge is more stable than a carboxylate, and the charge is localized on the side chain, the dipeptides are predicted to have canonical structures [53]. In this respect, they are similar to protonated dipeptides containing His [47, 49, 50, 55, 56] or Arg [27, 29, 35, 57], which contain basic side chains that sequester positive charge. We find that the sulfonated dipeptides dissociate similar to what has been reported for ArgGly and other dipeptides, with the formation of characteristic sequence ions, such as b₂ ions. However, unlike what is typically found for protonated dipeptides, we find that b₂ ion formation in the sulfonated

dipeptides involves not only loss of exchangeable protons on nitrogen and oxygen but also loss of protons from

carbon, which are generally not considered within the mobile proton model.

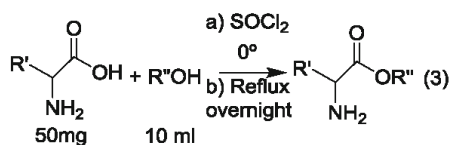


Experimental

Mass spectrometry experiments were carried out using a commercial LCQ-DECA (Thermo Electron Corporation, San Jose, CA, USA) quadrupole ion trap mass spectrometer, equipped with electrospray ionization (ESI) source. Samples were dissolved in a methanol:water mixture (1:1) and introduced into the source at a flow rate of 10 μ L/min. Electrospray and ion focusing conditions were varied so to maximize the signal of the ion of interest. Dissociation of ions was carried out by using MSⁿ experiments with mass-selected ions in the cell, with the helium buffer serving as the collision target. Reactant ions for CID were isolated at $q_z = 0.250$ and with a mass-width sufficient to avoid off-resonance excitation of the mass-selected ions. The energy of collision-induced dissociation (CID) in the cell is reflected in the "normalized collision energy," which ranges from 0 to 100%.

Synthesis of Amino Acid Esters

A 50 mg sample of the amino acid was dissolved in 10 mL of alcohol and cooled to 0 °C. Esterification was initiated by adding 3 mL of SOCl₂, dropwise, into the cold amino acid solution. After the solution warmed to room temperature, it was refluxed overnight to get desired amino acid ester (Equation 3).



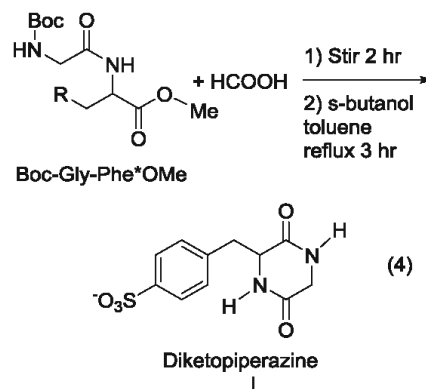
Synthesis of GlyPhe*OH and Phe*GlyOH Dipeptides

A sample of 0.09 mmol of Boc-Amino acid (Boc-R₁) was dissolved in 15 mL of dichloromethane (DCM), and 0.09 mmol of benzotriazol-1-yl-oxytriethylpyrrolidinophosphonium hexafluorophosphate (PyBop) was added. The solution was cooled to 0 °C and 0.14 mmol of di-isopropylethylamine base (DIEA) was added dropwise. After stirring for 20 min, the solution was brought to room temperature, and 0.09 mmol

of second residue amino acid methyl ester (R₂-OMe) was added. After stirring for an additional 40 min, the excess DCM was evaporated in vacuum. Formation of the dipeptide product (BocR₁-R₂OMe) was confirmed by mass spectrometry. The Boc group was removed by dissolving the product in excess trifluoroacetic acid (TFA) for 20 min, followed by evaporation of the TFA in vacuum, resulting in formation of the methyl ester. The ester, R₁-R₂OMe, can be hydrolyzed to R₁-R₂OH by treating their aqueous solution with concentrated sulfuric acid. The synthesis of GlyPhe*OMe is shown in Scheme S1 in the Supplementary Material.

Synthesis of Diketopiperazine

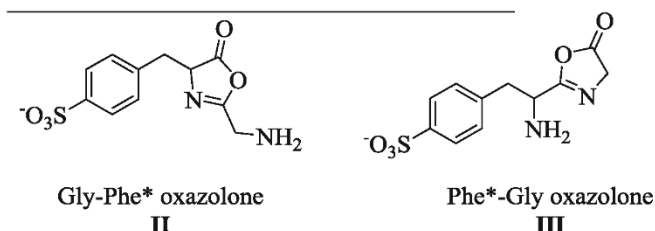
Diketopiperazine (**I**) was synthesized using the approach described previously [58]. Briefly, the solution containing 50 mg of Boc-GlyPhe*OMe and 10 mL formic acid (98%) was stirred at room temperature for 2 h (Equation 4). Excess formic acid was removed in vacuo and the crude product was dissolved in 15 mL of sec-butyl alcohol and 5 mL of toluene. The solution was boiled for 3 h and the solvent level maintained by addition of fresh butanol. After concentrating the solution to 5–10 mL and cooling to 0 °C, the product was obtained by filtration.



Synthesis of Oxazolones (GlyPhe* and Phe*Gly Oxazolones)

The syntheses of the oxazolones were carried out using procedures described previously [59]. Briefly, the solution containing 10 mmol of Boc-GlyPhe*OH and 15 mmol of 1, 3,-dicyclohexylcarbodiimide (DCC) were

dissolved in 10 mL of dichloromethane. The solution was stirred at room temperature for 3 h. Excess solvent was removed in vacuo and the resulting crude product was dissolved in 3 mL TFA to produce GlyPhe*-oxazolone (II). Similar procedure was adopted for synthesis of Phe*Gly-oxazolone (III).



Computational Methods

Geometries and electronic energies were calculated at the B3LYP/6-31+G* level of theory. Low-energy conformations were initially identified by using the Monte Carlo multiple minimum search method, with the Merck molecular force field (MMFF) as implemented in MacroModel (ver. 9.6) [60], and unique conformations were used as starting points in B3LYP optimizations. Single point energies for selected optimized structures were carried out at the MP2/6-311+G** level of theory in order to obtain a better description of van der Waals interactions and charge polarization. Energies are not corrected for zero-point energies or thermal energy contributions. B3LYP and MP2 calculations were carried out using QCHEM ver. 4.0 [61].

Results and Discussion

Analysis of GlyPhe*OH and Phe*GlyOH

The CID (MS²) mass spectra of GlyPhe*OH and Phe*GlyOH (*m/z* 301) are shown in Figure 1. Both isomers give the same products with the same intensities. Primary product ions include *m/z* 284 (*M* - NH₃), *m/z* 283 (*M* - H₂O), *m/z* 257 (*M* - CO₂), and *m/z* 244 (*M* - C₂ONH₃, net loss of glycine - H₂). Additional products can be attributed to secondary fragmentation of the primary products. In contrast, the CID spectra of the positive ions derived from the two dipeptides are markedly distinct (see [Supplementary Material](#)). The fact that both GlyPhe*OH and Phe*GlyOH give the same spectra upon negative ion CID indicates that they rearrange to a common structure before dissociation. Rearrangement of dipeptides upon low-energy CID has been reported previously by Farrugia and O'Hair for protonated ArgGly and GlyArg

[27]. As described in the introduction, protonated ArgGly/GlyArg is structurally similar to Phe*GlyOH/GlyPhe*OH because they both contain canonical dipeptides with the charges

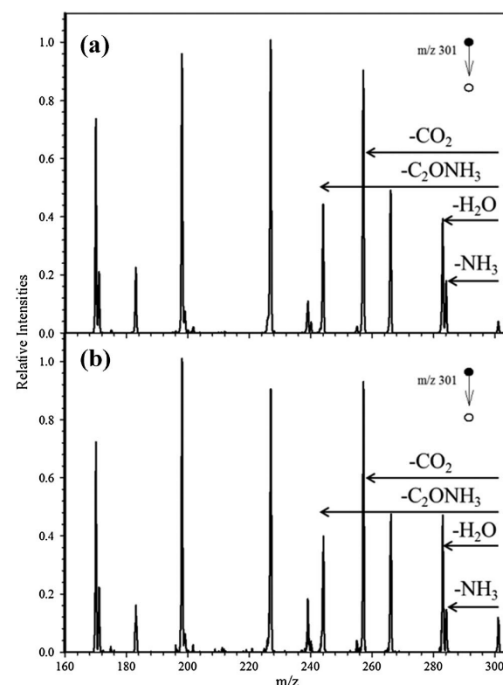


Figure 1. CID mass spectra for (a) GlyPhe*OH and (b) Phe*GlyOH

on the side chains. Therefore, the rearrangement of GlyPhe*OH and Phe*GlyOH dipeptides is likely similar to what was proposed previously by Farrugia and O'Hair for protonated ArgGly and GlyArg dipeptides [27], involving proton transfer within the dipeptide to form zwitterionic structures, which can rearrange to cyclic structure and eventually rearrange to form the common acid anhydride intermediate (Figure 2). Consequently, any of the structures in Figure 2 can be the common intermediate leading to the dissociation product(s), with the dissociation determined by the overall lowest energy pathway for the product [62]. Further CID of the product ions in Figure 1a and b are also similar, confirming that GlyPhe*OH and Phe*GlyOH give the same products upon CID.

Analysis of GlyPhe*OMe and Phe*GlyOMe

Support for the mechanism shown in Figure 2 comes from the experiments involving methyl esters. Farrugia and O'Hair [27] have shown previously that methylation of the C-terminus carboxylic acid inhibits the rearrangement reaction of protonated ArgGly and GlyArg, presumably by blocking the initial proton transfer step. Similarly, we have found that esterification of GlyPhe*OH and Phe*GlyOH inhibits their rearrangement as well. The

CID spectra of GlyPhe*OMe and Phe*GlyOMe, shown in Figure 3, are significantly different in both the identities of the products and the intensities. Although both ions dissociate to form products m/z 283 ($M - \text{MeOH}$), m/z 266 ($M - \text{MeOH} - \text{NH}_3$), and m/z 170, the relative intensities are very different. In particular, whereas the b_2 ion ($M - \text{CH}_3\text{OH}$ @ m/z 283) is one of the dominant peaks upon CID of Phe*GlyOMe, it is very weak upon CID of GlyPhe*OMe. In addition, peaks at m/z 298, 240, 226, 198, 185, and 171 are observed solely on CID of Phe*GlyOMe spectra, whereas m/z 266, 241, and 197 are observed solely on CID of GlyPhe*OMe spectra.

The $M - \text{CH}_3\text{OH}$ ions observed upon CID of GlyPhe*OMe and Phe*GlyOMe are the b_2 ions. The MS^3 spectra of b_2 ions obtained from GlyPhe*OMe and Phe*GlyOMe, shown in Figure 4a and b, are also different, consistent with different isomers giving different products, without rearranging to a common structure. The CID spectra of the b_2 ions obtained from Phe*GlyOH and GlyPhe*OH agree with that from that obtained from Phe*GlyOMe.

Comparison to Authentic Diketopiperazine and Oxazolones

In order to determine the structures of the b_2 ions, we have compared their CID spectra with those obtained for the most likely possibilities, including the diketopiperazine

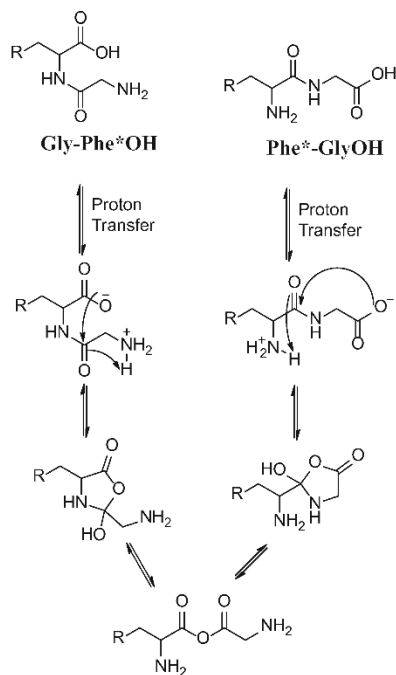


Figure 2. Proposed mechanism for formation of common structure from Phe*GlyOH and GlyPhe*OH

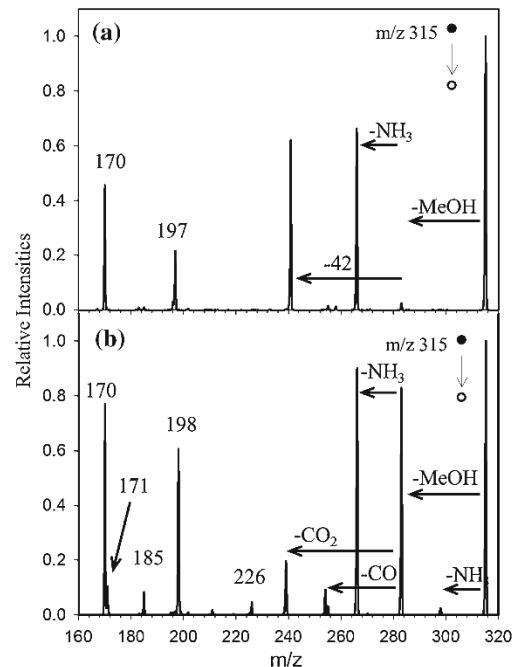


Figure 3. (a) CID of GlyPhe*OMe, and (b) CID of Phe*GlyOMe

importantly, that the rearrangement of GlyPhe*OH occurs before dissociation indicates that the barrier for the rearrangement is lower than the dissociation energy, and the barrier for dissociation of Phe*GlyOH is lower than that for dissociation of GlyPhe*OH [62].

Although the spectra of the Phe*GlyOMe b_2 ion and oxazolone **III** are superficially similar in that they form the same products, the relative intensities of the products do not match. In particular, the m/z 239 peak in the spectrum of **III** (Figure 5c) is much more intense than that in the spectrum of the b_2 ion (Figure 4b). It is possible that the difference in CID intensities for the two ions may result from differences in the manner in which they were generated. Because the b_2 ion is formed by CID whereas the authentic oxazolone comes directly from electrospray, the ions in the trap may initially have different amounts of internal energy, which can lead to differences in product intensities.

However, further analysis of the CID spectra suggests some patterns. For example, the ratios of m/z 239/ m/z 170 intensities in the two spectra are very similar (5.4 versus 5.9). Similarly, the ratio of the m/z 198 and m/z 266 products are also similar (1.7 versus 2.0). These results are consistent with the spectrum for an isobaric mixture of two components – one that dissociates to form m/z 239 and 170 (and possibly 266 and 198), and the other dissociates to form m/z 266 and 198 (and likely 255) – in different proportions, depending on the source of the ion.

The formation of an oxazolone structure for the b_2 ion from Phe*Gly is not surprising. As described in the introduction, oxazolones are expected for most b_2 , especially those formed from peptides with *trans* amide bonds. Indeed, the lowest energy conformations of Phe*GlyOH and Phe*GlyOMe are calculated to have *trans* amide bond structures, approximately 15 kcal/mol lower in energy than the *cis* geometry (see [Supplementary Material](#)). In contrast, formation of the diketopiperazine from GlyPhe*OMe is more unexpected. Both GlyPhe*OH and GlyPhe*OMe also have *trans* amide structures, with the *cis* structures, again, more than 10 kcal/mol less stable than *trans*. Perkins et al. [49] have observed diketopiperazine formation in the formation of HisAla b_2 ions, and initially suggested that having the charge on the backbone may have an effect. Subsequent studies of HisAla [47] and ArgGly [35] have also found diketopiperazine products, consistent with the proposal by Perkins et al. [49]. However, the b_2 ion for Phe*GlyOMe (or Phe*GlyOH) does not have diketopiperazine structure, despite having the backbone charge. For the *trans* dipeptides, Phe*GlyOH is calculated to be ~ 7 kcal/mol lower in energy than GlyPhe*OH, which accounts for the rearrangement of GlyPhe*OH before dissociation.

Deuterium Labeling

Deuterium labeling provides additional insight into the structure(s) of the product(s) of the b_2 ions. In order to determine which proton is involved in methanol loss in the formation of the b_2 ion, we examined three deuterated labeled compounds

d_3 -Phe*GlyOMe, Phe*Gly(2,2- d_2) OMe, and d_5 -Phe*GlyOMe (Figure 6). H/D exchange of the three labile protons of Phe*GlyOMe was carried out in 50:50 D_2O and MeOD solution. Upon CID, d_3 -Phe*GlyOMe loses MeOD and MeOH in a ratio of about 1:2 (Figure 6a). Loss of MeOD is consistent with what is expected formation of oxazolone **III**, with loss of methoxy from the C-terminus and loss of a mobile proton from one of the nitrogen positions. However, loss of CH_3OH is surprising, especially as the major product, because it requires loss of hydrogen from a carbon position, which would not normally be considered a “mobile” proton lost during dissociation. Scrambling involving hydrogen on α -carbon has been observed previously for dissociation of b_3 [63] and a_3 [64] fragment ions, but has not been observed in the simple formation of b_n ions.

Although the spectrum in Figure 6a shows that protons on carbon are involved in the dissociation, it does not specify which carbons are involved, whether they are from an α -carbon on Gly or Phe*, or from the aliphatic or aromatic region of the side chain. Additional deuterium labeling experiments, however, provide further insight. The spectrum for Phe*GlyOMe, where the Gly is labeled with deuterium in the α -position (2, 2- d_2), is shown in Figure 6b. Again, the ion

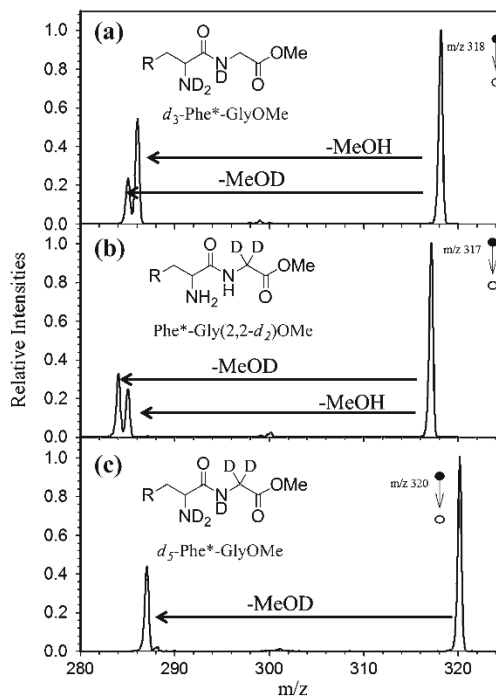
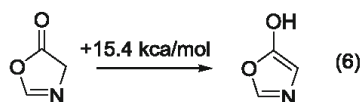


Figure 6. CID spectra showing b_2 ion formation from deuterated dipeptide esters (a) d_3 -Phe*-GlyOMe, (b) Phe*-Gly(2,2- d_2)OMe, (c) d_5 -Phe*-GlyOMe

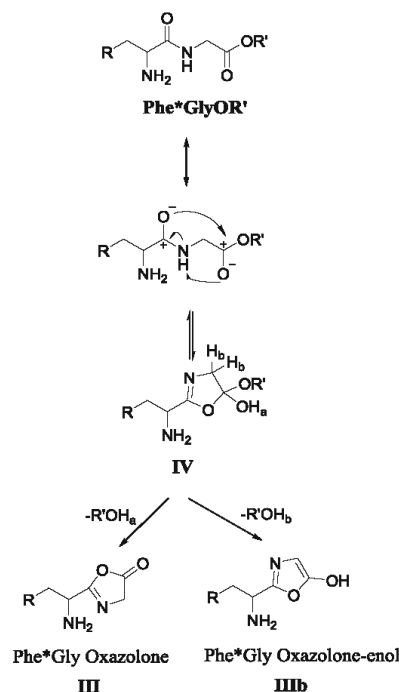
dissociates by loss of MeOH and MeOD, but in this case, the intensities are reversed, with loss of MeOD being the major b_2 product. In this experiment, loss of CH₃OH is consistent with formation of the oxazolone. Loss of CH₃OD as the major pathway for b_2 ion formation confirms that carbon-based hydrogens are involved and, in particular, it is the proton on the α -position of glycine. However, this result still does not rule out participation of other protons, such as those at the α -position of Phe* or those on the side chain. To test for the possibility, we also deuterated the nitrogen positions. The CID spectrum of the d_3 -Phe*GlyOMe, with deuterium at the α -position of Gly and at all the exchangeable positions, is shown in Figure 6c. In this case, the b_2 ion is formed almost exclusively (>98%) by loss of CH₃OD. Therefore, the b_2 ions are being formed either by loss of an exchangeable proton (from nitrogen) or from a proton α -position of the Gly, with the latter process being more prominent. The fact that b_2 ions are formed by multiple processes is consistent with the conclusion in the previous section that the b_2 ions are a mixture of multiple structures.

The deuterium labeling indicates that the two products formed involve loss of proton from nitrogen or from the Gly. A mechanism that accounts for the observed products is shown in Scheme 1. Nucleophilic attack of the Phe* carbonyl oxygen at the Gly carbonyl carbon accompanied by proton transfer leads to the hemiacetal-like structure, **IV**. Loss of alcohol with proton loss from the OH in **IV** (proton H_a in Scheme 1) leads to the standard oxazolone, **III**. In this pathway, the proton that is lost is a mobile proton, originally on the amide nitrogen. Alternatively, loss of alcohol from **IV** with the proton coming from the ring (proton H_b) would lead instead to a hydroxyoxazolone, **IIIb**, the enol structure of the oxazolone.

Computational studies support the assignment of the enol structure, **IIIb**, for the b_2 ion obtained from Phe*GlyOMe. Unlike phenols, hydroxyoxazolones are typically not more stable than the corresponding oxazolones. At the MP2/6-31+G**/B3LYP/6-31+G* level of theory, the simple oxazolone is computed to be 15.4 kcal/mol lower in energy than the hydroxyoxazolone (Equation 6). However, interaction between the hydroxy group and the sulfonate charge in the Phe*Gly b_2 ion is predicted to stabilize the enol structure. The relative energies of possible isomeric b_2 ion structures obtained from GlyPhe* and Phe*Gly are shown in Table 1. The most stable product is predicted to be the diketopiperazine, **I**, and the **II** and **III** oxazolone b_2 ions are calculated to be 14 and 20 kcal/mol higher in energy, respectively. The relative energies of the diketopiperazine and oxazolones are consistent with what has been found in previous studies [47, 49, 65].



At the MP2/6-31+G* level of theory, the lowest energy structure, aside from the diketopiperazine, is predicted to be the hydroxyoxazolone obtained from Phe*Gly, **IIIb**, as shown in



Scheme 1.

Scheme 1. In contrast, the hydroxyoxazolone obtained from GlyPhe*, **IIb**, is significantly higher in energy. The stability of the enol structure for the Phe*Gly b_2 can be attributed to a favorable hydrogen bond interaction between the OH and the sulfonate group, as shown in Figure 7, and accounts for the preference for losing proton from carbon, as opposed to from nitrogen. The oxazolone structure **II** obtained from GlyPhe* has a hydrogen bond between the N-H and sulfonate, which accounts for its stability compared to **III**. The other structures are not capable of having interactions with the sulfonate. The optimized geometries of all the possible b_2 structures are shown in Figure 7. An oxazolone-enol structure in peptide fragmentation has been proposed previously by Paizs and co-workers [64], but the proposed enol structure is inconsistent with the

Table 1. Calculated Relative Energies of b_2 Ions^a

Ion	MP2/6-31+G*
Diketopiperazine I	0
GlyPhe* Oxazolone II	14
GlyPhe* Oxazolone enol IIb	26
Phe*Gly Oxazolone III	20
Phe*Gly Oxazolone enol IIIb	12

^a Relative electronic energies (not corrected) in kcal/mol at B3LYP/6-31+G* optimized geometries.

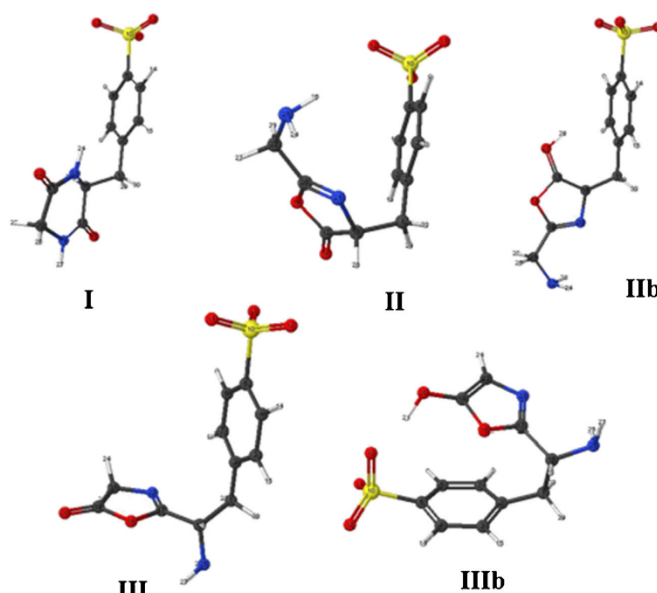


Figure 7. Lowest energy structures of possible b_2 ion structures

measured infrared multiphoton dissociation spectrum for the ion [63]. This is not surprising because the enol structure is nominally expected to be ~ 15 kcal/mol higher in energy than the keto form. However, in this work the enol is stabilized through intramolecular hydrogen bonding and is, therefore, predicted to be a low-energy isomer. Stabilization of the b_2 ion by intramolecular hydrogen bonding has been observed previously for HisPro [65], but in that system, the hydrogen bonding preferentially stabilized the diketopiperazine structure, by almost 20 kcal/mol.

Conclusions

The Phe*Gly and GlyPhe* dipeptides examined in this work dissociate upon collision-induced dissociation to form products similar to those typically formed for protonated dipeptides, including sequence specific ions, such as the b_2 ion. However, the Phe* containing peptides are distinct from typical ionized peptides in that they are anionic, with the charge localized on the side chain, such that the amino acid moieties have canonical structures. “Mobile protons” are still involved in the dissociation processes, but in this work, we find that b_2 ions are also formed by loss of backbone hydrogen atoms, typically not considered as part of the mobile proton model. The results highlight the importance of evaluating each modified amino acid individually, in respect to not only the effect on the peptide structure, but also the effect on the products.

Acknowledgements

This work was supported by the National Science Foundation (CHE11-11777 and CHE15-65755). Calculations were carried out using the resources of the Center for Computational Studies of Open-Shell and Electronically Excited Species (iopenshell.usc.edu), supported by the National Science Foundation through the CRIF:CRF program. The authors thank Professors Ben Bythell, Vicki Wysocki, and JC Poutsma for their valuable insights about b_2 ions and other discussions. The authors thank Scott McLuckey for his inspirational work and leadership, and are delighted that they actually have a bio-ion paper that they can contribute to this issue in his honor.

References

1. Banerjee, S., Mazumdar, S.: Electrospray ionization mass spectrometry: a technique to access the information beyond the molecular weight of the analyte. *Int. J. Anal. Chem.* **40**, 282574 (2012)
2. Ahmed, F.E.: Utility of mass spectrometry for proteome analysis: Part I. Conceptual and experimental approaches. *Expert Rev. Proteom.* **5**, 841–864 (2008)
3. Brodbelt, J.S.: Ion activation methods for peptides and proteins. *Anal. Chem.* (Washington, DC), **88**, 30–51 (2016)
4. Hirayama, K.: Structural studies of proteins by mass spectrometry. *J. Mass Spectrom. Soc. Jpn.* **60**, 51–64 (2012)
5. Hunt, D.F., Shabanowitz, J., Bai, D.L.: Peptide sequence analysis by electron transfer dissociation mass spectrometry: a web-based tutorial. *J. Am. Soc. Mass Spectrom.* **26**, 1256–1258 (2015)
6. Artemenko, K.A., Samgina, T.Y., Lebedev, A.T.: Mass-spectrometric de novo sequencing of peptides. *Mass-Spectrom.* **3**, 225–254 (2006)

7. Medzihradszky, K.F., Chalkley, R.J.: Lessons in de novo peptide sequencing by tandem mass spectrometry. *Mass Spectrom. Rev.* **34**, 43–63 (2015)
8. Seidler, J., Zinn, N., Boehm, M.E., Lehmann, W.D.: De novo sequencing of peptides by MS/MS. *Proteomics* **10**, 634–649 (2010)
9. Wysocki, V.H., Tsaprailis, G., Smith, L.L., Brei, L.A.: Mobile and localized protons: a framework for understanding peptide dissociation. *J. Mass Spectrom.* **35**, 1399–1406 (2000)
10. Boyd, R., Somogyi, A.: The mobile proton hypothesis in fragmentation of protonated peptides: a perspective. *J. Am. Soc. Mass Spectrom.* **21**, 1275–1278 (2010)
11. Dongre, A.R., Jones, J.L., Somogyi, A., Wysocki, V.H.: Influence of peptide composition, gas-phase basicity, and chemical modification on fragmentation efficiency: evidence for the mobile proton model. *J. Am. Chem. Soc.* **118**, 8365–8374 (1996)
12. Wysocki, V.H., Cheng, G., Zhang, Q., Hermann, K.A., Beardsley, R.L., Hilderbrand, A.E. Peptide fragmentation overview. *Prin. Mass Spectrom. Appl. Biomolecules* 279–300 (2006)
13. Paizs, B., Suhai, S.: Fragmentation pathways of protonated peptides. *Mass Spectrom. Rev.* **24**, 508–548 (2005)
14. Schlosser, A., Lehmann, W.D.: Five-membered ring formation in unimolecular reactions of peptides: a key structural element controlling low-energy collision-induced dissociation of peptides. *J. Mass Spectrom.* **35**, 1382–1390 (2000)
15. O'Hair, R.A.J.: The role of nucleophile-electrophile interactions in the unimolecular and bimolecular gas-phase ion chemistry of peptides and related systems. *J. Mass Spectrom.* **35**, 1377–1381 (2000)
16. Yalcin, T., Khouw, C., Csizmadia, I.G., Peterson, M.R., Harrison, A.G.: Why are b ions stable species in peptide spectra? *J. Am. Soc. Mass Spectrom.* **6**, 1165–1174 (1995)
17. Ambihapathy, K., Yalcin, T., Leung, H.-W., Harrison, A.G.: Pathways to immonium ions in the fragmentation of protonated peptides. *J. Mass Spectrom.* **32**, 209–215 (1997)
18. Bowie, J.H., Brinkworth, C.S., Dua, S.: Collision-induced fragmentations of the (M-H)-parent anions of underivatized peptides: an aid to structure determination and some unusual negative ion cleavages. *Mass Spectrom. Rev.* **21**, 87–107 (2002)
19. Bythell, B.J., Knapp-Mohammady, M., Paizs, B., Harrison, A.G.: Effect of the His residue on the cyclization of b ions. *J. Am. Soc. Mass Spectrom.* **21**, 1352–1363 (2010)
20. Chen, X., Tirado, M., Steill, J.D., Oomens, J., Polfer, N.C.: Cyclic peptide as reference system for b ion structural analysis in the gas phase. *J. Mass Spectrom.* **46**, 1011–1015 (2011)
21. Harrison, A.G.: To b or not to b: the ongoing saga of peptide b ions. *Mass Spectrom. Rev.* **28**, 640–654 (2009)
22. Rodríguez, C.F., Shoeib, T., Chu, I.K., Siu, K.W.M., Hopkinson, A.C.: Comparison between protonation, lithiation, and argination of 5-oxazolones: a study of a key intermediate in gas-phase peptide sequencing. *J. Phys. Chem. A* **104**, 5335–5342 (2000)
23. Bythell, B.J., Dain, R.P., Curtice, S.S., Oomens, J., Steill, J.D., Groenewold, G.S., Paizs, B., Van Stipdonk, M.J.: Structure of [M+H-H₂O]⁺ from protonated tetraglycine revealed by tandem mass spectrometry and IRMPD spectroscopy. *J. Phys. Chem. A* **114**, 5076–5082 (2010)
24. Chen, X., Yu, L., Steill, J.D., Oomens, J., Polfer, N.C.: Effect of peptide fragment size on the propensity of cyclization in collision-induced dissociation: oligoglycine b₂–b₈. *J. Am. Chem. Soc.* **131**, 18272–18282 (2009)
25. Chu, I.K., Shoeib, T., Guo, X., Rodríguez, C.F., Hopkinson, A.C., Siu, K.W.M., Lau, T.C.: Characterization of the product ions from the collision-induced dissociation of arginated peptides. *J. Am. Soc. Mass Spectrom.* **12**, 163–175 (2001)
26. Grewal, R.N., El Aribi, H., Harrison, A.G., Siu, K.W.M., Hopkinson, A.C.: Fragmentation of protonated tripeptides: the proline effect revisited. *J. Phys. Chem. B* **108**, 4899–4908 (2004)
27. Farrugia, J.M., O'Hair, R.A.J.: Involvement of salt bridges in a novel gas phase rearrangement of protonated arginine-containing dipeptides which precedes fragmentation. *Int. J. Mass Spectrom.* **222**, 229–242 (2003)
28. Farrugia, J.M., O'Hair, R.A.J., Reid, G.E.: Do all b₂ ions have oxazolone structures? Multistage mass spectrometry and ab initio studies on protonated N-acyl amino acid methyl ester model systems? *Int. J. Mass Spectrom.* **210/211**, 71–87 (2001)
29. Forbes, M.W., Jockusch, R.A., Young, A.B., Harrison, A.G.: Fragmentation of protonated dipeptides containing arginine. effect of activation method. *J. Am. Soc. Mass Spectrom.* **18**, 1959–1966 (2007)
30. Harrison, A.G.: Cyclization of peptide b₉ ions. *J. Am. Soc. Mass Spectrom.* **20**, 2248–2253 (2009)
31. Knapp-Mohammady, M., Young, A.B., Paizs, B., Harrison, A.G.: Fragmentation of doubly-protonated Pro-His-Xaa tripeptides: formation of b₂₂₊ ions. *J. Am. Soc. Mass Spectrom.* **20**, 2135–2143 (2009)
32. Nold, M.J., Wesdemiotis, C., Yalcin, T., Harrison, A.G.: Amide bond dissociation in protonated peptides. Structures of the N-terminal ionic and neutral fragments. *Int. J. Mass Spectrom. Ion Process.* **164**, 137–153 (1997)
33. Wysocki, V.H., Resing, K.A., Zhang, Q., Cheng, G.: Mass spectrometry of peptides and proteins. *Methods (San Diego, CA)* **35**, 211–222 (2005)
34. Yoon, S.H., Chamot-Rooke, J., Perkins, B.R., Hilderbrand, A.E., Poutsma, J.C., Wysocki, V.H.: IRMPD spectroscopy shows that AGG forms an oxazolone b₂₊ ion. *J. Am. Chem. Soc.* **130**, 17644–17645 (2008)
35. Zou, S., Oomens, J., Polfer, N.C.: Competition between diketopiperazine and oxazolone formation in water loss products from protonated ArgGly and GlyArg. *Int. J. Mass Spectrom.* **316/318**, 12–17 (2012)
36. Lee, V.W.M., Li, H., Lau, T.-C., Siu, K.W.M.: Structures of b and a product ions from the fragmentation of arginated peptides. *J. Am. Chem. Soc.* **120**, 7302–7309 (1998)
37. Bythell, B.J., Somogyi, A., Paizs, B.: What is the structure of b₂ ions generated from doubly protonated tryptic peptides? *J. Am. Soc. Mass Spectrom.* **20**, 618–624 (2009)
38. Eckart, K., Holthausen, M.C., Koch, W., Spiess, J.: Mass spectrometric and quantum mechanical analysis of gas-phase formation, structure, and decomposition of various b₂ ions and their specifically deuterated analogs. *J. Am. Soc. Mass Spectrom.* **9**, 1002–1011 (1998)
39. Paizs, B., Lendvay, G., Vvkey, K., Suhai, S.: Formation of b₂₊ ions from protonated peptides: an ab initio study. *Rapid Commun. Mass Spectrom.* **13**, 525–533 (1999)
40. Paizs, B., Suhai, S.: Towards understanding the tandem mass spectra of protonated oligopeptides. I: Mechanism of amide bond cleavage. *J. Am. Soc. Mass Spectrom.* **15**, 103–113 (2004)
41. Paizs, B., Suhai, S., Harrison, A.G.: Experimental and theoretical investigation of the main fragmentation pathways of protonated H-Gly-Gly-Sar-OH and H-Gly-Sar-Sar-OH. *J. Am. Soc. Mass Spectrom.* **14**, 1454–1469 (2003)
42. Polce, M.J., Ren, D., Wesdemiotis, C.: Dissociation of the peptide bond in protonated peptides. *J. Mass Spectrom.* **35**, 1391–1398 (2000)
43. Sinha, R.K., Ereleam, U., Bythell, B.J., Paizs, B., Maitre, P.: Diagnosing the protonation site of b₂ peptide fragment ions using IRMPD in the X-H (X = O, N, and C) stretching region. *J. Am. Soc. Mass Spectrom.* **22**, 1645–1650 (2011)
44. Wang, D., Gulyuz, K., Stedwell, C.N., Polfer, N.C.: Diagnostic NH and OH vibrations for oxazolone and diketopiperazine structures: b₂ from protonated triglycine. *J. Am. Soc. Mass Spectrom.* **22**, 1197–1203 (2011)
45. Armentrout, P.B., Clark, A.A.: The simplest b₂₊ ion: Determining its structure from its energetics by a direct comparison of the threshold collision-induced dissociation of protonated oxazolone and diketopiperazine. *Int. J. Mass Spectrom.* **316/318**, 182–191 (2012)
46. Bythell, B.J., Suhai, S., Somogyi, A., Paizs, B.: Proton-driven amide bond-cleavage pathways of gas-phase peptide ions lacking mobile protons. *J. Am. Chem. Soc.* **131**, 14057–14065 (2009)
47. Farrugia, J.M., Taverner, T., O'Hair, R.A.J.: Side-chain involvement in the fragmentation reactions of the protonated methyl esters of histidine and its peptides. *Int. J. Mass Spectrom.* **209**, 99–112 (2001)
48. Morrison, L.J., Chamot-Rooke, J., Wysocki, V.H.: IR action spectroscopy shows competitive oxazolone and diketopiperazine formation in peptides depends on peptide length and identity of terminal residue in the departing fragment. *Analyst (Cambridge, UK)* **139**, 2137–2143 (2014)
49. Perkins, B.R., Chamot-Rooke, J., Yoon, S.H., Gucinski, A.C., Somogyi, A., Wysocki, V.H.: Evidence of diketopiperazine and oxazolone structures for HA b₂₊ ion. *J. Am. Chem. Soc.* **131**, 17528–17529 (2009)
50. Gucinski, A.C., Chamot-Rooke, J., Nicol, E., Somogyi, A., Wysocki, V.H.: Structural influences on preferential oxazolone versus diketopiperazine b₂₊ ion formation for histidine analog-containing peptides. *J. Phys. Chem. A* **116**, 4296–4304 (2012)
51. Paizs, B., Suhai, S.: Combined quantum chemical and RRKM modeling of the main fragmentation pathways of protonated GGG. I. *Cis-trans*

- isomerization around protonated amide bonds. *Rapid Commun. Mass Spectrom.* **15**, 2307–2323 (2001)
52. Dunbar, R.C., Polfer, N.C., Berden, G., Oomens, J.: Metal ion binding to peptides: oxygen or nitrogen sites? *Int. J. Mass Spectrom.* **330/332**, 71–77 (2012)
53. Koirala, D., Kodithuwakkuge, S.R., Wenthold, P.G.: Mass spectrometric study of the decomposition pathways of canonical amino acids and α -lactones in the gas phase. *J. Phys. Org. Chem.* **28**, 635–644 (2015)
54. Wenthold, P.G., Koirala, D., Somogyi, A., Poutsma, J.C.: Infrared spectroscopic confirmation of α -lactone formation in the dissociation of a gaseous amino acid. *J. Phys. Org. Chem.* **30**, e3606 (2017)
55. Dunbar, R.C., Steill, J.D., Polfer, N.C., Oomens, J.: Gas-phase infrared spectroscopy of the protonated dipeptides H + PheAla and H + AlaPhe compared to condensed-phase results. *Int. J. Mass Spectrom.* **283**, 77–84 (2009)
56. Tsapralis, G., Nair, H., Zhong, W., Kuppanan, K., Futrell, J.H., Wysocki, V.H.: A mechanistic investigation of the enhanced cleavage at histidine in the gas-phase dissociation of protonated peptides. *Anal. Chem.* **76**, 2083–2094 (2004)
57. Tsapralis, G., Somogyi, A., Nikolaev, E.N., Wysocki, V.H.: Refining the model for selective cleavage at acidic residues in arginine-containing protonated peptides. *Int. J. Mass Spectrom.* **195/196**, 467–479 (2000)
58. Nitecki, D.E., Halpem, B., Westley, J.W.: Simple route to sterically pure dioxopiperazines. *J. Org. Chem.* **33**, 864–866 (1968)
59. Uraguchi, D., Asai, Y., Ooi, T.: Site-directed asymmetric quaternization of a peptide backbone at a C-terminal azlactone. *Angew. Chem. Int. Ed.* **48**, 733–737 (2009)
60. MacroModel, ver. 9.6, Schrödinger, LLC: New York, NY (2009)
61. Kong, J., White, C.A., Krylov, A.I., Sherrill, D., Adamson, R.D., Furlani, T.R., Lee, M.S., Lee, A.M., Gwaltney, S.R., Adams, T.R., Ochsenfeld, C., Gilbert, A.T.B., Kedziora, G.S., Rassolov, V.A., Maurice, D.R., Nair, N., Shao, Y., Besley, N.A., Maslen, P.E., Dombroski, J.P., Daschel, H., Zhang, W., Korambath, P.P., Baker, J., Byrd, E.F.C., Voorhis, T.V., Oumi, M., Hirata, S., Hsu, C.-P., Ishikawa, N., Florian, J., Warshel, A., Johnson, B.G., Gill, P.M.W., Head-Gordon, M., Pople, J.A.: Q-Chem 2.0: a high-performance ab initio electronic structure program package. *J. Comput. Chem.* **21**, 1532 (2000)
62. Hauptert, L.J., Poutsma, J.C., Wenthold, P.G.: The Curtin-Hammett principle in mass spectrometry. *Acc. Chem. Res.* **42**, 1480–1488 (2009)
63. Morrison, L., Somogyi, A., Wysocki, V.H.: The influence glutamic acid in protonated $b_3 \rightarrow b_2$ formation from VGEIG and related analogs. *Int. J. Mass Spectrom.* **325/327**, 139–149 (2012)
64. Cooper, T., Talaty, E., Grove, J., Van Stipdonk, M., Suhai, S., Paizs, B.: Isotope labeling and theoretical study of the formation of a_3^* ions from protonated tetraglycine. *J. Am. Soc. Mass Spectrom.* **17**, 1654–1664 (2006)
65. Gucinski, A.C., Chamot-Rooke, J., Steinmetz, V., Somogyi, A., Wysocki, V.H.: Influence of N-terminal residue composition on the structure of proline-containing b_2^+ ions. *J. Phys. Chem. A* **117**, 1291–1298 (2013)



Mass spectrometric detection of the Gibbs reaction for phenol analysis

Sabyasachy Mistry | Paul G. Wenthold

The Department of Chemistry and Biochemistry, Purdue University, 560 Oval Drive, West Lafayette, IN 47907, USA

Correspondence

Paul G. Wenthold, Department of Chemistry, Purdue University, 560 Oval Drive, West Lafayette, IN 47907, USA.
Email: pgw@purdue.edu

Funding information

National Science Foundation, Grant/Award Number: CHE15-65755

Abstract

This paper describes a new method for detecting phenols, by reaction with Gibbs reagent to form indophenols, followed by mass spectrometric detection. Unlike the standard Gibbs reaction, which uses a colorometric approach, the use of mass spectrometry allows for simultaneous detection of differently substituted phenols. The procedure is demonstrated to work for a large variety of phenols without *para*-substitution. With *para*-substituted phenols, Gibbs products are still often observed, but the specific product depends on the substituent. For *para* groups with high electronegativity, such as methoxy or halogens, the reaction proceeds by displacement of the substituent. For groups with lower electronegativity, such as amino or alkyl groups, Gibbs products are observed that retain the substituent, indicating that the reaction occurs at the *ortho* or *meta* position. In mixtures of phenols, the relative intensities of the Gibbs products are proportional to the relative concentrations, and concentrations as low as 1 $\mu\text{mol/L}$ can be detected. The method is applied to the qualitative analysis of commercial liquid smoke, and it is found that hickory and mesquite flavors have significantly different phenolic composition.

KEYWORDS

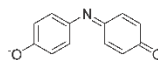
ESI-MS, Gibbs reaction, indophenols, liquid smoke, phenols

1 | INTRODUCTION

Phenols are ubiquitous in our world and are found in all types of natural and non-natural systems. Examples of phenolic compounds that occur naturally include biological molecules, such as tyrosine and L-dopa, food components, such as capsaicin or red wine tannins, and even drugs, such as morphine and tetrahydrocannabinol. Alternatively, phenols are present due to anthropogenic sources. In particular, industrial waste can have phenol concentrations as high as 10 g/L.¹ Many methods have been used to detect phenols,² mostly relying on some sort of chromatography (LC or GC) prior to detection. Mass spectrometric detection has an advantage in that it can be used to carry out simultaneous detection of multiple phenol derivatives without requiring prior separation. However, although it is possible to detect phenols directly by using mass spectrometry, it is not specific to phenol detection. Consequently, a common approach used for the specific detection of phenols involves the use of reagents to selectively derivatize the phenols prior to

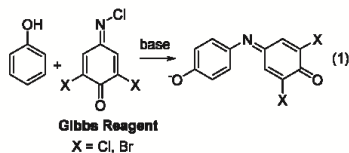
detection to make them more amenable for analysis by chromatography,³⁻¹⁰ or for direct detection by mass spectrometry.^{11,12}

In this work, we describe an approach for the analysis of phenols by using mass spectrometric detection of indophenol derivatives. The conversion of phenols to indophenols can be traced back almost 200 years, to the detection of orcinol.^{13,14} For example, Liebermann¹⁵⁻¹⁷ showed that phenols, including phenol, orcinol and thymol, can be transformed into dark-blue-colored indophenol dyes by reaction with sulfuric acid and ammonia.



Indophenol

In 1927, Gibbs reported a convenient reagent for the detection of phenols^{18,19} by converting them to indophenols. The Gibbs reaction (Equation 1), utilizing the Gibbs reagent, 2,6-dichloro- or dibromo-4-(chloroimino)cyclohexa-2,5-dien-1-one, has since been a standard approach for the detection of phenols.^{20,21}



One of the key features that make the Gibbs procedure a useful approach for the detection of phenols is the robust color of the indophenol product,²² which allows for easy spectrophotometric detection. In recent years, applications of the Gibbs procedure have been reported for the detection of phenol-based pharmaceuticals,^{23–34} capsaicin,^{35–37} and for monitoring the presence of phenol.³⁸ In all of these applications, the indophenol is detected spectrophotometrically.

One of the limitations of the Gibbs approach for detection of phenols is that the absorption peak is not very sensitive to substitution of the phenol. Consequently, while the standard Gibbs method is useful for determining total phenol content,^{37,39} it is generally not capable of distinguishing between individual substituted phenols. Therefore, a separation step is required for the detection of specific phenol derivatives. It is possible to detect the Gibbs indophenol product with other, non-colorimetric methods. For example, Lowe et al⁴⁰ have examined and detected the Gibbs reaction using electrochemistry and cyclic voltammetry and have shown that it can be used to detect THC. Similarly, Josephy and Lenkinski⁴¹ have characterized the Gibbs product formed from *tert*-butylhydroxyanisole by using electron ionization mass spectrometry, and electron-ionization spectra for some protonated indophenols (neutral phenols) are generally available.⁴²

Herein, we describe the detection of Gibbs products by using simple electrospray-ionization mass spectrometry (ESI-MS). Considering that indophenols are naturally anionic, they are readily detected by ESI-MS. An important advantage of using mass spectrometry for the detection of indophenols is that it readily distinguishes between different types of substituted phenols. In this work, we report ESI mass spectra for indophenols obtained in the Gibbs reaction of simple substituted phenols and show its application for simultaneous detection of components in a mixture, including quantification. This approach using the Gibbs reagent to form indophenols provides an alternative to previously reported derivatization methods, such as acetylation¹¹ or conversion to the imidazolium ether.¹²

2 | EXPERIMENTAL

2.1 | Sample preparation—general procedures

Samples were prepared by mixing 5 mL of a solution of Gibbs reagent in methanol (60 mmol/L) with 10 mL of an aqueous potassium phosphate dibasic solution (deionized water, 40 mmol/L, pH 9.5)⁴³ containing substrate. After mixing, the solutions were stirred at room temperature for the allotted time, after which 50 μ L of the solution was diluted to 4 mL in water-methanol solution (1:1), for ESI-MS analysis. Solutions for individual samples contained 0.25 mmol of substrate in the phosphate buffer, similar to the concentration of Gibbs reagent. Spectra are measured 5 minutes after mixing, unless otherwise noted.

For the mixture of phenol and *o*-cresol, 10 mL of the initial solution containing *o*-cresol and phenol was mixed with 5-mL methanol solution of Gibbs reagent (100 mmol/L). The reaction mixture was stirred for 5 and 30 minutes before diluting with 1:1 methanol as described above, followed by mass spectrometric analysis. The concentration of *o*-cresol in the initial solution was chosen so to obtain a concentration of 3 μ mol/L in the final (electrosprayed) solution. Similarly, the concentration of phenol in the initial solution was chosen so to obtain concentrations of 1, 2, 5, 10, 25 and 50 μ mol/L in the final solution, with an excess of Gibbs reagent.

2.2 | Sample preparation—liquid smoke

K_2HPO_4 (1 mmol, 174 mg) was added directly to 5 mL of the corresponding commercial smoke sample directly and mixed with 10-mL methanol solution of Gibbs reagent (1 mmol, 210 mg). The reaction mixture was stirred at room temperature for 5 minutes. Two hundred microliter reaction mixture was dissolved in 4-mL water-methanol (1:1) solution for MS analysis.

2.3 | Spectra collection

Electrospray ionization mass spectra were obtained on a commercial LCQ-DECA (Thermo Electron Corporation, San Jose, CA, USA) quadrupole ion trap mass spectrometer, equipped with ESI source, operating in negative ion mode. Substrate solutions in a methanol: water mixture (1:1) and introduced into the source directly at a flow rate of 10 μ L/min. Electrospray and ion focusing conditions were varied to maximize the signal of the ion of interest.

2.4 | Spectral analysis

One important advantage of using the Gibbs reagent for derivatization is that the chlorine atoms make products containing the Gibbs reagent readily detectable by the isotopic pattern. Therefore, the spectra are deconvoluted using the isotope pattern for ions containing two chlorine atoms (1:0.648:0.105) to eliminate the peaks that cannot contain the Gibbs reagent. In the deconvolution, the maximum intensity of the peak at mass M is set to be the minimum of the intensity at mass M , $I(M + 2)/0.648$, or $I(M + 4)/0.105$. Although this deconvolution approach does not identify peaks that must contain two chlorine atoms, as coincidental peak ratios are possible, it can be used to explicitly rule out all the signals that cannot have two chlorine atoms. For example, if the signal at mass M is 100 000, but the signal at $M + 2$ is only 100, then the signal M that contains two chlorines (and therefore could be a Gibbs product) is only 952. Technically, the intensities of the peaks remaining after deconvolution are upper limits to the signal for two-chlorine containing products, as coincidental peak ratios can result in false positives. The difference between the peak height and the Gibbs-product signal is largest when there is extensive overlap of product signals. However, the ability to specifically eliminate non-Gibbs products where possible makes the Gibbs approach preferable to simple ESI-MS of the mixture. The deconvolution is carried out using Excel.

2.5 | Materials

All the phenols used in this work were obtained from commercial sources and used as received. The methanol was "Reagent Grade" and used without further purification.

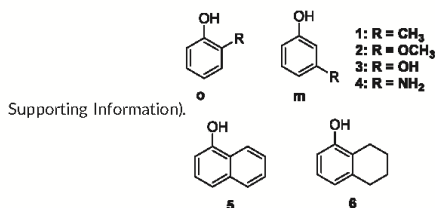
3 | RESULTS

3.1 | Phenol

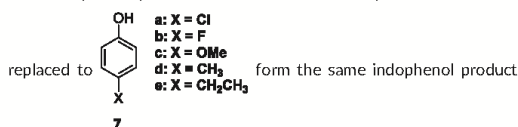
Figure 1 shows the ESI-MS obtained for samples of Gibbs reagent (Figure 1A) and phenol (Figure 1B). In the absence of phenol, the MS of the Gibbs reagent is non-descript and shows a large number of unidentifiable ionic products. It is possible to detect phenoxide (m/z 93) directly under these conditions (Figure 1B). However, in the presence of other acidic substrates, the phenoxide product would be expected to be a minor product. Figure 1C shows the spectrum obtained 5 minutes after mixing Gibbs reagent and phenol in the buffer solution. The spectrum is dominated by the Gibbs indophenol product, as indicated by the characteristic isotopic pattern. Moreover, despite having phenol at the same concentration as in Figure 1B, the absolute intensity increases by a factor of approximately 100 for the detection of the Gibbs product, not taking into account the fact that signal is distributed over multiple isotope peaks. Therefore, the total signal of the phenol derivative in Figure 1C is nearly 200 times greater than that of phenol in Figure 1B (the peak below m/z 100 in Figure 1C is m/z 96, and not phenoxide, m/z 93). It has been shown previously that the detection sensitivity of phenols in mass spectrometry can be increased by derivatization, such as acetylation, before detection.¹¹ Finally, Figure 1D shows the spectrum obtained after deconvolution, to account for the isotope peaks. Although the initial spectrum was originally very clean, the deconvoluted spectrum is even moreso, with more than 85% of the signal attributable to indophenol.

3.2 | Substituted phenols

Gibbs products are also readily detected by ESI-MS for other substituted phenols, included *o*- and *m*-cresol (**1o** and **1m**), *o*- and *m*-hydroxyanisole (**2o** and **2m**), catechol (**3o**), resorcinol (**3m**), 2-aminophenol (**4**), 1-naphthol (**5**) and tetrahydro-1-naphthol (**6**) (see



While **1** to **6** all lack substitution in the *para*-position, it is also possible to detect Gibbs products for some *para*-substituted phenols,^{44,45} as well, including *p*-chloro-, fluoro-, and methoxyphenols (**7a-c**, respectively). For these substrates, the *para*-substituent is



as obtained with phenol (Equation 1).⁴⁵ In addition, indophenol products are also observed with *p*-cresol (**7d**) and *p*-ethylphenol (**7e**), but in these cases, the indophenol products contain the substituent, indicating substitution at a non-*para* position. Moreover, even in those systems where substitution occurs at the *para* position, additional products are observed that complicate the analysis. The mechanism of the reaction, including the reaction with *para*-substituted systems, is outside of the scope of this work and will be described in a future report.

3.3 | Isomer distinction

A limitation of the mass spectra of the indophenol products of the Gibbs reaction is that it cannot distinguish between isomeric phenols,

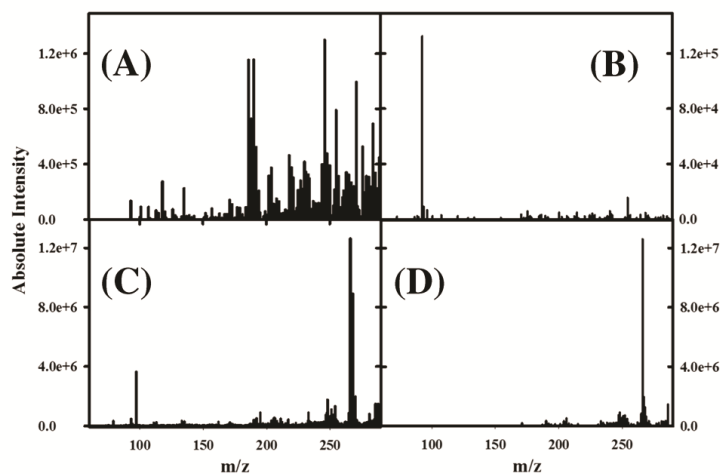


FIGURE 1 ESI mass spectra of products of phenol reaction with the Gibbs reagent. A, Gibbs reagent alone in buffer; B, phenol alone in buffer; C, phenol and Gibbs reagent mixture in buffer, 5 minutes after mixing; D, mixture mass spectrum deconvoluted for the 2-chlorine isotope pattern

which have the same mass-to-charge ratio. However, for most of the ions examined, the isomers can be distinguished on the basis of their CID spectrum. For example, Figure 2 shows the CID spectra of the indophenols formed from *ortho*- (2a) and *meta*-cresol (2b). Significant differences are observed between the spectra, with methyl loss being a major dissociation pathway for the *ortho*-isomer, but not observed for *meta*, whereas *m/z* 252, 208, and 180 are exclusively observed for the *meta*-isomer. Although not all isomeric pairs show such dramatic differences (see Supporting Information), this shows that CID of the indophenols can be used to distinguish between isomeric phenols.

3.4 | Mixture analysis and signal time dependence

One of the advantages of using mass spectrometry to detect the indophenol products of the Gibbs reaction is that it can be used for simultaneous detection of multiple phenol derivatives without separation. This is illustrated by the spectrum of 1:1 mixture of phenol and *o*-cresol (**1o**), each at 0.25 mmol/L concentration, shown in Figure 3. The presence of peaks at *m/z* 266 and *m/z* 280 in the deconvoluted mass spectrum indicates the presence of phenol and **1o**, respectively.

Although the phenol and **1o** have equal concentrations, at 5 minutes, the signal for the cresol is nearly 25 times larger than that for phenol. However, after 30 minutes, the absolute signal for phenol increases by nearly a factor of 5, whereas that for *o*-cresol increases by less than 5%, which shows that under these buffer conditions, the reaction with *o*-cresol occurs much faster than that with phenol. The dependence of the rate of the Gibbs reaction on solvent/pH/substrate has been a subject of investigation since the original work of Gibbs in 1927.²⁸

3.5 | Sensitivity

To use this method for the quantitative detection of phenol, we have used *o*-cresol as an internal standard. Calibration curves for the ratio I

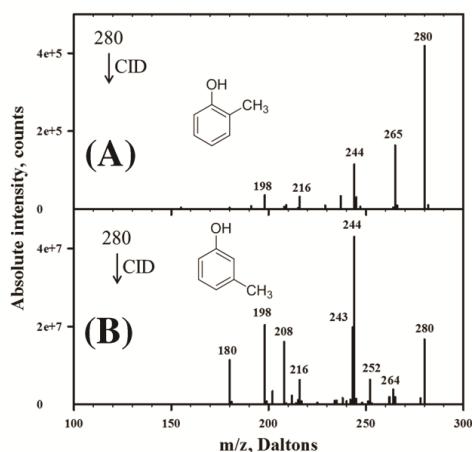


FIGURE 2 CID spectra of indophenols formed from (A) *ortho*-cresol and (B) *meta*-cresol, with a normalized energy of 25%

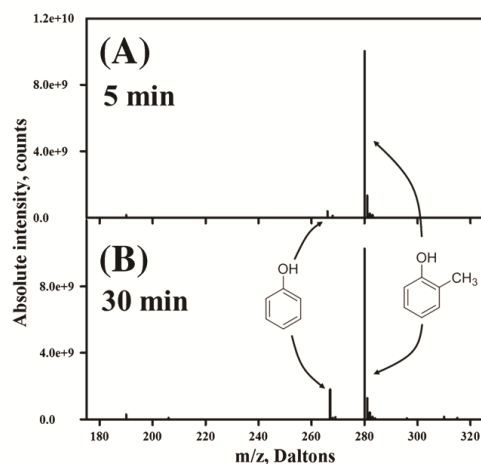


FIGURE 3 Deconvoluted ESI-mass spectrum of Gibbs products obtained from a 1:1 mixture of phenol and *o*-cresol, taken (A) 5 minutes and (B) 30 minutes after mixing. The spectrum in Figure 2A was taken 5 minutes after mixing the phenols with the Gibbs reagent

(*m/z* 266)/I (*m/z* 280) vs phenol concentration, for samples where the internal standard concentrations are 3.0 $\mu\text{mol/L}$, at 5 and 30 minutes post-mix are shown in Figure 4. Under the conditions used in this work, the reaction of the Gibbs reagent with *o*-cresol is faster than that with phenol, such that the relative amount of the Gibbs

product for phenol, *m/z* 266, compared to the Gibbs product for phenol, *m/z* 280, at longer reaction time (~ 0.2) is larger than that at short reaction time (~ 0.05). Nonetheless, the ratio of phenol Gibbs product to *o*-cresol Gibbs product is essentially linear ($r^2 = 0.99$) over the range of phenol concentration from 1 to 50 $\mu\text{mol/L}$. Colorimetric detection of the phenols by using the Gibbs reaction typically has detection limits of approximately 1 $\mu\text{mol/L}$,^{29,46} similar to what we find for phenol in this work. Alternatively, Aberici and co-workers have reported a detection limit near 0.1 $\mu\text{mol/L}$ or less for acetylated

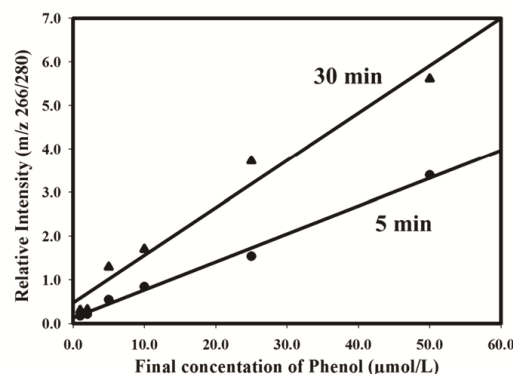
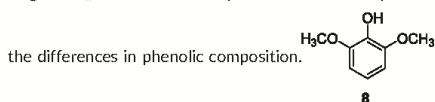


FIGURE 4 Relative intensities of phenol (*m/z* 266) and *o*-cresol (*m/z* 280) Gibbs products as a function of phenol concentration. The *o*-cresol is present at a concentration of 3 $\mu\text{mol/L}$

phenols when using trap-and-release membrane introduction mass spectrometry.¹¹

4 | APPLICATION: ANALYSIS OF "HICKORY" AND "MESQUITE" LIQUID SMOKE

The mass spectrometric detection of Gibbs products can be used to analyze any sample that contains significant amounts of phenols. An example of this type of product is "liquid smoke," a common additive used for flavoring⁴⁷ and preservation,⁴⁸ which consists of wood smoke condensates. Phenols make up approximately one third of commercially available liquid smoke,⁴⁹ with guaiacol (**2o**), pyrocatechol (**3o**), and syringol (**8**) among the most important components.⁴⁹⁻⁵³ As an illustration of how this method can be used to analyze mixtures, we have carried out an analysis of two commercially available liquid smoke products, sold by The Colgin Companies (Dallas, TX, www.colgin.com), a "Natural Hickory" and "Natural Mesquite" to determine



The deconvoluted mass spectra for the hickory and mesquite flavors of liquid smoke upon reaction with the Gibbs reagent, taken 5 minutes after mixing, are shown in Figure 5. Gibbs products formed from guaiacol (m/z 296), pyrocatechol (m/z 282), and syringinol (m/z

326) are readily observed in both products, although the relative amounts are very different for the two flavorings. Additional signals in the spectrum near masses 349, 351, and 420 are unidentified products that are commonly observed in spectra of phenol-containing samples with Gibbs reagents. Based on the peak ratios and apparent isotope pattern, they likely contain multiple Gibbs reagent structures.

For both samples, the Gibbs product for catechol (which could also contain resorcinol) is the most abundant. However, hickory flavor contains relatively higher amounts of the methoxy-substituted phenols, guaiacol, and syringinol.

In a detailed analysis of Code 10-Poly full-strength liquid smoke, Montazeri et al⁴⁷ found additional, less abundant products, including isomeric methoxymethylphenols and 3-methoxy-1,2-benzenediol. These appear to be present in the spectra in Figure 5, at m/z 310 and 312, respectively. However, in both spectra, there is a product at m/z 311 that is similar in abundance to those at m/z 310 and 312. The odd m/z value would require a nitrogen containing product and could, in principle, be attributed to an amino-methoxyphenol. However, as with the products at m/z 349, 351, and 420, the m/z 311 product is observed in other samples we have examined and therefore is likely a side-product formed from Gibbs reagent.

Assuming the reactions of hydroxy- and methoxyphenols with Gibbs reagents occur at approximately the same rates, then the relative intensities of the peaks in Figure 5 reflect the relative concentrations of the phenolic components. However, that assumption is not necessarily true, and proper relative and absolute quantification of the phenols in liquid smoke requires measurements with an internal

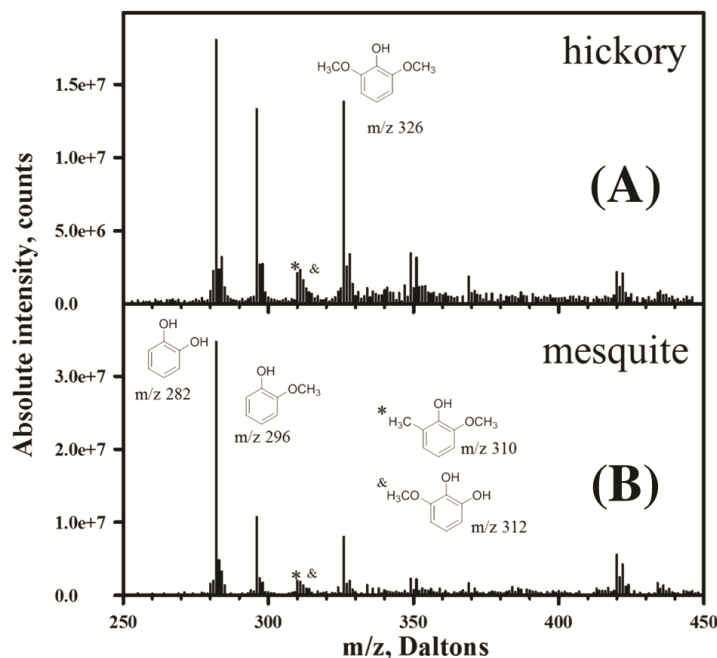


FIGURE 5 Deconvoluted mass spectrum of the Gibbs products obtained from analysis of (A) natural hickory and (B) natural mesquite flavors of Colgin brand liquid smoke

standard and calibration. Similarly, control experiments are required to determine the products of the Gibbs reagent with *para*-substituted phenols present in liquid smoke.⁴⁷

5 | CONCLUSIONS

While the Gibbs reagent has long been used as a phenolic assay, the use of mass spectrometry to detect the indophenol product allows for a more specific determination of phenol composition. The relative yields of Gibbs products additionally allow for quantification of phenol components, by measuring intensity against an internal standard. Mass spectrometric analysis also allows for investigation of the product structures, particularly for the reactions with *para*-substituted phenols, which can react either by direct substitution of the substituent, or at another site within the phenol, preserving the *para* substituent. Finally, the method is shown to work for the analysis of liquid smoke and is therefore amenable for the analysis of wood-smoke condensates.

ACKNOWLEDGEMENTS

This work was supported by the National Science Foundation (CHE15-65755).

ORCID

Paul G. Wenthold  <http://orcid.org/0000-0002-8257-3907>

REFERENCES

- Arutchelvan V, Kanakasabai V, Nagarajan S, Muralikrishnan V. Isolation and identification of novel high strength phenol degrading bacterial strains from phenol-formaldehyde resin manufacturing industrial wastewater. *J Hazard Mater*. 2005;127(1-3):238-243.
- Nollet LML, Leen SP, eds. *Handbook of Water Analysis*. 3rd ed. Boca Raton, Fla: CRC Press; 2014:613-646.
- Yu Y-J, Zhong S, Su G-Y, et al. Trace analysis of phenolic compounds in water by in situ acetylation coupled with purge and trap-GC/MS. *Anal Methods*. 2012;4(7):2156-2161.
- Helaleh MIH, Fujii S, Korenaga T. Column silylation method for determining endocrine disruptors from environmental water samples by solid phase micro-extraction. *Talanta*. 2001;54(6):1039-1047.
- Llompert M, Lourido M, Landin P, Garcia-Jares C, Cela R. Optimization of a derivatization-solid-phase microextraction method for the analysis of thirty phenolic pollutants in water samples. *J Chromatogr a*. 2002;963(1-2):137-148.
- Lourenco ELB, Ferreira A, Pinto E, Yonamine M, Farsky SHP. On-fiber derivatization of SPME extracts of phenol, hydroquinone and catechol with GC-MS detection. *Chromatographia*. 2006;63(3-4):175-179.
- Polo M, Llompert M, Garcia-Jares C, Gomez-Noya G, Bollaín M-H, Cela R. Development of a solid-phase microextraction method for the analysis of phenolic flame retardants in water samples. *J Chromatogr a*. 2006;1124(1-2):11-21.
- Regueiro J, Becerril E, Garcia-Jares C, Llompert M. Trace analysis of parabens, triclosan and related chlorophenols in water by headspace solid-phase microextraction with in situ derivatization and gas chromatography-tandem mass spectrometry. *J Chromatogr a*. 2009;1216(23):4693-4702.
- Schummer C, Groff C, Al Chami J, Jaber F, Millet M. Analysis of phenols and nitrophenols in rainwater collected simultaneously on an urban and rural site in east of France. *Sci Total Environ*. 2009;407(21):5637-5643.
- Yu Y-J, Liu H-L, Dai X-L, Cai H-X, Li C-Y, Yu H-X. Trace analysis of phenols and chlorophenols in water by in situ derivatization headspace solid-phase microextraction coupled with gas chromatography/mass spectrometry. *Fenxi Huaxue*. 2010;38:1243-1248.
- Sparrapan R, Eberlin MN, Alberici RM. Quantitation of trace phenolic compounds in water by trap-and-release membrane introduction mass spectrometry after acetylation. *Rapid Commun Mass Spectrom*. 2008;22(24):4105-4108.
- Zhu H, Janusson E, Luo J, et al. Phenol-selective mass spectrometric analysis of jet fuel. *Analyst*. 2017;142(17):3278-3284.
- Dumas J, Liebig J. On the orcinol. *Chem Zentralbl*. 1838;9:690-692.
- Robiquet. Neue Beobachtungen über das Orein. *Ann Pharm*. 1835;15(3):289-300.
- Liebermann C. Ueber die Einwirkung der salpetrigen Säure auf Phenole. *Berichte der Deutschen Chemischen Gesellschaft*. 1874;7(1):247-250.
- Liebermann C. Ueber die aus aromatischen Oxyverbindungen und salpetriger Säure entstehenden Farbstoffe. *Berichte der Deutschen Chemischen Gesellschaft*. 1874;7(2):1098-1102.
- Liebermann C. Ueber Orcein. *Berichte der Deutschen Chemischen Gesellschaft*. 1875;8(2):1649-1651.
- Gibbs HD. Phenol tests. IV. Velocity of indophenol formation-2,6-dibromobenzenoindophenol. *J Phys Chem*. 1927;31:1053-1081.
- Gibbs HD. Phenol tests. III The Indophenol Test. *J Biol Chem*. 1927;72:649-664.
- Ettinger MB, Ruchhoff CC. Determination of phenol and structurally related compounds by the Gibbs method. *Anal Chem*. 1948;20(12):1191-1196.
- Mohler EF, Jacob LN. Determination of phenolic-type compounds in water and industrial waste waters comparison of analytical methods. *Anal Chem*. 1957;29(9):1369-1374.
- Brooker LGS, Sprague RH. Color and constitution. IV. The absorption of phenol blue. *J Am Chem Soc*. 1941;63(11):3214-3215.
- Gurupadaya BM, Shankar MS, Manohara YN. Spectrophotometric methods for the estimation of butorphanol tartrate in bulk and pharmaceutical formulations. *Int J Chem Sci*. 2007;5:109-116.
- Ankita M, Gurupadaya BM, Chandra A. Colorimetric estimation of acenocoumarol in bulk and pharmaceutical formulations. *Asian J Chem*. 2008;20:5001-5004.
- Gowrisankar D, Sarsambi PS, Raju SA. Development and validation of new spectrophotometric methods for the estimation of cefprozil in pure form and in pharmaceutical formulations. *J Indian Counc Chem*. 2008;25:106-108.
- Bartzatt RL. Spectrophotometric and colorimetric methodology to detect and quantify hydrazide based chemotherapeutic drugs. *Environ Sci: Indian J*. 2010;5:86-91.
- Patel K, Patel C, Panigrahi B, Parikh A, Patel H. Development and validation of spectrophotometric methods for the estimation of mesalamine in tablet dosage forms. *J Young Pharm*. 2010;2(3):284-288.
- Tuljarani G, Sankar DG, Kadgpathi P, Suthakaran R, Satyanarayana B. Quantitative determination of bisoprolol fumarate in bulk and pharmaceutical dosage forms by spectrophotometry. *Int. J. Chem. Sci*. 2010;8:2253-2258.
- Chandan RS, Vasudevan M, Deecaraman; Gurupadaya, B M; Indupriya, M, Spectrophotometric determination of lamotrigine using Gibb's and MBTH reagent in pharmaceutical dosage form. *J Pharm Res*. 2011;4:1813-1815.
- Gousuddin M, Raju SA, Sultanuddin, Manjunath S. Development and validation of spectrophotometric methods for estimation of Fometrol bulk drug and its pharmaceutical dosage forms. *Int. J Pharm Pharm Sci*. 2011;3:306-309.
- Sowjanya K, Thejaswini JC, Gurupadaya BM, Indupriya M. Spectrophotometric determination of Pregabalin using Gibb's and MBTH

- reagent in pharmaceutical dosage form. *Pharma Chem.* 2011;3:112-122.
32. Somisetty VSR, Bichala PK, Rao CMMP, Kirankumar V. Development and validation of newer analytical methods for the estimation of deferasirox in bulk and in tablet dosage form by calorimetric method. *Int J Pharm Pharm Sci.* 2013;5:521-525.
33. Prabhu PP, Das P, Kaneri A, Reddy MJ. Simple spectrophotometric estimation of labetalol in bulk and marketed formulation. *Eur J Biomed Pharm Sci.* 2014;1:108-114.
34. Rajapandi R, Aswathy SR, Sreedharan B. Spectrophotometric method development and validation for estimation of enrofloxacin in pure and dosage forms. *World J Pharm Res.* 2016;5:1402-1410.
35. Jeong H-J, Hwang D, Ahn JT, et al. Development of a simple method for detecting capsaicinoids using Gibb's reagent in pepper. *Weon'ye Gwahag G'sulji.* 2012;30:294-300.
36. Thompson RQ, Chu C, Gent R, Gould AP, Rios L, Vertigan TM. Visualizing Capsaicinoids: calorimetric analysis of chilli peppers. *J Chem Educ.* 2012;89(5):610-612.
37. Ryu W-K, Kim H-W, Kim G-D, Rhee H-I. Rapid determination of capsaicinoids by calorimetric method. *J Food Drug Anal.* 2017;25(4):798-803.
38. Karimi M, Hassanshahian M. Isolation and characterization of phenol degrading yeasts from wastewater in the coking plant of Zarand, Kerman. *Braz J Microbiol.* 2016;47(1):18-24.
39. Montazeri N, Oliveira ACM, Himelbloom BH, Leigh MB, Crapo CA. Chemical characterization of commercial liquid smoke products. *Food Sci. Nutr. (Hoboken, NJ, U. S.).* 2013;1:102-115.
40. Lowe ER, Banks CE, Compton RG. Indirect detection of substituted phenols and cannabis based on the electrochemical adaptation of the Gibbs reaction. *Anal Bioanal Chem.* 2005;383(3):523-531.
41. Josephy PD, Lenkinski RE. Reaction of Gibbs reagent (2,6-dichlorobenzoquinone-4-chloroimine) with the antioxidant BHA (3-tert-butyl-4-hydroxyanisole): isolation and identification of the major product. *J Chromatogr.* 1984;294:375-379.
42. SDBSWeb: <http://sdbs.db.aist.go.jp> (National Institute of Advanced Industrial Science and Technology, accessed December 2017)
43. Kang D, Ricci F, White RJ, Plaxco KW. Survey of redox-active moieties for application in multiplexed electrochemical biosensors. *Anal Chem.* 2016;88(21):10452-10458.
44. Dacre JC. Nonspecificity of the Gibbs reaction. *Anal Chem.* 1971;43(4):589-591.
45. Josephy PD, Van Damme A. Reaction of Gibbs reagent with para-substituted phenols. *Anal Chem.* 1984;56(4):813-814.
46. Tulus R, Konyali H. Spectrophotometric determination of some drugs by their phenolic groups. *Istanbul Univ Eczacilik Fak Mecm.* 1980;16:56-72.
47. Rozum JJ, Flavor S. In: Tarté R, ed. *Ingredients in Meat Products: Properties, Functionality and Applications.* New York, NY: Springer New York; 2009:211-226.
48. Lingbeck JM, Cordero P, O'Bryan CA, Johnson MG, Ricke SC, Crandall PG. Functionality of liquid smoke as an all-natural antimicrobial in food preservation. *Meat Sci.* 2014;97(2):197-206.
49. Montazeri N, Oliveira AC, Himelbloom BH, Crapo CA, Leigh MB. Chemical characterization of commercial liquid smoke products. *Food Sci Nutr.* 2013;1(1):102-115.
50. Budaraga IK, Arnim, Marlida Y, Bulanin U. Analysis of liquid smoke chemical components with GC MS from different raw materials variation production and pyrolysis temperature level. *Int J ChemTech Res.* 2016;9:694-708.
51. Simon R, de la Calle B, Palme S, Meier D, Anklam E. Composition and analysis of liquid smoke flavouring primary products. *J Sep Sci.* 2005;28(9-10):871-882.
52. Wittkowski, R. Analysis of liquid smoke and smoked meat volatiles by headspace gas chromatography, in *Agriculture, Food Chemistry and the Consumer. Proceedings of the 5th European Conference on Food Chemistry (Vol. 2);* INRA: Paris, Fr, 1989; Vol. 2, p 639-643.
53. Wittkowski R, Baltes W, Jennings WG. Analysis of liquid smoke and smoked meat volatiles by headspace gas chromatography. *Food Chem.* 1990;37(2):135-144.

SUPPORTING INFORMATION

Additional supporting information may be found online in the Supporting Information section at the end of the article.

How to cite this article: Mistry S, Wenthold PG. Mass spectrometric detection of the Gibbs reaction for phenol analysis. *J Mass Spectrom.* 2018;53:947-953. <https://doi.org/10.1002/jms.4261>

APPENDIX. PATENT



US 20190228955A1

(19) **United States**
(12) **Patent Application Publication** (10) **Pub. No.: US 2019/0228955 A1**
Wenthold et al. (43) **Pub. Date: Jul. 25, 2019**

(54) **METHODS OF DETECTING CHEMICALS**

Publication Classification

(71) Applicant: **Purdue Research Foundation**, West Lafayette, IN (US)

(51) **Int. Cl.**
H01J 49/00 (2006.01)
H01J 49/16 (2006.01)
G01N 33/02 (2006.01)

(72) Inventors: **Paul G. Wenthold**, West Lafayette, IN (US); **Sabyaschy Mistry**, West Lafayette, IN (US)

(52) **U.S. Cl.**
CPC **H01J 49/0031** (2013.01); **G01N 33/02** (2013.01); **H01J 49/165** (2013.01)

(73) Assignee: **Purdue Research Foundation**, West Lafayette, IN (US)

(57) **ABSTRACT**

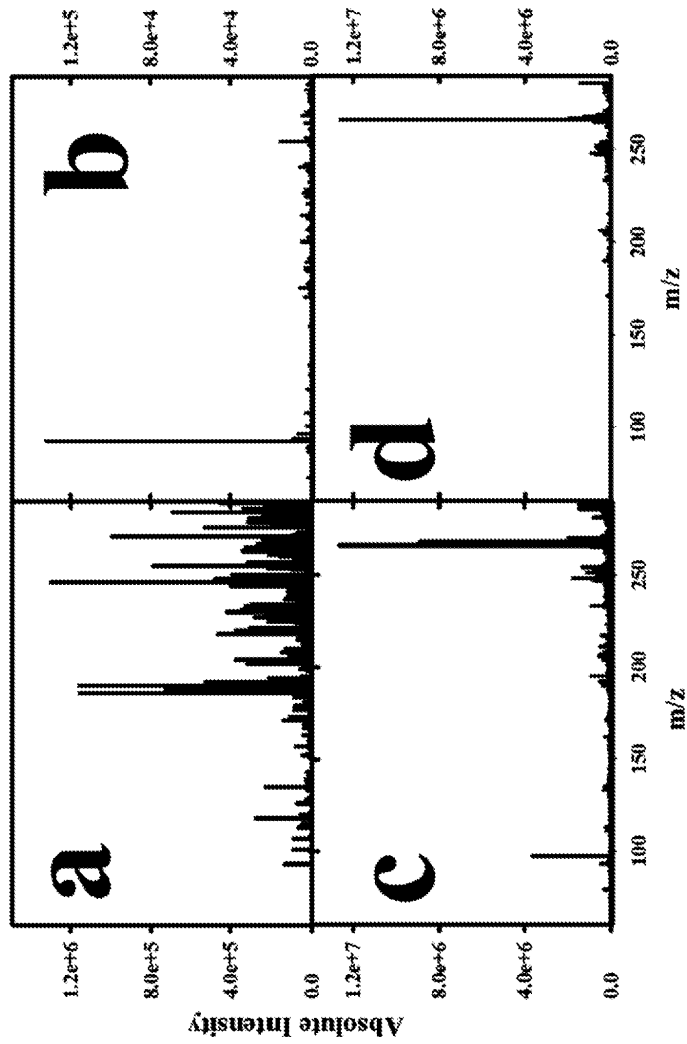
(21) Appl. No.: **16/252,676**

(22) Filed: **Jan. 20, 2019**

Related U.S. Application Data

(60) Provisional application No. 62/620,066, filed on Jan. 22, 2018.

A method of identifying phenolic compounds in a compound under test (CUT) is disclosed. The method includes mixing the CUT with a buffer solution to generate a buffered compound, mixing the buffered compound with a Gibbs reagent and allowing reaction for a predetermined amount of time to generate an indophenol; inputting the indophenol to a mass spectrometer, generating spectra of the indophenol, and analyzing the spectra to determine presence of phenolic compounds in the indophenols.



FIGs. 1a, 1b, 1c, and 1d

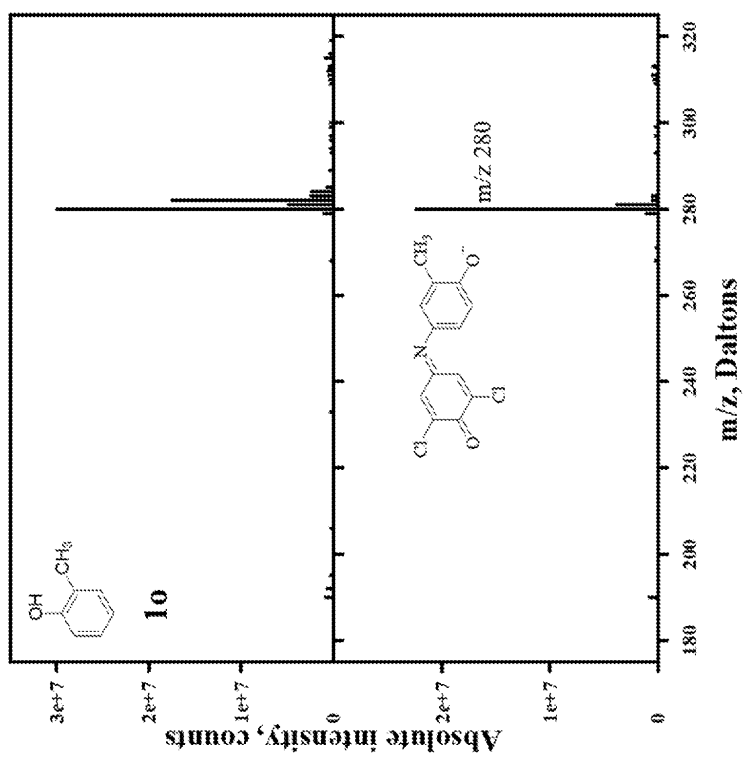


FIG. 2

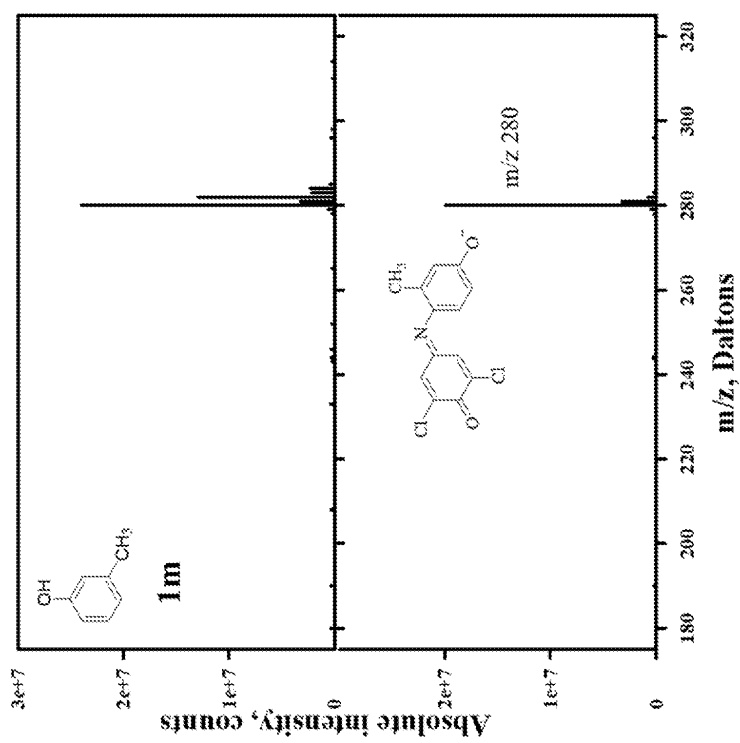


FIG. 3

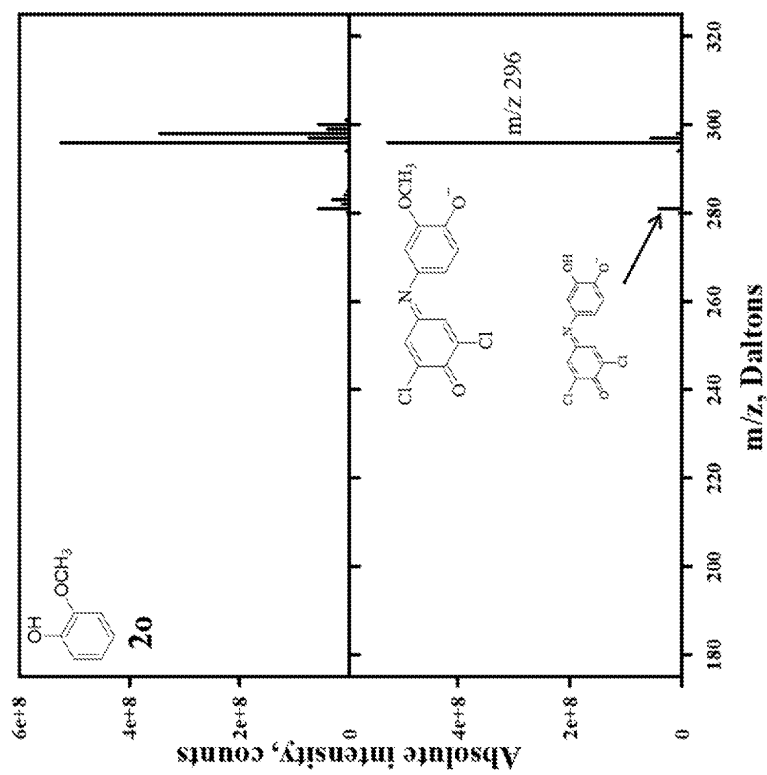


FIG. 4

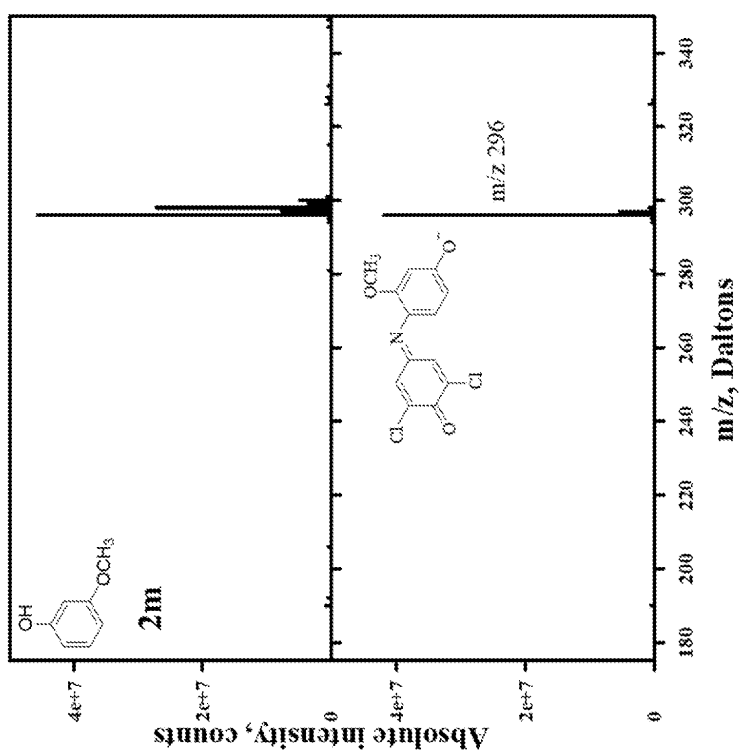
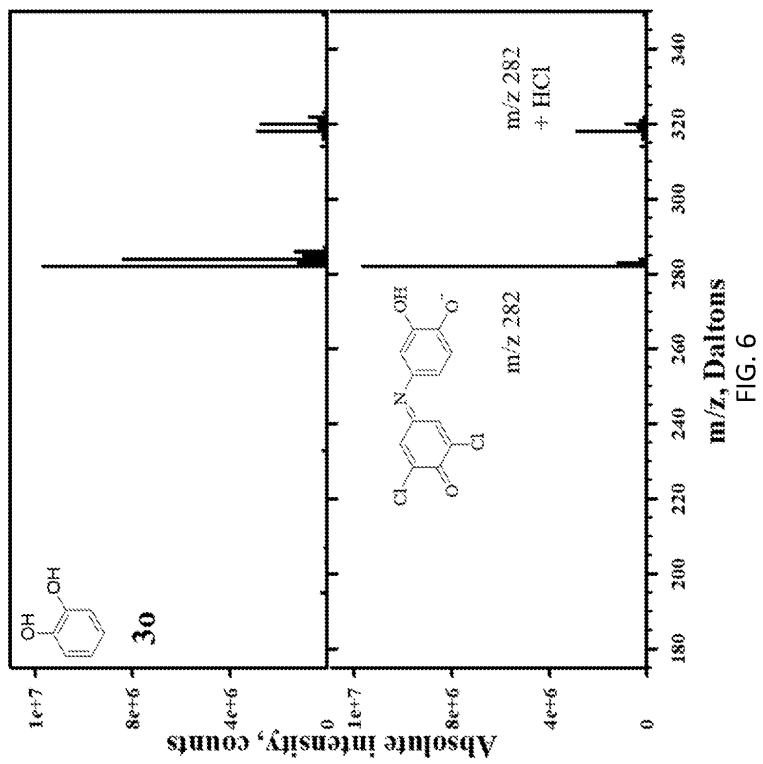
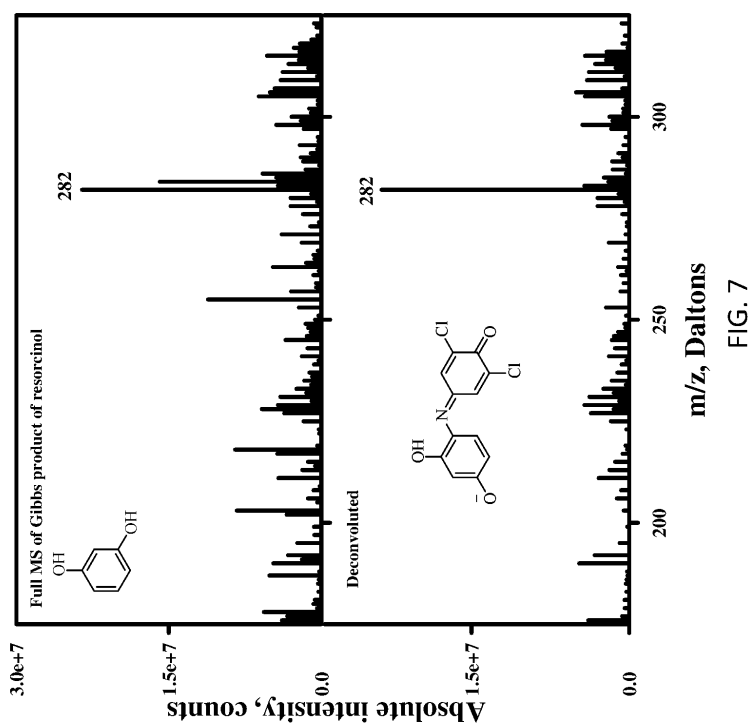


FIG. 5





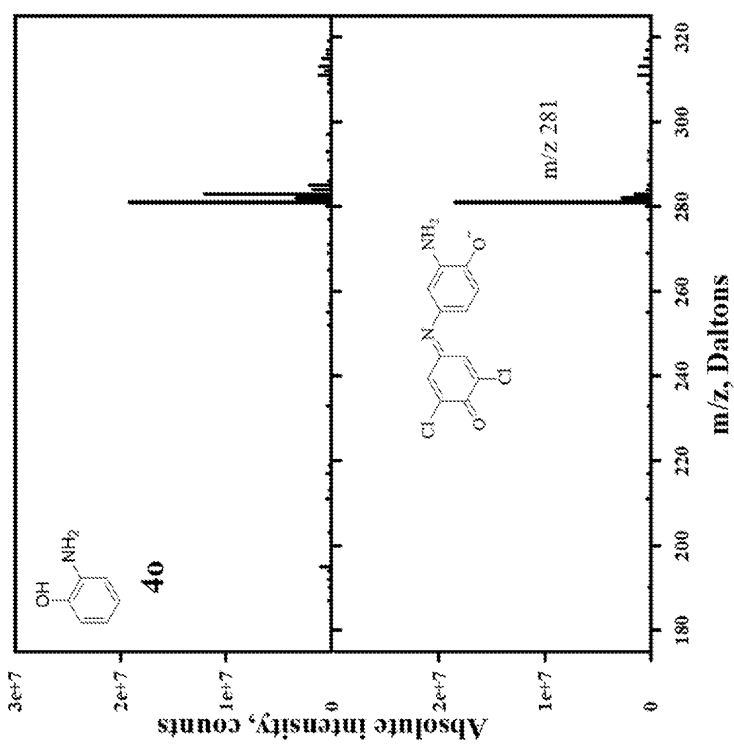


FIG. 8

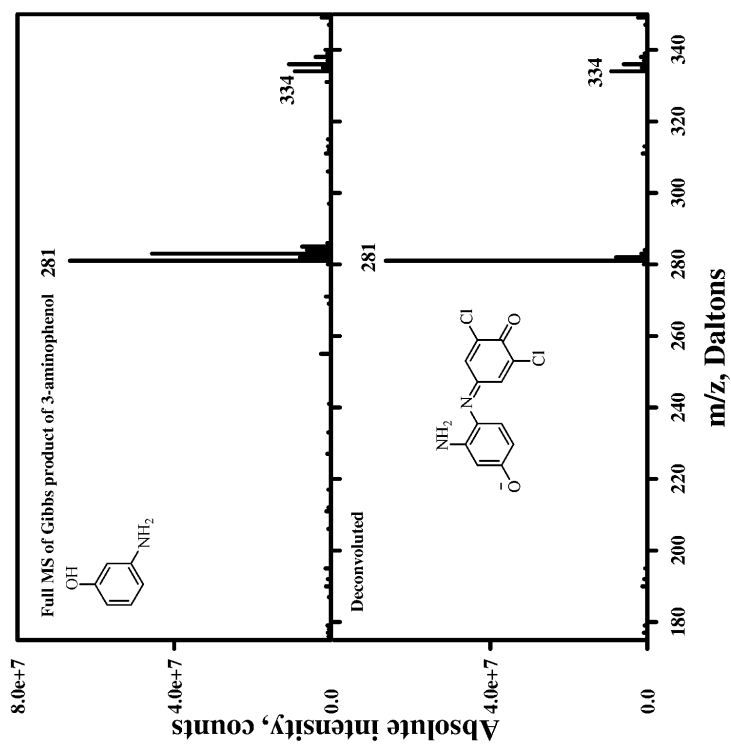


FIG. 9

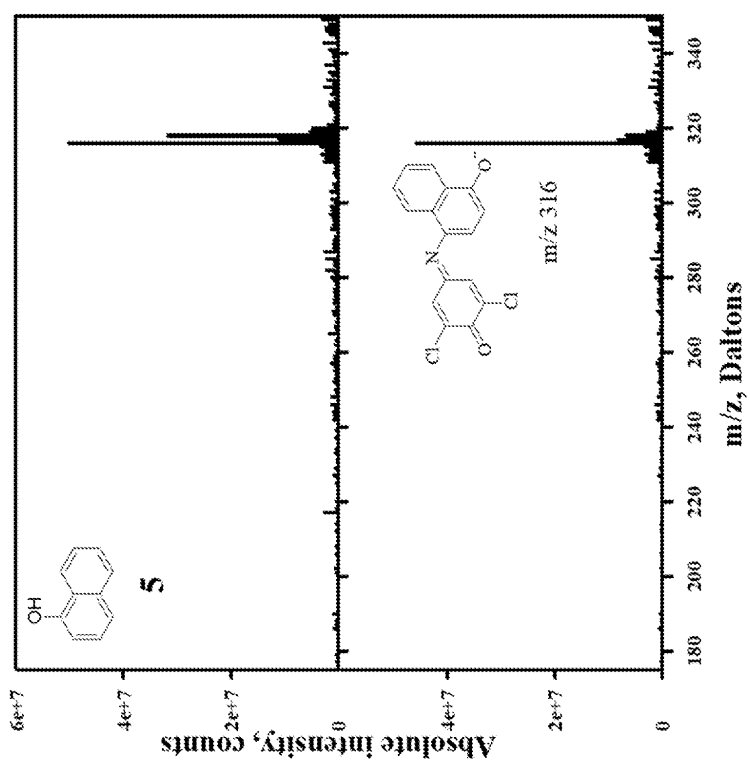
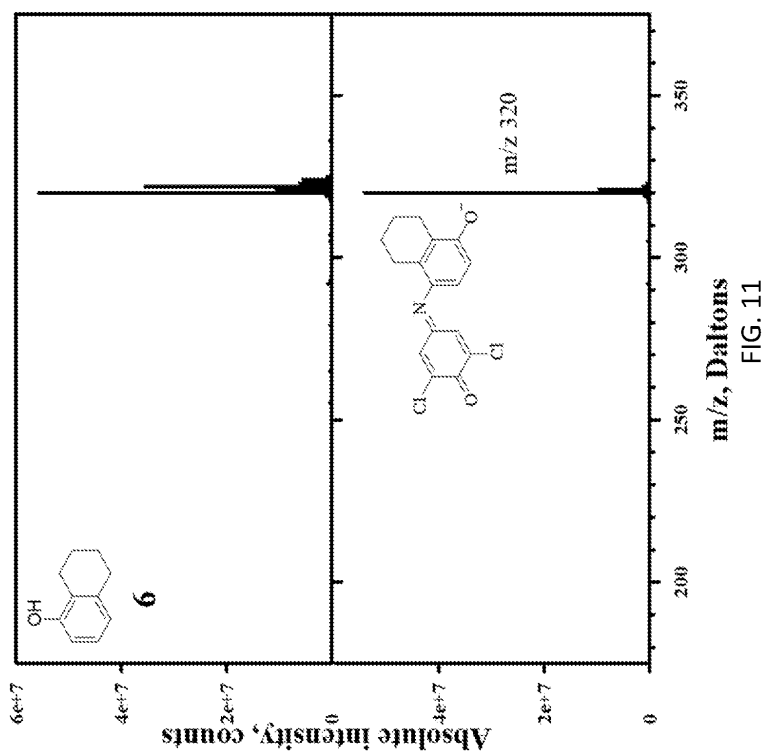
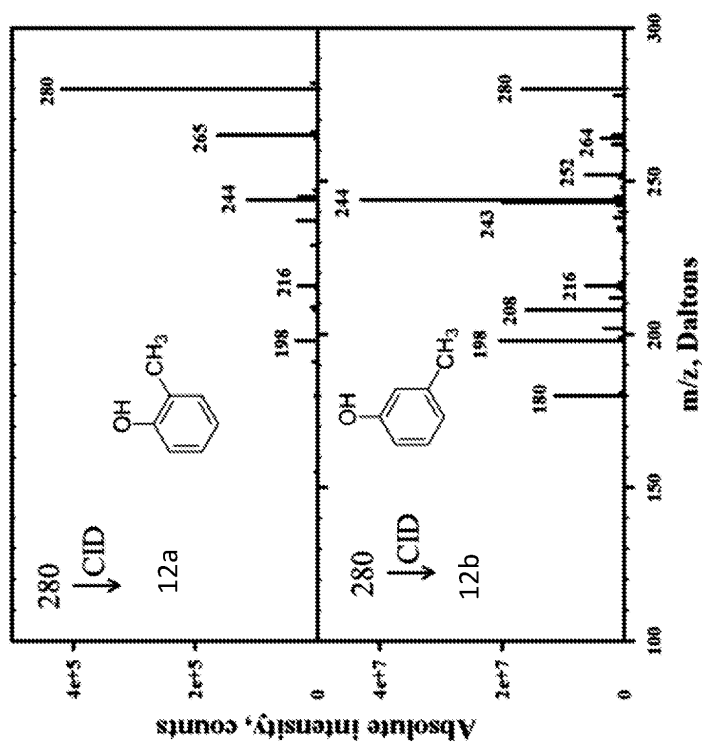


FIG. 10





FIGs. 12a and 12b

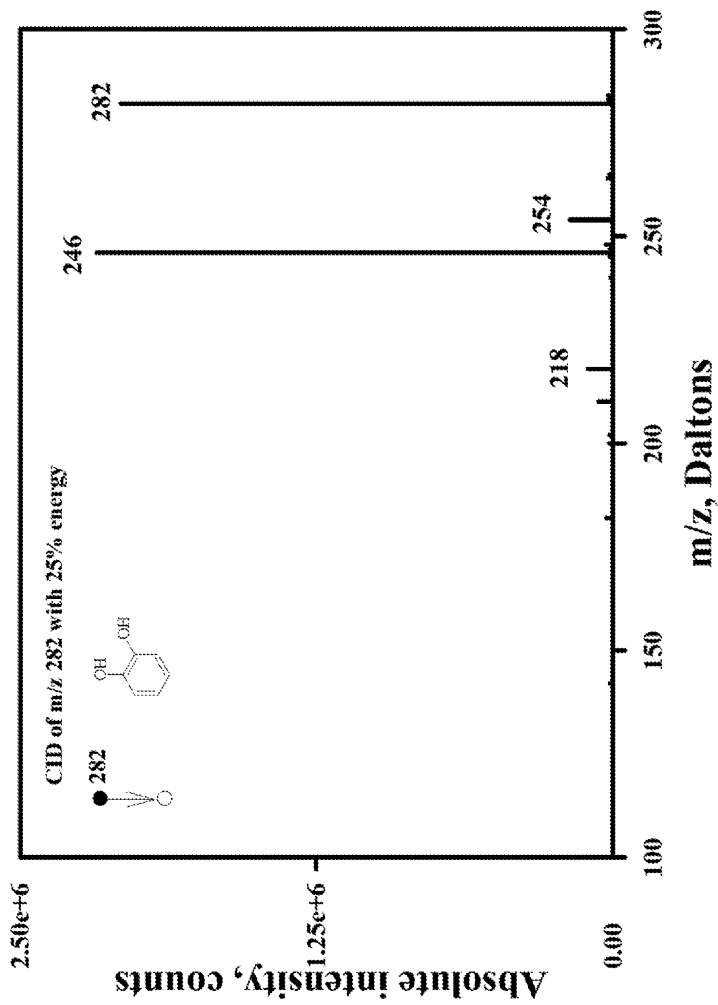


FIG. 12c

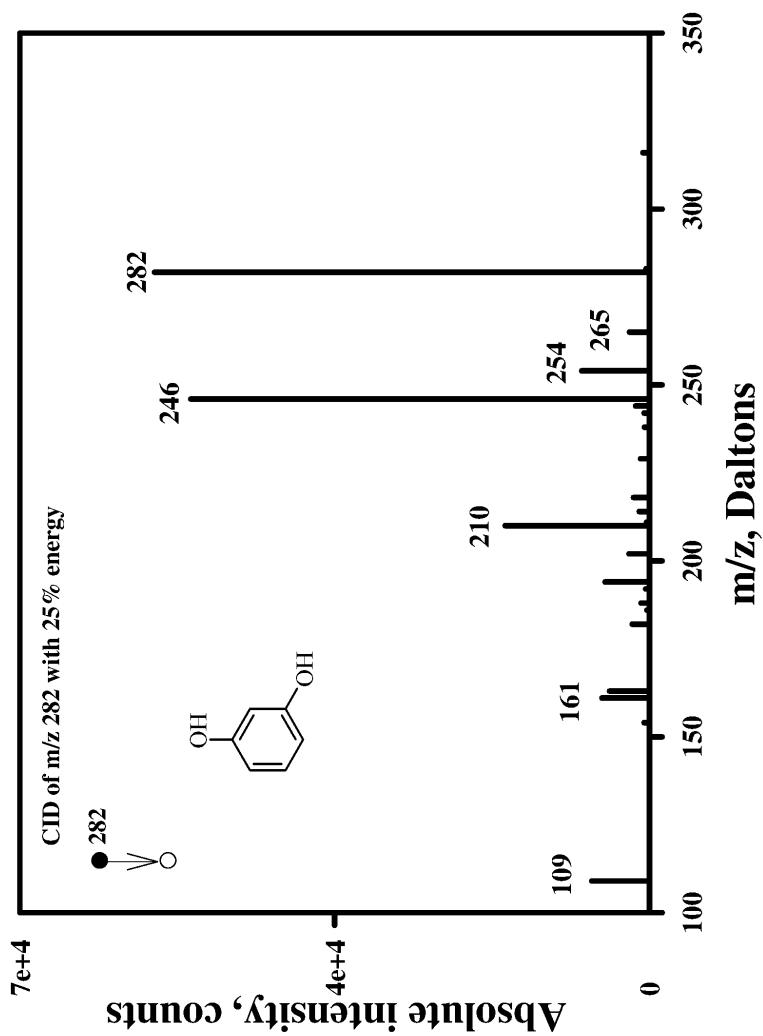


FIG. 12d

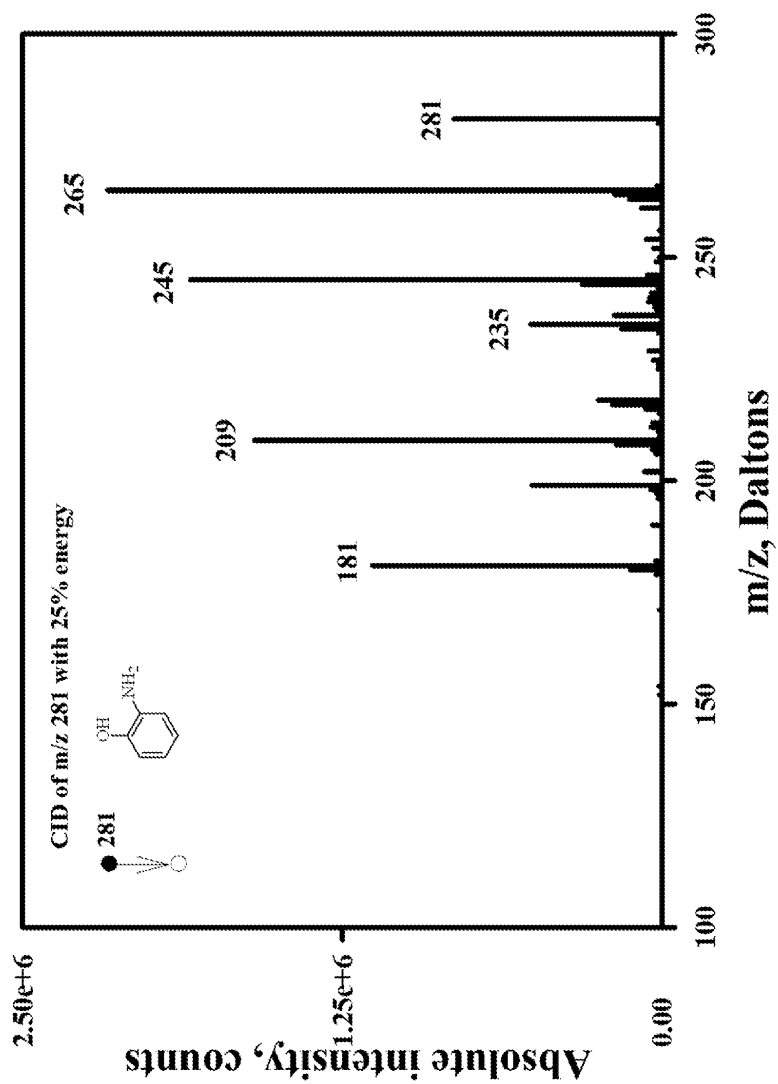


FIG. 12e

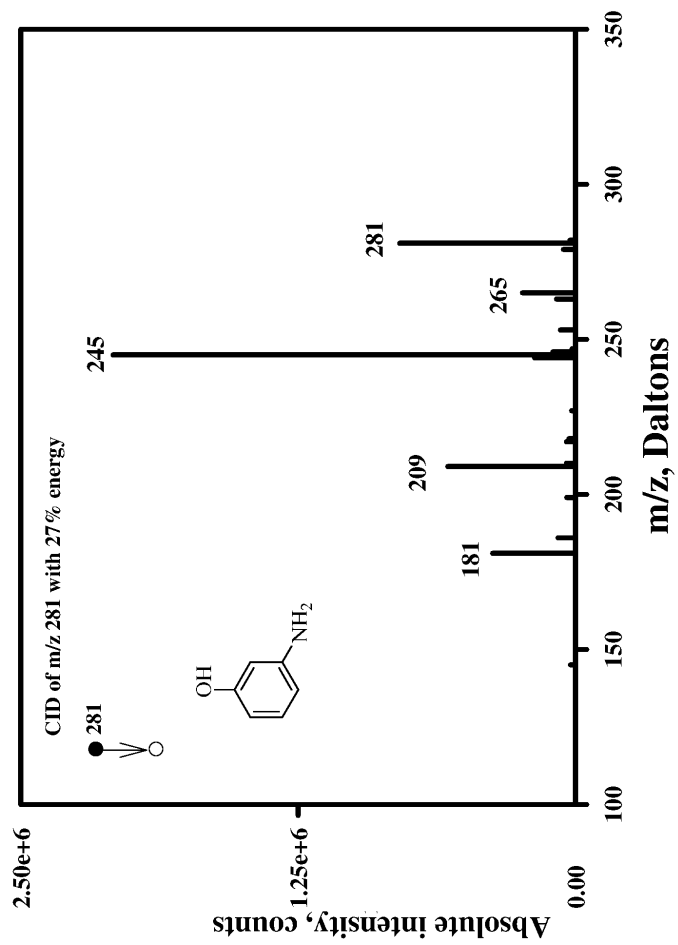
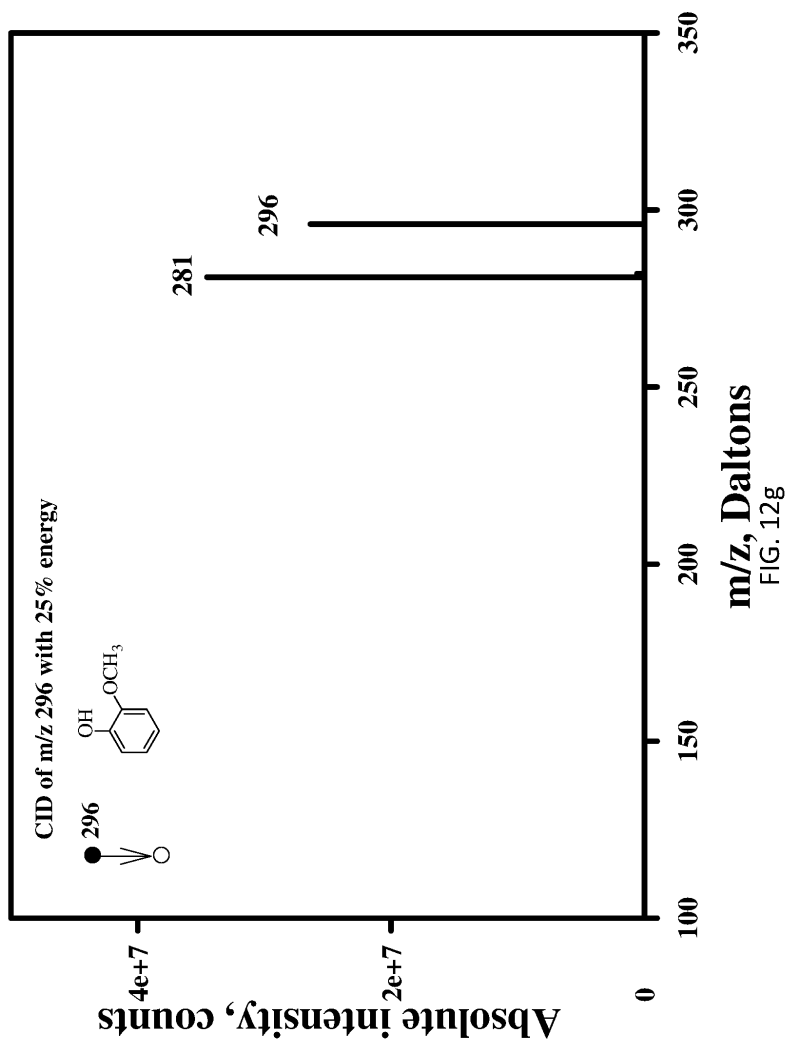
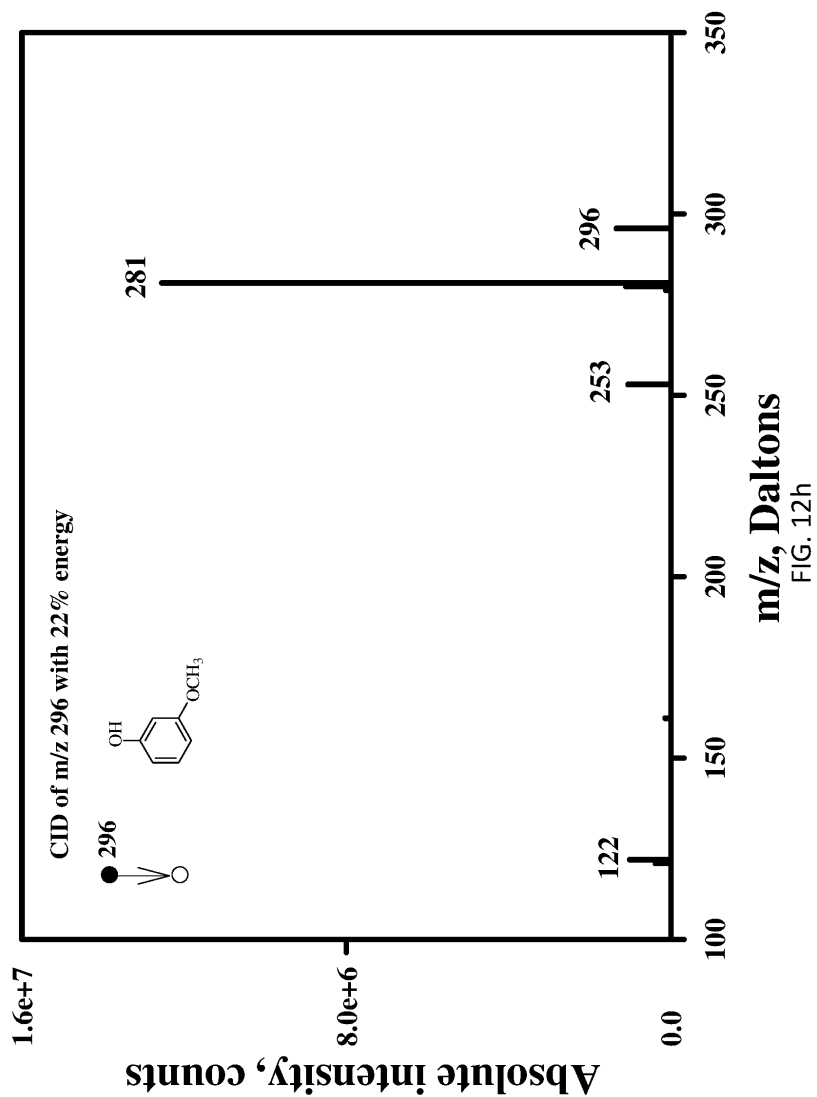


FIG. 12f





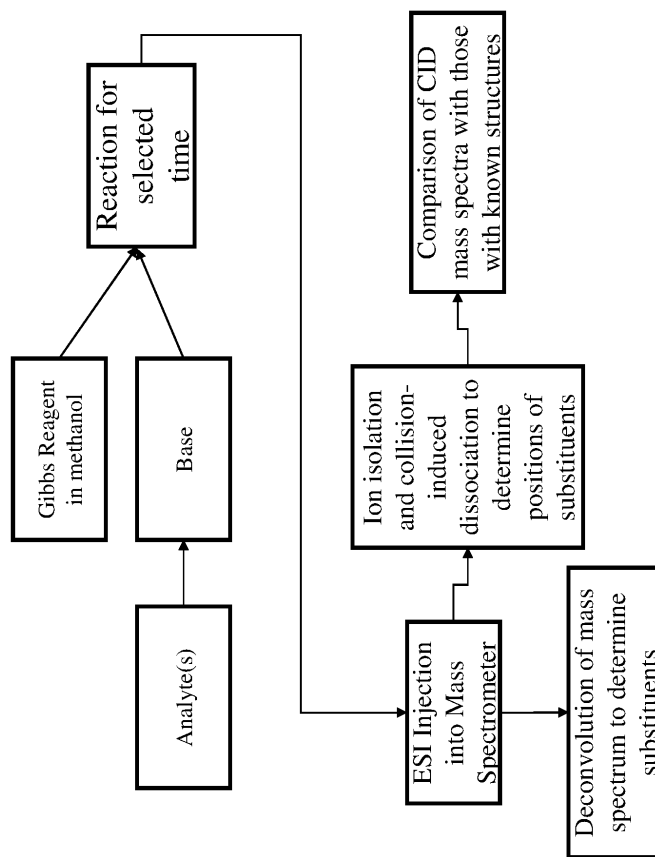
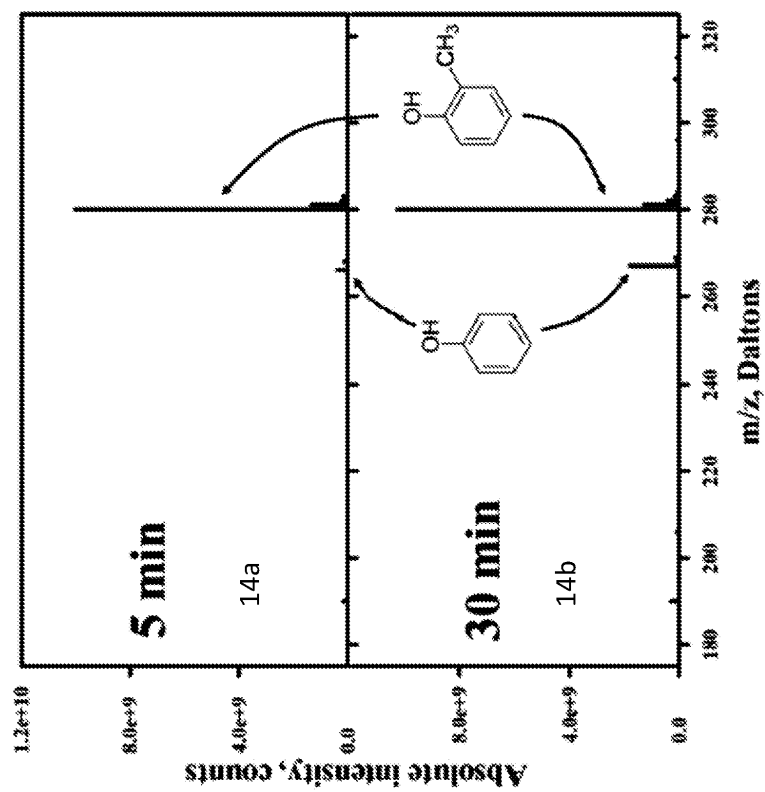


FIG. 13



FIGs. 14a and 14b

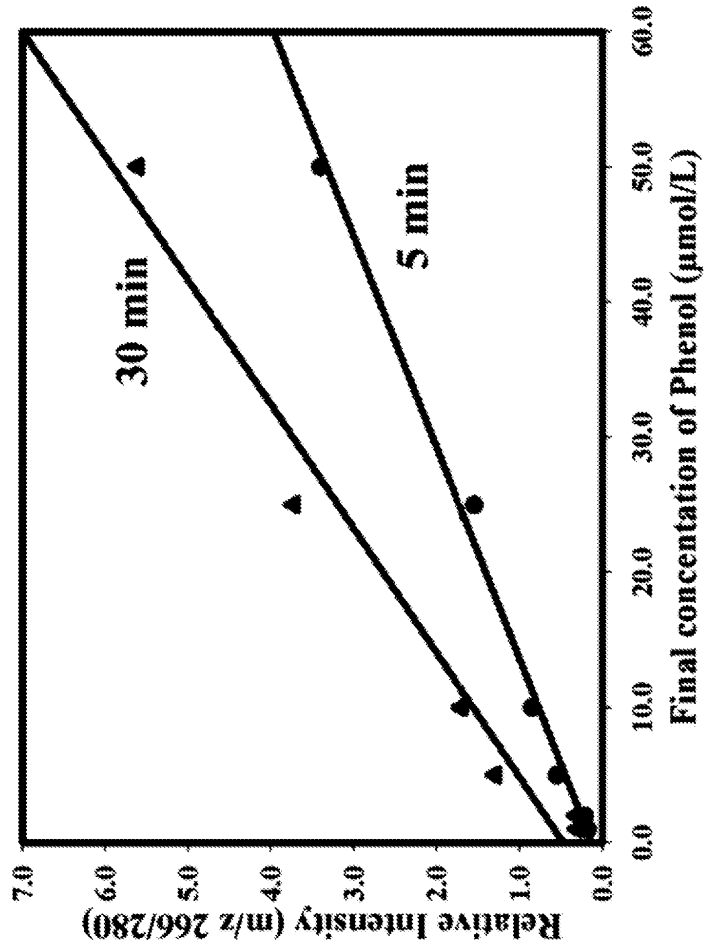


FIG. 15

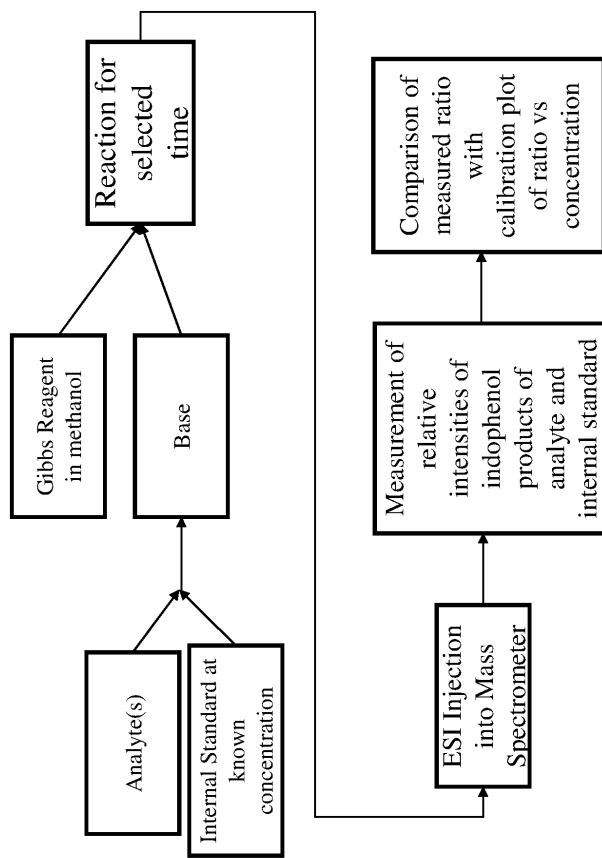
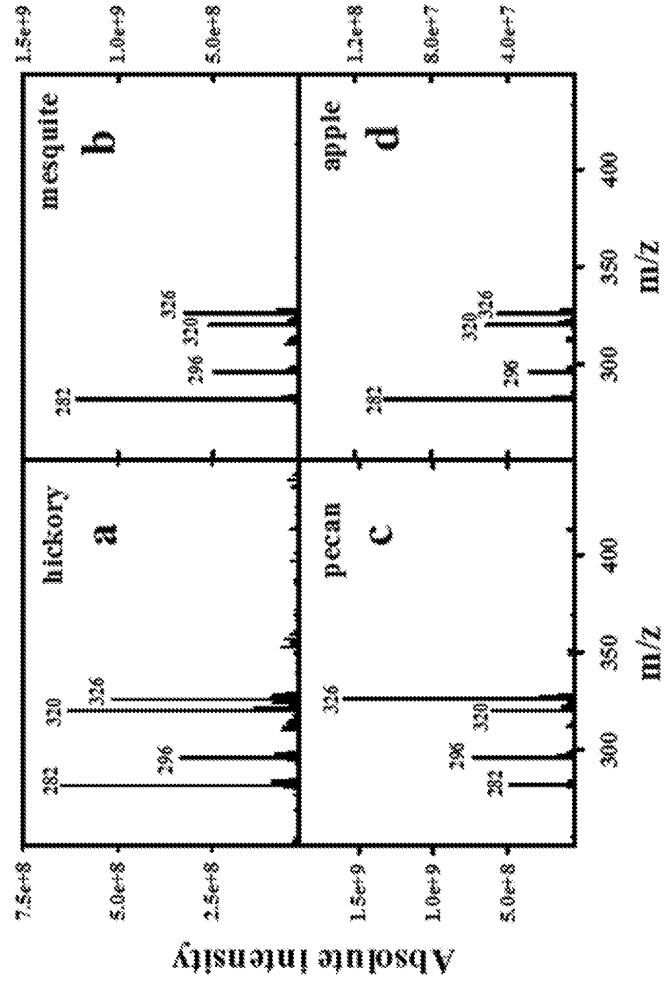


FIG. 16



FIGs. 17a, 17b, 17c, and 17d

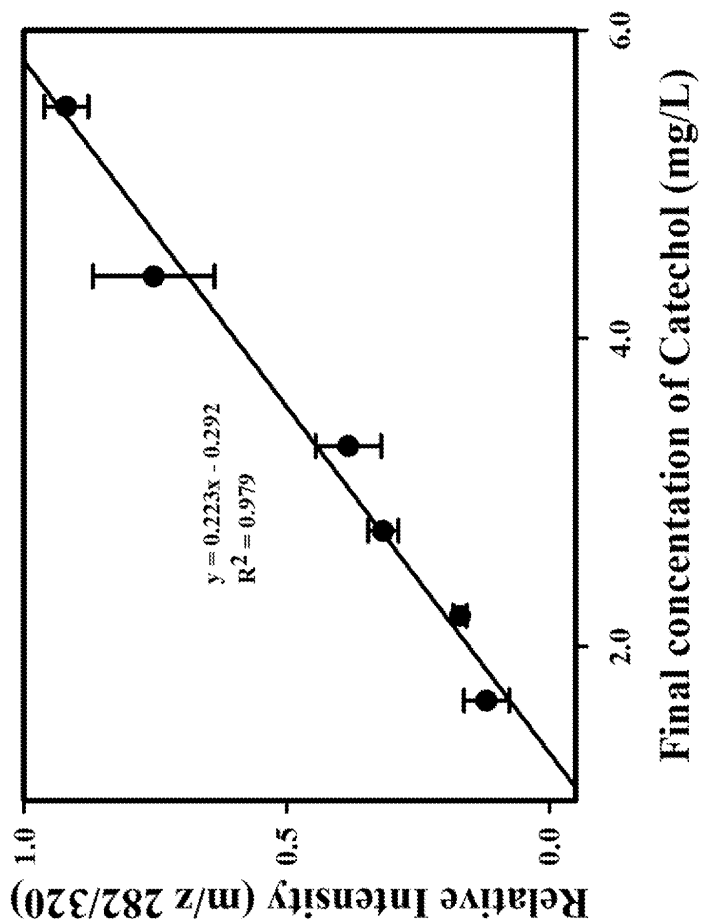


FIG. 18

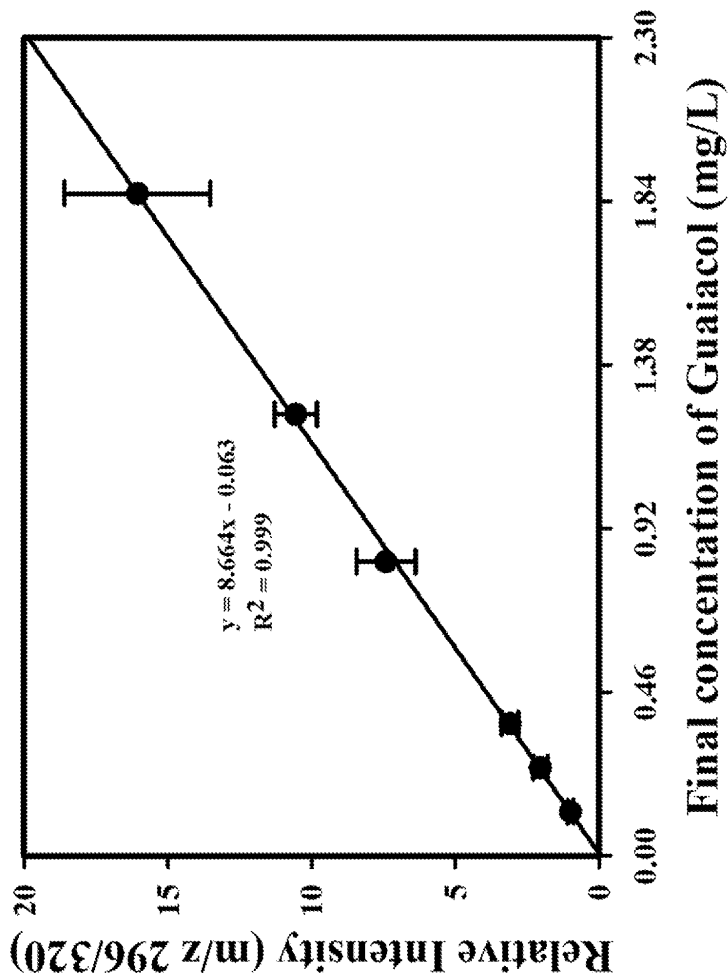


FIG. 19

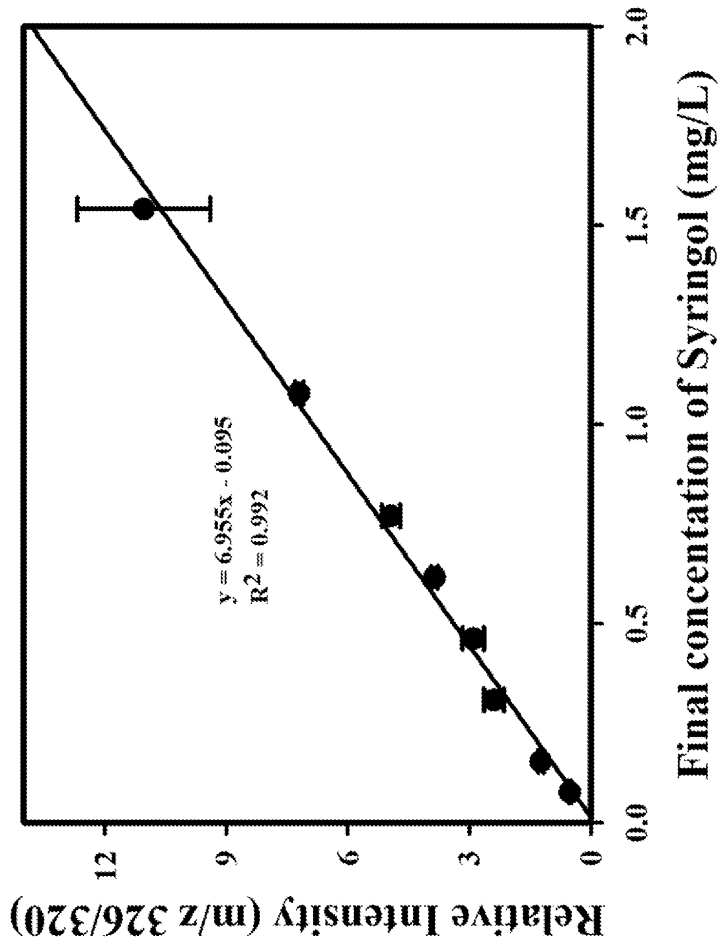


FIG. 20

METHODS OF DETECTING CHEMICALS

CROSS-REFERENCE TO RELATED APPLICATIONS

[0001] The present patent application is related to and claims the priority benefit of U.S. Provisional Patent Application Ser. No. 62/620,066 filed Jan. 22, 2018, the content of which is hereby incorporated by reference in its entirety into the present disclosure.

STATEMENT REGARDING GOVERNMENT FUNDING

[0002] This invention was made with government support under CHE15-65755 awarded by the National Science Foundation. The government has certain rights in the invention.

TECHNICAL FIELD

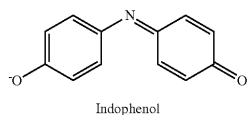
[0003] The present disclosure generally relates to a method of detecting and measuring chemical contents, and in particular, to a method of detecting phenol-based compounds using mass spectrometry.

BACKGROUND

[0004] This section introduces aspects that may help facilitate a better understanding of the disclosure. Accordingly, these statements are to be read in this light and are not to be understood as admissions about what is or is not prior art.

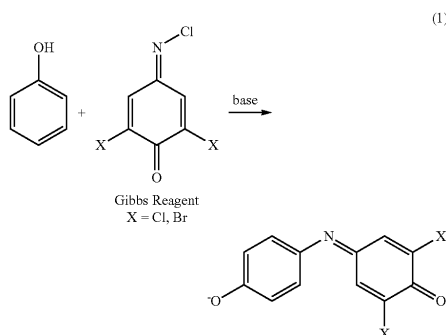
[0005] Phenol-based compounds are found all around us. They can be seen in naturally-occurring materials as well as man-made materials. In the naturally-occurring category, examples include biological molecules, such as tyrosine and L-dopa, food components, such as capsaicin or red wine tannins, and even drugs, such as morphine and tetrahydrocannabinol. In the man-made category, examples include industrial waste which can have phenol concentrations as high as 10 g/L. For a variety of reasons, e.g., food and drug safety, it is of import to identify composition of material, and in particular presence and concentration of phenolic compounds.

[0006] There have been many methods developed to detect phenols. One such method is colorimetric detection of phenols. Such methods can be traced back almost 200 years, to the detection of orcinol. For example, Liebermann in late 1800's showed that phenols, including phenol, orcinol and thymol, can be transformed into dark-blue-colored indophenol dyes by reaction with sulfuric acid and ammonia as shown below.



Then in 1927, Gibbs reported a convenient reagent for the detection of phenols by converting them to indophenols. The Gibbs reaction (eq 1), utilizing the Gibbs Reagent, 2,6-

dichloro- or dibromo-4-(chloroimino)cyclohexa-2,5-dien-1-one, has since been a standard approach for the detection of phenols.



[0007] One of the key features that makes the Gibbs procedure a useful approach for the detection of phenols is the robust color of the indophenol product, which allows for easy spectrophometric detection. In recent years, applications of the Gibbs procedure have been reported for the detection of phenol-based pharmaceuticals, capsaicin, and for monitoring the presence of phenol. In all of these applications, the indophenol is detected spectrophometrically.

[0008] However, one of the limitations in spectrophometric detection methodology of the Gibbs approach for detection of phenols is that the absorption peak is not very sensitive to substitution of the phenol. Consequently, while the standard Gibbs method is useful for determining total phenol content, it is generally not capable of distinguishing between individual substituted phenols. To address this limitations, several other approaches have been developed.

[0009] To address the above-stated limitation, a separation step is needed for the detection of specific phenol derivatives. Other non-colorometric methods have been utilized in the prior art to detect phenols in compounds. One such method has been established by Lowe et al. who have examined and detected the Gibbs reaction using electrochemistry and cyclic voltammetry, and have shown that it can be used to detect, various compounds, e.g., tetrahydrocannabinol (THC).

[0010] According to yet another non-colorometric method, to further selectively separate phenol compounds, liquid chromatography or gas chromatography methods have also been used to establish presence of different phenol substitutions.

[0011] According to still yet another non-colorometric method, Josephy and Lenkinski have characterized the Gibbs product formed from tert-butylhydroxyanisole (BHA) by using electron ionization mass spectrometry based on electron-ionization spectra for some protonated indophenols (neutral phenols) which are generally available.

[0012] All the above methods, however, suffer from lack of sensitivity, lack of selectivity, or lack of ability to identify position of the substituent (i.e., ortho, meta, or para) on the phenol ring.

[0013] Therefore, there is an unmet need for a novel approach that can identify concentration of phenols in a compound, simultaneously and selectively detect multiple phenol derivatives without requiring prior separation, and further provide position of the substituent on the phenol ring.

SUMMARY

[0014] A method of identifying phenolic compounds in a compound under test (CUT) is disclosed. The method includes mixing the CUT with a buffer solution to generate a buffered compound. The method also includes mixing the buffered compound with a Gibbs reagent and allowing reaction for a predetermined amount of time to generate an indophenol. In addition, the method includes inputting the indophenol to a mass spectrometer. Furthermore, the method includes generating spectra of the indophenol, and analyzing the spectra to determine presence of phenolic compounds in the indophenols.

[0015] A method of identifying isomeric phenolic compounds in a compound under test (CUT), is also disclosed. The method includes mixing the CUT with a buffer solution to generate a buffered compound. The method also includes mixing the buffered compound with a Gibbs reagent and allowing reaction for a predetermined amount of time to generate an indophenol. Furthermore, the method includes inputting the indophenol to a mass spectrometer, and generating spectra of the indophenol. The method also includes disassociating ions utilizing a collision induced disassociation (CID) stage, and analyzing the spectra to determine i) presence of phenolic compounds in the indophenols, and ii) identify isomers of the phenolic compounds.

[0016] A method of quantifying phenolic concentration of compounds in a compound under test, is also disclosed. The method include mixing the CUT with a buffer solution to generate a buffered compound, mixing the buffered compound with a Gibbs reagent and allowing reaction for a first predetermined amount of time to generate a first set of one or more indophenols, inputting the first set of one or more indophenols to a mass spectrometer, generating spectra of the first set of one or more indophenols, identifying a first set of one or more peaks associated with the first set of one or more indophenols, identifying a phenolic compound to be used as an internal standard with a peak for a corresponding indophenol of the internal standard at an m/z having a separation from the first set of one or more peaks of at least 5, mixing the first set of one or more indophenols with the internal standard having a predetermined concentration for a second predetermined amount of time to generate a second set of one or more indophenols, inputting the second set of one or more indophenols to the mass spectrometer, generating spectra of the second set of one or more indophenols, generating calibration curves for each of the first set of one or more indophenols, wherein the calibration curve represents a ratio of intensity of each of the first set of one or more indophenols to intensity of the internal standard vs. concentration of each of the first set of one or more indophenols, and obtaining the concentration of each of the first set of indophenols.

BRIEF DESCRIPTION OF DRAWINGS

[0017] FIG. 1a is a mass spectrum of the Gibbs reagent.

[0018] FIG. 1b is a mass spectrum of a phenol.

[0019] FIG. 1c is a mass spectrum of an indophenol of the phenol and the Gibbs reagent.

[0020] FIG. 1d is a deconvoluted version of the mass spectrum of FIG. 1c.

[0021] FIG. 2 is mass spectra for the indophenol of the ortho-cresol ($R=CH_3$) after mixing with the Gibbs reagent (the top panel represents the full spectrum of the indophenol while the bottom panel represents the deconvoluted spectrum).

[0022] FIG. 3 is mass spectra for the indophenol of the meta-cresol ($R=CH_3$) after mixing with the Gibbs reagent (the top panel represents the full spectrum of the indophenol while the bottom panel represents the deconvoluted spectrum).

[0023] FIG. 4 is mass spectra for the indophenol of the ortho-hydroxyanisole ($R=OCH_3$) after mixing with the Gibbs reagent (the top panel represents the full spectrum of the indophenol while the bottom panel represents the deconvoluted spectrum).

[0024] FIG. 5 is mass spectra for the indophenol of the meta-hydroxyanisole ($R=OCH_3$) after mixing with the Gibbs reagent (the top panel represents the full spectrum of the indophenol while the bottom panel represents the deconvoluted spectrum).

[0025] FIG. 6 is mass spectra for the indophenol of the catechol ($R=OH$) after mixing with the Gibbs reagent (the top panel represents the full spectrum of the indophenol while the bottom panel represents the deconvoluted spectrum).

[0026] FIG. 7 is mass spectra for the indophenol of the resorcinol ($R=OH$) after mixing with the Gibbs reagent (the top panel represents the full spectrum of the indophenol while the bottom panel represents the deconvoluted spectrum).

[0027] FIG. 8 is mass spectra for the indophenol of the ortho-aminophenol ($R=NH_2$) after mixing with the Gibbs reagent (the top panel represents the full spectrum of the indophenol while the bottom panel represents the deconvoluted spectrum).

[0028] FIG. 9 is mass spectra for the indophenol of the meta-aminophenol ($R=NH_2$) after mixing with the Gibbs reagent (the top panel represents the full spectrum of the indophenol while the bottom panel represents the deconvoluted spectrum).

[0029] FIG. 10 is mass spectra for 1-naphthol and the corresponding Gibbs reagent indophenol (the top panel represents the full spectrum of the indophenol while the bottom panel represents the deconvoluted spectrum).

[0030] FIG. 11 is mass spectra for tetrahydro-1-naphthol and the corresponding Gibbs reagent indophenol (the top panel represents the full spectrum of the indophenol while the bottom panel represents the deconvoluted spectrum).

[0031] FIGS. 12a and 12b are collision induced disassociation (CID) spectra of the indophenols formed from ortho- (12a) and meta-cresol (12b), respectively.

[0032] FIGS. 12c and 12d are CID spectra of the indophenols of catechol ($R=OH$) or resorcinol ($R=OH$), respectively.

[0033] FIGS. 12e and 12f are CID spectra of the indophenols of ortho-aminophenol ($R=NH_2$) and meta-aminophenol ($R=NH_2$), respectively.

[0034] FIGS. 12g and 12h are CID spectra of the indophenols of guaiacol and meta-hydroxyanisole ($R=OCH_3$), respectively.

[0035] FIG. 13 is a flowchart according to the present disclosure of a process by which substituents in a compound under test are identified using the Gibbs reagent and mass spectrometry.

[0036] FIGS. 14a and 14b are deconvoluted mass spectra of Gibbs products obtained from a 1:1 mixture of phenol and o-cresol taken at 5 min of mixing (FIGS. 14a) and 30 min of mixing (FIG. 14b).

[0037] FIG. 15 is a calibration graph of intensity vs. concentration of phenols in $\mu\text{mol/L}$ with o-cresol used as an internal standard.

[0038] FIG. 16 is a flow chart according to the present disclosure of a process for quantifying concentrations of phenolic compounds in a compound under test utilizing an internal standard.

[0039] FIGS. 17a, 17b, 17c, and 17d are deconvoluted mass spectra for various liquid smoke (hickory (17a), mesquite (17b), pecan (17c), and apple (17d)).

[0040] FIG. 18 is a calibration graph of intensity vs. concentration of catechol in mg/L with 5,6,7,8-tetrahydro-1-naphthol (THN) used as an internal standard.

[0041] FIG. 19 is a calibration graph of intensity vs. concentration of guaiacol in mg/L with 5,6,7,8-tetrahydro-1-naphthol (THN) used as an internal standard.

[0042] FIG. 20 is a calibration graph of intensity vs. concentration of syringol in mg/L with 5,6,7,8-tetrahydro-1-naphthol (THN) used as an internal standard.

DETAILED DESCRIPTION

[0043] For the purposes of promoting an understanding of the principles of the present disclosure, reference will now be made to the embodiments illustrated in the drawings, and specific language will be used to describe the same. It will nevertheless be understood that no limitation of the scope of this disclosure is thereby intended.

[0044] In the present disclosure, the term “about” can allow for a degree of variability in a value or range, for example, within 10%, within 5%, or within 1% of a stated value or of a stated limit of a range.

[0045] In the present disclosure, the term “substantially” can allow for a degree of variability in a value or range, for example, within 90%, within 95%, or within 99% of a stated value or of a stated limit of a range.

[0046] A novel approach is disclosed herein that can identify concentration of phenols in a compound, simultaneously and selectively detect multiple phenol derivatives without requiring prior separation, and further provide position of the substituent on the phenol ring.

[0047] Accordingly, the present disclosure describes detection of Gibbs products by using electrospray-ionization mass spectrometry (ESI-MS). This approach is contrary to accepted wisdom because use of the Gibbs reagent for detection of phenols has been since the early days of the Gibbs reagent been limited to colorimetric approaches. However, the inventors found that use of mass spectrometry surprisingly provides robust selectivity in identifying phenolic compounds based on the Gibbs reagent and the indophenols resulting therefrom. Since indophenols are naturally anionic, they are readily detected by ESI-MS. An important advantage of using mass spectrometry for the detection of indophenols is that it readily distinguishes between different substituents when in the ortho- and meta-positions. In the present disclosure, ESI mass spectra for indophenols obtained in the Gibbs reaction of simple sub-

stituted phenols are provided, which show a robust application for simultaneous detection of components in a mixture, including identification and quantification.

[0048] Accordingly, the present disclosure provides a novel method for detecting phenols of unknown concentration in a compound, by reacting the compound with the Gibbs Reagent to form indophenols, followed by mass spectrometric detection. Unlike the standard Gibbs reaction, which uses a colorimetric approach, the use of mass spectrometry allows for simultaneous detection of differently substituted phenols.

[0049] Use mass spectrometry to detect the indophenol product allows for a more specific determination of phenol composition. The relative yields of Gibbs products additionally allows for quantification of phenol components, by measuring intensity against an internal standard. Mass spectrometric analysis also allows for investigation of the product structures, particularly for the reactions with para-substituted phenols, which can react either by direct substitution of the substituent, or at another site within the phenol, preserving the para substituent. The method is shown to work for the analysis of liquid smoke, and is therefore amenable for the analysis of wood-smoke condensates

[0050] The procedure is demonstrated to work for a large variety of phenols without para-substitution. With para-substituted phenols, Gibbs products are still often observed, but the specific product depends on the substituent. For para groups with high electronegativity, such as methoxy or halogens, the reaction proceeds by displacement of the substituent. For groups with lower electronegativity, such as amino or alkyl groups, Gibbs products are observed that retain the substituent, indicating that the reaction occurs at the ortho or meta positions. In mixtures of phenols, the relative intensities of the Gibbs products are proportional to the relative concentrations, and concentrations as low as 1 $\mu\text{mol/L}$ can be detected. In one example, the novel method of the present disclosure is thus applied to a qualitative analysis of commercial liquid smoke, and it is found that hickory, mesquite, pecan, and apple flavors represent significantly different phenolic composition.

[0051] Exemplary aspects of the novel methodology of the present disclosure is now provided.

Sample Preparation (General Procedure)

[0052] Samples were prepared by mixing an exemplary volume (e.g., 5 mL) of a solution of the Gibbs Reagent in methanol (e.g., 60 mmol/L) with 10 mL of an aqueous potassium phosphate dibasic solution (deionized water, 40 mmol/L , pH 9.5) containing substrate. After mixing, the solutions were stirred at room temperature for the allotted time, after which 50 μL of the solution was diluted to 4 mL in water-methanol solution (1:1), for ESI-MS analysis. Solutions for individual samples contained 0.25 mmol of substrate in the phosphate buffer. Spectra are measured 5 minutes after mixing—unless otherwise noted.

[0053] For the mixture of phenol and o-cresol, 10 mL of the initial solution containing o-cresol and phenol were mixed with 5 mL methanol solution of the Gibbs Reagent (100 mmol/L). The reaction mixtures were stirred for 5 minutes and 30 minutes, respectively, before diluting with 1:1 methanol as described above, followed by mass spectrometric analysis. The concentration of o-cresol in the initial solution was chosen so to obtain a concentration of 3 $\mu\text{mol/L}$ in the final electrosprayed solution. Similarly, the

concentration of phenol in the initial solution was chosen so to obtain concentrations of 1, 2, 5, 10, 25 and 50 $\mu\text{mol/L}$ in the final solution.

ESI-MS

[0054] Electrospray ionization mass spectra were obtained on a commercial LCQ-DECA (THERMO ELECTRON CORPORATION, San Jose, Calif., USA) quadrupole ion trap mass spectrometer, equipped with an ESI source, operating in negative ion mode. Substrate solutions in a methanol: water mixture (1:1) were introduced into the source directly at a flow rate of 10 $\mu\text{L}/\text{min}$. Electrospray and ion focusing conditions were varied to maximize the signal of the ion of interest.

Sample Preparation (Liquid Smoke)

[0055] K_2HPO_4 (0.5 mmol, 87 mg) was added directly to 5 mL of the corresponding commercial smoke sample directly and mixed with 10 mL methanol solution of the Gibbs Reagent (0.5 mmol, 105 mg). The reaction mixture was stirred at room temperature for 5 minutes. 200 μL of the reaction mixture was dissolved in 4 mL water-methanol (1:1) solution for spectrometric analysis.

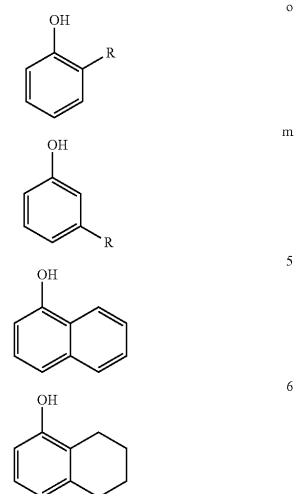
Spectral Analysis

[0056] An important advantage of using the Gibbs Reagent for derivatization is that the chlorine atoms make products containing the Gibbs Reagent readily detectable by the isotopic pattern. Therefore, the spectra are deconvoluted using the isotope pattern for ions containing two chlorine atoms (1:0.648:0.105, where 1 represents the first peak, 0.648 represents the second peak and the 0.105 represents the third peak) to eliminate the peaks that cannot contain the Gibbs Reagent. Thus, the deconvolution process acts as a filter to eliminate peaks that do not have the double chlorine ions (i.e., peaks associated with non-indophenols). It is this ability to specifically detect phenoxides and eliminate non-Gibbs products that makes the Gibbs approach preferable to the spectrometric analysis of the mixture using ESI-MS.

[0057] Referring to FIGS. 1a, 1b, and 1c, spectra obtained from the ESI-MS of the Gibbs reagent alone in buffer (FIG. 1a), phenol alone in buffer (FIG. 1b), phenol and the Gibbs reagent in buffer 5 minutes after mixing (FIG. 1c) are provided. As shown in FIG. 1a, in the absence of phenol, the MS of the Gibbs reagent is non-descript, and shows a large number of unidentifiable ionic products. FIG. 1b provides a clear indication of phenoxide (m/z 93). However, in the presence of other acidic substrates, the phenoxide product would be expected to be a minor product. FIG. 1c shows the spectrum obtained 5 minutes after mixing Gibbs reagent and phenol in the buffer solution. The spectrum is dominated by the Gibbs indophenol product, as indicated by the characteristic isotopic pattern. Moreover, despite having phenol at the same concentration as in FIG. 1b, the absolute intensity increases by a factor of about 100 for the detection of the Gibbs product, not considering the fact that signal is distributed over multiple isotope peaks. Therefore, the total signal of the phenol derivative in FIG. 1c is nearly 200 times greater than that of phenol in FIG. 1b. For example, in FIG. 1c, the intensity is 1.2×10^5 for the phenoxide. However, the intensity of the indophenol is about 1.2×10^7 , evidencing the robust ionic nature of the indophenols, making mass spectrometry a viable choice for detection of phenols using the

Gibbs reagent. FIG. 1d provides the spectrum obtained after deconvolution, to account for the isotope peaks. Although the initial spectrum was originally very clean, the deconvoluted spectrum is even more so, with more than 85% of the signal attributable to indophenol. The deconvolution process is a filtering process based on the two chlorine ions in the indophenols, further described below.

[0058] Gibbs products are also readily detected by ESI-MS for other substituted phenols, included ortho- and meta-cresol (1o and 1m), ortho- and meta-hydroxyanisole (2o and 2m), catechol (3o), resorcinol (3m), 2-aminophenol (4), 1-naphthol (5), and tetrahydro-1-naphthol (6) as provided below:



- 1: R = CH₃
- 2: R = OCH₃
- 3: R = OH
- 4: R = NH₂

[0059] Spectra for each of these constituents at the ortho and meta positions in the indophenols resulting from mixing with the Gibbs reagent for those positions are shown in FIGS. 2-8. For example, FIG. 2 shows the spectra for the indophenol of the ortho-cresol (R=CH₃) after mixing with the Gibbs reagent. The top panel of FIG. 2 represents the full spectrum of the indophenol while the bottom panel represents the deconvoluted spectrum. FIG. 3 shows the spectra for the indophenol of the meta-cresol (R=CH₃) after mixing with the Gibbs reagent. The top panel of FIG. 3 represents the full spectrum of the indophenol while the bottom panel represents the deconvoluted spectrum. A comparison of FIGS. 2 and 3 reveals a peak at m/z of 280 which represents the indophenol of cresol (R=CH₃) regardless of the ortho or meta-positions. FIG. 4 shows the spectra for the indophenol of the ortho-hydroxyanisole (R=OCH₃) after mixing with the Gibbs reagent. The top panel of FIG. 4 represents the full spectrum of the indophenol while the bottom panel represents the deconvoluted spectrum. FIG. 5

shows the spectra for the indophenol of the meta-hydroxyanisole ($R=OCH_3$) after mixing with the Gibbs reagent. The top panel of FIG. 5 represents the full spectrum of the indophenol while the bottom panel represents the deconvoluted spectrum. A comparison of FIGS. 4 and 5 reveals a peak at m/z of 296 which represents the indophenol of hydroxyanisole ($R=OCH_3$) regardless of the ortho or meta positions. FIG. 6 shows the spectra for the indophenol of the catechol ($R=OH$) after mixing with the Gibbs reagent. The top panel of FIG. 6 represents the full spectrum of the indophenol while the bottom panel represents the deconvoluted spectrum. FIG. 7 shows the spectra for the indophenol of the resorcinol ($R=OH$) after mixing with the Gibbs reagent. The top panel of FIG. 7 represents the full spectrum of the indophenol while the bottom panel represents the deconvoluted spectrum. A comparison of FIGS. 6 and 7 reveals a peak at m/z of 282 which represents the indophenol of catechol or resorcinol ($R=OH$), respectively. FIG. 8 shows the spectra for the indophenol of the ortho-aminophenol ($R=NH_2$) after mixing with the Gibbs reagent. The top panel of FIG. 8 represents the full spectrum of the indophenol while the bottom panel represents the deconvoluted spectrum. FIG. 9 shows the spectra for the indophenol of the meta-aminophenol ($R=NH_2$) after mixing with the Gibbs reagent. The top panel of FIG. 9 represents the full spectrum of the indophenol while the bottom panel represents the deconvoluted spectrum. A comparison of FIGS. 8 and 9 reveals a peak at m/z of 281 which represents the indophenol of aminophenol ($R=NH_2$) regardless of the ortho or meta positions. FIG. 10 shows the spectra for 1-naphthol and the corresponding Gibbs reagent indophenol. The top panel of FIG. 10 represents the full spectrum of the indophenol while the bottom panel represents the deconvoluted spectrum. A closer look at FIG. 10 reveals a peak at m/z of 316 which represents the indophenol of 1-naphthol. FIG. 11 shows the spectra for tetrahydro-1-naphthol and the corresponding Gibbs reagent indophenol. The top panel of FIG. 11 represents the full spectrum of the indophenol while the bottom panel represents the deconvoluted spectrum. A closer look at FIG. 11 reveals a peak at m/z of 320 which represents the indophenol of tetrahydro-1-naphthol.

[0060] While mass spectrometry provides a robust approach for detection of phenol when mixed with the Gibbs reagent, thus generating indophenols as shown in eq. 1, mass spectrometry by itself is not well suited to distinguish between isomers of phenols. This limitation was already observed in the ortho and meta positions of the same substituents (see pairs of FIGS. 2 and 3, 4 and 5, 5 and 7, and 8 and 9). Thus in order to distinguish between these isomers (which have the same mass to charge ratio but have substituents at different positions), an additional step is needed. The extra step includes a collision induced disassociation (CID) stage, known to a person having ordinary skill in the art (e.g., U.S. Pat. No. 6,590,203 to Kato, contents of which is hereby incorporated by reference into the present disclosure in its entirety), and the associated CID spectrum of fragments. To demonstrate this added step, reference is now made to FIGS. 12a and 12b which show the CID spectra of the indophenols formed from ortho-(12a) and meta-cresol (12b), respectively. Significant differences are observed between the spectra, with methyl loss being a major dissociation pathway for the ortho-isomer, but not observed for meta, whereas m/z 252, 208, and 180 are exclusively observed for the meta-isomer. Therefore, in reference to

FIG. 12a, for an indophenol of cresol ($R=CH_3$) at the ortho position, the CID spectrum represents peaks at m/z of 198, 216, 244, 265, and 280, while in reference to FIG. 12b, for an indophenol of cresol ($R=CH_3$) at the meta position, the CID spectrum represents peaks at m/z of 180, 198, 208, 216, 243, 244, 252, 264, and 280. Further reference is made to FIGS. 12c and 12d which show the CID spectra of the indophenols of catechol ($R=OH$) or resorcinol ($R=OH$), respectively. Therefore, in reference to FIG. 12c, for the indophenol of catechol ($R=OH$), the CID spectrum represents peaks at m/z of 218, 246, 254, and 282, while in reference to FIG. 12d, for the indophenol of resorcinol ($R=OH$), the CID spectrum represents peaks at m/z of 109, 161, 210, 246, 254, 265, and 282. Further reference is made to FIGS. 12e and 12f which show the CID spectra of the indophenols of ortho-aminophenol ($R=NH_2$) and meta-aminophenol ($R=NH_2$), respectively. Therefore, in reference to FIG. 12e, for the indophenol of ortho-aminophenol ($R=NH_2$), the CID spectrum represents peaks at m/z of 181, 199, 209, 235, 245, 265, and 281, while in reference to FIG. 12f, for the indophenol of meta-aminophenol ($R=NH_2$), the CID spectrum represents peaks at m/z of 181, 209, 245, 265, and 281. Further reference is made to FIGS. 12g and 12h which show the CID spectra of the indophenols of guaiacol, the CID spectrum represents peaks at m/z of 281 and 296 (FIG. 12g) and meta-hydroxyanisole ($R=OCH_3$), the CID spectrum represents peaks at m/z of 122, 253, 281, and 296. Although not all isomeric pairs show such dramatic differences, FIGS. 12a, 12b, 12c, 12d, 12e, 12f, and 12g show that CID of the indophenols can be used to distinguish between isomeric phenols.

[0061] Therefore, according to one embodiment of the present disclosure, initially a mass spectrum of a phenolic Gibbs product (i.e., an indophenol as in eq. 1) is obtained. Reviewing the spectrum, phenolic compounds based on different substituents can be identified based on the m/z numbers (see FIGS. 2-11). In order to clean up the spectra from unwanted peaks, the spectra can be deconvoluted to remove peaks lacking the two chlorine ions of the indophenols. Once the phenolic compounds have been identified, then isomers (i.e., identification of positions of substituents) can be identified by subsequently or simultaneously using the CID spectra. Referring to FIG. 13, a flowchart is provided showing the steps described above.

[0062] The next topic addressed in the present disclosure is sensitivity. As discussed above, an advantage of using mass spectrometry to detect the indophenol products of the Gibbs reaction is that it can be used for simultaneous detection of multiple phenol derivatives without separation. This is illustrated by the spectrum of 1:1 mixture of phenol and o-cresol (1o), each at 0.25 mmol/L concentration, shown in FIGS. 14a and 14b which are spectra of indophenols of cresol ($R=CH_3$) at the ortho position taken at 5 min of mixing (FIGS. 14a) and 30 min of mixing (FIG. 14b). The presence of peaks at m/z 266 and m/z 280 in the deconvoluted mass spectrum indicate the presence of phenol and o-cresol (1o), respectively.

[0063] Although the phenol and o-cresol in the indophenols have equal concentrations, at 5 minutes the signal for the cresol is nearly 25 times larger than that for phenol. However, after 30 minutes, the absolute signal for phenol increases by nearly a factor of 5, whereas that for o-cresol

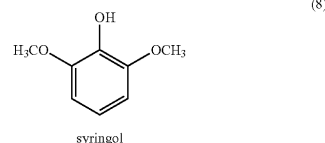
increases by less than 5%, which shows that under these buffer conditions, the reaction with o-cresol occurs much faster than that with phenol.

[0064] To use this method for the quantitative detection of phenol, a phenolic compound not present in the compound being tested can be used as an internal standard. Importantly, the compound under test (CUT) should be evaluated to determine what phenolic compounds exist in the CUT (based on the above described methods), then a phenolic compound not present in the CUT can be used as an internal standard based on an indophenol having an m/z separation of at least 5 as compared to the m/z of all other peaks found in the spectra. In one example o-cresol having a concentration of 3.0 μmol/L is used as an internal standard, although a host of other phenolic compounds are also possible. Calibration curves for the ratio I(m/z 266)/I(m/z 280) vs phenol concentration, for samples where the above-stated internal standard at 5 min and 30 min post-mix are shown in FIG. 15, which is a graph of intensity vs. concentration of phenols in μmol/L. This graph (FIG. 15) can then be used to quantify concentration of phenol compounds. Under the conditions used according to the present disclosure, the reaction of the Gibbs reagent with o-cresol is faster than that with phenol, such that the relative amount of the Gibbs product for phenol, m/z 266, compared to the Gibbs product for phenol, m/z 280, at longer reaction time is larger than that at short reaction time (based on a comparison of 30 minutes and 5 minutes reaction times). Nonetheless, the ratio of phenol Gibbs product to o-cresol Gibbs product is essentially linear (r^2 is about 0.99) over the range of phenol concentration from 1-50 μmol/L.

[0065] The quantification approach described above is shown in FIG. 16, which is a flowchart of the quantification aspect of the present disclosure. Initially the analyte is mixed with a buffer and mixed with the Gibbs reagent for a selected time (producing an indophenol) which is then provided to the mass spectrometer for analysis of what phenolic compounds are present. Once the phenolic compounds are identified, then a phenolic compound as an internal standard at a known concentration is chosen and the process repeated, this time with the internal standard generating a peak not seen in the previous run. Next, relative intensities of indophenol products of analyte and internal standard are obtained followed by a comparison of measured ratio with calibration plot of ratio vs concentration.

[0066] With the above description of the novel method, two compounds with unknown phenolic contents are now analyzed based on this method. Hickory, mesquite, pecan, and apple liquid smoke compounds are now described.

[0067] The mass spectrometric detection of Gibbs products can be used to analyze any sample that contains significant amounts of phenols. An example of this type of product is "liquid smoke," a common additive used for flavoring and preservation, which includes wood smoke condensates. Phenols make up approximately 1/5 of commercially available liquid smoke, with guaiacol (2o), pyrocatechol (3o) and syringol (8) (shown below) are among the most important components. As an illustration of how this method can be used to analyze mixtures, four commercially available liquid smoke products, sold by The COLGIN COMPANIES (Dallas, Tex.), a "Natural Hickory", "Natural Mesquite", "pecan", and "apple" are analyzed to determine the differences in phenolic composition.



[0068] The deconvoluted mass spectra for hickory, mesquite, pecan, and apple flavors of liquid smoke upon reaction with the Gibbs reagent, taken 5 minutes after mixing, are shown in FIGS. 17a, 17b, 17c, and 17d which are deconvoluted spectra for hickory (17a), mesquite (17b), pecan (17c), and apple (17d). Once substituents are observed, then an internal standard having an m/z separation of at least 5 is chosen. In this case, an internal standard of 5,6,7,8-tetrahydro-1-naphthol (THN) is used which produces an indophenol with a peak at m/z 320.

[0069] In FIG. 17a, significant peaks are at m/z 282, 296, 326 for Gibbs product of catechol, guaiacol, and syringol, respectively. As mentioned, the peak at m/z 320 is due to the Gibbs product of internal standard, THN. The spectra show that hickory contains more methoxy phenol than mesquite (17b), which is abundant with hydroxy phenol. Pecan flavored has mostly syringol (m/z 326) (FIG. 17c) and apple flavored has mostly catechol (m/z 282) (FIG. 17d). Interestingly, for this analysis 2 mL of the corresponding liquid smoke is taken for all flavored liquid smokes but apple, which is 8 mL to get significant signal of the Gibbs product.

[0070] In each case of forming calibration curves, the intensity ratio of the corresponding compound and that of the internal standard, i.e., 5,6,7,8-tetrahydro-1-naphthol (THN), is provided against the concentration of the corresponding compound after five minutes reaction time. FIGS. 18, 19, and 20 show the calibration curves by plotting I(m/z282)/I(m/z320) vs. catechol concentration (FIG. 18), I(m/z 296)/I(m/z320) vs. guaiacol concentration (FIG. 19), I(m/z 326)/I(m/z320) vs. syringol concentration (FIG. 20), respectively, where 5,6,7,8-tetrahydro-1-naphthol (m/z 320) Gibbs products is used as the internal standard in each. The 5,6,7,8-tetrahydro-1-naphthol is present at a concentration of 0.20 mg/L. The ratio of catechol Gibbs product to the internal standard Gibbs product is substantially linear ($r^2=0.993$) over the range of catechol concentration from 1.65-5.50 mg/L. Similarly, in the other two calibration curves the ratios are substantially linear ($r^2=0.997$ for guaiacol, and $r^2=0.998$ for syringol) over the range of guaiacol concentration of 0.12-1.86 mg/L and over the concentration of syringol of 0.08-1.08 mg/L.

[0071] The concentrations (milligrams per liter and mmole per liter) of the phenolic compounds are presented in Table 1. The results are of an average of at least five set of experiments. The results show that the mostly plentiful compound in all four-different flavored liquid smoke is catechol and the least present amount is guaiacol. Catechol is present in mesquite flavored as high as 6.728±0.687 g/L (61.051±1.530 mmol/L). However, a low amount of catechol is contained in apple flavored liquid smoke (1.486±0.045 g/L, 13.488±0.409 mmol/L). Hickory flavored liquid smoke contains approximately half of catechol (3.444±0.141 g/L, 31.257±1.277 mmol/L) as compared to mesquite flavored, whereas pecan contains almost double of it

(2.773±0.084 g/L, 25.167±0.759 mmol/L) than the apple flavored. The compound with the lowest amount contained is guaiacol, which is mostly present in pecan flavored (71.937±2.683 mg/L, 0.602±0.059 mmol/L) and least amount present in apple flavored liquid smoke (3.651±0.174 mg/L, 0.029±0.001 mmol/L). Interestingly, presence of guaiacol in mesquite flavored liquid smoke (61.672±3.553 mg/L, 0.497±0.029 mmol/L) is quite similar of pecan flavored and hickory flavored which contain around one-third guaiacol (23.029±2.654 mg/L, 0.186±0.021 mmol/L) of that in mesquite flavored. The third compound present in these liquid smokes is syringol. Pecan flavored contains the highest amount of it (209.420±8.963 mg/L, 1.351±0.086 mmol/L), while apple flavored liquid smoke contains lowest amount (20.904±0.642 mg/L, 0.132±0.004 mmol/L). Hickory (91.417±5.022 mg/L, 0.579±0.033 mmol/L) and mesquite (94.779±5.508 mg/L, 0.601±0.036 mmol/L) flavored contain similar amount of syringol.

TABLE 1

Concentration of catechol, guaiacol, and syringol in mmol/L and mg/L in four different flavored liquid smoke								
Analyte	Pecan		Apple		Hickory		Mesquite	
	mg/L	mM	mg/L	mM	mg/L	mM	mg/L	mM
Catechol	2772.680 (83.677)	25.167 (0.759)	1486.470 (45.127)	13.488 (0.409)	3444.196 (140.810)	31.257 (1.277)	6728.430 (168.696)	61.051 (1.530)
Guaiacol	71.937 (2.683)	0.602 (0.059)	3.651 (0.174)	0.029 (0.001)	23.029 (2.654)	0.186 (0.021)	61.672 (3.553)	0.497 (0.029)
Syringol	209.420 (8.963)	1.351 (0.086)	20.904 (0.642)	0.132 (0.004)	91.417 (5.022)	0.579 (0.033)	94.779 (5.508)	0.601 (0.036)

[0072] In a detailed analysis of Code 10-Poly full-strength liquid smoke, Montazeri et al. found additional, less abundant products, including isomeric methoxymethylphenols and 3-methoxy-1,2-benzenediol. These appear to be present in the spectra in FIGS. 17a and 17b, at m/z 310 and 312, respectively. However, in both spectra, there is a product at m/z 311 that is similar in abundance to those at m/z 310 and 312. The odd m/z value would require a nitrogen containing product, and could, in principle, be attributed to an amino-methoxyphenol. Additional products are also observed at m/z 349, 351 and 420. The product at m/z 420 is important because, while a minor peak in the analysis at 5 min, it is the most abundant product at 30 min. From the isotope pattern and collision induced dissociation experiments, it is found that the product at m/z 420 contains chlorine. Since the reactions of hydroxy- and methoxyphenols with Gibbs reagents are fast, then the relative intensities of the peaks in FIGS. 17a and 17b reflect the relative concentrations of the phenolic components.

[0073] Those having ordinary skill in the art will recognize that numerous modifications can be made to the specific implementations described above. The implementations should not be limited to the particular limitations described. Other implementations may be possible.

1. A method of identifying phenolic compounds in a compound under test (CUT), comprising:
 - mixing the CUT with a buffer solution to generate a buffered compound;
 - mixing the buffered compound with a Gibbs reagent and allowing reaction for a predetermined amount of time to generate an indophenol;

- inputting the indophenol to a mass spectrometer; generating spectra of the indophenol; and analyzing the spectra to determine presence of phenolic compounds in the indophenols.
2. The method of claim 1, wherein the buffered solution is basic.
 3. The method of claim 2, wherein the buffered solution is potassium phosphate dibasic.
 4. The method of claim 1, wherein a peak at m/z of 280 represents the indophenol of cresol (R=CH₃) at an ortho or meta positions, a peak at m/z of 296 represents the indophenol of hydroxyanisole (R=OCH₃) at the ortho or meta positions, a peak at m/z of 282 represents the indophenol of catechol or resorcinol (R=OH), a peak at m/z of 281 represents the indophenol of aminophenol (R=NH₂) at the ortho or meta positions, a peak at m/z of 316 represents the indophenol of 1-naphthol, and a peak at m/z of 320 represents the indophenol of tetrahydro-1-naphthol.

5. The method of claim 1, wherein the Gibbs reagent is one of 2,6-dichloroquinone-4-chloroimide and 2,6-dibromoquinone-4-chloroimide.
6. The method of claim 5, further comprising deconvoluting the generated spectra and whereby the analyzing step is based on the deconvoluted step, where the spectral deconvolution removes peaks that are unrelated to double chlorine or bromine ions present in the indophenols.
7. The method of claim 1, wherein the mass spectrometer is an electrospray ionization mass spectrometer.
8. A method of identifying isomeric phenolic compounds in a compound under test (CUT), comprising:
 - mixing the CUT with a buffer solution to generate a buffered compound;
 - mixing the buffered compound with a Gibbs reagent and allowing reaction for a predetermined amount of time to generate an indophenol;
 - inputting the indophenol to a mass spectrometer; generating spectra of the indophenol;
 - disassociating ions utilizing a collision induced dissociation (CID) stage; and
 - analyzing the spectra to determine i) presence of phenolic compounds in the indophenols, and ii) identify isomers of the phenolic compounds.
9. The method of claim 8, wherein the buffered solution is basic.
10. The method of claim 9, wherein the buffered solution is potassium phosphate dibasic.
11. The method of claim 8, wherein a peak at m/z of 280 represents the indophenol of cresol (R=CH₃) at an ortho or meta positions, a peak at m/z of 296 represents the indo-

phenol of hydroxyanisole (R=OCH₃) at the ortho or meta positions, a peak at m/z of 282 represents the indophenol of catechol or resorcinol (R=OH), a peak at m/z of 281 represents the indophenol of aminophenol (R=NH₂) at the ortho or meta positions, a peak at m/z of 316 represents the indophenol of 1-naphthol, and a peak at m/z of 320 represents the indophenol of tetrahydro-1-naphthol.

12. The method of claim 8, wherein the Gibbs reagent is one of 2,6-dichloroquinone-4-chloroimide and 2,6-dibromoquinone-4-chloroimide.

13. The method of claim 12, further comprising deconvoluting the generated spectra and whereby the analyzing step is based on the deconvoluted step, where the spectral deconvolution removes peaks that unrelated to double chlorine or bromine ions present in the indophenols.

14. The method of claim 8, wherein for an indophenol of cresol (R=CH₃) at an ortho position, the CID spectrum represents peaks at m/z of 198, 216, 244, 265, and 280; for an indophenol of cresol (R=CH₃) at a meta position, the CID spectrum represents peaks at m/z of 180, 198, 208, 216, 243, 244, 252, 264, and 280; for an indophenol of catechol (R=OH), the CID spectrum represents peaks at m/z of 218, 246, 254, and 282; for an indophenol of resorcinol (R=OH), the CID spectrum represents peaks at m/z of 109, 161, 210, 246, 254, 265, and 282; for an indophenol of aminophenol (R=NH₂) at the ortho position, the CID spectrum represents peaks at m/z of 181, 199, 209, 235, 245, 265, and 281; for an indophenol of aminophenol (R=NH₂) at the meta position, the CID spectrum represents peaks at m/z of 181, 209, 245, 265, and 281; for an indophenol of guaiacol, the CID spectrum represents peaks at m/z of 281, and 296; and for an indophenol of meta-hydroxyanisole (R=OCH₃), the CID spectrum represents peaks at m/z of 122, 253, 281, and 296.

15. A method of quantifying phenolic concentration of compounds in a compound under test (CUT), comprising:

- mixing the CUT with a buffer solution to generate a buffered compound;
- mixing the buffered compound with a Gibbs reagent and allowing reaction for a first predetermined amount of time to generate a first set of one or more indophenols;
- inputting the first set of one or more indophenols to a mass spectrometer;
- generating spectra of the first set of one or more indophenols;

identifying a first set of one or more peaks associated with the first set of one or more indophenols;

identifying a phenolic compound to be used as an internal standard with a peak for a corresponding indophenol of the internal standard at an m/z having a separation from the first set of one or more peaks of at least 5;

mixing the first set of one or more indophenols with the internal standard having a predetermined concentration for a second predetermined amount of time to generate a second set of one or more indophenols;

inputting the second set of one or more indophenols to the mass spectrometer;

generating spectra of the second set of one or more indophenols;

generating calibration curves for each of the first set of one or more indophenols, wherein the calibration curve represents a ratio of intensity of each of the first set of one or more indophenols to intensity of the internal standard vs. concentration of each of the first set of one or more indophenols; and

obtaining the concentration of each of the first set of indophenols.

16. The method of claim 15, wherein the buffered solution is basic.

17. The method of claim 16, wherein the buffered solution is potassium phosphate dibasic.

18. The method of claim 15, wherein a peak at m/z of 280 represents the indophenol of cresol (R=CH₃) at an ortho or meta positions, a peak at m/z of 296 represents the indophenol of hydroxyanisole (R=OCH₃) at the ortho or meta positions, a peak at m/z of 282 represents the indophenol of catechol or resorcinol (R=OH), a peak at m/z of 281 represents the indophenol of aminophenol (R=NH₂) at the ortho or meta positions, a peak at m/z of 316 represents the indophenol of 1-naphthol, and a peak at m/z of 320 represents the indophenol of tetrahydro-1-naphthol.

19. The method of claim 15, wherein the Gibbs reagent is one of 2,6-dichloroquinone-4-chloroimide and 2,6-dibromoquinone-4-chloroimide.

20. The method of claim 15, further comprising deconvoluting the generated spectra and whereby the analyzing step is based on the deconvoluted step, where the spectral deconvolution removes peaks that are unrelated to double chlorine or bromine ions present in the indophenols.

* * * * *